Glutaminase Inhibition as a Potential Therapeutic Strategy in Diffuse Large B-cell Lymphoma

Dissertation

der Mathematisch-Naturwissenschaftlichen Fakultät

der Eberhard Karls Universität Tübingen

zur Erlangung des Grades eines

Doktors der Naturwissenschaften

(Dr. rer. nat.)

vorgelegt von

Beatriz Gomez Solsona

aus Castellon de la Plana, Spanien

Tübingen

2023

Gedruckt mit Genehmigung der Mathematisch-Naturwissenschaftlichen Fakultät der Eberhard Karls Universität Tübingen.

Tag der mündlichen Qualifikation:	04.07.2023
Dekan:	Prof. Dr. Thilo Stehle
1. Berichterstatter:	Prof. Dr. Stephan Hailfinger
2. Berichterstatter:	Prof. Dr. Klaus Schulze-Osthoff

A todas las mujeres de
mi vida y, en especial, a mi madre.
Por todo su apoyo, cariño, humildad y coraje, que me han impulsado a seguir adelante.

Table of contents

Abbreviations I

CHAPTER 1

Summary VII
Zusammenfassung IX
1. Introduction 1
1.1 Non-Hodgking lymphoma 1
1.2 Diffuse large B-cell lymphoma 2
1.2.1 Pathogenesis of germinal center B-cell-like DLBCL 5
1.2.2 Pathogenesis of activated B-cell-like DLBCL 6
1.3 Antiapoptotic Bcl-2 protein in DLBCL 8
1.4 Therapeutic strategies targeting DLBCL 8
1.5 Glutamine metabolism and its role in cancer 11
1.5.1 Role of glutamine as a carbon and nitrogen donor 11
1.5.2 Role of glutamine in gene expression regulation 12
1.5.3 Role of glutamine in the induction of signaling pathways 13
1.5.4 Glutamine metabolism and redox homeostasis 14
1.6 Glutaminase 14
1.6.1 The role of glutaminase in cancer 16
1.7 c-Myc in DLBCL and glutamine metabolism 17
1.8 Aims of the study 19

2. Results 20
2.1 Effects of glutaminase-1 inhibition in DLBCL 20
2.1.1 GLS1 and GLS2 expression in DLBCL cell lines 20
2.1.2 Glutaminolysis regulation via c-Myc in DLBCL cell lines 20
2.1.3 DLBCL cell survival depends on GLS1 activity 21
2.1.4 GLS1 silencing and glutamine deprivation affect DLBCL survival 24
2.1.5 Primary non-transformed B cells are refractory to GLS1 inhibition 25
2.2 Molecular mechanism of GLS1 inhibition in DLBCL 25
2.2.1 Effects of GLS1 inhibition on intracellular signaling pathways and post-translational modifications 26
2.2.2 Nucleotide supplementation does not rescue cell viability after GLS1 inhibition 30
2.2.3 The abundance of metabolic intermediaries is diminished upon CB-839 treatment 31

2.2.4 GLS1 inhibition provokes oxidative stress in DLBCL 34
2.2.5 GLS1 inhibition does not affect mitochondrial integrity 36
2.2.6 α-Tocopherol abrogates the effects of GLS1 inhibition 38
2.3 Synergystic approaches for the treatment of DLBCL 41
2.3.1 GLS1 inhibition acts synergystically with the Bcl-2 inhibitor ABT-199 41

3. Discussion 44
3.1 Importance of glutamine metabolism for DLBCL survival 44
3.2 Mechanisms of action of GLS inhibitors in DLBCL 47
3.3 Synergistic aproaches for the treatment of DLBCL 53

CHAPTER 2

4. Introduction 55
4.1 Hepatocellular carcinoma 55
4.1.1 Current HCC treatment options 55
4.1.2 Risk factors involved in hepatocarcinogenesis 56
4.1.3 The role of inflammation in HCC development 57
4.1.3.1 IL-6/STAT3 signaling pathway in the development of HCC 58
4.1.3.2 Role of NF-κB in HCC development 59
4.1.3.3 NF-κB function in the tumor microenvironment 60
4.2 The transcription factor NF-κB 62
4.3 Atypical IκB members 64
4.3.1 The atypical protein IκBζ 65
4.3.2 Role of IκBζ in cancer 68
4.4 Functions of Brd4 and its relationship with NF-κB 69
4.5 Aims of the study 72

5. Results 73
5.1 Potential IκBζ interaction partners 73
5.1.1 IκBζ induction 73
5.1.2 IκBζ interaction partners 74
5.1.2.1 Brd4 binding to IκBζ 74
5.1.2.2 Cdk9 binding to IκBζ 76
5.1.2.3 STAT3 binding to IκBζ 77
5.1.3 Mapping of IκBζ and Brd4 interaction 78
5.1.4 Oncogenic Ras induction of IκBζ and its role in senescence 79

5.2 Identification of novel IκBζ target genes 82
5.2.1 Novel IκBζ-dependent target genes 82
5.3 Liver-specific *NFKBIZ* overexpression in mice 84
5.3.1 *NFKBIZ* overexpression *in vivo* has detrimental effects on mouse livers 84
5.3.2 Characterization of the IκBζ-induced phenotypic alterations 88
5.4 *NFKBIZ* expression in liver disease patients 90
5.4.1 *NFKBIZ* expression is elevated in human liver disease 90

6. Discussion 92
6.1 IκBζ induction and regulation in human HCC cell lines 92
6.2 Oncogenic Ras-mediated IκBζ induction and its role in senescence 98
6.3 Novel IκBζ target genes 100
6.4 Effects of liver-specific IκBζ overexpression *in vivo* 102
6.5 IκBζ expression in human liver disease 105

7. Materials and Methods 108
7.1 Materials 108
7.1.1 Cell culture consumables 108
7.1.2 Cell culture media, supplements and antibiotics 109
7.1.3 Chemicals and reagents 109
7.1.4 Immortalized human cell lines 111
7.1.5 Formulations 111
7.1.6 Kits and systems 113
7.1.7 Materials for qPCR 113
7.1.8 Oligonucleotides 113
7.1.9 Materials for protein expression systems 115
7.1.9.1 Transient expression 115
7.1.9.2 Lentiviral expression 116
7.1.10 Antibodies 116
7.1.11 Pharmacological inhibitors 117
7.1.12 Biological reagents and agents used for stimulation 118
7.1.13 Devices 118
7.1.14 Software for data analysis 119
7.1.15 Mouse strains 119
7.2 Methods and protocols 121
7.2.1 Cell culture methods 121
7.2.1.1 Culture of immortalized cell lines 121

7.2.1.2 Isolation and culture of human primary B cells 121
7.2.1.3 Freezing and thawing of cells 121
7.2.1.4 Determination of cell number, proliferation and viability... 121
7.2.2 Transient and stable expression systems..... 122
7.2.2.1 Calcium phosphate transfection..... 122
7.2.2.2 Lentiviral transduction 123
7.2.3 RNA methods 123
7.2.3.1 RNA isolation and cDNA generation 123
7.2.3.2 Real time-quantitative PCR..... 124
7.2.3.3 RNAscope® 124
7.2.4 Protein methods 125
7.2.5 Enzyme-linked immunosorbent assay (ELISA) 128
7.2.6 Senescence assays..... 128
7.2.6.1 Senescence induction..... 128
7.2.6.2 β-Galactosidase staining (SA-β-gal) 128
7.2.7 Fluorescence activated cell sorting (FACS)..... 129
7.2.7.1 Surface staining 129
7.2.7.2 Intracellular staining 131
7.2.8 Luminescence and fluorescence assays..... 132
7.2.8.1 Quantification of cellular GSH levels..... 132
7.2.8.2 Quantification of cellular NADPH levels..... 132
7.2.8.3 Quantification of cellular ATP levels..... 133
7.2.8.4 CellTiter-Fluor™ cell viability assay 133
7.2.8.5 Microscopy..... 133

8. Acknowledgements 134

9. References 136

Abbreviations

ABC	Activated B-cell subtype
AID	Activation-induced cytidine deaminase
ALD	Alcoholic liver disease
AMA	Antimycin A
ANK	Ankyrin repeat
AP-1	Activator protein-1
ATL	Adult T cell Leukemia
ATP	Adenosine triphosphate
BAD	Bcl-2-associated death promoter
BAFFR	B-cell-activating factor receptor
BAK	Bcl-2 homologous antagonist killer
BAX	Bcl-2-associated X protein
BCL	B-cell lymphoma
BCR	B-cell receptor
BD	Bromodomain
BET	Bromodomain and extra terminal domain
BH3	Bcl-2 homology 3
BID	Basic residue-rich interaction domain
BL	Burkitt lymphoma
BLIMP1	B lymphocyte-induced maturation protein-1
Brd4	Bromodomain-containing protein 4
BSA	Bovine serum albumin
BTK	Bruton's tyrosine kinase
C/EBPβ	CCAAT/enhancer binding protein β
CAD	Carbamoyl-phosphate synthetase 2 aspartate transcarbamylase and dihydroorotase
CARD	Caspase recruitment domain-containing protein
CBM	CARD11, BCL10 and MALT1
CBP	CREB-binding protein
CC	Consensus cluster
CCL	CC-chemokine ligand
CD	Cluster of differentiation
CD40L	Cluster of differentiation 40 ligand
CDK	Cyclin-dependent kinase
CDKN2A	Cyclin-dependent kinase inhibitor 2A
cDNA	Complementary DNA
ChIP	Chromatin immunoprecipitation
CHX	Cycloheximide
cIAP	Cellular inhibitor of apoptosis
CK2	Casein kinase 2
c-Myc	Avian myelocytomatosis virus oncogene cellular homolog
CoA	Coenzyme-A
COO	Cell of origin
CR	Complete response
CRC	Colorectal cancer
CREB	cAMP response element-binding protein
CREBBP	CREB binding protein

Csf-1	Colony stimulating factor-1
CSR	Class switch recombination
CTP	CTP synthetase
CTCL	Cytotoxic T-lymphocyte associated protein
CXCL	Chemokine (C-X-C motif) ligand
DA-EPOCH	Dose adjusted – etoposide, prednisone, vincristine, cyclophosphamide, doxorubicin
DAG	Diacylglycerol
DAMP	Danger-associated molecular pattern
DAPI	4 ',6-diamino-2-fenilindol
DBE	Dimethyl succinate
DEN	Diethylnitrosamine
DLBCL	Diffuse large B-cell lymphoma
DMEM	Dulbecco's modified eagle medium
DMF	Dimethyl fumarate
DM-KG	Dimethyl ketoglutarate
DMSO	Dimethyl sulfoxide
DNA	Dimethyl sulfoxide
dNTP	2'-Deoxynucleoside 5'-triphosphate
Dox	Doxycycline
EBV	Epstein-Barr virus
ECL	Enhanced chemoluminiscence
EDTA	Ethylenediaminetetraacetic acid
EFS	Event-free survival
ELISA	Enzyme-linked immunosorbent assay
EP300	E1A-binding protein p300
ER	Endoplasmatic reticulum
ETC	Electron transport chain
ERK	Extracellular signal–regulated kinase
FACS	Fluorescence-activated cell sorting
FAD	Flavin adenine dinucleotide
FADD	FAS-associated death domain protein
FCS	Fetal calf serum
FITC	Fluorescein isothiocyanate
FL	Follicular lymphoma
FLIP	FLICE inhibitory protein
GAC	Glutaminase C
GADD45β	Growth arrest and DNA-damage-inducible, beta
GAPDH	Glyceraldehyde-3-phosphate dehydrogenase
GBP-1	Guanylate binding protein-1
GCB	Germinal center B-cell like
GCL	Glutamate-cysteine ligase
G-CSF	Granulocyte colony-stimulating factor
GDH	Glutamate dehydrogenase
GLS	Glutaminase
GLUD	Glutamate dehydrogenase
GM-CSF	Granulocyte macrophage colony-stimulating factor
GOT	Glutamate-oxaloacetate transaminase
gRNA	Guide-RNA
GSH	Glutathione

GTPase	Guanosine triphosphate hydrolase
H3K4	Lysine 4 of histone 3
HAT	Histone acetyltransferase
HBV	Hepatitis B virus
HCV	Hepatitis C virus
HCC	Hepatocellular carcinoma
HDACs	Histone deacetylases
HEPES	4-(2-Hydroxyethyl) piperazine-1-ethanesulfonic acid
HIF-1	Hypoxia-inducible factor-1
HIV	Human immunodeficiency virus
HL	Hodgkin lymphoma
HPV	Human papillomavirus
HR	Host response
HRP	Horseradish peroxidase
HTLV	Human T-lymphotropic virus
IFN	Interferon
Ig	Immunoglobulin
IGH	Immunoglobulin heavy chain
IGL	Immunoglobulin light chain
IHC	Immunohistochemistry
IKK	IκB kinase
IL	Interleukin
IP	Immunoprecipitation
IRAK	IL-1R-associated kinase
IRF	Interferon regulatory factor
ITAM	Immunoreceptor tyrosine-based activation motif
IκB	Inhibitor of κB/inhibitor of NF-κB
IκBα	Inhibitor of κB/inhibitor of NF-κB α
IκBNS	Nuclear factor of kappa light polypeptide gene enhancer in B-cells inhibitor
IκBζ	Inhibitor of κB/inhibitor of NF-κBζ
JAK	Janus-associated kinase
JHMD	Jumonji C histone demethylases
JNK	c-Jun amino-terminal kinase
KD	Knock-down
kDa	Kilo Dalton
KGA	Kidney glutaminase
KO	Knockout
LAT1	L-Type amino acid transporter
LCN	Lipocalin-2
LGA	Liver-trype glutaminase
LPS	Lipopolysaccharide
LTα	Lymphotoxin α
LTβ	Lymphotoxin β
MAIL	Molecule possessing ankyrin repeats induced by lipopolysaccharide
MALT1	Mucosa-associated lymphoid tissue
MAPK	Mitogen-activated protein kinase
MCL	Mantle cell lymphoma
M-CSF	Macrophage colony-stimulating factor
MDH	Malate dehydrogenase

ME	Malic enzyme
MFI	Mean fluorescence intensity
MiRNA	MicroRNA
mitoROS	Mitochondrial ROS
MM	Multiple myeloma
MOMP	Mitochondrial outer membrane permeabilization
MPO	Myeloperoxidase
mRNA	Messenger RNA
mTOR	Mammalian Target of rapamycin
MyD88	Myeloid differentiation primary response protein 88
NAC	N-acetylcysteine
NADP	Nicotinamide adenine dinucleotide phosphate
NAFLD	Non-alcoholic fatty liver disease
NASH	Non-alcoholic steatohepatitis
NEAA	Non-essential amino acid
NEMO	NF-κB essential modulator
NF-κB	Nuclear factor kappa light chain enhancer of activated B cells
NHL	Non-Hodgkin lymphoma
NIK	NF-κB-inducible kinase
NK	Natural killers
NLS	Nuclear localization signal
NOTCH	Neurogenic locus notch homolog protein
NPS	N-terminal cluster of CK2 phosphorylation sites
OAA	Oxaloacetate
ORR	Objective response rate
OS	Overall survival
OIS	Oncogene-induced senescence
OxPhos	Oxidative phosphorylation
P/I	PMA and Ionomycin
PAGE	Polyacrylamide gel electrophoresis
PAMP	Pathogen-associated molecular pattern
PBS	Phosphate-buffered saline
PBST	Phosphate buffered saline with Tween-20
PCa	Prostate cancer
PCR	Polymerase chain reaction
PDAC	Pancreatic ductal adenocarcinoma
PDID	phosphorylation-dependent interaction domain
PFS	Progression-free survival
PI3K	Phosphoinositide 3 kinase
PKC	Protein kinase C
PMA	Phorbol 12-myristate 13-acetate
PMBL	Primary mediastinal B-cell lymphoma
PRMD1	PR domain zinc finger protein 1
PRR	Pattern recognition receptor
PTEN	Phosphatase and Tensin homolog
qPCR	Quantitative polymerase chain reaction
qRT-PCR	Quantitative reverse transcription-polyermase chain reaction
R-ACVBP	Rituximab, doxorubicin, cyclophosphamide, vindesine, bleomycin, prednisone
RANK	Receptor activator of nuclear factor κB

RANKL	Receptor activator of nuclear factor κB ligand
RB	Retinoblastoma protein
R-CHOP	Rituximab-Cyclophosphamide,Hydroxydaunorubicin, Vincristine(Oncovin™)
RHD	Rel homology domain
RNA	Ribonucleic acid
RNApolII	RNA polymerase II
RNAseq	RNA sequencing
ROS	Reactive oxygen species
RPL37A	Ribosomal protein L37a
RSK	Ribosomal protein L37a
RT	Room temperature
rtTA	Reverse tetracycline transactivator
SD	Standard deviation
SDHA	Succinate dehydrogenase complex, subunit
SDS	Sodium dodecyl sulphate
SFK	Src family kinase
shRNA	Short hairpin RNA
S100A	S100 Calcium Binding Protein A8
STAT	Signal transducers and activators of transcription
SYK	Spleen tyrosine kinase
TAB	TAK1-binding protein
TAD	Transactivation domain
TAE	Tris acetic acid EDTA
TACE	Transarterial chemoembolization
TAK1	TGF-β-activated kinase 1
T-ALL	T-cell acute lymphoblastic leukaemia
TBP	TATA-binding protein
TCA	Tricarboxylic acid
TCR	T cell receptor
TED	TET DNA demethylases
Tet	Tetracycline
TET	Ten-eleven translocation (TET) methylcytosine dioxygenases
TF	Transcription factor
TGFβ	Transforming growth factor β
Th	T helper cell
TIR	Toll/interleukin-1 receptor
TLR	Toll-like receptor
TNFAIP3	Tumor necrosis factor, alpha-induced protein 3 or A20
TMRE	Tetramethylrhodamin, Ethylester, Perchlorat (TMRE)
TNF	Tumor necrosis factor
TNFR	Tumor necrosis factor receptor
TP53	Tumor protein 53
TRAF	TNF receptor-associated factor
Tris	Tris(hydroxymethyl)aminomethane
TSS	Transcription start site
Tween	Polysorbat 20
TYK2	Tyrosine kinase 2
Ub	Ubiquitin
UTR	Untranslated region

VEGF	Vascular endothelial growth factor
WT	Wild-type
α-KG	α-ketoglutarate
κB site	NF-κB binding site

CHAPTER 1

Summary

Diffuse large B-cell lymphoma (DLBCL) is a highly heterogeneous disease and the most prevalent lymphoma in adulthood. Despite the existence of a first-line chemoimmunotherapy regime, approximately one-third of patients remain unresponsive and succumb to the disease, highlighting the need to find novel treatment strategies. In this regard, tumor cells frequently exhibit metabolic reprogramming and become addicted to glutamine, relying on this amino acid and its metabolism to fulfill their bioenergetic and biosynthetic demands, and to maintain homeostasis. This dependency on glutamine becomes a vulnerability that can be exploited therapeutically. Taking this into account, the aim of this study was to investigate the dependence of DLBCL cells on glutaminolysis, as well as exploring the effects and potential of targeting the enzyme glutaminase-1 (GLS1) for the treatment of DLBCL.

In the present study, we could show that GLS1 is robustly expressed in multiple DLBCL cell lines. Accordingly, we demonstrated that both pharmacological inhibition and genetic knockdown of GLS1 induce cell death in DLBCL cells independent of their subtype classification and genetic characteristics. Conversely, primary human B-cells remained refractory to this treatment. Interestingly, GLS1 inhibition provoked a stark decrease in common tricarboxylic acid cycle (TCA) intermediaries and, most importantly, significantly increased the levels of cytosolic and mitochondrial reactive oxygen species (ROS). We noticed that the accumulation of ROS upon glutaminase inhibition in DLBCL cells can be partially attributed to the decrease in reduced glutathione (GSH) levels. In this context, we demonstrated that supplementation with a membrane-permeable form of α-ketoglutarate or with the potent antioxidant α-tocopherol recovered the pool of reduced GSH, attenuated oxidative stress and abrogated the cytotoxicity caused by GLS1 inhibition. Moreover, we examined the effects of combining the GLS1 inhibitor CB-839 with the Bcl-2 inhibitor ABT-199 and observed that this combination not only increases ROS production dramatically, but also induces DLBCL cytotoxicity in a synergistic manner. Collectively, our data defines the crucial role of glutaminolysis for the survival of DLBCL cells through the

maintenance of redox homeostasis and highlight the potential of targeting GLS1 and Bcl-2 simultaneously for the treatment of DLBCL patients.

Kapitel 1

Zusammenfassung

Das diffuse große B-Zell-Lymphom (DLBCL) ist eine hochgradig heterogene Erkrankung und das häufigste Lymphom in Erwachsenen. Trotz des Vorhandenseins einer Erstbehandlung in Form einer Chemotherapie-Immuntherapie, reagieren etwa ein Drittel der Patienten nicht darauf und erliegen der Krankheit. Dies unterstreicht die Notwendigkeit, neue Behandlungsstrategien zu finden. In diesem Zusammenhang zeigen Tumorzellen häufig eine Umstellung des Stoffwechsels und werden abhängig von Glutamin. Dadurch sind sie auf die Aminosäure und ihre Verstoffwechselung angewiesen, um ihre bioenergetischen und biosynthetischen Anforderungen zu erfüllen und die Homöostase aufrechtzuerhalten. Diese Abhängigkeit von Glutamin wird zu einer Schwachstelle, die therapeutisch genutzt werden kann. Vor diesem Hintergrund hatte die vorliegende Studie zum Ziel, die Abhängigkeit von DLBCL-Zellen von der Glutaminolyse zu untersuchen, sowie die Auswirkungen und das Potenzial der gezielten Hemmung des Enzyms Glutaminase-1 (GLS1) zur Behandlung von DLBCL zu erforschen.

In der vorliegenden Studie konnten wir zeigen, dass GLS1 in mehreren DLBCL-Zelllinien stark exprimiert wird. Entsprechend konnten wir nachweisen, dass sowohl die pharmakologische Hemmung als auch die genetische Abschaltung von GLS1 den Zelltod in DLBCL-Zellen unabhängig von ihrer Subtyp-Klassifizierung oder ihren genetischen Merkmalen auslösen. Im Gegensatz dazu blieben primäre humane B-Zellen unempfindlich gegenüber dieser Behandlung. Interessanterweise führte die Hemmung von GLS1 zu einem deutlichen Rückgang der Tricarbonsäurezyklus- (TCA-) Zwischenprodukte und vor allem zu signifikant erhöhten Mengen an reaktiven Sauerstoffspezies (ROS) im Zytosol und in den Mitochondrien. Wir stellten fest, dass die Akkumulation von ROS durch die Hemmung der Glutaminase in DLBCL-Zellen teilweise auf den Rückgang der reduzierten Glutathion- (GSH-) Mengen zurückzuführen ist. In diesem Zusammenhang konnten wir nachweisen, dass eine membranpermeable Form von α-Ketoglutarat oder das starke Antioxidans α-Tocopherol den Pool an reduziertem GSH wiederherstellte, oxidativen Stress abschwächte und die durch die Hemmung von GLS1 verursachte Zytotoxizität aufhob.

Darüber hinaus untersuchten wir die Auswirkungen der Kombination des GLS1-Inhibitors CB-839 mit dem Bcl-2-Inhibitor ABT-199 und stellten fest, dass diese Kombination nicht nur die ROS-Produktion dramatisch erhöht, sondern auch die DLBCL-Zytotoxizität in synergistischer Weise induziert.

Zusammenfassend zeigen unsere Daten eine entscheidende Rolle der Glutaminolyse für das Überleben von DLBCL-Zellen durch die Aufrechterhaltung der Redox- Homöostase und unterstreicht das Potenzial, GLS1 und Bcl-2 gleichzeitig als Ziel für die Behandlung von DLBCL-Patienten anzustreben.

1 Introduction

1.1 Non-Hodgkin lymphoma

Non-Hodgkin lymphoma (NHL) is the most common hematological malignancy worldwide and comprises a heterogeneous group of cancers that originate from lymphocytes and manifest predominantly in the lymph nodes (Armitage et al., 2017; Bowzyk Al-Naeeb et al., 2018). The classification of NHL is complex, since each lymphoma subtype differs widely in terms of cell of origin, molecular characteristics, pathogenesis and prognosis. The great majority of NHLs arise from B lymphocytes, with only 10-15% deriving from NK and T lymphocytes. This diverse group of malignancies ranges from more indolent or low-grade subtypes, such as follicular lymphoma (FL), to the more aggressive diffuse large B-cell lymphoma (DLBCL) (Bowzyk Al-Naeeb et al., 2018; Shankland et al., 2012; Staudt & Dave, 2005). Studies have defined a series of risk factors that promote the development of NHL including immunosuppression, infection by human immunodeficiency virus (HIV), Epstein-Barr virus (EBV), human herpes virus (HPV)-8 or *Helicobacter pylori*, each of which is associated with the development of a specific lymphoma subtype (Armitage et al., 2017; Singh et al., 2020; Staudt & Wilson, 2002). Lymphomagenesis occurs mainly due to defects during normal B-cell development in the germinal center. During the germinal center reaction, B cells undergo two DNA modifications: somatic hypermutation of their immunoglobulin variable region that alters their antigen affinity, and class-switch recombination of the immunoglobulin heavy-chain (IgH) (Y. Wang et al., 2020). These physiological modifications can alter the genome of B cells, giving rise to gene amplifications or deletions, mutations and chromosomal translocations (Lenz & Staudt, 2010; Staudt & Wilson, 2002). In fact, studies have determined the association of specific acquired chromosomal translocations with different lymphoma subtypes. For instance, the t(3;14) translocation, found in FL and DLBCL patients, causes the juxtaposition of the *BCL6* gene on chromosome 3 to the transcriptionally active IgH locus on chromosome 14. Similarly, the t(14;18) translocation, also observed in FL and DLBCL patients, places the anti-apoptotic *BCL2* gene under the control of IgH locus enhancers, thereby causing apoptosis resistance in these cells. In Burkitt lymphoma (BL) the translocation t(8;14) joins *MYC* with the IgH locus, thereby causing c-Myc overexpression that leads to unchecked cell proliferation, while in

mantle cell lymphomas (MCL) it is common to find cyclin D1 overexpression due to translocation of *CCND1* in chromosome 11 to the IgH locus in chromosome 14 (t(11;14)), leading to a deregulation of the cell cycle (Armitage et al., 2017; Lenz & Staudt, 2010; Nogai et al., 2011; Staudt & Dave, 2005; Zeppa & Cozzolino, 2017). The survival rate for NHL has increased in the past years with the introduction of immunotherapies. However, since the incidence of NHL is on the rise and certain subtypes still exhibit high mortality rates, there is an impending need for novel treatment strategies (Singh et al., 2020; Thandra et al., 2021).

1.2 Diffuse large B-cell lymphoma

Diffuse large B-cell lymphoma is the most common and aggressive type of B-cell lymphoma in adults, accounting for 30-40% of all newly diagnosed NHL cases (Mamgain et al., 2022; Rosenwald et al., 2002; Schneider et al., 2011). The standard-of-care first-line treatment for DLBCL patients, known as R-CHOP, consists of an anthracycline-based chemotherapy regimen that includes cyclophosphamide, hydroxydaunorubicin, oncovin (vincristine sulfate) and prednisone (CHOP), combined with the anti-CD20 monoclonal antibody rituximab (Lenz & Staudt, 2010; Roschewski et al., 2014). More than half of DLBCL patients achieve complete remission following standard treatment. However, approximately 30% do not respond to initial treatment or relapse and eventually succumb to the disease, underlying the need to find novel treatment strategies (Roschewski et al., 2014). DLBCL is characterized by being a highly heterogeneous disease regarding its pathogenesis and clinical outcome (Martelli et al., 2013; Nogai et al., 2011; Rosenwald et al., 2002; Schneider et al., 2011; Staudt & Dave, 2005). In this context, gene-expression profiling allowed for the distinction of three molecular subtypes based on the cell of origin (COO): germinal center B-cell-like (GCB)-DLBCL, activated B-cell-like (ABC)-DLBCL and primary mediastinal B-cell lymphoma (PMBC), with the GCB and ABC subtypes accounting for 80% of all DLBCL cases (Alizadeh et al., 2000; Küppers, 2005; Lenz & Staudt, 2010; Nogai et al., 2011; Schneider et al., 2011; G. Wright et al., 2003). These subtypes have distinctive gene expression signatures, exhibit different processes of malignant transformation, and differ in their prognosis, with the ABC subtype being more prone to remain unresponsive. Survival has been proved to be partially determined by the

gene expression signature, with those characteristic of germinal center B cells or with a stromal-1 signature being associated with better outcomes (Lenz, Wright, Dave, et al., 2008; Rosenwald et al., 2002). Other attempts at classifying DLBCL have relied on clustering methods, in which consensus clusters (CC) are defined by similar transcriptional profiles. In this case, DLBCLs were divided into three distinct subgroups, namely oxidative phosphorylation (OxPhos)-DLBCL, enriched in genes involved in oxidative phosphorylation, B-cell receptor (BCR)/proliferation (BCR)-DLBCL, characterized by enrichment in cell-cycle-related genes, and a third and final subgroup named host response (HR)-DLBCL, enriched in genes related with T-cell immune responses (Caro et al., 2012; Monti et al., 2005).

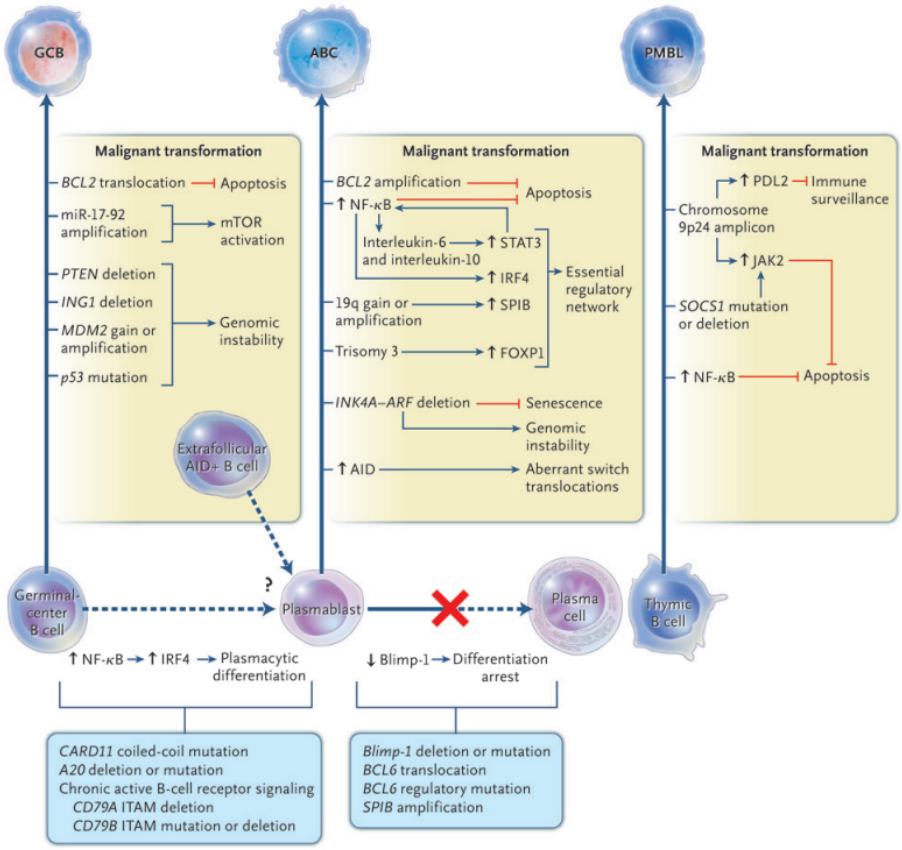

Figure 1.1 Oncogenic pathways of the three DLBCL subtypes. Diffuse large B-cell lymphoma can be classified into three distinct molecular subtypes based on the cell of origin: the germinal center B-cell-like (GCB) subtype, the activated B-cell-like (ABC) subtype and primary mediastinal B-cell lymphoma (PMBL). These subtypes originate from different stages of B-cell differentiation and exhibit distinct genetic lesions that drive malignant transformation. AID, activation-induced cytidine deaminase; ITAM, immunoreceptor tyrosine-based activation motifs; mTOR, mammalian target of rapamycin; and NF-κB, nuclear factor-κB. Obtained from (Lenz & Staudt, 2010).

However, the most recent studies have focused on classifying DLBCL into distinct genetic subtypes based on shared genetic abnormalities, including recurrent mutations, somatic copy number alterations, structural variations, and characteristic gene signatures (Chapuy et al., 2018; Schmitz et al., 2018; G. W. Wright et al., 2020). Furthermore, these genetic subtypes of DLBCL underscore the existence of distinct immune microenvironments within each category and their vulnerabilities towards specific targeted therapies. The first attempts at classifying DLBCL in this manner resulted in the identification of four or five prominent genetic subsets or subtypes, depending on the clustering method and genomic analysis used. One research group identified four genetic subtypes based on common genetic aberrations, namely the MCD, BN2, N1 and EZB subtypes, whereas another study was able to identify five robust clusters (C1-C5) based on genetic driver alterations (Chapuy et al., 2018; Schmitz et al., 2018). Each one of these clusters resembles the distinct subtypes identified in the former study (Schmitz et al., 2018). For instance, the MCG subtype, characterized by the co-occurrence of $MyD88^{L265P}$ and CD79B mutations, is closely related to the C5 subset, also exhibiting frequent mutations in MyD88 and CD79B.
Based on the latter genetic classification, there are two genetically distinct GCB DLBCL-related clusters (C3 and C4), two ABC DLBCL clusters (C1 and C5), and an ABC/GCB DLBCL cluster (C2). The DLBCLs classified as C3 or C4 (characteristic of GCB DLBCLs) harbor mutations affecting *BCL2* and chromatin modifiers, as well as mutations leading to *PTEN* downregulation or loss. DLBCLs identified as belonging to the C1 or C5 subset (ABC DLBCL-related clusters) sustain mutations that affect *BCL2*, *MALT1*, *MYD88*, *CD79B*, *PRMD1*, as well as NOTCH2 or BCL6 signaling, and generally, any NF-κB pathway member which is frequently mutated in ABC DLBCL, such as *BCL10* and *TNFAIP3*. Finally, the fifth cluster, C2, corresponds to DLBCLs which harbor frequent inactivation of *TP53*, and often exhibit loss of *CDKN2A* and *RB1* (Chapuy et al., 2018).

The most recent attempt at genetic subclassification allowed for the identification of seven subtypes based on genetic features that differ with respect to activated oncogenic pathways, gene expression profile, immune microenvironment, survival rates and best therapeutic options (G. W. Wright et al., 2020). The characteristics of these seven genetic subtypes are schematically presented in Figure 1.2.

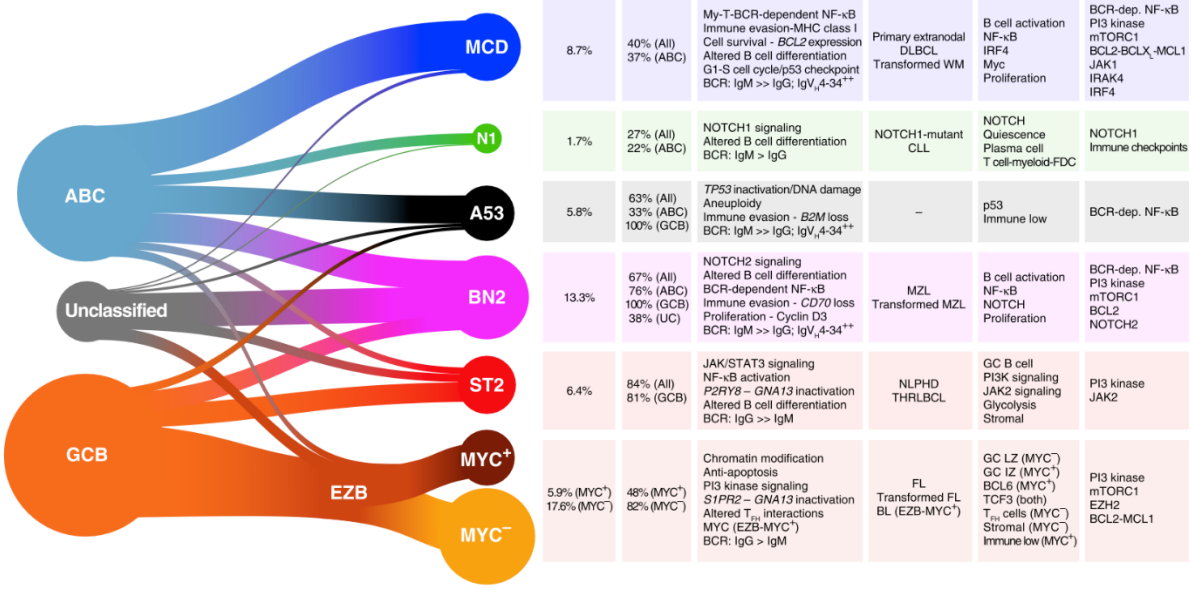

	Prevalence	5-yr overall survival	Genetic themes	Genetically related lymphomas	Gene expression signatures	Potential therapeutic targets
MCD	8.7%	40% (All) 37% (ABC)	My-T-BCR-dependent NF-κB Immune evasion-MHC class I Cell survival - *BCL2* expression Altered B cell differentiation G1-S cell cycle/p53 checkpoint BCR: IgM >> IgG; $IgV_H4\text{-}34^{++}$	Primary extranodal DLBCL Transformed WM	B cell activation NF-κB IRF4 Myc Proliferation	BCR-dep. NF-κB PI3 kinase mTORC1 BCL2-BCLX$_L$-MCL1 JAK1 IRAK4 IRF4
N1	1.7%	27% (All) 22% (ABC)	NOTCH1 signaling Altered B cell differentiation BCR: IgM > IgG	NOTCH1-mutant CLL	NOTCH Quiescence Plasma cell T cell-myeloid-FDC	NOTCH1 Immune checkpoints
A53	5.8%	63% (All) 33% (ABC) 100% (GCB)	*TP53* inactivation/DNA damage Aneuploidy Immune evasion - *B2M* loss BCR: IgM >> IgG; $IgV_H4\text{-}34^{++}$	–	p53 Immune low	BCR-dep. NF-κB
BN2	13.3%	67% (All) 76% (ABC) 100% (GCB) 38% (UC)	NOTCH2 signaling Altered B cell differentiation BCR-dependent NF-κB Immune evasion - *CD70* loss Proliferation - Cyclin D3 BCR: IgM >> IgG; $IgV_H4\text{-}34^{++}$	MZL Transformed MZL	B cell activation NF-κB NOTCH Proliferation	BCR-dep. NF-κB PI3 kinase mTORC1 BCL2 NOTCH2
ST2	6.4%	84% (All) 81% (GCB)	JAK/STAT3 signaling NF-κB activation *P2RY8 – GNA13* inactivation Altered B cell differentiation BCR: IgG >> IgM	NLPHD THRLBCL	GC B cell PI3K signaling JAK2 signaling Glycolysis Stromal	PI3 kinase JAK2
EZB	5.9% (MYC^+) 17.6% (MYC^-)	48% (MYC^+) 82% (MYC^-)	Chromatin modification Anti-apoptosis PI3 kinase signaling *S1PR2 – GNA13* inactivation Altered T_{FH} interactions MYC (EZB-MYC^+) BCR: IgG > IgM	FL Transformed FL BL (EZB-MYC^+)	GC LZ (MYC^-) GC IZ (MYC^+) BCL6 (MYC^+) TCF3 (both) T_{FH} cells (MYC^-) Stromal (MYC^-) Immune low (MYC^+)	PI3 kinase mTORC1 EZH2 BCL2-MCL1

Figure 1.2. Genetic DLBCL subtypes and their characteristic genetic features and potential therapeutic targets. DLBCL can be genetically classified into seven different subtypes based on frequent genetic aberrations and gene expression signatures, namely MCD, N1, A53, BN2, ST2, EZB-MYC+ and EZB-MYC-. This schematic representation underlines the link between the DLBCL subgroups as defined by COO to the corresponding genetic subtypes. The table on the left exhibits the specific characteristics of each genetic subtype, including prevalence, overall survival, genetic themes, related lymphomas, gene expression signatures and potential therapeutic targets. Dep, dependent; FDC, follicular dendritic cell; LZ, light zone; IZ, intermediate zone. Obtained from (G. W. Wright et al., 2020).

1.2.1 Pathogenesis of germinal center B-cell-like DLBCL

Molecular analyses have permitted the characterization and definition of DLBCL subtypes, each with distinct driver mutations (Reddy et al., 2017). In this regard, GCB DLBCLs are thought to arise from normal germinal center B cells, considering they exhibit a gene-expression profile typical of non-malignant germinal center B cells, continue to undergo somatic hypermutation and frequently show IgH class switch (Lenz & Staudt, 2010; Nogai et al., 2011). It is believed that this expression profile is associated with favorable prognosis and survival rates, with 70-80% of patients achieving complete remission. Even though there are certain genetic abnormalities that are common in more than one DLBCL subset, some are particular to each subtype. In the case of GCB DLBCL, it is frequent to observe translocation events involving *BCL2* and/or *MYC* genes, which lead to malignant transformation through unchecked proliferation and apoptosis evasion (Lenz & Staudt, 2010; Nogai et al., 2011;

Rosenwald et al., 2002; Schneider et al., 2011). Furthermore, it is common to find tumor suppressor genes such as *PTEN* and *TP53* deleted, mutated or repressed, thereby upregulating the phosphatidylinositol-3-kinase (PI3K) pathway (Abubaker et al., 2007; Lenz & Staudt, 2010; Olive et al., 2009). Dysregulated activation of the PI3K pathway further promotes cell survival, proliferation and growth through constitutive activation of AKT and mTORC1 signaling (Olive et al., 2009; Shaffer et al., 2012). Conversely, mutations occurring in genes encoding for epigenetic modifiers such as E1A-binding protein p300 (EP300) or CREB-binding protein (CREBBP) are observed both in ABC and GCB DLBCL (Nogai et al., 2011; Pasqualucci et al., 2011; Shaffer et al., 2012). GCB DLBCL can also be distinguished from the ABC subtype by the lack of chronic active BCR signaling and the independence from the NF-κB pathway to thrive. Furthermore, GCB lymphomas have generally undergone class switch recombination and preferentially express an IgG BCR (Lenz et al., 2007). This IgG isotype has been characterized by producing strong ERK, MAPK and calcium responses that rather promote differentiation, which could render this subtype less aggresive than its ABC DLBCL counterpart, which is characterized by expressing IgM BCR, known to promote proliferation rather than terminal differentiation (Lenz et al., 2007; Ruminy et al., 2011; Shaffer et al., 2012).

1.2.2 Pathogenesis of activated B-cell-like DLBCL

ABC DLBCLs have an expression profile very similar to that of plasma cells, with constitutive activation of NF-κB that increases the expression of the transcription factor interferon regulatory factor 4 (*IRF4*), typical of end stage memory B cells (Davis et al., 2001; Lam et al., 2005; Lenz & Staudt, 2010). Expression of *IRF4* is essential not only for B-cell proliferation, but also to drive B cells towards plasma B-cell differentiation (Klein et al., 2006). However, in the context of ABC DLBCL, acquired mutations impede proper expression of BLIMP1, which blocks full differentiation into plasma cells (Iqbal et al., 2007; Mandelbaum et al., 2010; Pasqualucci et al., 2006; Shaffer et al., 2000). In contrast to the GCB subtype, ABC DLBCLs do not usually undergo class switch recombination; however, they do exhibit high amounts of the enzyme activation-induced cytidine deaminase (AID), which ultimately leads to their IgH genes being heavily mutated (Lenz & Staudt, 2010). Contrary to GCB DLBCL, *BCL2* tends to be overexpressed by amplification of its locus rather than by a translocation event in ABC DLBCLs (Lenz, Wright, Emre, et al., 2008), and the tumor suppressors p16 and

p14ARF are deleted in 30% of the cases, thus leading to cell death resistance (Lenz & Staudt, 2010; Shaffer et al., 2012). Furthermore, they exhibit the highest expression of *MYC,* consistent with their origin from a post-germinal center B-cell and likely partly owing to the constitutive NF-κB activity (Amandine David et al., 2017; Y. Xia & Zhang, 2020). Importantly, 30% of ABC DLBCLs present a dysregulated BCL6 activity due to the t(3;14) translocation (Schneider et al., 2011). Constitutive expression of *BCL6* causes the repression or transactivation of a wide array of genes that ultimately lead to an increase in survival and proliferation, genomic instability and block in B-cell differentiation (Shaffer et al., 2012). Nonetheless, the pathogenic hallmark of ABC DLBCL is the constitutive activation of the NF-κB pathway, which in 20% of the cases is caused by mutations in the B-cell receptor subunits CD79A and CD79B, while in 10% of the cases is originated by activating mutations in the BCR downstream target caspase recruitment domain-containing protein 11 (CARD11) (Davis et al., 2001, 2010; Grondona et al., 2018; Lenz, Davis, et al., 2008; Lenz & Staudt, 2010). Both frequently occurring mutations lead to constitutively active BCR signaling. Gain-of-function mutations in myeloid differentiation primary response gene (88) (*MyD88*) are also frequent in the ABC DLBCL subtype, as well as inactivating mutations in the negative NF-κB regulator A20, which typically coexist with other genetic alterations affecting the NF-κB pathway (Compagno et al., 2009; Knittel et al., 2016; Ngo et al., 2011; Shaffer et al., 2012). Chronic activation of NF-κB not only leads to apoptosis evasion through transcriptional activation of a set of antiapoptotic Bcl2 members, but also promotes survival (Davis et al., 2001). One of the most important mechanisms through which constitutive NF-κB can lead to pro-survival signaling pathways is through the induction of interleukin (IL)-6 and IL-10 expression (Gupta et al., 2012; Hashwah et al., 2019; Lam et al., 2008; Ngo et al., 2011).The secreted cytokines then act in an autocrine and paracrine manner activating Janus kinases in the surface of B cells. JAK1 activation leads to phosphorylation, and thus dimerization, of STAT3 that ultimately induces the activation of a set of genes required for the survival of ABC DLBCL cells (Ding et al., 2008; Lam et al., 2008; J. Yang et al., 2007). The broad genetic lesions observed in ABC DLBCL that converge in constitutive NF-κB activation likely explain the aggressiveness of this DLBCL subtype, due to the induction of antiapoptotic, pro-survival and pro-proliferative genes.

1.3 Antiapoptotic Bcl-2 protein in DLBCL

The Bcl-2 family of proteins, key regulators of the mitochondrial apoptotic pathway, is comprised of three functionally and structurally different subfamilies: (1) the pro-apoptotic executioner proteins Bax and Bak, that directly mediate the mitochondrial outer membrane permeabilization (MOMP) for the release of cytochrome c, (2) the pro-apoptotic BH3-only proteins, which aid in the induction of the MOMP by binding and oligomerizing Bax and Bak or by neutralizing anti-apoptotic family members, and (3) the anti-apoptotic members Bcl-2, Bcl-x_L, Mcl-1, Bcl-w and A1, that sequester the effector proteins (Correia et al., 2015; Shamas-Din et al., 2013). Evading apoptosis is a hallmark of cancer cells, which tend to exhibit an imbalance of pro-apoptotic and anti-apoptotic proteins (Czabotar et al., 2014; Delbridge et al., 2016). The anti-apoptotic member Bcl-2 is frequently dysregulated in DLBCL (Shaffer et al., 2012). For instance, the amplification of the *BCL2* genomic locus is a recurrent lesion in ABC DLBCL patients, causing its overexpression at protein level. Additionally, constitutive NF-κB activation in this lymphoma subtype also leads to *BCL2* upregulation, while more than 30% of GCB DLBCL cases exhibit the previously discussed t(8;14) translocation (Dunleavy & Wilson, 2011; Shaffer et al., 2012). In both scenarios, *BCL2* overexpression is correlated with a poor prognosis and therapy resistance, especially when occurring concurrently with a *MYC* translocation, as observed in double hit lymphomas (Dunleavy, 2014; Hermine et al., 1996; Johnson et al., 2012). However, BH3-mimmetics provide a promising avenue of treatment for DLBCL patients with *BCL2* lesions. Venetoclax (ABT-199), which specifically targets the Bcl-2-BAX or -BAK axis, is among the most promising BH3-mimmetics, owing to the encouraging results observed in multiple clinical trials performed in Bcl-2-driven cancers, including a phase I trial performed in NHL patients (Davids et al., 2014; Kuo et al., 2017; Pan et al., 2014; Peirs et al., 2014; Roberts et al., 2015; Souers et al., 2013).

1.4 Therapeutic strategies targeting DLBCL

As mentioned previously, the introduction of the anti-CD20 monoclonal antibody rituximab to the anthracycline-based chemotherapy regime (CHOP) has managed to greatly increase overall survival (OS) of DLBCL patients and has remained the standard-of-care for more than one decade (Coiffier et al., 2010; Fu et al., 2008;

Pfreundschuh et al., 2011). Subsequent studies investigating the efficacy of modified chemotherapy regimens, such as R-ACVBP or DA-EPOCH-R, showed superiority in terms of event-free survival (EFS), progression-free survival (PFS) and OS, but exhibited high toxicity in older patients or were efficient only in certain DLBCL subtypes, respectively (Récher et al., 2011; Wyndham H. Wilson et al., 2012). Thanks to gene-expression profiling analyses and the discovery of specific genetic lesions driving lymphomagenesis, it is now possible to target these oncogenic pathways for more precise treatment approaches. For instance, targeting of the antiapoptotic protein Bcl-2 could be a promising approach for all DLBCL subsets. In fact, the Bcl-2 inhibitor venetoclax (ABT-199) has proved to be effective in a variety of B-cell lymphomas and is currently being tested in a phase II clinical trial (Davids et al., 2014; Souers et al., 2013; US National Library of Medicine, 2012). On the other hand, the use of the immunomodulator lenalidomide, which causes DNA synthesis arrest, inhibition of inflammatory cytokine production, a decrease in NF-κB signaling and enhanced antibody-dependent cell-mediated cytotoxicity, led to striking improvements in objective response rate (ORR) and complete responses (CR) when combined with R-CHOP both in GCB and non-GCB DLBCL patients (Camicia et al., 2015). In the case of ABC DLBCLs, an interesting approach is the targeting of specific activating mutations responsible for the constitutive activation of the NF-κB pathway. In this context, the use of proteasome inhibitors such as bortezomib, which blocks the degradation of the NF-κB inhibitory member IκBα, showed impressive results in non-GCB-DLBCL cases when combined with DA-EPOCH (Dunleavy et al., 2009; Roschewski et al., 2014; Ruan et al., 2010). Another possibility is to target essential effector molecules downstream of the BCR. In this regard, ibrutinib, a small-molecule inhibitor that targets Bruton tyrosine kinase (BTK), was shown to induce encouraging clinical responses in ABC DLBCL patients with wild-type and mutated CD79B (Advani et al., 2012; Wilson et al., 2012, 2021; Younes et al., 2013). However, BTK inhibitors show no toxicity for cells with *CARD11* mutations. In these cases, inhibitors of MALT1 – an essential component of the CARD11-BCL10-MALT1 signaling hub that is required for NF-κB activation – make promising targeted agents for the treatment of ABC DLBCLs (Camicia et al., 2015; Fontan et al., 2012; Fontán & Melnick, 2013; Hailfinger et al., 2009, 2011). Protein kinase C β-type (PKC-β), a serine/threonine kinase essential in propagating BCR signaling, is of relevance in B-cell malignancies and is highly expressed in refractory DLBCL (Camicia et al., 2015). In this regard,

Enzastaurin, a selective inhibitor of PKC-β, has shown promising results in DLBCL patients, achieving a 1-year PFS of 71% (Riihijärvi et al., 2010; Robertson et al., 2007; Roschewski et al., 2014). In the case of GCB DLBCLs, the frequent loss of *PTEN* correlates with the constitutive activation of the PI3K pathway, making targeting of this kinase or of downstream effectors very attractive (Roschewski et al., 2014). Consequently, development of inhibitors targeting downstream effectors of this pathway are currently underway. However, preliminary studies with the mTOR inhibitors everolimus and temsirolimus demonstrated modest activity across several DLBCL subtypes (Smith et al., 2010; Witzig et al., 2011). Other potentially effective inhibitors targeting the frequently deregulated c-Myc and Bcl-6 are being examined at present (Roschewski et al., 2014). However, the significant molecular heterogeneity of DLBCL makes it complicated to design and develop drugs that could be beneficial for several DLBCL subtypes at once, and thus, for a high number of patients. This makes targeting of metabolic pathways, that are likely altered in multiple lymphoma subtypes, attractive in terms of novel treatment strategies. On this matter, targeting of the enzyme glutaminase (GLS) has been proved effective in several different hematological and solid tumors, making it a potential candidate for DLBCL treatment.

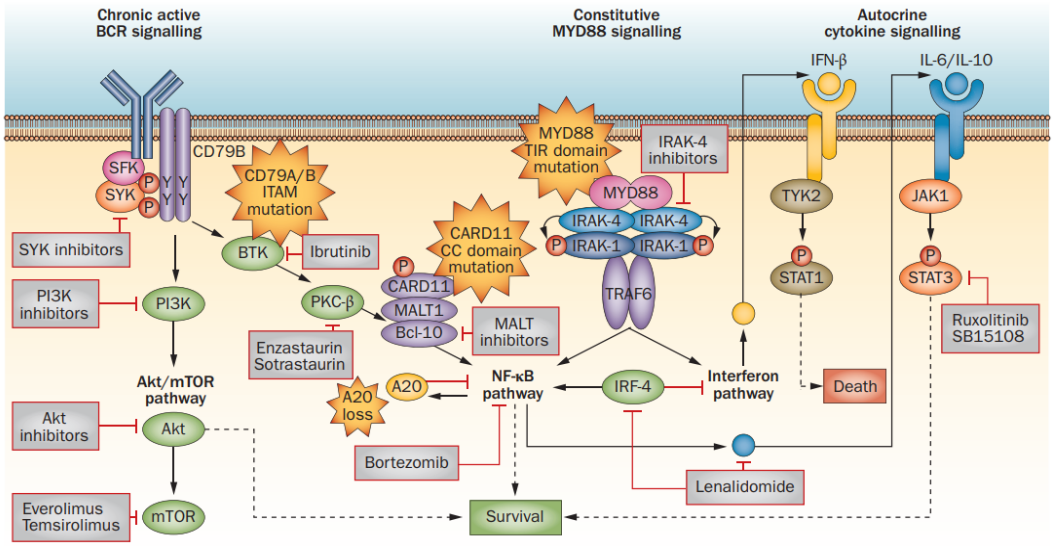

Figure 1.3. Key deregulated intracellular signaling pathways in ABC DLBCL and novel targeted agents. Constitutive activation of the NF-κB pathway is a hallmark of ABC DLBCL and can be achieved by several oncogenic mechanisms. Inhibitors such as ibrutinib, enzastaurin, SYK inhibitors and PI3K inhibitors target tyrosine kinases crucial in chronic active BCR signaling. Targeting of downstream effectors with bortezomib, a proteasome inhibitor, or lenalidomide, which downregulates IRF4, have also shown efficacy against ABC DLBCL. Abbreviations: Bcl-10, B-cell lymphoma/leukemia 10; BTK, Bruton's tyrosine kinase; CARD11, caspase recruitment domain-containing protein 11; IFNβ, interferon β; IRAK-4, interleukin-1

receptor-associated kinase 4; IRF-4, interferon regulatory factor 4; JAK, Janus activating kinase; mTOR, mammalian target of rapamycin; PKCβ, protein kinase C β; SFK, Src family kinase; STAT, signal transducer and activator of transcription; SYK, spleen tyrosine kinase; TRAF6, TNF receptor associated factor 6; TYK2, tyrosine kinase 2. Obtained from (Roschewski et al., 2014).

1.5 Glutamine metabolism and its role in cancer

Glutamine is the most abundant amino acid in the blood and it is indispensable for the survival of highly proliferative cells (Curi R. et al., 2007; Yoo et al., 2020). It belongs to a group of amino acids that are considered *conditionally* essential, meaning that in physiological conditions it can be readily synthesized *de novo* by the action of glutamine synthetase. However, under pathological conditions, glutamine consumption increases dramatically, to the point where the rate at which it can be synthesized cannot fulfill the energy requirements of the cells (Lacey & Wilmore, 1990; Lukey et al., 2013; Yoo et al., 2020). In fact, fast-proliferating cancer cells tend to become addicted to glutamine, relying on this amino acid to support the biosynthetic, bioenergetic and homeostatic needs for cell growth and division (Masisi et al., 2020; Zhang et al., 2017). Many tumor types have been reported to undergo apoptosis upon depletion of this amino acid, owing to its key role in a wide range of cellular functions and pathways (T. Nguyen & Durán, 2018).

1.5.1 Role of glutamine as a carbon and nitrogen donor

Glutamine is an indispensable donor of reduced nitrogen required for *de novo* synthesis of purine and pyrimidine bases, the building blocks of nucleic acids, thereby directly supporting cell growth and division (T. Nguyen & Durán, 2018; Zhang et al., 2017). Apart from being utilized for the synthesis of nucleotides, the γ-nitrogen of glutamine is used to produce other non-essential amino (NEAA) acids via the action of aminotransferases. Similarly, glutamine-derived carbons are essential for the synthesis and maintenance of amino acid pools in the cells, generating up to 50% of the intracellular NEAAs and being one of the most important molecules for cellular biogenesis (Altman et al., 2016; Hosios et al., 2016; Yoo et al., 2020). More importantly, glutamine-derived glutamate is catabolized either by glutamate dehydrogenase (GLUD) or transaminases to produce α-ketoglutarate (α-KG), an essential metabolic

intermediary that fuels the tricarboxylic acid (TCA) cycle for the generation of ATP via generation of NADH and $FADH_2$ equivalents (DeBerardinis et al., 2007; van der Heiden et al., 2009). Cancer cells can thus exploit glutamine-derived α-KG for anaplerosis of the TCA cycle, and thus, cover for the increased bioenergetic demands (T. Nguyen & Durán, 2018; Zhang et al., 2017). Glutamine-derived α-KG can also be reduced by a process termed reductive carboxylation in hypoxic conditions through consumption of NADPH to generate citrate, which is required for the synthesis of fatty-acids (Metallo et al., 2012; R. C. Sun & Denko, 2014; L. Yang et al., 2017). Altogether, many cancer cells rely heavily on glutamine consumption not only for energy generation, but also for biomass accumulation through the synthesis of the building blocks required for macromolecule production.

1.5.2 Role of glutamine in gene expression regulation

Albeit in an indirect manner, intermediaries derived from glutamine metabolism can alter gene expression through the regulation of chromatin organization. In this context, glutamine-derived α-KG serves as a co-substrate for dioxygenase enzymes from the TET and Jumonji-C domain-containing family, which catalyze histone and DNA demethylation (Abla et al., 2020; T. Nguyen & Durán, 2018; Tsukada et al., 2006). On the other hand, glutamine-derived metabolites can be a substrate for acetyl-CoA generation through the process of reductive carboxylation. Considering histone acetylation depends on intermediary metabolism to supply acetyl-CoA, glutamine can ultimately play a role in global histone acetylation and alteration of gene expression (Teperino et al., 2010; C. Yang et al., 2014). In summary, cancer cells might exploit glutamine metabolism for chromatin structure modification, which could lead to histone hypermethylation and repression of tumor suppressor and differentiation-related genes.

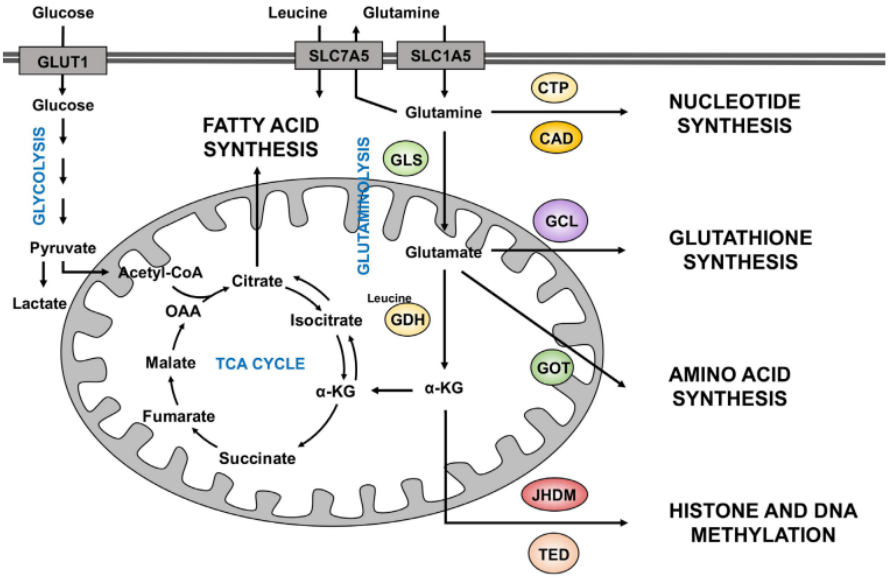

Figure 1.4. Roles of glutamine in the cell. After import into the cells through the SLC1A5 transporter, glutamine is converted to glutamate by glutaminase, thereby aiding in the synthesis of glutathione. It is further converted into α-ketoglutarate, which enters the TCA cycle to produce energy for the cell or participates in fatty acid synthesis via reductive carboxylation. Glutamine-derived α-ketoglutarate also regulates DNA and histone methylation serving a co-substrate of dioxygenase enzymes. Moreover, glutamine metabolism also contributes in nucleotide and amino acid synthesis. CAD: carbamoyl-phosphate synthetase 2 aspartate transcarbamylase, and dihydroorotase; CTP: CTP synthetase; GCL: glutamate-cysteine ligase; GDH: glutamate dehydrogenase; GOT: glutamate-oxaloacetate transaminase; JHMD: Jumonji C histone demethylases; TED: TET DNA demethylases. Obtained from (T. Nguyen & Durán, 2018).

1.5.3 Role of glutamine in the induction of signaling pathways

Apart from its anaplerotic functions and influence in gene expression via epigenetic modifications, glutamine can orchestrate growth promoting intracellular signaling events. The mTOR kinase complex, for instance, can sense amino acid availability, including glutamine, thereby becoming activated. Once active, mTOR will promote protein translation, autophagy regulation, fatty acid synthesis and cell growth (Nicklin et al., 2009). In this context, glutamine is exported out of the cytoplasm by the antiporter LAT1/SLC7A5 allowing for the influx of leucine, an amino acid capable of activating mTOR (Lukey et al., 2013; T. Nguyen & Durán, 2018). Furthermore, recent studies have demonstrated that glutamine can directly activate mTOR in a Rag GTPase-independent manner (Meng et al., 2020). Additionally, a recent study provided evidence that glutamine can directly activate STAT3, a transcription factor particularly important in the mediation of ABC DLBCL proliferation and survival (Cacace et al., 2017). Other transcription factors whose activity can be regulated by glutamine include

hypoxia-inducible factor-1 (HIF-1) and c-Myc, which also regulate metabolism and promote cell growth and proliferation (Dejure et al., 2017; Yoo et al., 2020).

1.5.4 Glutamine metabolism and redox homeostasis

Tumor cells rely on moderate levels of reactive oxygen species (ROS) to support pro-tumorigenic signaling. However, cancer cells tend to generate excessive levels of ROS that can damage macromolecules such as proteins, lipids and nucleotides, ultimately triggering apoptosis (Nakamura & Takada, 2021; Panieri & Santoro, 2016). Glutamine can mitigate ROS levels through synthesis of the antioxidant molecule glutathione (GSH) (Altman et al., 2016; Lukey et al., 2013; T. Nguyen & Durán, 2018; Yoo et al., 2020; Zhang et al., 2017). Glutathione is a tripeptide comprised of glutamate, cysteine and glycine, that can scavenge peroxide free radicals (Franco & Cidlowski, 2009; Roth et al., 2002). As a matter of fact, glutamine availability is the rate-limiting step for glutathione synthesis, since its catabolism is required for the provision of the amino acid components comprising GSH (Gong et al., 2022; Masisi et al., 2020). Furthermore, glutamine aids in the production of the reducing equivalent NADPH, which essential for the restoration of reduced GSH via at least two different metabolic pathways (Masisi et al., 2020; T. Nguyen & Durán, 2018). One of these pathways depends on the glutaminase-driven conversion of glutamine into glutamate, which is subsequently metabolized into α-ketoglutarate via the action of GLUD while concomitantly reducing $NADP^+$ to NADPH (Botman et al., 2014). On the other hand, the other pathway involves the action of aspartate aminotransferase (GOT1), which metabolizes glutamine-derived aspartate into oxaloacetate (OAA). OAA is thereafter reduced to malate by malate dehydrogenase 1 (MDH1), which is then converted into pyruvate through the action of malic enzyme 1 (ME1), generating NADPH in the process (Son et al., 2013; Ying et al., 2021). All in all, glutamine metabolism contributes to the maintenance of redox homeostasis by providing the intermediaries required for the synthesis of antioxidant molecules to scavenge free radicals.

1.6 Glutaminase

Glutamine plays a role in a wide range of cellular functions, many of which require its catabolism in order to provide for metabolic precursors. Glutaminase is the key enzyme

in glutamine metabolism and hydrolyzes its conversion to glutamate and ammonia (Masisi et al., 2020; L. Yang et al., 2017). Glutamate is subsequently catabolized into α-KG, which can fuel the TCA cycle and generate further metabolic intermediaries. Glutaminase exists as two different isozymes: kidney-type glutaminase (GLS), which has been extensively studied, and liver-type glutaminase (GLS2 or LGA). Even though both glutaminase isoforms are encoded by different genes localized in different chromosomes, their catalytic domains align nearly identically (Katt et al., 2017). Kidney-type glutaminase is encoded by the *GLS* gene and can be expressed as three different splice variants: a longer form called kidney glutaminase (KGA), a shorter version called glutaminase C (GAC) and a significantly shorter catalytically inactive version known as GAM. KGA and GAC are practically identical except for their C-terminal region, which is shorter in GAC, while their N-terminal region is conserved and is responsible for their localization to the mitochondria (Katt et al., 2017; Márquez et al., 2016). The liver-type glutaminase, encoded by the *GLS2* gene, also exists as three transcriptional variants that differ at their N-terminus. GLS exists either as a dimer or as a tetramer, but its oligomerization is not required for full catalytic activity. Rather, they require phosphate for their activation and to increase their catalytic activity (Katt et al., 2017). These enzymes have a key role particularly in highly proliferative cells to enable the use of glutamine as a biosynthetic precursor and energy source (Marquez et al., 2015).

While GLS is widely accepted as a tumor promoter, the role of GLS2 is unclear, having been suggested to act as a tumor suppressor or a tumor promoter depending on the cancer type (Katt et al., 2017; Marquez et al., 2015; Márquez et al., 2016; Matés et al., 2018; Saha et al., 2019). Regarding its role as a tumor suppressor, GLS2 expression is almost completely abolished in several tumor types, including glioblastoma, gastric cancer and hepatocellular carcinoma (Lukey et al., 2013; Suzuki et al., 2022; Szeliga M. et al., 2009; L. Xu et al., 2020). Further findings showed that its expression is regulated by a group of tumor suppressors and stress-related proteins including p53, p63 and p73 (Márquez et al., 2016). Additionally, owing to the observed role of GLS2 in protecting from oxidative-stress-induced apoptosis and DNA damage, its overexpression in the T98G glioblastoma or H1299 non-small cell lung carcinoma cell lines induced significant reductions in cell growth and survival, further supporting that GLS2 repression is a trait associated with tumorigenesis (W. Hu et al., 2010; Suzuki

et al., 2010, 2022). Finally, a study demonstrated that ectopic expression of GLS2 in a HCC xenograft model significantly reduced tumor size by promoting ferroptosis, a form of cell-death that relies on an iron-dependent accumulation of lipid peroxides (Suzuki et al., 2022). Nevertheless, despite these findings, it is important to point out that in some instances GLS2 has been observed to function as a tumor promoter (Lukey et al., 2019). Considering the dual roles of GLS2, pharmacological targeting of GLS1 seems the more promising option for cancer treatment (X. Xu et al., 2019).

1.6.1 The role of glutaminase in cancer

Glutaminase has emerged as a critical player in the progression of several cancer types, and its expression and activity have been observed to be increased in several tumors through different mechanisms (Márquez et al., 2016; Matés et al., 2018; L. Yang et al., 2017). For instance, NF-κB and c-Myc, both of which are frequently deregulated in tumor cells including DLBCL, can indirectly prompt *GLS* upregulation through repression of the microRNA (miRNA)-23 (Gao et al., 2009; Rathore et al., 2012). On the other hand, c-Jun can directly bind the *GLS* promoter thereby enhancing its expression (Lukey et al., 2016). Overexpression of *GLS* in tumor cells can be a sign of metabolic reprogramming and can be indicative of glutamine addiction. In this context, a study reported that both *GLS1* as well as the glutamine transporter *ASCT2* are found upregulated in multiple myeloma (MM) cases. In this setting, targeting of GLS1 with the inhibitor GLS-IN-968 induced growth inhibition and apoptosis of MM cells, as well as *MYC* loss through proteasomal degradation, thereby impeding pathogenesis of a pre-malignant cell line *in vivo* (Effenberger et al., 2017). Similarly, Myc-induced HCC tumors in mice exhibited *GLS* overexpression (B. Li et al., 2019). Strikingly, loss of only one copy of *GLS* was enough to decrease cell proliferation, tumor burden and increase survival (B. Li et al., 2019). Likewise, treatment of the B-cell lymphoma cell line P493 with the GLS inhibitor BPTES (bis-2-(5-phenylacetamido-1,2,4-thiadiazol-2-yl) ethyl sulfide) led to DNA replication arrest, cell death and fragmentation, and was enough to diminish tumorigenesis in a B-cell lymphoma xenograft (Xiang et al., 2015). Additionally, c-Myc has been shown to be deregulated both in colorectal cancer (CRC), due to alterations in the WNT pathway, as well as in ovarian carcinoma. A study on CRC showed that glutamine deprivation caused a reversible cell cycle arrest, decreased the levels of ATP and caused stalling of RNA polymerase II on multiple genes (Dejure et al., 2017). Interestingly, supplementation

with a membrane permeable form of α-KG (DM-KG) or adenosine was enough to rescue cell proliferation and survival. Comparably, in ovarian carcinoma cell lines, *MYC* overexpression positively correlated with high *GLS* expression and increased GSH levels. Glutaminase inhibition in this context provoked an increase in ROS that could be abrogated with supplementation of DM-KG and the antioxidant N-acetylcysteine (NAC) (Shen et al., 2020). Excessive ROS were also observed in acute myeloid leukemia and pancreatic adenocarcinoma (PDAC) cell lines after treatment with the GLS inhibition CB-839 or glutamine deprivation, respectively (Gregory et al., 2019; Zhang et al., 2019). Altogether, the role of glutamine in providing intermediaries for the replenishment of the TCA cycle, nucleic acid synthesis, ATP generation and redox homeostasis seems to be essential for the survival of multiple tumor entities, making GLS1 inhibition an attractive treatment strategy.

1.7 c-Myc in DLBCL and glutamine metabolism

MYC is an oncogene found frequently deregulated in several malignancies including DLBCL (L. Nguyen et al., 2017; Schaub et al., 2018). It encodes for a transcription factor that forms heterodimers with the related protein MAX. These heterodimers bind to promoters of already transcriptionally active genes, thus acting as an activator of pre-existent transcriptional programs. *MYC* modulates the expression of genes related with cell growth and proliferation, DNA replication, protein biosynthesis, metabolism, angiogenesis and stem-cell self-renewal (Meyer & Penn, 2008). A paradoxical function of c-Myc is the induction of apoptosis. Owing to this role, alterations in the expression of *MYC* alone are not enough to induce tumorigenesis. Hence, *MYC* lesions require the presence of other oncogenic alterations to induce malignant transformation (L. Nguyen et al., 2017). In this regard, 7-14% of DLBCL patients exhibit *MYC* translocations usually in the context of complex karyotypes accompanied by *BCL2* and/or *BCL6* translocations (Dunleavy, 2014; Ladanyi et al., 1991). These double or triple hit lymphomas carry dismal prognoses (Nowakowski & Czuczman, 2015). An interesting function of c-Myc in human malignancies is its role as a regulator of metabolism. Tumor cells undergo a metabolic shift in order to fulfill their bioenergetic and biosynthetic needs by performing aerobic glycolysis (a phenomenon known as the Warburg effect), and/or becoming addicted to glutamine (vander Heiden et al., 2009).

Myc plays an important role in the latter through distinct mechanisms. On the one hand, Myc has been shown to promote the expression of the glutamine transporters SLC1A5 (ASCT2), SN2 and SLC38A5, thereby enhancing its uptake (Wise et al., 2008; Zhao et al., 2019). Furthermore, studies on the B-cell lymphoma line P493 and on prostate cancer (PCa) cell lines proved that c-Myc can directly affect GLS1 protein levels by post-transcriptional regulation. This is mediated by direct repression of miR-23a and miR-23b, thereby increasing the expression of GLS1 protein and enhancing glutaminolysis (Gao et al., 2009). Interestingly, glutamine itself can alter c-Myc expression. A recent study provided evidence indicating that glutamine deprivation suppresses translation of endogenous c-Myc by provoking a reduction in adenosine-nucleotide levels in the CRC cell line HCT116 (Dejure et al., 2017). Furthermore, a study on multiple myeloma showed that loss of GLS1 expression was related with decrased c-Myc protein levels via proteasomal degradation (Effenberger et al., 2017). All in all, the current state of findings suggests that *MYC*-driven malignancies exhibit a glutamine-addicted phenotype through the upregulation of glutamine uptake and catabolism. Knowing that *MYC* is one of the most prevalently altered genes in NHL and that it is correlated with a poor prognosis, the question arises whether DLBCL require exogenous glutamine for survival and whether targeting of glutamine metabolism could be a potential therapeutic strategy in this context.

1.8 Aims of the study

DLBCL, the most common B-cell lymphoma in adulthood, represents a highly heterogeneous disease that can be classified into multiple subtypes depending on the genetic characteristics and gene expression profiles. Some DLBCL subtypes are characteristically aggressive and tend to remain refractory to the existing standard-of-care, known as R-CHOP, thus highlighting the need for novel therapeutic strategies. Multiple tumors reprogram their metabolism during malignant transformation and become addicted to glutamine, relying on it to maintain homeostasis. Glutaminase, the enzyme responsible for the conversion of glutamine to glutamate, is overexpressed in a variety of tumors and is associated with poor prognosis, thereby identifying it as a promising therapeutic target. Accordingly, investigating the expression of GLS1 in several DLBCL subtypes and the effects of targeting this enzyme in this tumor entity, is pivotal to uncover its therapeutic potential in DLBCL patients.

Therefore, the aims of the study were to:

- Investigate the expression of GLS in DLBCL cells to determine whether it is a potential druggable target.
- Determine whether c-Myc expression in DLBCL cells correlates with GLS1 expression and expose any underlying dependences between the two.
- Elucidate the effects of inhibiting GLS1 in DLBCL and the therapeutic potential of glutaminolysis inhibitors for lymphoma treatment, as well as their mechanisms of action.
- Uncover synergistic therapeutic combinations between GLS1 inhibitors and other approved or experimental substances that have previously shown efficacy in lymphoma.

2 Results

2.1 Effects of glutaminase-1 inhibition in DLBCL

Previous studies have demonstrated that GLS1 plays a pro-tumorigenic role and is upregulated in multiple tumors, while GLS2 expression is correlated with differentiated cell states and can act as a tumor suppressor (Katt et al., 2017; Márquez et al., 2016). To address the question whether GLS1 inhibitors could potentially be used as therapeutic agents for the treatment of DLBCL, we first analyzed the expression of both GLS1 and GLS2 in different DLBCL cell lines and explored the effects of inhibiting glutaminase-1.

2.1.1 GLS1 and GLS2 expression in DLBCL cell lines

To determine whether GLS1 could be a potential target in the treatment of diffuse large B-cell lymphoma, we first examined the protein expression of GLS1 and GLS2 by immunoblotting in a variety of cell lines spanning various DLBCL subtypes. Both isoforms were detected at protein level in all cell lines tested independent of their classification as ABC or GCB DLBCL (Fig. 2A). However, while we did not detect any distinctive pattern regarding GLS2 expression, ABC DLBCL cell lines exhibited an increase in GLS1 expression when compared to their GCB DLBCL counterparts. Studies have reported that c-Myc levels are associated with GLS1 expression, suggesting the existence of a feedback regulatory mechanism between the two (Dejure et al., 2017; Effenberger et al., 2017). However, despite the increase in GLS1 expression observed in ABC DLBCL cell lines, this did not correlate with an increase in c-Myc protein levels (Fig. 2A). These findings suggest that DLBCLs could potentially be sensitive to GLS1 inhibition and that glutaminase does not influence c-Myc expression in these cell lines.

2.1.2 Glutaminolysis regulation via c-Myc in DLBCL cell lines

c-Myc is known to increase not only glutamine uptake, but also its metabolism via induction of glutaminase-1 expression (Gao et al., 2009; Zhao et al., 2019). To evaluate whether c-Myc controls GLS1 expression in DLBCL, both ABC and GCB DLBCL cells were treated with the Brd4 inhibitor JQ1, known to downregulate *MYC* expression (Otto et al., 2019; Pang et al., 2022; Zuber et al., 2011). Even though JQ1 treatment led to

a decrease in c-Myc protein levels in all cell lines tested, GLS1 levels remained unaltered (Fig. 2B), indicating that glutaminase-1 expression is not controlled by c-Myc in DLBCL cell lines.

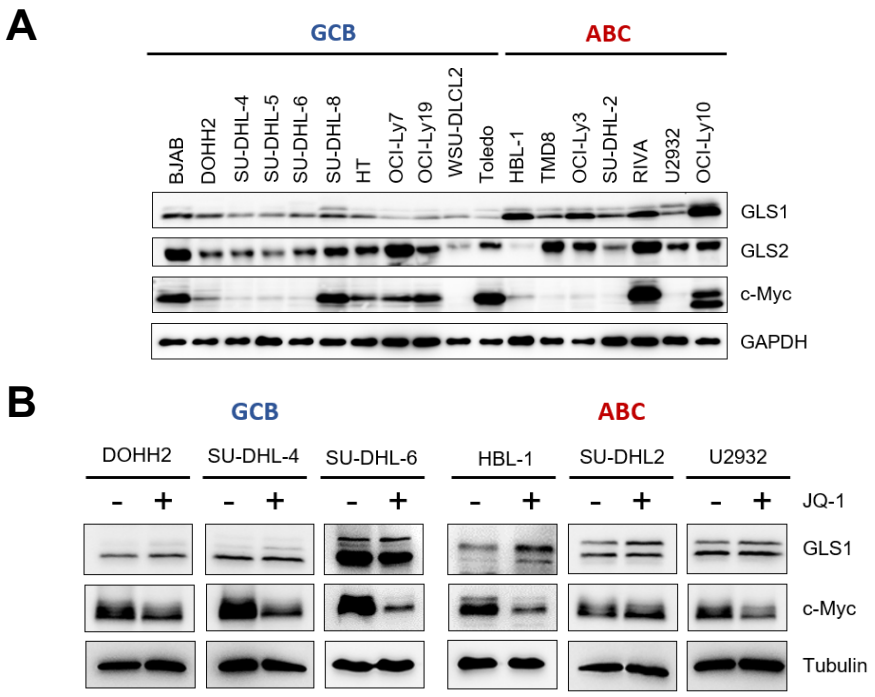

Figure 2. GLS1 and GLS2 expression in human DLBCL cell lines. (A) GLS1, GLS2 and c-Myc protein expression in various ABC and GCB DLBCL cell lines was analyzed by immunoblotting. GAPDH served as loading control. **(B)** GLS1 and c-Myc protein expression was analyzed by immunoblotting in various ABC and GCB DLBCL cell lines treated with solvent or 1 µM JQ1 for 24 h. Tubulin served as loading control.

2.1.3 DLBCL cell survival depends on GLS1 activity

Knowing that GLS1 is expressed in multiple DLBCL cell lines, we investigated whether inhibition of this enzyme could affect the survival of lymphoma cells. For this purpose, ABC and GCB DLBCL cell lines were treated with the selective GLS1 inhibitor CB-839 (Telaglenastat) for six consecutive days. Interestingly, the survival of all cell lines tested was markedly reduced in the presence of CB-839 (Fig. 3). To further validate the cytotoxicity of GLS1 inhibition and exclude potential CB-839 side effects, cells were treated with a different selective glutaminase-1 inhibitor known as BPTES (bis-2-(5-phenylacetamido-1,3,4-thiadiazol-2-yl) ethyl sulfide). Similar to CB-839, BPTES managed to reduce the survival of ABC DLBCL and GCB DLBCL cell lines (Fig. 4A). To investigate the cause of the CB-839-mediated reduction in cell numbers, we performed a cell-cycle analysis and assessed apoptosis induction via flow cytometry. Interestingly, treatment with CB-839 did not provoke a cell-cycle arrest in DLBCL cells,

albeit a modest increase in the percentage of cells in the G0/G1 phase could be detected (Fig. 4B). However, CB-839 treatment for 24 h was enough to significantly increase the number of 7-AAD/AnnexinV-double positive cells, thus indicating that glutaminase-1 inhibition induces apoptotic cell death in DLBCL cell lines (Fig. 4C). These results suggest that DLBCL cells are dependent on the activity of glutaminase-1 for survival.

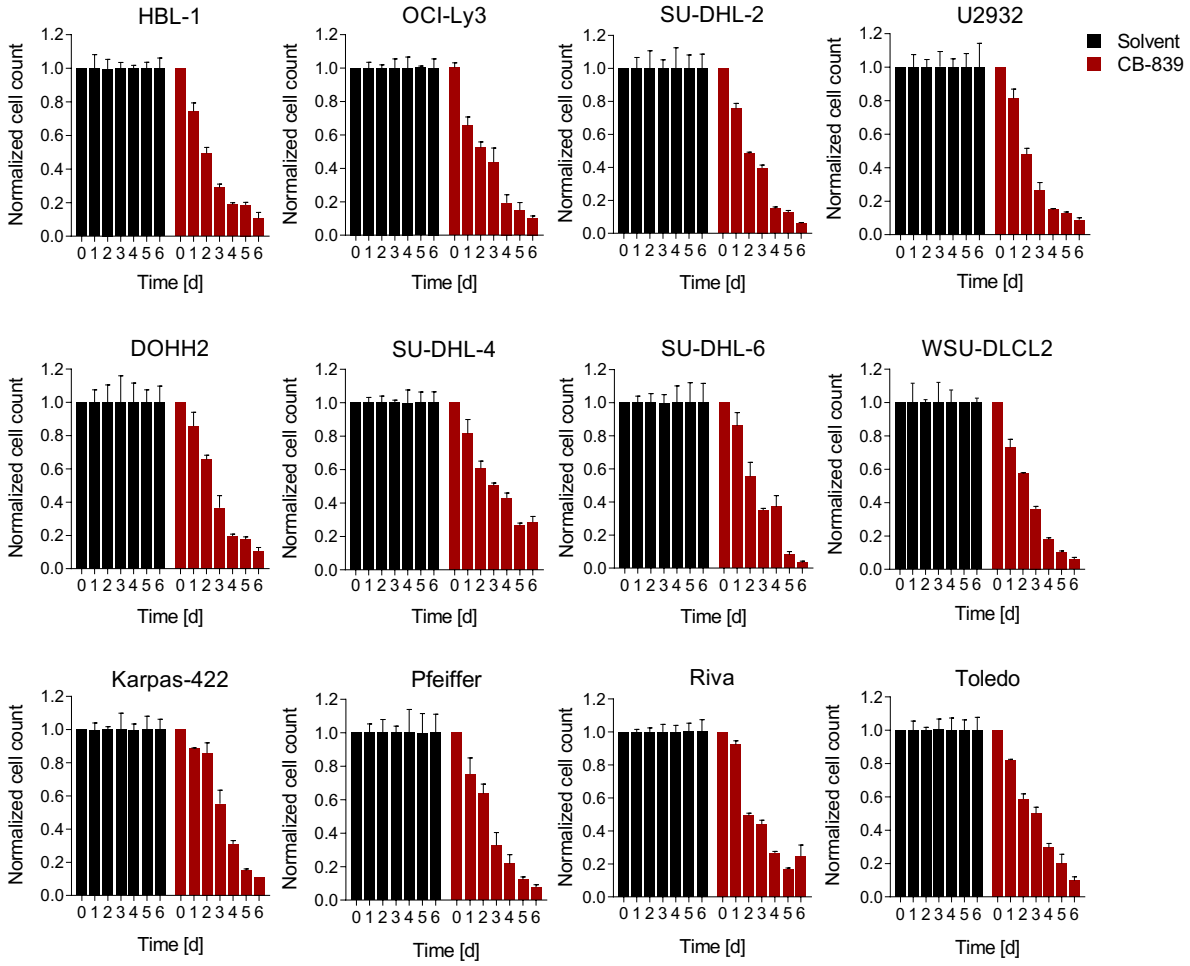

Figure 3. CB-839 induces cytotoxicity in DLBCL. Various ABC DLBCL and GCB DLBCL cell lines were treated daily with solvent or 400 nM CB-839 and incubated for the indicated time. Cell numbers were determined daily and normalized to the solvent control. Error bars correspond to the mean ± SD. Data is representative of at least three independent experiments.

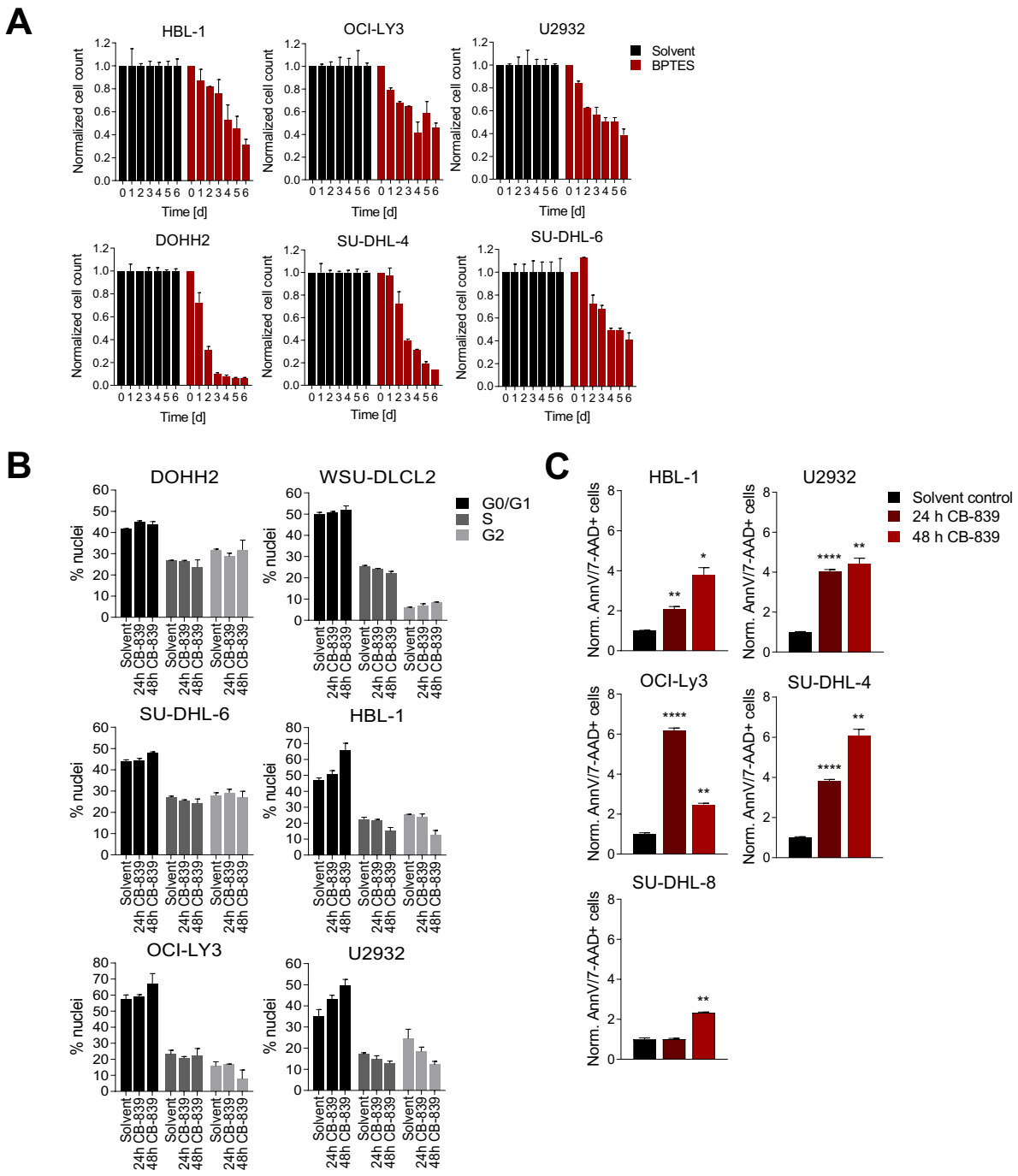

Figure 4. GLS1 inhibition triggers apoptosis in DLBCL cells. (A) ABC and GCB DLBCL cell lines were treated daily with solvent or 1 μM BPTES. Cell numbers were determined as indicated and normalized to the solvent control. **(B)** ABC and GCB DLBCL cell lines were treated with solvent or 400 nM CB-839 for 24 or 48 h. Graphs show the relative distribution of cells in the different phases of the cell cycle. Solvent-treated cells were used as controls. **(C)** ABC and GCB DLBCL cells were treated with solvent or 400 nM CB-839 for 24 or 48h. The relative percentage of apoptotic cells was analyzed by flow cytometry using Annexin-V/7-AAD staining. Solvent-treated cells were used as control for normalization. Error bars correspond to the mean ± SD. Data is representative of at least three **(A-C)** independent experiments. *p* values were calculated by *t* test (unpaired, two tailed), $*p < 0.05$, $**p < 0.01$, $***p < 0.001$, ****p<0.0001.

2.1.4 GLS1 silencing and glutamine deprivation affect DLBCL survival

To exclude possible side effects from the GLS1 inhibitors, we investigated whether glutaminase-1 silencing via small hairpin RNA (shRNA) mediated knock-down also impacted DLBCL survival. As expected, GLS1 silencing decreased cell numbers independent of the DLBCL subtype (Fig. 5A-B). Similarly, deprivation of glutamine from the culture medium led to cytotoxicity both in ABC and GCB DLBCL cells (Fig. 5C). These results indicate that the cytotoxic effects observed are specifically dependent on the inhibition of glutamine metabolism and are not caused by side effects derived from the use of GLS inhibitors.

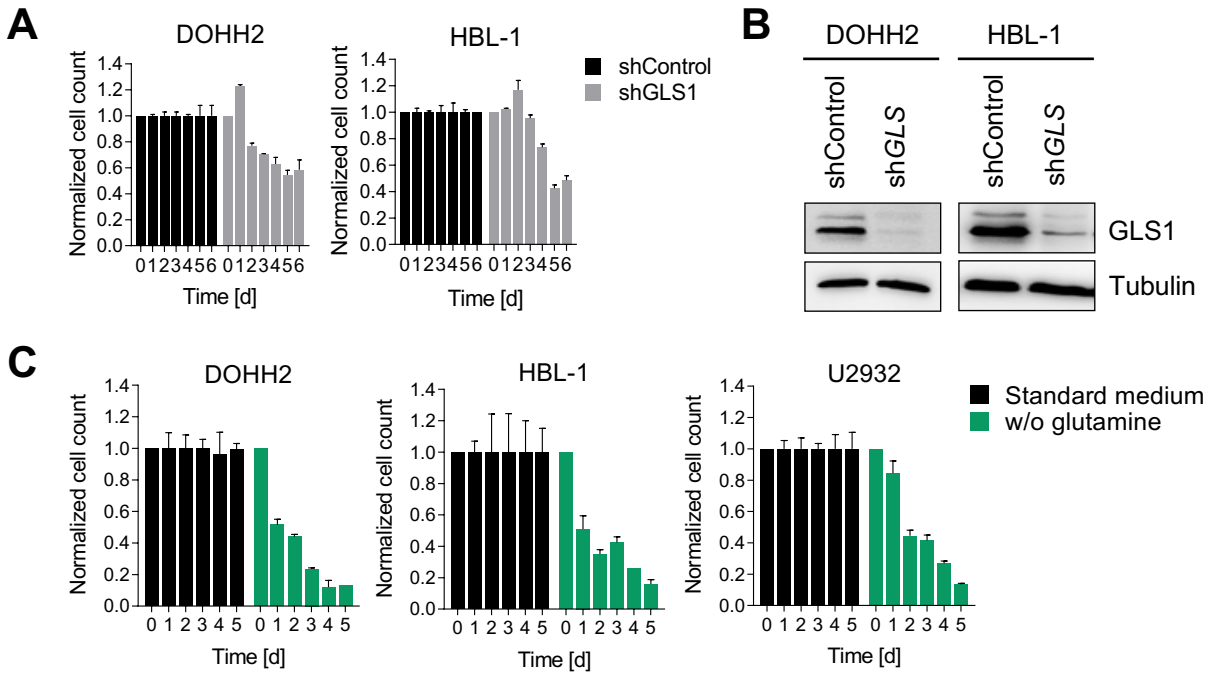

Figure 5. Glutaminolysis inhibition and glutamine deprivation abrogate DLBCL survival. **(A)** DOHH2 and HBL-1 cells were transduced with either a non-targeting vector control or an shRNA targeting *GLS*. After transduction, cell numbers were determined as indicated and normalized to the non-targeting control. **(B)** The efficacy of the shRNA-mediated knockdown of GLS1 in DOHH2 and HBL-1 cells was controlled by immunoblotting. Tubulin served as a loading control. **(C)** ABC and GCB DLBCL cell lines were cultured in standard or glutamine-deprived medium. Cell numbers were determined and normalized to the standard medium control. Error bars correspond to the mean ± SD. Data is representative of three two **(A, C)** independent experiments.

2.1.5 Primary non-transformed B cells are refractory to GLS1 inhibition

When it comes to cancer treatment, it is essential to exploit targets that render tumor cells susceptible to cell death while keeping non-malignant cells unaffected. For this reason, we next evaluated the effects of GLS1 inhibition on primary non-transformed B cells isolated from peripheral blood mononuclear cells (PBMCs). Strikingly, CB-839 treatment did not impair the survival of primary B cells (PBCs) (Fig. 6). Furthermore, phytohemagglutinin (PHA) or IL-4/CD40L-stimulated PBCs remained refractory to CB-839, exhibiting only a slight decrease in cell numbers by day six, thus indicating that only transformed DLBCL cells are sensitive to glutaminase inhibition and rely on glutamine metabolism for survival.

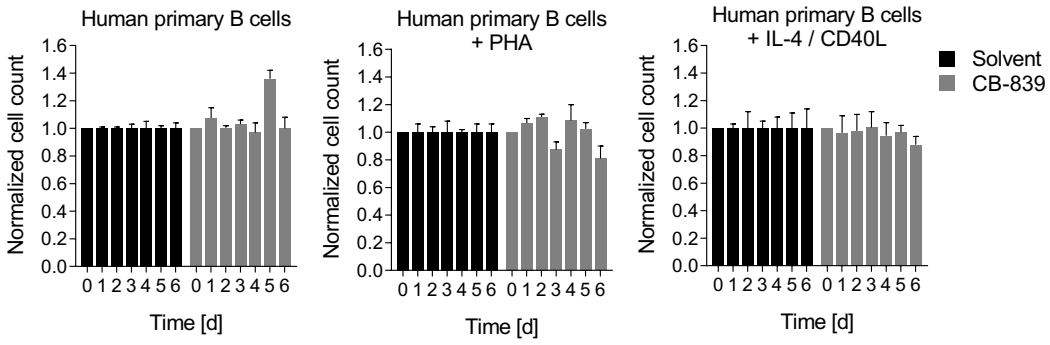

Figure 6. Primary B cells are refractory to CB-839 treatment. Human primary B cells were treated daily with solvent or 400 nM CB-839. Cell numbers were determined daily and normalized to the solvent control. Error bars correspond to the mean ± SD. Data is representative of at least two independent experiments.

2.2 Molecular mechanism of GLS1 inhibition in DLBCL

Glutamine plays a key role in multiple cellular processes and is essential for redox homeostasis, DNA replication, fatty acid and amino acid synthesis, proliferation, metabolism and survival (Z. Wang et al., 2020; L. Yang et al., 2017; Yoo et al., 2020). Hence, the inhibition of glutaminolysis blunts several intracellular pathways and diminishes the abundance of TCA cycle intermediaries that are crucial to fulfill the biosynthetic and bioenergetic needs of cancer cells. Nevertheless, the molecular mechanisms that account for the cytotoxicity observed after glutaminase-1 inhibition in DLBCL cells remain to be elucidated.

2.2.1 Effects of GLS1 inhibition on intracellular signaling pathways and post-translational modifications

To gain insights into the molecular mechanism of CB-839-mediated cytotoxicity, we first explored the protein levels of different kinases known to be activated and important for the survival of DLBCL cells and their phosphorylation state. Immunoblotting revealed that GLS1 inhibition or silencing via shRNA in DLBCLs did not hamper the phosphorylation of ERK, AKT, IκBα or c-Jun (Fig. 7A).

Glutamine has also been shown to regulate signal transduction and act as a signaling molecule to activate intracellular signaling pathways, such as the mTORC pathway (L. Yang et al., 2017). The kinase mTORC1, critical for cell growth and proliferation, has been shown to become activated by directly sensing the presence of glutamine (Meng et al., 2020). Furthermore, glutaminolysis inhibition has been observed to impair mTORC1 activation due to the drop in non-essential amino acid pool (Altman et al., 2016; Hosios et al., 2016). Hence, we next examined the protein levels and phosphorylation of well-known mTORC1 targets after CB-839 treatment in DLBCL cell lines. While rapamycin, a specific mTOR inhibitor, managed to reduce the levels of phosphorylated 4E-BP1 and S6, CB-839 failed to do so (Fig. 7B). All in all, our data confirmed that CB-839 treatment does not impair the activation of multiple kinases important for the proliferation, growth and survival of DLBCLs.

On a different note, glutamine metabolism influences global histone acetylation and methylation in an indirect manner through the supply of essential metabolic intermediaries. One such example is glutamine-derived α-ketoglutarate, which not only regulates the synthesis of TCA cycle substrates but can also act as an epigenetic regulator serving as a cofactor for Jumonji-C containing histone lysine demethylases (Teperino et al., 2010; Tsukada et al., 2006b; W.-H. Yang et al., 2021). On the other hand, glutamine can produce acetyl-CoA via reductive carboxylation, a metabolite that serves as a substrate of histone acetyltransferases (Bradshaw, 2021; C. Yang et al., 2014). Hence, glutamine metabolism could ultimately lead to alterations in the gene expression pattern of cells. Taking this into consideration, we next assessed the capacity of glutaminase to induce changes in the methylation status of two well-known H3 lysine residues. We found that knockdown of GLS1 in ABC DLBCL and GCB DLBCL cell lines did not lower the repressive histone methyl marks in H3K9 and H3K27

that could have explained potential changes in gene expression related with DLBCL survival (Fig. 7C).

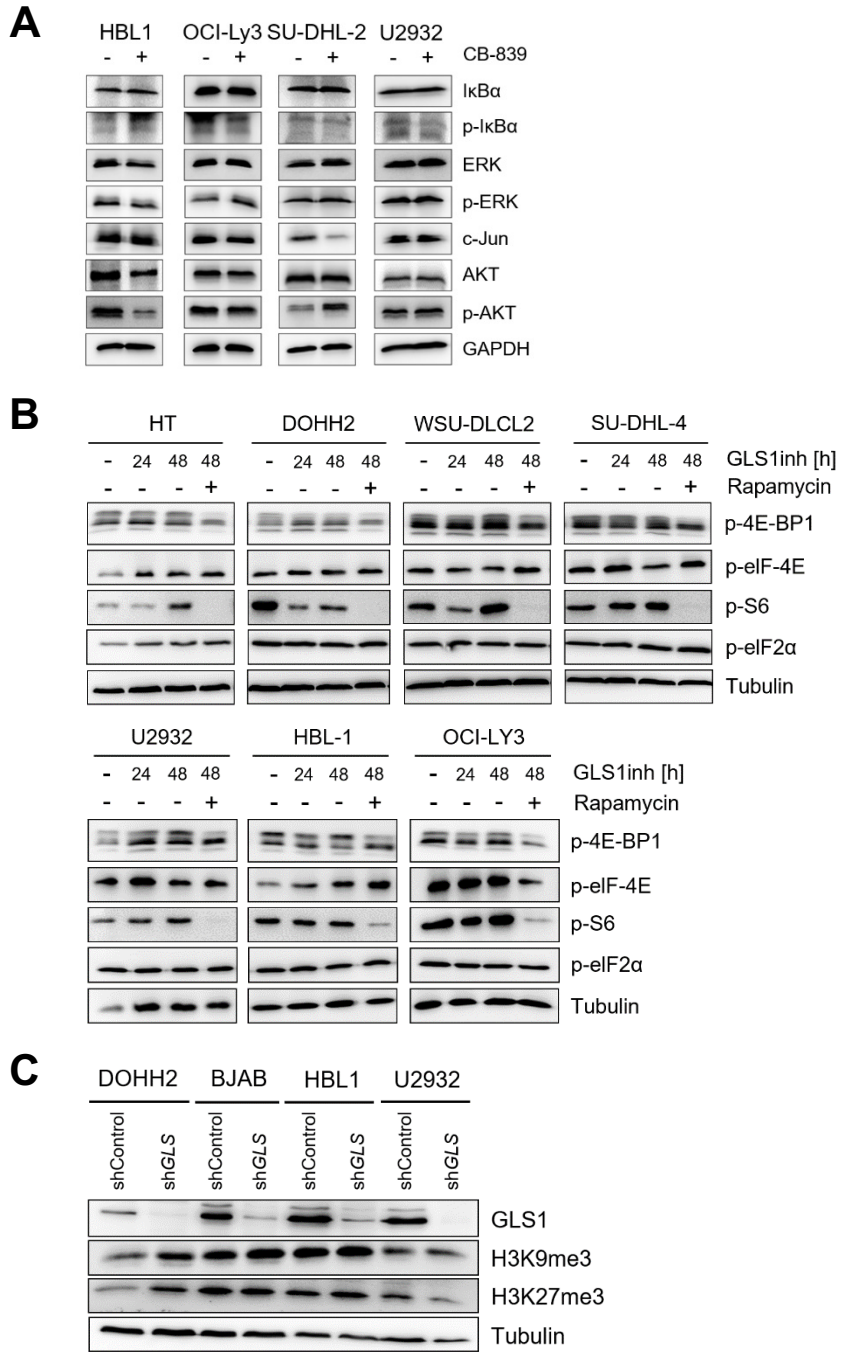

Figure 7. CB-839 does not affect signaling pathways important for DLBCL survival. (A-B) ABC and GCB DLBCL cell lines were treated with solvent or 500 nM CB-839 for 24 h and the phosphorylation of **(A)** central regulators of the NF-kB, MAPK, AP-1 and PI3K signaling pathways and **(B)** mTORC1 downstream targets were analyzed by immunoblotting. Cells were treated with 1 μM rapamycin as a positive control. **(C)** ABC and GCB DLBCL cell lines were transduced either with a non-targeting vector control or an shRNA targeting *GLS*. The methylation status of H3K9 and H3K27 was analyzed by immunoblotting. **(A)** GAPDH served as a loading control. **(B, C)** Tubulin served as loading control.

Characteristically, ABC DLBCL cells exhibit constitutive NF-κB activation which eventually leads to STAT3 phosphorylation via the production and secretion of IL-6 and IL-10, which act in an autocrine and paracrine manner activating Janus kinases (JAKs) (Ding et al., 2008). Interestingly, when examining the activation of STAT3 in CB-839-treated ABC DLBCL cells, it was noted that GLS1 inhibition led to a decrease in STAT3 phosphorylation that could be rescued via addition of exogenous IL-6 and IL-10 (Fig. 8A). ELISAs performed for IL-6 and IL-10 detection revealed a significant decrease in the secretion of both cytokines after 48 h treatment of ABC DLBCL cells with CB-839 (Fig. 8B). All in all, this suggested that the observed decrease in STAT3 activity was a consequence of the lack of autocrine/paracrine stimuli necessary to activate the Janus kinases responsible for the phosphorylation of STAT3, rather than the direct inhibition of STAT3 by CB-839. Knowing that sustained STAT3 activity is essential for the proliferation and survival of ABC DLBCL cells, we questioned whether the observed impairment in survival after glutaminase-1 inhibition was due to the decrease in STAT3 activation after CB-839 treatment. To answer this, we analyzed the viability of ABC DLBCL cells after CB-839 treatment and supplementation of exogenous IL-6 and IL-10, which recover the levels of STAT3 phosphorylation. Notably, ABC DLBCL cell lines remained sensitive to the GLS1 inhibitor despite STAT3 activation (Fig. 8C). For further validation, HBL-1 and U2932 cells were transduced to express a hyperactive STAT3 mutant (STAT3C) and treated with CB-839. These cells, however, continued to undergo cell death in response to GLS1 inhibition (Fig. 8D). Altogether, our data confirmed that the CB-839-mediated inhibition of STAT3 is not responsible for the observed cytotoxicity in ABC DLBCL.

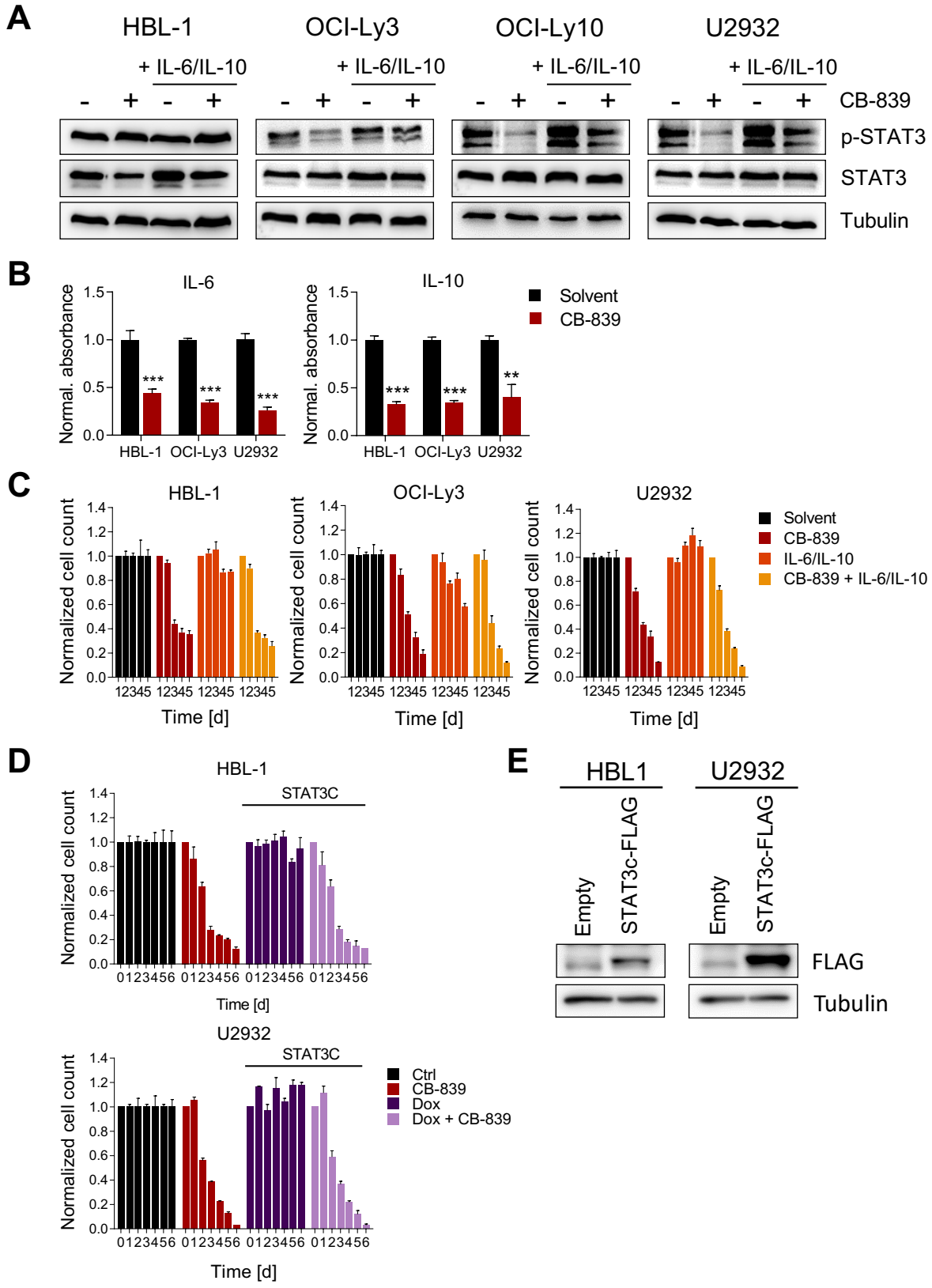

Figure 8. CB-839 reduces IL-6/IL-10 secretion and impairs STAT3 activation. (A) ABC DLBCL cell lines were treated with solvent, 500 nM CB-839 and/or 5 ng/ml rhIL-6 and rhIL-10 as indicated, and the phosphorylation of STAT3 was assessed by immunoblot analysis. **(B)** ABC DLBCL cell lines were treated with solvent or 500 nM CB-839 for 48 h. Secreted IL-6 and IL-10 was quantified by ELISA and normalized to the solvent control. **(C)** HBL-1 and U2932

cells were treated with solvent, 500 nM CB-839 and/or 5 ng/ml rhIL-6 and rhIL-10 as indicated. Cell numbers were determined and normalized to the solvent control. **(D-E)** HBL-1 and U2932 cells expressing control vector or FLAG-STAT3C were treated daily with 1 µg/ml doxycycline. **(D)** The vector control and STAT3C-expressing cells were then treated with solvent or 500 nM CB-839 as indicated. Cell numbers were quantified and normalized to the respective solvent controls. **(E)** The efficacy of the retroviral transduction of STAT3C in HBL-1 and U2932 cells was controlled by immunoblotting. **(A, E)** Tubulin served as loading control. Error bars correspond to the mean ± SD. Data is representative of at least three (**B-C**) or two **(A, D-E)** independent experiments. *p* values were calculated by *t* test (unpaired, two tailed), *$p < 0.05$, **$p < 0.01$, ***$p < 0.001$, ****p<0.0001.

** Retroviral transduction of STAT3C ABC DLBCL cells was kindly performed by Wendan Xu.*

2.2.2 Nucleotide supplementation does not rescue cell viability after GLS1 inhibition

Glutamine is an indispensable donor of reduced nitrogen, required for the synthesis of both purine and pyrimidine bases. The former constitute the building blocks of nucleic acids, and an abundance of these are especially important for highly proliferative cells (L. Yang et al., 2017). Therefore, we investigated whether adenosine supplementation was enough to decrease the toxicity of the GLS1 inhibitor in DLBCL cells. In all cell lines examined, addition of adenosine did not salvage viability (Fig. 9), likely indicating that the role of glutamine as a nitrogen donor is dispensable for the survival of DLBCL cells.

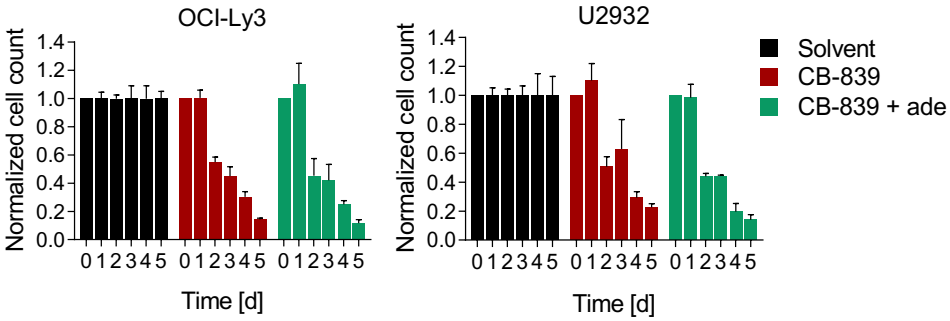

Figure 9. Adenosine fails to protect against CB-839-mediated cell death. ABC and GCB DLBCL cells were treated with solvent or 500 nM CB-839, or in combination with 150 µM adenosine daily. Cell numbers were determined as indicated and normalized to the solvent control. Data is representative of at least three independent experiments. Error bars correspond to the mean ± SD. Data is representative of at least three independent experiments.

2.2.3 The abundance of metabolic intermediaries is diminished upon CB-839 treatment

Highly proliferative cells require continuous replenishing of the TCA cycle and mainly rely on glutamine metabolism to serve as the source of carbons. To verify metabolic alterations after GLS1 inhibition, we analyzed the metabolome of CB-839 treated and control cells. As expected, most of the major TCA cycle intermediaries commonly derived from glutamine metabolism were markedly reduced in DOHH2 and WSU-DLCL2 cells after 24 h CB-839 treatment, while glutamine levels were enriched (Fig. 10A). Glutamate and α-ketoglutarate, two of the main metabolites derived from glutamine, showed reductions of up to 70% when compared to the solvent control (Fig. 10A). Surprisingly, we also noticed a clear decrease in the concentrations of well-characterized intracellular antioxidant molecules such as α-tocopherol, glutathione (GSH) and the reduced form of NADP+ (NADPH) (Fig. 10B). Carbons derived from glutamine metabolism also contribute to ATP production through their oxidation in the TCA cycle, as well as by supporting the oxidative phosphorylation pathway via the electron transport chain (ETC) (DeBerardinis et al., 2007). Accordingly, CB-839 treatment of ABC DLBCL and GCB DLBCL cells provoked a significant decrease in ATP levels, especially after 48 h of glutaminase inhibition (Fig. 10C).

Considering the substantial deprivation of key metabolic intermediaries as a result of GLS1 inhibition, we investigated whether this played a role in the cytotoxic effects observed with CB-839. Supplementation with DM-KG, a membrane permeable form of α-ketoglutarate, resulted in a complete rescue of DOHH2, SU-DHL-2 and SU-DHL-4 cells from the CB-839-mediated cytotoxicity; while achieving a partial rescue in HBL-1, OCI-Ly3, SU-DHL-4 and WSU-DLCL cells (Fig. 11D). Furthermore, addition of DM-KG in glutamine-free medium managed to fully recover the viability of U2932 cells, while partially rescuing DOHH2 and HBL-1 cells (Fig. 11E). The TCA cycle intermediary α-ketoglutarate plays various roles in the cell, from serving as a cofactor for demethylating enzymes, to acting as a precursor for the synthesis of other amino-acids and antioxidant molecules (Abla et al., 2020). Hence, the rescue potential of DM-KG cannot be fully ascribed to its role in the refueling of the TCA cycle. Taking into consideration the previous findings, DM-KG is presumably capable of rescuing DLBCL

from CB-839-mediated cytotoxicity through its capacity to maintain the pool of reducing equivalents.

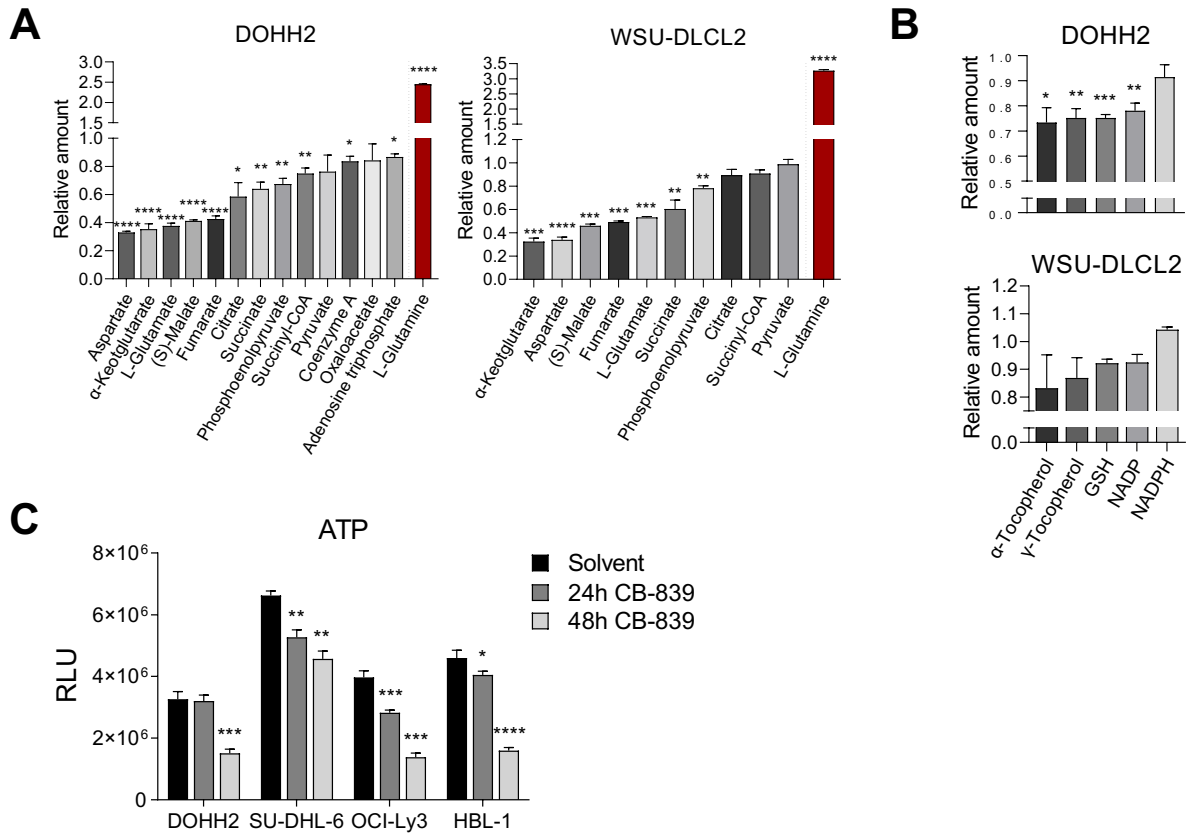

Figure 10. TCA cycle metabolites and antioxidant molecules are reduced upon CB-839 treatment. (A-B) DOHH2 and WSU-DLCL2 cells were treated with solvent or 500 nM CB-839 for 24 h. Metabolites were quantified by mass spectrometry and normalized to the solvent control. **(C)** ABC and GCB DLBCL cell lines were treated with solvent or 500 nM CB-839 for 24 h and 48 h. ATP levels were quantified and normalized to the respective solvent-treated controls. Error bars correspond to the mean ± SD. Data is representative of at least three independent experiments. *p* values were calculated by *t* test (unpaired, two tailed), **p* < 0.05, ***p* < 0.01, ****p* < 0.001, ****p<0.0001, n.s. not significant.

** Mass spectrometry was kindly performed by Dr. Mattia Zmpieri and Laurentz Schuhknecht (ETH Zürich, Switzerland).*

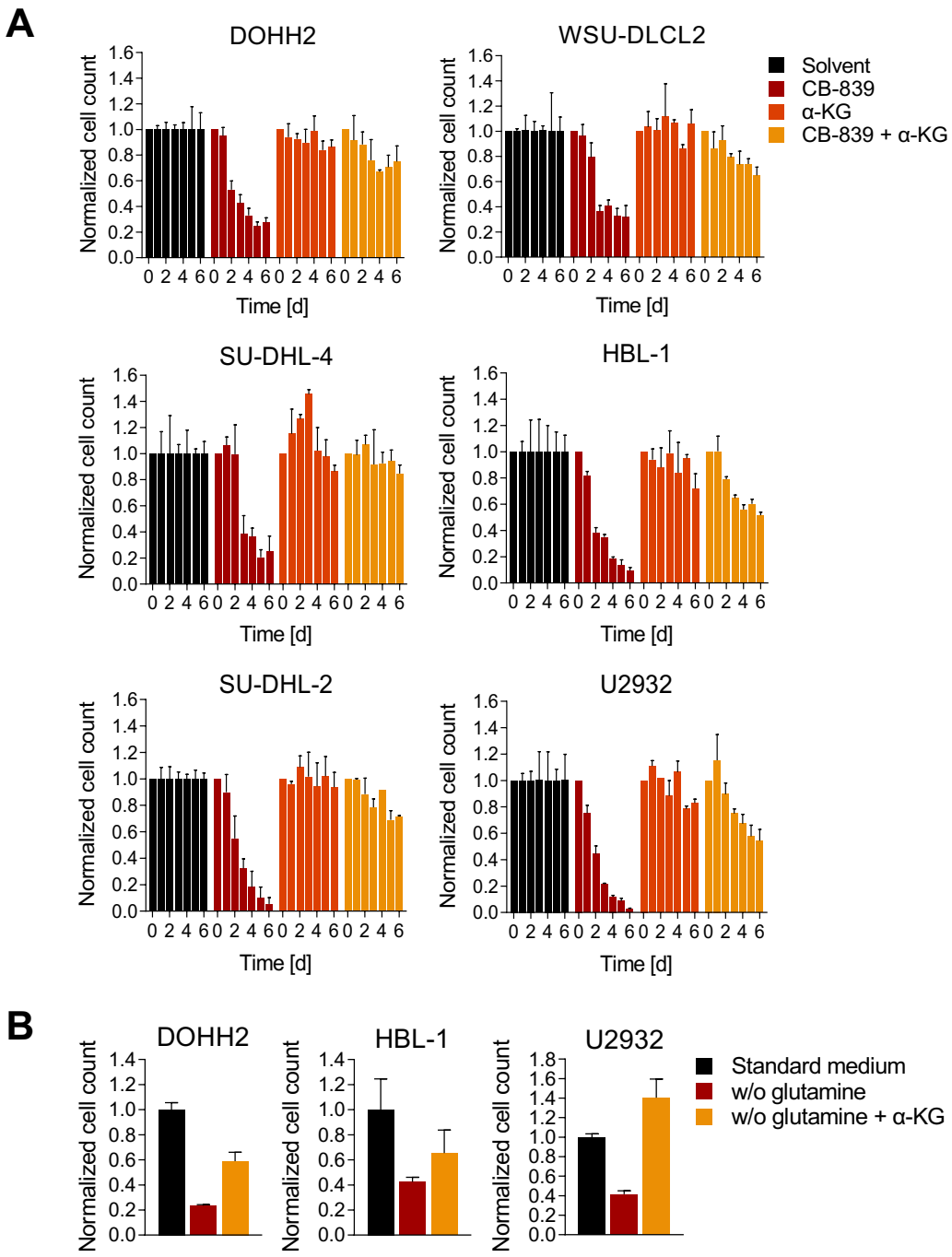

Figure 11. DM-KG protects against CB-839-mediated cell death. (A-D) ABC and GCB DLBCL cells were treated with solvent or 500 nM CB-839 alone or in combination with 0.5 mM DM-KG daily. **(B)** ABC and GCB DLBCL cell lines were cultured in standard or glutamine-deprived medium with or without 0.5 mM DM-KG. **(A-B)** Cell numbers were determined as indicated and normalized to the solvent control. Error bars correspond to the mean ± SD. Data is representative of at least two **(B)** or three **(A)** independent experiments.

2.2.4 GLS1 inhibition provokes oxidative stress in DLBCL

Cells rely on glutamine metabolism to maintain the pool of intracellular antioxidant molecules, such as NADPH and GSH, by providing a source of intermediaries required for their synthesis (T. Nguyen & Durán, 2018; Roth et al., 2002). Knowing that CB-839 treatment caused a stark reduction not only of metabolites such as glutamate, but also of intracellular antioxidants, we investigated the capacity of CB-839 to deplete reduced glutathione. Interestingly, we noticed that GLS1 inhibition effectively reduced the GSH pool, especially in GCB DLBCL cell lines (Fig. 12A). Strikingly, addition of DM-KG reestablished the levels of GSH after CB-839 treatment in all cell lines tested (Fig. 12A). NADPH levels were also analyzed, but results were not consistent amongst the DLBCL cell lines (Fig. 12B). While many of the cells examined exhibited decreases in the pool of reduced NADPH that could be efficiently recovered by DM-KG supplementation, this reduction was only modest (Fig. 12B).

Depletion of GSH typically leads to an accumulation of reactive oxygen species (ROS) due to the inability of the cells to clear these radicals fast enough via other mechanisms. We therefore quantified cytosolic and mitochondrial ROS, as well as lipid peroxidation, by flow cytometry in multiple DLBCL cell lines after treatment with CB-839. Interestingly, treatment for 48 h with a low dose of CB-839 was enough to induce significant increases in ROS, especially those derived from and accumulating in mitochondria (Fig. 12C). Strikingly, GLS1 inhibition also induced lipid peroxidation. However, the increase observed was weak when compared to the effects achieved by DMF treatment, which is a well-known ferroptosis inducer (Fig. 13A). To further assess the correlation between glutamine metabolism and redox homeostasis, we quantified ROS after glutamine deprivation. As expected, the lack of glutamine led to a strong increase in both mitochondrial and cytosolic ROS (Fig. 13B). Collectively, this data confirms that GLS1 inhibition leads to the accumulation of cytosolic and mitochondrial ROS likely through the depletion of the antioxidant GSH.

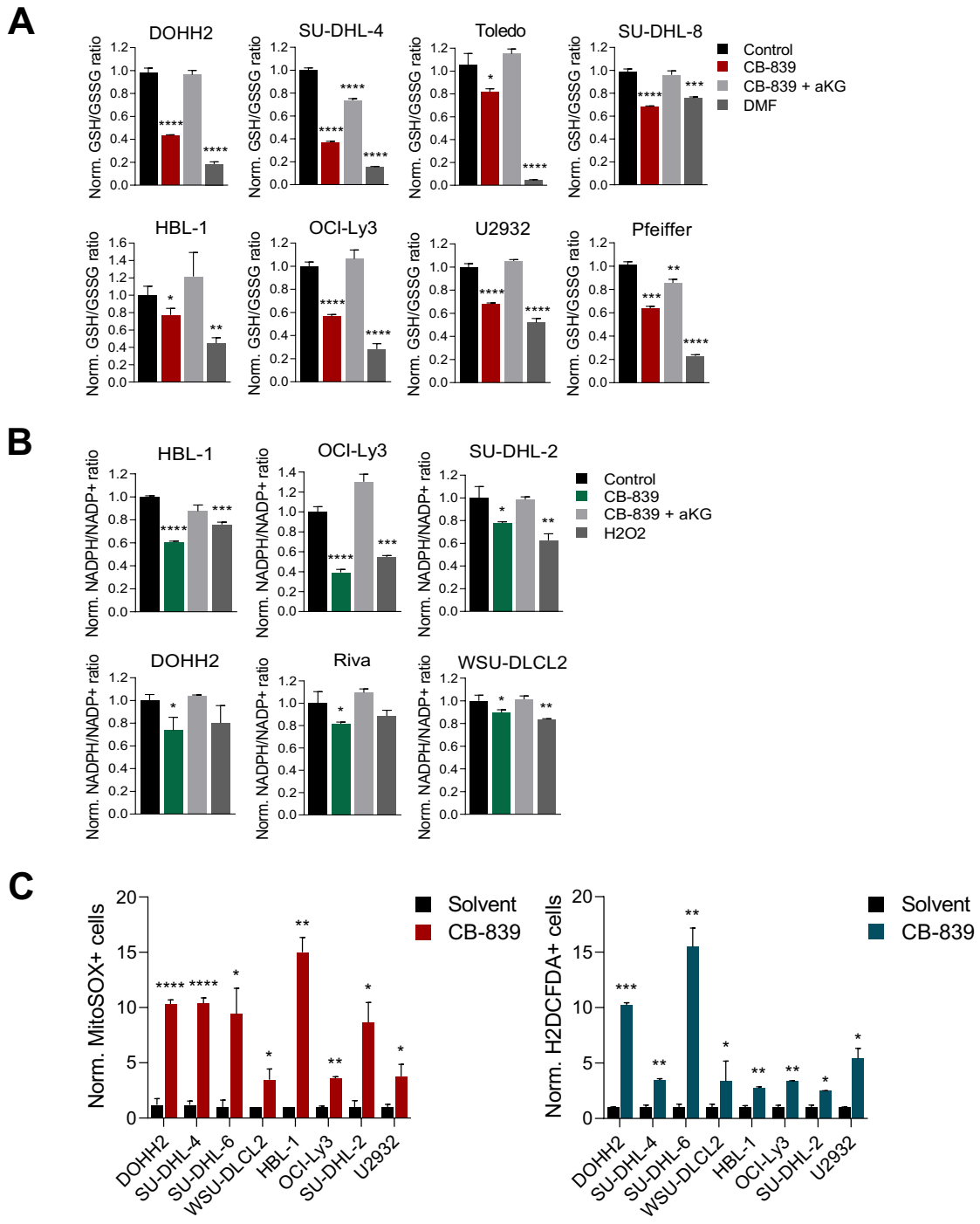

Figure 12. CB-839 induces ROS and reduces GSH levels in DLBCL. (A-B) The indicated DLBCL cell lines were treated with the GSH-depleter dimethyl fumarate (DMF, 20 μM) or 500 nM CB-839 for 24 hours alone or in combination with 0.5 mM of DM-KG. The ratio of reduced to oxidized **(A)** glutathione, or **(B)** NADPH was determined and normalized to the respective solvent-treated controls. **(C)** DLBCL cells were treated for 48 h with solvent or 500 nM CB-839 alone before quantifying the mitochondrial (left panel) or cytosolic (right panel) ROS by flow cytometry. The percentage of MitoROS-positive cells or H2DCFDA-positive cells in CB-839 treated samples were normalized to the percentage of the solvent control. Error bars correspond to the mean ± SD. Data is representative of at least three independent experiments **(A-C)**. *p* values were calculated by *t* test (unpaired, two tailed), **p* < 0.05, ***p* < 0.01, ****p* < 0.001, ****p<0.0001.

2.2.5 GLS1 inhibition does not affect mitochondrial integrity

The lack of indispensable TCA cycle metabolites post-GLS1 inhibition could potentially provoke alterations in the electron transport chain (ETC) that could compromise the mitochondrial membrane potential. Taking this into consideration, we next investigated whether CB-839 had a detrimental effect on mitochondria that could lead to an excessive leakage of ROS. For this, we used tetramethylrhodamine, ethyl ester (TMRE), a positively charged dye that accumulates in active mitochondria, to assay mitochondrial integrity after GLS1 inhibition. DLBCL cells did not exhibit any alterations in the mitochondrial membrane potential (MMP) after CB-839 treatment (data not shown). Interestingly, there seemed to be a modest correlation between the number of active mitochondria and the sensitivity of each specific cell line to accumulate ROS in response to CB-839 treatment (Fig. 13C). However, whether these two are related or not remains to be determined.

Because of the potential alterations that the complexes that constitute the ETC could suffer after GLS1 inhibition, we next evaluated the effects of using complex I and complex III inhibitors (rotenone and antimycin A respectively) on the accumulation of mitochondrial ROS (mito-ROS). As expected, rotenone markedly increased mitochondrial ROS and cotreatment with CB-839 further increased the amount of mito-ROS (Fig. 13D, lower panel). However, although antimycin A alone increased mito-ROS, its addition to CB-839 treatment did not increment the ROS levels any further than the ones observed with CB-839 alone (Fig. 13D, upper panel). Nevertheless, it is important to note that complex III directly depends on the proper functioning of complex II, which delivers electrons directly from succinate. Succinate is a TCA cycle metabolite that can derive from glutamine metabolism. Hence, the observation that antimycin A does not further increase ROS levels after co-treatment with CB-839 could be indicative of the fact that CB-839 indirectly affects complex II, and thus, complex III due to the lack of succinate caused by glutaminase-1 inhibition. All in all, this suggests that GLS1 inhibition does not have a detrimental effect on the overall function of the ETC and that the increase in ROS observed after CB-839 treatment is independent of the ETC.

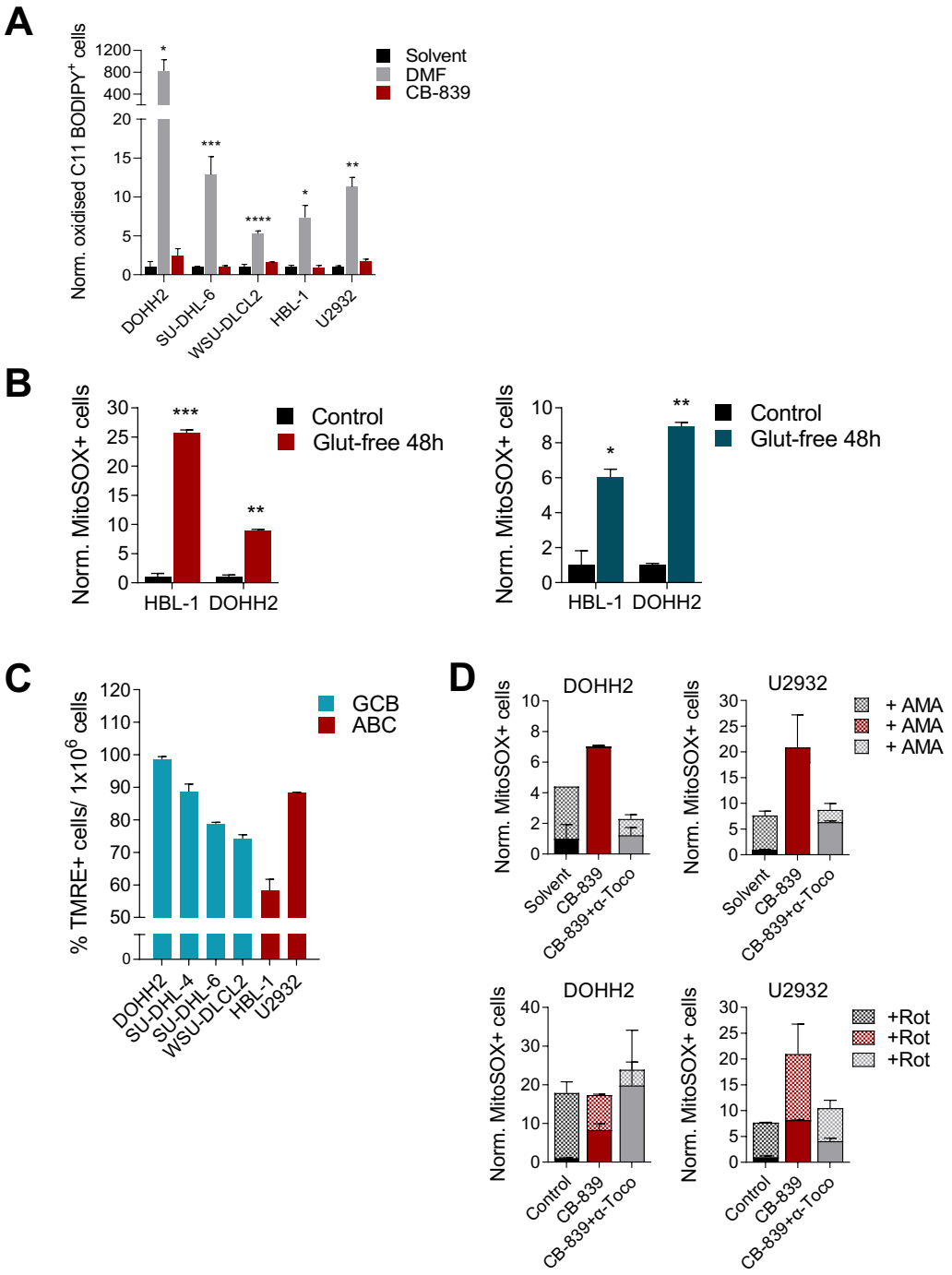

Figure 13. CB-839 treatment does not compromise mitochondrial integrity. (A) DLBCL cell lines were treated with solvent, 500 nM CB-839 or 20 μM DMF for 48 hours. Lipid peroxidation was quantified by flow cytometry using the oxidation-sensitive fluorescent probe BODIPY C11. **(B)** $1x10^6$ DLBCL cells were stained with TMRE. The percentage of TMRE-positive cells were quantified via flow cytometry. **(D)** DOHH2 and U2932 cells were treated with 500 nM CB-839 alone or in combination with 1 μM antimycin A (upper panels) or 1 μM rotenone (lower panels). The mitochondrial ROS levels were quantified by flow cytometry. The percentage of MitoSOX-positive cells in CB-839 treated samples was normalized to the solvent control. Error bars correspond to the mean ± SD. Data is representative of at least two **(B)** or three **(A, C-D)**. independent experiments. *p* values were calculated by *t* test (unpaired, two tailed), *$p < 0.05$, **$p < 0.01$, ***$p < 0.001$, ****p<0.0001.

2.2.6 α-Tocopherol abrogates the effects of GLS1 inhibition

Because excessive ROS levels cause damage to multiple macromolecules (proteins, lipids, nucleic acids, etc) thereby leading to cell death, we assessed the effect of hydrophilic (N-Ac, Trolox, ascorbic acid) and lipophilic antioxidants (α-tocopherol, mitoTEMPO) on CB-839-induced ROS accumulation and apoptosis. The hydrophilic antioxidants N-Ac and ascorbic acid, as well as the mitochondrial-targeted antioxidant mitoTEMPO, failed to protect cells from CB-839-dependent cytotoxicity (Fig. 14A, B and D). Trolox, a hydrophilic analog of α-tocopherol, also failed to rescue the cells after GLS1 inhibition (Fig. 14C). Conversely, and similar to α-ketoglutarate, α-tocopherol prevented the CB-839-mediated cytotoxicity (Fig. 15A). Viability rescue was especially prominent in the OxPhos DLBCL cell lines, indicating that this DLBCL subtype might be particularly sensitive to CB-839-induced ROS accumulation. The rescue observed after treatment with α-tocopherol directly correlated with its capacity to reduce the levels of intracellular and mitochondrial ROS (Fig. 15B-C). Interestingly, the use of the ferroptosis inhibitor ferrostatin-1 could only partially rescue viability of DOHH2, OCI-Ly3 and Toledo cells (data not shown), indicating that the CB-839-dependent cytotoxicity is likely not ferroptosis-mediated.

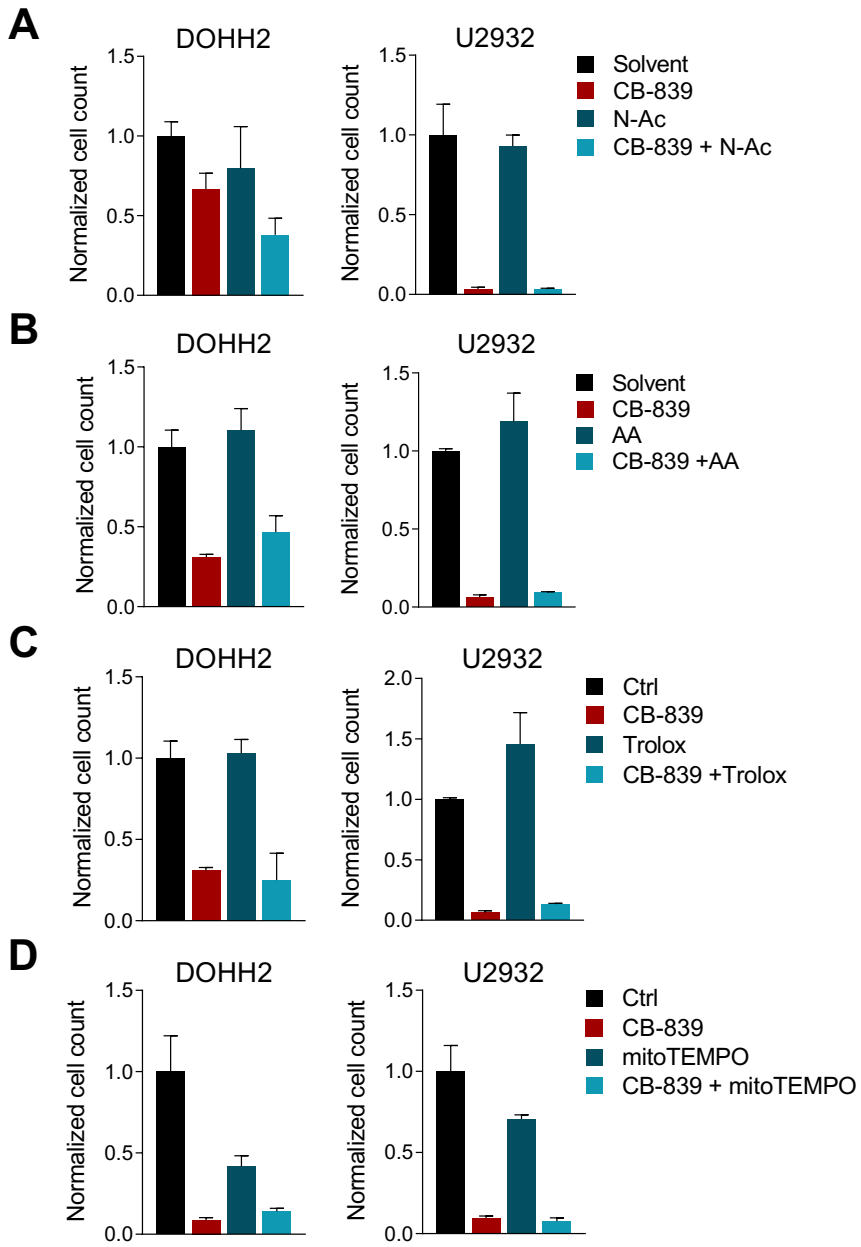

Figure 14. Hydrophilic antioxidants fail to salvage DLBCL cells from CB-839-mediated cytotoxicity. (A-D) ABC and GCB DLBCL cells were treated with solvent or 500 nM CB-839 alone or in combination with **(A)** 5-10 µM N-Acetylcysteine, **(B)** 50 µM ascorbic acid and **(C)** 10 µM Trolox for 5 days, or **(D)** 500 nM mitoTEMPO for 4 days. Cell numbers were determined as indicated and normalized to the solvent control. Error bars correspond to the mean ± SD. Data is representative of at least three **(A-D)** independent experiments.

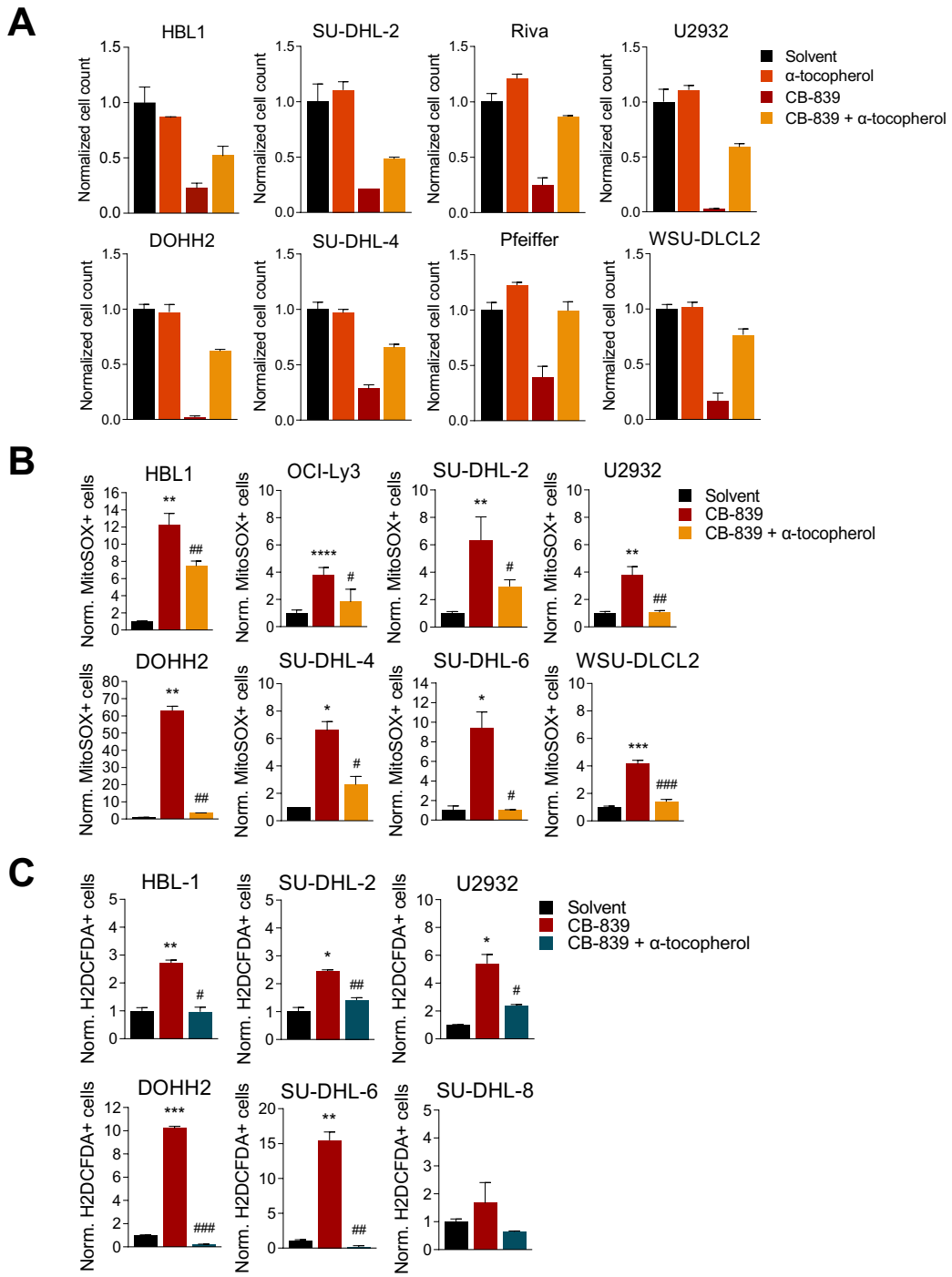

Figure 15. α-Tocopherol abrogates CB-839-induced ROS accumulation. (A) ABC and GCB DLBCL cells were treated with solvent or 500 nM CB-839 alone or in combination with 100 µM α-tocopherol for 6 d. Graphs depict cell numbers determined at day 6 normalized to the solvent control. **(B-C)** DLBCL cells were treated with solvent or 500 nM CB-839 alone or in combination with 100 µM α-tocopherol for 48 to quantify **(B)** mitochondrial ROS and **(C)** cytosolic ROS by flow cytometry. The percentage of **(B)** MitoSOX-positive cells and **(C)** cellROX-positive cells in CB-839 treated samples was normalized to the percentage of the solvent control. Error bars correspond to the mean ± SD. Data is representative of at least three independent experiments (**A-C**). *p* values were calculated by *t* test (unpaired, two tailed), **p* < 0.05, ***p* < 0.01, ****p* < 0.001, ****p<0.0001. * Were used to indicate significance between solvent and CB-839-treated samples; # were used to indicate significance between CB-839 and CB-389 + α-tocopherol-treated samples.

2.3 Synergistic approaches for the treatment of DLBCL

2.3.1 GLS1 inhibition acts synergistically with the Bcl-2 inhibitor ABT-199

To investigate promising synergistic approaches with CB-839, we sought out a drug previously described to be effective in B-cell lymphoma patients, but that would also have the potential to disrupt redox homeostasis in the cells. The Bcl-2 inhibitor ABT-199 has been described to induce mitochondrial ROS generation in T cells through respiratory chain supercomplex inhibition (Peirs et al., 2014). Hence, we first evaluated its capacity to increase ROS accumulation in DLBCL cell lines. Strikingly, ABT-199 alone was enough to significantly increase mitochondrial ROS both in ABC DLBCL and GCB DLBCL cell lines in a dose dependent manner (Fig. 16A). Accordingly, and as anticipated, the combination of both ABT-199 and CB-839 resulted in a drastic increase in both cytosolic and mitochondrial ROS accumulation in all cell lines tested (Fig. 16B-C). Notably, this effect was significantly diminished by the addition of the antioxidant α-tocopherol (Fig. 16B-C).

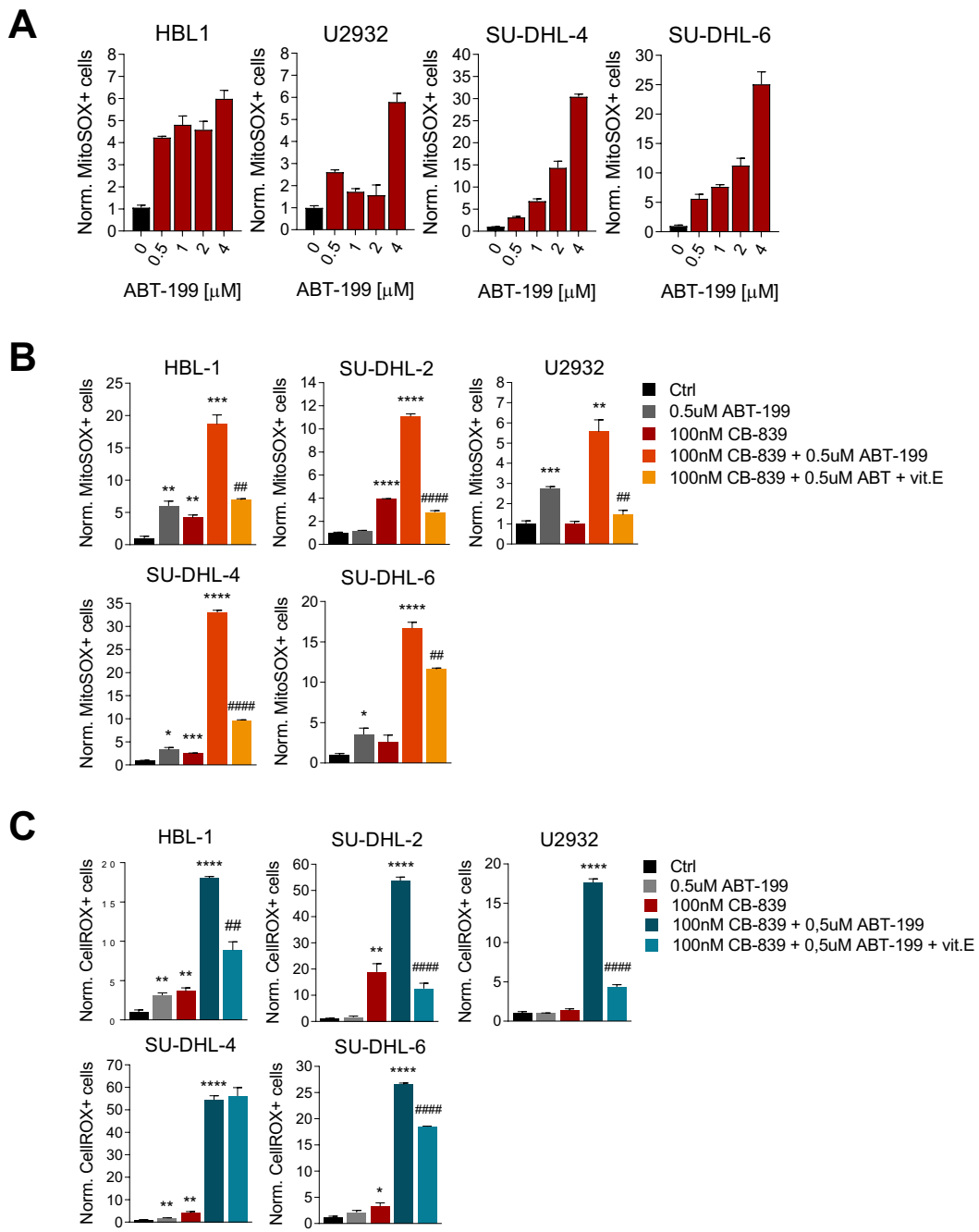

Figure 16. Synergistic ROS induction in DLBCL cell lines by the combined inhibition of GLS1 and BCL2. (A) ABC and GCB DLBCL cell lines were treated with ABT-199 for 48 h as indicated. Mitochondrial ROS levels were quantified by flow cytometry. The percentage of MitoSOX-positive cells in ABT-199 treated samples was normalized to the percentage of the solvent control. **(B-C)** DLBCL cells were treated for 48 h with solvent, 0.5 μM ABT-199 or 250 nM CB-839 alone or in combination, with or without 100 μM α-tocopherol. Mitochondrial ROS levels were quantified by flow cytometry. The percentage of **(B)** MitoSOX-positive cells or **(C)** cellROX-positive cells in CB-839 treated samples was normalized to the percentage of the solvent control. **(A-C)** Error bars correspond to the mean ± SD. Data is representative of at least three independent experiments. *p* values were calculated by *t* test (unpaired, two tailed), $*p < 0.05$, $**p < 0.01$, $***p < 0.001$, ****p<0.0001, n.s. not significant. * Were used to indicate significance between solvent and CB-839-treated samples; # were used to indicate significance between CB-839 and CB-389 + α-tocopherol-treated samples.

Next, we examined the combinatorial effects of both drugs in terms of viability and found that, whereas low doses of CB-839 only modestly affect survival of ABC DLBCL and GCB DLBCL cells, addition ABT-199 strongly sensitizes the cells to CB-839 inhibition (Fig. 17A). Hence, as determined by the Loewe additivity model, ABT-199 and CB-839 act in a synergistic manner to induce cytotoxicity in DLBCL cells over various concentrations, indicating the predisposition of DLBCL cell lines to undergo ROS-mediated cell death (Fig. 17B). Altogether, these results suggest that this combinatorial regime could be of interest for the treatment of DLBCL.

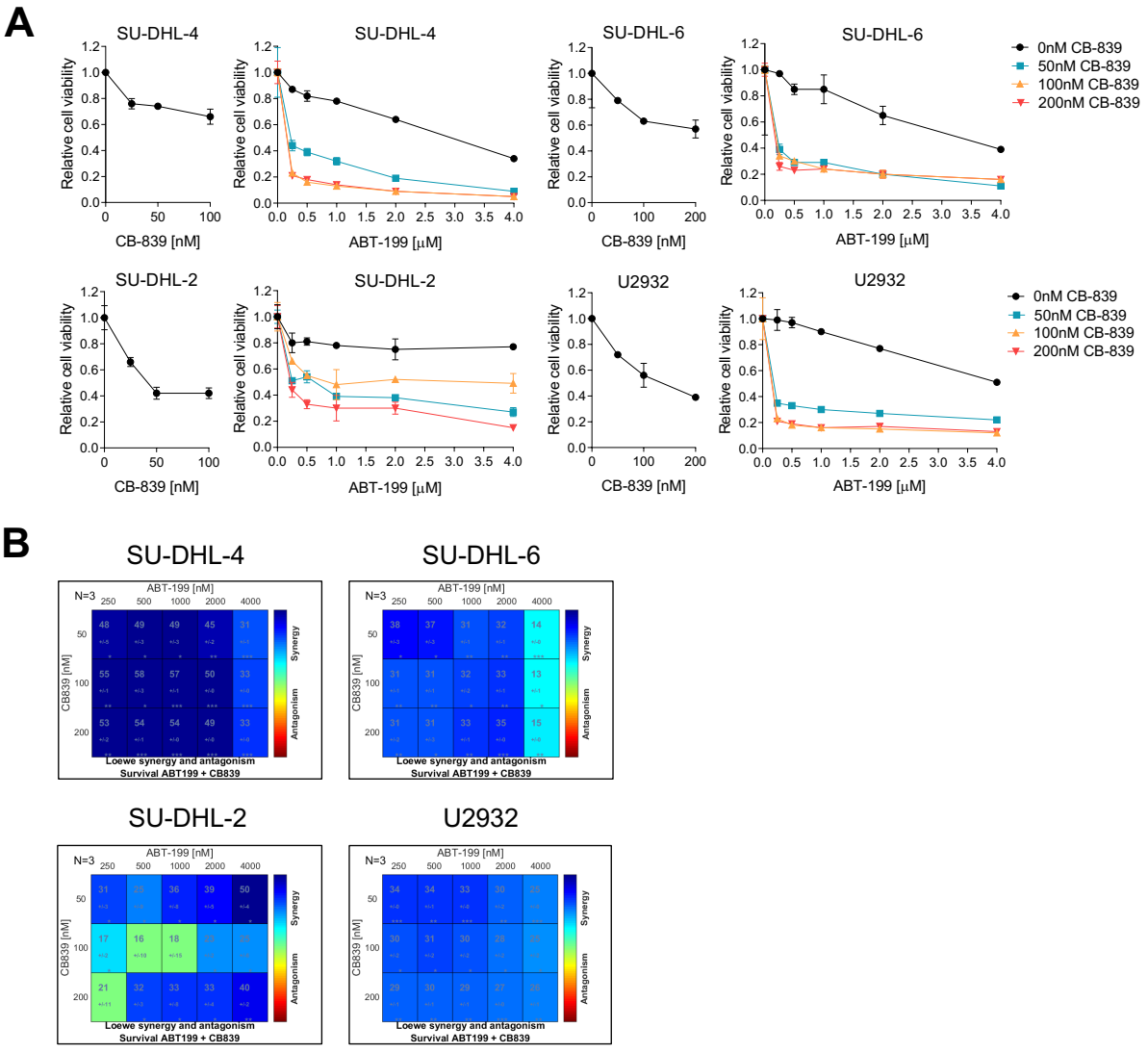

Figure 17. Synergistic killing of DLBCL cell lines by the combined inhibition of GLS1 and BCL2. (A) DLBCL cells were treated with CB-839 alone or in combination with ABT-199. Cell survival was quantified by MTS assay after 48 h and combination treatment was normalized to the CB-839 single treatment. **(B)** The Loewe additivity model was used to identify synergism between the CB-839 and ABT-199 doses assayed. Error bars correspond to the mean ± SD. Data is representative of at least three independent experiments.

3 Discussion

With more than 500,000 cases per year, NHL remains one of the most prevalent cancer types worldwide, with approximately 50% of the patients succumbing to the disease (Sung et al., 2021). Diffuse large B-cell lymphoma, being the most common lymphoid malignancy in adults, accounts for more than 30% of all diagnosed NHLs (Lenz & Staudt, 2010). Despite the existence of a well-established standard of treatment known as R-CHOP, approximately 30% of patients will still develop relapsed disease (Camicia et al., 2015). This is attributable to the pronounced heterogeneity observed amongst DLBCL cases and their vast complexity at a molecular level, which limits the therapeutic options (Cheson et al., 2021; M. Y. He & Kridel, 2021; Lenz & Staudt, 2010; Martelli et al., 2013). ABC DLBCLs are especially aggressive, owing to their constitutive NF-κB activation, which drives the expression of anti-apoptotic and proliferation-related genes (Davis et al., 2001, 2001; Grondona et al., 2018; Lam et al., 2008). A current avenue of treatment aims at exploiting metabolic deregulations that are a common feature in cancer cells. This strategy could be potentially effective in all DLBCL subtypes and, thus, could benefit a high number of patients.

3.1 Importance of glutamine metabolism for DLBCL survival

The reprogramming of energy metabolism is a hallmark of cancer. Rapidly proliferating tumor cells have a heightened demand for metabolic intermediaries to fulfil their intracellular biomass requirements, thereby providing them with a growth advantage (Van der Heiden et al., 2009; Wise & Thompson, 2010; Yoo et al., 2020). In this context, the phenomenon known as the Warburg effect or aerobic glycolysis, whereby cells preferentially convert glucose into lactate even in the presence of oxygen, is a characteristic feature of tumor cells. Even in the presence of intact mitochondria, cancer cells undergo this metabolic shift that yields less energy but produces glycolytic intermediaries at a higher rate, at the same time as supporting a faster ATP generation (DeBerardinis et al., 2007; Liberti & Locasale, 2016; vander Heiden et al., 2009). Similarly, cancer cells frequently undergo another metabolic rewiring by which they become addicted to glutamine (Franchina et al., 2018; Marquez et al., 2015; L. Yang et al., 2017; Yoo et al., 2020). Studies have emphasized the reliance of numerous

tumors on glutamine to replenish the TCA cycle and to supply the necessary building blocks for *de novo* synthesis of amino acids, nucleotides and fatty acids essential for cell survival (Altman et al., 2016; Yoo et al., 2020; Zhang et al., 2017). However, the dependence of tumor cells on these alternative pathways becomes a vulnerability that can be targeted (Gong et al., 2022; Gregory et al., 2019; Lukey et al., 2013; Shen et al., 2020).

One such strategy of considerable interest is to inhibit the enzyme glutaminase – responsible for the deamination of glutamine into glutamate – in glutamine addicted cancers (Katt et al., 2017; Márquez et al., 2016). Previous studies have revealed frequent upregulation of glutamine transporters as well as glutaminase in multiple hematological and solid tumors (Masisi et al., 2020; Wise et al., 2008; Zhao et al., 2019). These showed dependence on glutamine metabolism for proliferation and survival and were susceptible to GLS inhibition and/or glutamine deprivation (Effenberger et al., 2017; Gross et al., 2014; B. Li et al., 2019; Shen et al., 2020; Xiang et al., 2015). Therefore, to elucidate whether glutaminase is targetable in DLBCL, we first focused on analyzing the expression levels of both GLS isoforms in distinct DLBCL subtypes. Accordingly, GLS1 was found to be expressed in all lymphoma cell lines investigated, albeit ABC DLBCL cells exhibiting higher GLS1 protein levels (Fig. 2A). Interestingly, GLS2 was expressed in all cell lines independent of their subtype classification (Fig. 2A), even though GLS2 expression has previously been described to be restricted to liver, pancreas and brain (null et al., 2015; Saha et al., 2019; Z. Wang et al., 2020). Hence, liver-type glutaminase expression in lymphoma cell lines could be an indicative of the metabolic rewiring occurring during malignant transformation.

c-Myc has been identified as the main post-transcriptional regulator of glutaminase expression by directly repressing miR-23a and miR-23b, known to target *GLS'* 3' UTR (Gao et al., 2009). Considering that *MYC* is frequently overexpressed in DLBCLs either through genomic translocation or amplification (Ladanyi et al., 1991; Y. Xia & Zhang, 2020), we hypothesized that c-Myc might control the expression of GLS1 in lymphoma cells. However, GLS1 expression was not impaired by the JQ1-mediated downregulation of c-Myc at protein level (Fig. 2B). Conversely, glutamine deprivation has been shown to directly suppress c-Myc translation, while loss of GLS1 expression

has been associated with a faster c-Myc degradation via proteasome (Dejure et al., 2017; Effenberger et al., 2017). However, we could not detect a correlation between the expression of GLS1 and c-Myc in this context (Fig. 2A) and GLS1 inhibition did not lead to c-Myc downregulation (data not shown). Collectively, these observations suggest that c-Myc is not responsible for the regulation of GLS1 expression in DLBCL. Consequently, other transcription factors are likely to participate in the regulation of glutaminase and, thus, play a role in the cancer-related glutamine addiction. In aggressive ABC DLBCL, MALT1 protease activity was reported to be required for *GLS* expression (X. Xia et al., 2018). However, MALT1-mediated constitutive NF-κB activation in this DLBCL subtype is not a characteristic feature of GCB DLBCLs. Since GLS1 expression was observed in all DLBCL cell lines, this speaks against a MALT1-dependent regulation of glutaminase-1 expression in this setting. c-Jun, on the other hand, has been identified as a key regulator of mitochondrial glutaminase levels in human breast cancer cells (Lukey et al., 2016). However, we failed to find evidence to support a c-Jun-mediated regulation of GLS1 in ABC DLBCL cell lines (data not shown), which likely indicates the implication of an alternative transcription factor.

When assessing the susceptibility of DLBCL cells to glutaminase inhibition, we found that exposure of ABC and GCB DLBCL cells to two different selective GLS1 inhibitors, namely CB-839 and BPTES, was enough to induce cytotoxicity in a time-dependent manner (Fig. 3, Fig. 4A). Moreover, silencing of *GLS1* via small hairpin RNA or glutamine deprivation significantly reduced cell viability in a timely manner in all cell lines tested (Fig. 5A, C). GLS1 inhibition has prompted much interest as a therapeutic strategy against cancer, owing to its detrimental effect on tumor cell survival while sparing non-tumorigenic cells (Masisi et al., 2020; Matés et al., 2018; X. Xu et al., 2019). To this effect, we observed that non-malignant primary B cells remained unaffected to the treatment with CB-839 (Fig. 6). Nevertheless, these results must be taken with caution, since some studies point out to glutamine addiction being an artifact of *in vitro* culture due to the supraphysiological levels of glutamine in culture media (Quek et al., 2022; vande Voorde et al., 2023; Wise & Thompson, 2010). Indeed, GLS1 expression could only be detected in around 50% of DLBCL biopsies (data not shown). Thus, evaluation of GLS1 expression in DLBCL patient specimens becomes a requirement previous to treatment with a GLS1 inhibitor.

3.2 Mechanisms of action of GLS inhibitors in DLBCL

As mentioned previously, glutamine has proven to be of extreme importance for TCA cycle anaplerosis, as a carbon and nitrogen donor for nucleotide, fatty acid and amino acid synthesis, for the induction of growth and survival-related signaling pathways and for redox homeostasis (Curi R. et al., 2007; Yoo et al., 2020; Zhang et al., 2017). Cancer cells display an increased demand for amino acids, nucleotides and fatty acids in order to maintain their biomass requirements. Furthermore, tumor cells require constant TCA cycle replenishment to support their bioenergetic needs. Hence, most cancers end up relying on glutamine uptake and metabolism for growth and survival (Masisi et al., 2020; Z. Wang et al., 2020; L. Yang et al., 2017) . Accordingly, we observed that glutaminase inhibition via the GLS1-specific inhibitor CB-839 selectively induced DLBCL cell death while having low toxicity toward primary B cells. We thus hypothesized that GLS1 inhibition can provoke cytotoxicity through four different mechanisms: 1) by impairing the activation of well-known pro-survival signaling pathways in B cells, 2) by reducing the nucleotide supply, 3) by depleting the reservoir of metabolic intermediaries and/or 4) by compromising redox homeostasis.

Several studies have underlined the role of glutamine in the activation of the growth-promoting mTOR pathway (L. Yang et al., 2017). Glutamine not only can stimulate this kinase directly, but also participates in the import of other amino acids such as leucine, that can be sensed by and activate mTOR (Meng et al., 2020; Nicklin et al., 2009). Despite the evidence reported, the phosphorylation status of common mTOR downstream targets remained unaffected after CB-839 treatment. Furthermore, glutamine-derived α-ketoglutarate has been found to indirectly alter gene transcription through modifications of the chromatin methylation and acetylation status (Abla et al., 2020; T. Nguyen & Durán, 2018; Teperino et al., 2010). However, immunoblotting assays revealed that the try-methylation marks in H3K9 and H3K27 remained unaltered in DLBCL cells after CB-839 treatment (Fig. 7B-C). Conversely, STAT3 phosphorylation was decreased upon GLS1 inhibition (Fig. 8A), which is in accordance with published data showing that glutamine can directly activate STAT3, whereas glutaminolysis inhibition leads to a downregulation of STAT3 phosphorylation (Cacace et al., 2017; X. Xia et al., 2018). Nevertheless, in contradiction with these findings, in DLBCL cells STAT3 abrogation was caused by a significant reduction in the secretion

of IL-6 and IL-10 after CB-839 treatment (Fig. 8B). These cytokines, which are commonly produced by ABC DLBCL cells owing to the constitutive NF-κB activation, act in an autocrine and paracrine manner to stimulate JAKs and thus activate STAT3. Accordingly, when we supplemented the medium with exogenous recombinant human IL-6 and IL-10, the levels of phosphorylated STAT3 increased (Fig. 8A). Knowing the crucial role of the STAT3 pathway for the survival of B cells (Ding et al., 2008), we questioned whether recovery of STAT3 phosphorylation would abrogate the CB-839-mediated cytotoxicity. However, neither the supplementation with exogenous IL-6/IL-10, nor the inducible expression of a hyperactive STAT3 (STAT3C) mutant were able to mitigate the cytotoxicity caused by CB-839 (Fig. 8C-D). Given these results, we suggest that the reduction in cytokine production and secretion observed after glutaminase inhibition is rather a consequence of the decrease in biomass available for peptide and protein biosynthesis, as has also been observed for T cells (Sener et al., 2016).

We next evaluated our second hypothesis, in which we speculated that the notable reduction in cell viability after GLS1 inhibition was caused by glutamine-dependent alterations in nucleotide levels. Previous findings have shown that upon glutamine deprivation the intracellular pools of nucleotides decrease significantly owing to the role of glutamine as a donor of amino groups for the synthesis of purines and pyrimidines (T. Nguyen & Durán, 2018; Zhang et al., 2017). On the contrary, other studies reported that nucleotide biosynthesis does not require the action of glutaminase (Cory & Cory, 2006; Thangadurai et al., 2022; Zhang et al., 2017). Furthermore, a research group demonstrated that glutamine-dependent availability of adenosine in the CRC cell line HCT116 could be sensed specifically by the 3'UTR of *MYC* mRNA to drive its translation, thereby inducing cell growth and proliferation (Dejure et al., 2017). However, in DLBCL cells we failed to identify a regulatory pathway involving GLS1 and c-Myc, thus making this scenario improbable in lymphoma cells. Taking this evidence into consideration, we speculated that the CB-839-mediated cytotoxicity would likely not be due to alterations in the nucleotide pools of DLBCL cells. As expected, supplementing the media of CB-839-treated DLBCL cells with adenosine did not restore cell viability (Fig. 9).

A major function of glutamine is to supply intermediaries to fuel the TCA cycle after its conversion to glutamate and α-ketoglutarate, and thereby provide the required equivalents for ATP generation (Wise & Thompson, 2010; Yoo et al., 2020). Consequently, treatment of DLBCL cells with CB-839 led to a decrease in ATP levels, particularly after 48 h treatment (Fig. 10C), that correlated with the decrease in cell viability. However, we could not determine whether this decrease was due to a deprivation of necessary TCA cycle metabolites for ATP production or as a result of the cytotoxicity caused by the inhibitor. Consistent with the role of glutamine as an anaplerotic substrate, CB-839 treatment in DLBCL cells led to a rapid decrease in steady-state levels of common TCA cycle intermediaries including aspartate, α-ketoglutarate, glutamate, fumarate and succinate amongst others, which was accompanied by an enrichment of glutamine (Fig. 10A). This is in accordance with multiple studies that have evaluated the impact of glutamine deprivation and glutaminase inhibition on the metabolome (Ruiz-Rodado et al., 2020; C. Yang et al., 2014; W.-H. Yang et al., 2021). These results fueled the idea of the crucial role of glutamine metabolism in supporting the survival and proliferation of lymphoma cells via its anaplerotic functions. Hence, we initially hypothesized that CB-839 treatment induced cell death in DLBCL cells as a result of the depleted state of essential metabolites required for amino acid synthesis and energy production. However, we also noticed a significant decrease in the relative abundance of well-known antioxidant molecules, such as α-tocopherol, glutathione (GSH) and reduced NADPH in CB-839-treated DLBCL cells (Fig. 10B). In agreement with these findings, the ratio of reduced to oxidized glutathione decreased after GLS1 blockade in multiple DLBCL cell lines but was restored after addition of a membrane permeable form of α-ketoglutarate (DM-KG) (Fig. 12A). These results can be explained on at least two levels. First, glutamine-derived glutamate, which can also be generated from α-ketoglutarate, is one of the three amino acids comprising the antioxidant molecule glutathione (Franco & Cidlowski, 2009; Masisi et al., 2020; Roth et al., 2002). Furthermore, glutamate can be exported in exchange for cystine by the system x_c- antiporter. Cystine is then reduced to cysteine, which is an essential substrate for the synthesis of GSH (Lewerenz et al., 2012). Second, α-ketoglutarate has been shown to protect against oxidative stress effectively by stimulating endogenous antioxidant defense and restoring the pool of reducing equivalents (Abla et al., 2020; L. He et al., 2018). Accordingly, DM-KG not only restored the ratio of reduced/oxidized glutathione after CB-839 treatment to basal

levels but was also capable of rescuing cells from the CB-839-mediated cell death (Fig. 11A).

Consequently, we next assessed whether CB-839 treatment could provoke the accumulation of reactive oxygen species in DLBCL cell lines. To this effect, flow cytometry analyses were performed in multiple DLBCL cell lines that had been either cultured in absence of glutamine or exposed to CB-839 for 48 h and revealed a significant increase both in mitochondrial and cytosolic ROS (Fig. 12C, 13B). Overall, these results indicate that, even though glutamine is the primary source of carbons for the TCA cycle in some tumors, we suggest that in DLBCL the anaplerotic role of glutamine providing energy supply for the cell, or its role as a nitrogen donor for amino acid and nucleotide biosynthesis, are not primarily essential for DLBCL survival. Thus, we propose that the CB-839-mediated cytotoxicity is mainly driven by ROS induction.

Basal levels of ROS have been proved to be necessary and beneficial for cancer cell proliferation. In fact, hyperproliferation of tumor cells is usually concomitant to increased ROS production, but these cells are adapted to sustain aberrant redox homeostasis, usually by increasing their antioxidant status (Hayes et al., 2020). Moreover, ABC DLBCL cell lines have been shown to have a predisposition for increased basal levels of ROS, likely owing to their constitutive BCR pathway activation, which is associated with alterations in respiration and metabolism leading to increased ROS (Zhu et al., 2019). Increased ROS in this setting augments cytokine signaling, thus leading to increased proliferation, activation and survival. However, it has been well-established that excessive ROS accumulation causes irreversible damage that triggers cell death (Hayes et al., 2020). Paradoxically, glutamine itself can indirectly lead to ROS production through its anaplerotic entry into the TCA cycle, which is subsequently coupled with the electron transport chain (ETC). Electrons continuously leak from the ETC and react with oxygen, resulting in the generation of ROS (Raimondi et al., 2020). Conversely, glutaminolysis is crucial for the maintenance of redox homeostasis, mainly by supplying the intermediaries and amino acids required for the synthesis of antioxidant entities such as glutathione, as well as other reducing equivalents, like NADPH (Gong et al., 2022). As mentioned previously, upon GLS1 inhibition, increased ROS levels were detected in all DLBCL cells analyzed. This increase is not only observed in DLBCL, but also in many other tumor entities such as

AML, CRC and ovarian cancer (Pan et al., 2014; Shen et al., 2020). To prove that the CB-839-dependent cytotoxicity was derived from ROS accumulation, we investigated the effect of several different antioxidants for their ability to rescue cell viability post-CB-839 treatment. Interestingly, from all the screened antioxidants, α-tocopherol could effectively abrogate the CB-839-mediated cell death (Fig. 15A). In addition, α-tocopherol was capable of significantly reducing both mitochondrial and cytosolic ROS induced by CB-839 treatment in lymphoma cells (Fig. 15B-C). Taken together, we suggest that glutamine metabolism plays a key role in the maintenance of redox homeostasis by increasing the antioxidant potential of lymphoma cells. In this regard, high levels of reduced GSH have been correlated with tumorigenesis and therapy resistance in cancer (Godwin et al., 1992; Masamha & LaFontaine, 2018). Indeed, inactivating GLS1 in DLBCL cells compromised redox homeostasis, reduced GSH and increased ROS accumulation, which contributed substantially to the observed CB-839 anti-lymphoma effect.

α-Tocopherol is a lipophilic antioxidant known to be a ferroptosis inhibitor (Q. Hu et al., 2021). Ferroptosis is a programmed form of cell death dependent on iron and characterized by the accumulation of lipid peroxides (Jiang et al., 2021). Our research group has previously reported a broad antitumor effect by dimethyl fumarate (DMF) on both DLBCL subtypes mediated by the induction of ferroptosis (A. Schmitt et al., 2021). In this scenario, GCB DLBCL cells, which generally exhibited lower GSH levels, were particularly sensitive to this treatment. Based on our observation that GLS1 inhibition diminished the GSH pool in DLBCL cells and that α-tocopherol was the only antioxidant able to abrogate CB-839-mediated ROS-induced cell death, we initially hypothesized that DLBCL cells were undergoing ferroptosis after GLS1 blockade. To investigate this, we quantified lipid peroxidation after GLS1 inhibition and observed that, while DMF strongly induced lipid peroxidation after just a 4 h exposure, CB-839 failed to provoke such a stark increase (Fig. 13A), suggesting that the CB-839-mediated oxidative cell death cannot be characterized as ferroptosis.

Next, we wanted to further investigate the mechanism of action of CB-839 in DLBCL cells. We suspected that GLS1 inhibition provokes the accumulation of ROS due to redox imbalance. It is known that glutamine undergoes catabolism to fuel the TCA cycle, which subsequently supplies the ETC with NADH and $FADH_2$ required for the

proper functioning of the complex I and II of the ETC (DeBerardinis et al., 2007; vander Heiden et al., 2009). Theoretically, the inhibition of glutaminolysis and the subsequent deprivation of TCA cycle metabolites would lead to a lack of crucial reductive equivalents to feed the ETC, hence impairing its normal function. With an ETC impairment, one would expect a reduction in electron leakage from the mitochondria, thus diminishing ROS generation. However, this is not what we observed in lymphoma cells after GLS1 inhibition. Contrary to the aforementioned theory, we speculated that the lack of equivalents necessary to supply the ETC could lead to a disruption in the mitochondrial membrane potential, which would provoke an excessive electron leakage for ROS production. Evidence has shown that impairment of the mitochondrial electron transport chain leads to an increase in intracellular oxidative stress, disruption of the proton gradient, insufficient ATP production and even cell death (Indo et al., 2007). In fact, inhibitors of complex I and III, such as rotenone and antimycin A (AMA) respectively, have been used as ROS generators in biological systems. AMA-treated cells exhibited a loss of mitochondrial membrane potential, Bcl-2 downregulation, Bax upregulation, GSH depletion and marked ROS increase (W. H. Park et al., 2007). Rotenone induces cell death in a similar fashion (N. Li et al., 2003). Consequently, considering the observed increase in mitochondrial reactive oxygen species we observed after GLS1 inhibition, we next investigated the relationship between CB-839-induced cytotoxicity and mitochondrial membrane potential. Contrary to what we hypothesized, we could not observe any alterations in the mitochondrial membrane potential via TMRE staining. However, an interesting finding demonstrated that those DLBCL cell lines with higher amounts of active mitochondria (as determined by TMRE), exhibited higher cytosolic ROS levels after GLS1 blockade, likely indicating the source of CB-839-derived ROS. Strikingly, addition of rotenone to CB-839 increased the levels of mitochondrial ROS observed in DLBCL cells (Fig. 13D). On the contrary, addition of antimycin A to CB-839 could not further enhance ROS generation in lymphoma cells (Fig. 13D). In this context, further analyses are required in order to examine in detail the effects of CB-839 on the ETC to investigate whether CB-839 can provoke an excess in ROS production through alterations of the ETC.

Collectively, these observations suggest a crucial role for glutaminase in the maintenance of redox homeostasis in DLBCL by supplying sufficient intermediaries to fulfil the increased demand of reductive equivalents and antioxidant molecules. DLBCL

cells undergo cell death after GLS1 blockade owing to the lack of glutamine-derived glutamate required for glutathione synthesis. Furthermore, the data imply that GLS1 inhibition might affect the upkeep of the ETC which can further enhance ROS generation.

3.3 Synergistic approaches for the treatment of DLBCL

Current treatment schemes for NHL aim at combining agents that target different dysregulated pathways or cooperating mutations in order to achieve higher response rates (Roschewski et al., 2014). Combination strategies with different targeted agents have yielded promising results both in DLBCL cell lines and in phase I and II clinical trials. For instance, the PKC-β inhibitor enzastaurin has been tested in combination with the standard therapy R-CHOP in a phase II study and demonstrated an encouraging increase in 1-year progression free survival (PFS) of 71% versus 52% of those patients treated only with R-CHOP (Hainsworth et al., 2016). Furthermore, the Bruton tyrosine kinase inhibitor ibrutinib entered a phase Ib clinical trial where it was tested in combination with R-CHOP and has shown promising results (Younes et al., 2014). This combination is currently being tested in a phase III clinical trial with patients diagnosed with non-GCB DLBCL. The current challenge is to properly identify rational combination therapies and define mechanism-based synergistic approaches that avoid at all costs possible side effects.

To this effect, we proposed the combination between the Bcl-2 selective inhibitor venetoclax (ABT-199) and CB-839. We opted for this drug combination based on the observed mechanistic functions of ABT-199. On the one hand, venetoclax is a drug that has already been described to be effective in B-cell lymphoma patients and is undergoing phase I and II clinical trials (Davids et al., 2014; Kuo et al., 2017; Souers et al., 2013). Furthermore, since lesions causing Bcl-2 overexpression are frequent in both DLBCL subtypes, ABT-199 treatment would directly aim at the pro-survival mechanisms of DLBCL cells and tilt the balance in favor of apoptosis (Dunleavy & Wilson, 2011; Johnson et al., 2012). On the other hand, ABT-199 has been shown to enhance ROS production in T cells by reducing the formation of respiratory chain supercomplexes, while GSH levels remained unaffected (Peirs et al., 2014). Thus, we proposed that since CB-839 provokes ROS accumulation in a different manner than

ABT-199, the combination of both would likely synergistically enhance ROS levels in DLBCL cells. Furthermore, we could further exploit the fact that ABT-199 inhibits the anti-apoptotic protein Bcl-2, which would lower the threshold by which DLBCL cells undergo apoptosis in these conditions. For this, we first assessed the ability of ABT-199 to induce ROS in multiple DLBCL cell lines and demonstrated a dose-dependent increase in mitochondrial and cytosolic ROS induction upon Bcl-2 blockade (Fig. 16A). As expected, while single ABT-199 and CB-839 treatment led to moderate ROS accumulation, the combination of both agents resulted in a dramatic increase in ROS formation that could be almost fully abrogated by addition of α-tocopherol (Fig. 16B-C). This excessive ROS induction upon CB-839 and ABT-199 combination treatment subsequently provoked cytotoxicity in a synergistic manner independent of the DLBCL cell line (Fig. 17A-B).

In conclusion, considering that this drug combination has previously been shown to exhibit encouraging results in AML (Pan et al., 2014), and taking into account our observation that ABT-199 further sensitizes cells to ROS-mediated cell death when combined with CB-839, we propose that this drug combination might represent a promising novel strategy for the treatment of all DLBCL subtypes. However, GLS1 and Bcl2 expression should first be confirmed in DLBLC biopsies before considering the combinatorial GLS1/Bcl2 inhibitor treatment.

CHAPTER 2

The importance of IκBζ in liver disease

4 Introduction

4.1 Hepatocellular carcinoma

Hepatocellular carcinoma (HCC) accounts for ~90% of all newly diagnosed primary liver cancers and is the fourth leading cause of cancer-related death worldwide, with its incidence on the rise (Llovet, Kelley, et al., 2021; Sung et al., 2021). The prognosis of HCC patients remains dismal, owing to the severity of this tumor and a lack of effective treatment strategies. The molecular pathogenesis of HCC is complex, since it varies depending on the etiology and genotoxic insults that lead to hepatocarcinogenesis (Forner et al., 2018; J. D. Yang et al., 2019). Furthermore, targeting of the most frequent oncogenic drivers remains a challenge, considering some of the most frequently mutated genes, such as *TP53*, *CTNNB1*, *CCND1* and *TERT*, are considered undruggable (Llovet, Kelley, et al., 2021). Currently, the standard treatment consists in hepatic resection, transplantation and ablation for early diagnosed patients, and systemic treatment with the multi-kinase inhibitor sorafenib for cases of advanced hepatocellular carcinoma (Llovet, Kelley, et al., 2021). However, 70% of HCC patients relapse before 5 years and succumb to the disease (Forner et al., 2018; Villanueva, 2019).

4.1.1 Current HCC treatment options

Effective treatment strategies for the management of HCC are limited, owing to the scarcity of druggable targets. The most desirable treatment option is surgical resection of the tumor. However, only patients diagnosed at early stages with no dissemination are electable for resection and 70% will still develop recurrent HCC (Llovet, Kelley, et al., 2021). The most promising treatment for early diagnosed patients is liver transplantation, which not only gets rid of the tumor tissue, but also of the partial dysfunctional liver (Llovet, Kelley, et al., 2021; J. D. Yang et al., 2019). However, scarcity in organ donations limits this treatment (J. D. Yang et al., 2017). Another potentially curative treatment is local ablation using radiofrequency or microwave

ablation, which causes tumor necrosis not only of the tumor cells but also of the surrounding blood vessels (Llovet, De Baere, et al., 2021; Llovet, Kelley, et al., 2021). Survival after ablation ranges between 50-70%, making it one of the most effective treatment strategies for early diagnosed patients (Llovet, De Baere, et al., 2021; Shiina et al., 2018; J. Yu et al., 2017). Transarterial chemoembolization (TACE), whereby cytotoxic agents and embolization particles are infused directly into the tumor, is the treatment of choice for patients with large or multifocal tumors, but survival rates remain low (Lencioni et al., 2016; Llovet et al., 2002; Yin et al., 2014). Finally, sorafenib has remained the first-line systemic treatment option for patients with advanced-stage HCC for more than a decade (Llovet et al., 2008; Llovet, Kelley, et al., 2021). However, recently the combination of the anti-PDL1 antibody atezolizumab with the anti-VEGF antibody bevacizumab has proved to be more effective than sorafenib in improving overall survival (Cheng et al., 2022; Finn et al., 2020). Current treatment strategies are focusing on exploiting the inflammatory nature of this tumor and high immune presence in HCC to achieve better response rates. In this regard, immune checkpoint inhibitors combined with anti-angiogenic agents have shown promising results (Llovet, Kelley, et al., 2021; US National Library of Medicine, 2019).

4.1.2 Risk factors involved in hepatocarcinogenesis

In 90% of the cases, HCC occurs in a setting of chronic inflammation and cirrhosis, owing to a pre-existing liver disease (J. D. Yang et al., 2019; YM. Yang et al., 2019). There are several well-known risk factors for the development of HCC and their incidence reflects geographical variations (J. D. Yang & Roberts, 2010). For instance, chronic infection with hepatitis B virus (HBV) accounts for approximately 60% of HCC cases in eastern Asia and sub-Saharan Africa, while it only accounts for 20% of cases in the West (Global Burden of Disease Liver Cancer Collaboration et al., 2017; Llovet, Kelley, et al., 2021). HBV is a DNA virus that can integrate into the host genome, thereby inducing genetic mutations that cause oncogene activation and hepatocarcinogenesis (Levrero & Zucman-Rossi, 2016; Trépo et al., 2014; Yuen et al., 2018). Additionally, the early-onset cases of HCC observed in Africa are due to exposure to the mycotoxin aflatoxin B1, which acts synergistically with HBV increasing the risk of hepatocellular carcinoma (Gouas et al., 2009; TURNER et al., 2002; J. D. Yang et al., 2019). Conversely, hepatitis C virus (HCV) is the most common virus-related cause of HCC in North America, Europe, Japan and northern Africa (J. D.

Yang et al., 2019). In these cases, considering the inability of HCV to integrate in the genome, the development of HCC is limited to the patients that develop chronic liver damage and cirrhosis (Khatun et al., 2021; Llovet, Kelley, et al., 2021; J. D. Yang & Roberts, 2010). Notably, in developed countries, non-alcoholic fatty liver disease (NAFLD) and non-alcoholic steatohepatitis (NASH) have become one of the major attributors of HCC development and account for roughly 20% of the cases due to the rising prevalence of metabolic disorders such as diabetes mellitus and obesity (Welzel et al., 2013; J. D. Yang et al., 2019; Younossi et al., 2015). Interestingly, approximately 30% of NASH-associated HCCs occur in the absence of cirrhosis, making it hard to surveille these patients for the onset of liver cancer (Welzel et al., 2013). Furthermore, excessive alcohol intake leads to alcoholic liver disease (ALD), which increases the hepatocarcinogenic potential threefold (El-Serag & Mason, 2000; Ganne-Carrié & Nahon, 2019). Currently, alcohol abuse is the second most common risk factor in the USA and Europe and is accountable for 15-30% of HCC cases (J.-W. Park et al., 2015). Moreover, alcohol consumption increases the risk of HCC development when combined with other risk factors. For instance, HBV carriers who consume alcohol have increased risk of developing liver cancer (Donato et al., 2002; Hassan et al., 2002). In summary, HCC is a typical inflammation-related cancer, where the great majority of the associated risk factors pose a hepatocarcinogenic burden due to the prolonged inflammation and fibrosis arising from HBV/HCV infection, chronic alcohol intake, NAFLD and NASH and/or cirrhosis.

4.1.3 The role of inflammation in HCC development

The pathogenesis of HCC frequently involves inflammatory signaling pathways, immune cell infiltration and the tolerogenic environment characteristic of the liver. In fact, more than 80% of HCC cases are driven by an underlying cirrhosis caused by chronic inflammation (YM. Yang et al., 2019). The sequence leading to hepatocarcinogenesis consists of a multi-step process by which an initial insult, stemming from a viral infection, metabolic disorder, excessive alcohol consumption or exposure to toxins, ultimately results in hepatic epithelial cell damage (Villanueva, 2019; J. D. Yang & Roberts, 2010; YM. Yang et al., 2019). The damage induced to hepatocytes not only leads to inflammation, excessive ROS production and DNA damage, but also prompts compensatory proliferation in the hopes of resolving the injury. However, the coupling of increased hepatocyte proliferation with the elevated

susceptibility of suffering DNA mutations rises the likelihood of developing hepatocellular carcinoma (YM. Yang et al., 2019). Studies performed in HCC mouse models have uncovered several inflammation-related pathways that are critical mediators in hepatocarcinogenesis, including the IL-6/STAT3 signaling axis, as well as the nuclear factor kappa-light-chain-enhancer of activated B cells (NF-κB), the c-Jun N-terminal kinase (JNK) and the tumor necrosis factor (TNF)-α pathways (Refolo et al., 2020; YM. Yang et al., 2019).

4.1.3.1 IL-6/STAT3 signaling pathway in the development of HCC

The signaling axis involving IL-6/STAT3 is a well-characterized signaling pathway involved in the promotion of hepatocellular carcinogenesis, owing to its function in hepatocyte repair and replication (Svinka et al., 2013; YM. Yang et al., 2019). In fact, the disparity observed between men and women regarding HCC incidence is partly due to the differences observed in IL-6 levels due to sex hormones (Nakagawa et al., 2009; Naugler et al., 2007).

IL-6 levels have been shown to be increased in the serum of viral and alcoholic hepatitis patients, steatohepatitis patients, as well as in liver cirrhosis and HCC patients (Aleksandrova et al., 2014; Fontes-Cal et al., 2021; Nakagawa et al., 2009; Shakiba et al., 2018; Sheron et al., 1991; Wong et al., 2009). Studies in the murine diethylnitrosamine (DEN) model of HCC demonstrated that impairment of both the classical and trans-signaling IL-6 pathways protect from HCC development, generally by abrogating STAT3-dependent compensatory proliferation, DNA damage accumulation, hepatic injury, necrosis, macrophage infiltration and angiogenesis (Bergmann et al., 2017). In this context, Kupffer cells (KCs), which are liver specific macrophages, were the major source of soluble IL-6 receptor (sIL-6R) upon DNA damage and hepatocyte necrosis through MyD88 activation downstream of Toll-like receptors (TLRs). Furthermore, a study performed on a mouse model of obesity and hepatosteatosis, where HCCs were induced via administration of DEN at different time points, further demonstrated the implications of chronic IL-6-STAT3 axis activation on proliferation and progression of transformed hepatocytes (E. J. Park et al., 2010). Notably, obesity and lipid accumulation led to low-grade inflammation as demonstrated by elevated production of TNF and IL-6. In this setting, IL-6 signaling through STAT3 and ERK was observed to subsequently reduce apoptosis while stimulating cell

proliferation of transformed hepatocytes. In this scenario, knocking-out either STAT3, IL-6 or TNFR1 all abrogated the tumor-promoting effect of obesity, as observed by the reduction in HCC formation in this mouse model. Moreover, in a different obesity-associated HCC murine model, hepatocarcinogenesis was shown to be significantly reduced after IL-1β ablation, owing to the subsequent blockage in the senescence-associated secretory phenotype (SASP), which includes IL-6 and IL-8 secretion (Yoshimoto et al., 2013).

STAT3 phosphorylation was also shown to be enhanced in the livers of obese mice that had been fed a high fat diet (HFD) (Grohmann et al., 2018). In this context, the inactivation of the STAT3 phosphatase T-cell protein tyrosine phosphatase (TCPTP) increased IL-6 expression and STAT3 activity and promoted the development of hepatocellular carcinoma. Additionally, another study in the MUP-uPA mouse model of liver damage provided evidence of the requirement of the IL6-STAT3 autocrine loop for the malignant progression of HCC progenitor cells (HcPCs) (G. He et al., 2013). Silencing of IL-6 either in HcPCs or in hepatocytes reduced DEN-induced tumorigenesis in the liver in this specific setting.

Finally, retrospective studies in chronically infected HBV and HCV patients have revealed a correlation between high IL-6 levels in serum and the increased risk in developing HCC (Nakagawa et al., 2009; Shakiba et al., 2018; Wong et al., 2009). In fact, 16% of biopsies obtained from human HCV-infected livers exhibited IL-6 expression and STAT3 activation (G. He et al., 2013). Altogether, these studies highlight the crucial role of the IL-6-STAT3 signaling axis in the development and progression of hepatocellular carcinoma.

4.1.3.2 Role of NF-κB in HCC development

NF-κB is known as a master regulator of inflammation, that not only coordinates the initiation of inflammatory responses, but also regulates the intensity and duration of the response (Luedde & Schwabe, 2011). NF-κB is one of the most important pathways involved in the typical injury-inflammation-regeneration cycle observed during HCC development. However, the role of NF-κB in hepatocarcinogenesis remains controversial and can be contradictory. In this regard, the cytokines lymphotoxin (LT)-α and -β, known to induce both classical and alternative NF-κB signaling, have been shown to be upregulated in livers of HBV and HCV-induced hepatitis patients

(Haybaeck et al., 2009). In fact, heightened liver-specific LT-α and -β expression in a transgenic mouse line were shown to lead to an upregulation in the expression of chemokines and cytokines, as well as cell-growth-related genes, and led to an increase in hepatocyte proliferation and to a pronounced influx of lymphocytes and macrophages, all of which ultimately induced the development of hepatitis and HCC. Interestingly, ablation of either lymphocytic infiltration or liver-specific IKKβ expression in this context was shown to abrogate the development of hepatitis and HCC, thus underlining the tumor-promoting function of NF-κB in hepatocytes (Haybaeck et al., 2009). Additionally, an $Mdr2^{-/-}$ mouse model of cholestatic hepatitis that progresses to HCC over time showed that carcinogenesis in this setting is majorly dependent on the TNFα-induced NF-κB activity in hepatocytes (Pikarsky et al., 2004). $Mdr2^{-/-}$ mice expressing a liver-specific IκBα-supper-repressor, which sequesters NF-κB dimers in the cytoplasm, dramatically decreased HCC progression but not tumor initiation. This study provided evidence that NF-κB becomes essential for tumor promotion by protecting transformed hepatocytes against apoptosis via upregulation of the anti-apoptotic proteins GADD45β, A1 and c-IAP1 (Pikarsky et al., 2004).

In contrast, the IKK subunit NF-κB essential modulator (NEMO), which is essential for NF-κB activation, has been identified as a tumor suppressor in the liver. Liver-specific ablation of the NEMO/IKKγ subunit in mice was shown to cause spontaneous development of chronic steatohepatitis followed by HCC, owing to an increase in hepatocyte apoptosis and subsequent reactive proliferation prompted by FAS-associated death domain protein (FADD)-mediated and oxidative-stress-related liver injury (Luedde et al., 2007). Similarly, in a mouse model of DEN-induced hepatocarcinogenesis, hepatocyte-specific deletion of IKKβ resulted in a three-fold increase in tumor load and size, due to the JNK-mediated increase in ROS accumulation, hepatocyte death and compensatory proliferation (Maeda et al., 2005). These studies reinforce the observation that in some instances, especially in the absence of chronic inflammation, NF-κB can protect against HCC development.

4.1.3.3 NF-κB function in the tumor microenvironment

Constitutive activation of NF-κB not only occurs in tumor cells, but also in the cells comprising the tumor microenvironment. Furthermore, NF-κB activation in premalignant or malignant hepatocytes can be induced by cytokines and inflammatory

factors emanating from surrounding nonparenchymal liver cells. To this effect, hepatocarcinogenesis could be partially attributed to the activation of NF-κB in intrahepatic lymphocytes in the transgenic mouse model of liver-specific LT-α and LT-β overexpression. In this scenario, liver-infiltrating lymphocytes were responsible for the release of pro-inflammatory cytokines and chemokines that led to the recruitment and activation of myeloid cells, which subsequently caused tissue destruction and hepatocyte proliferation. Hence, lymphocyte depletion in this context abrogated HCC development in these mice (Haybaeck et al., 2009). Additionally, the observed NF-κB activation in hepatocytes of $Mdr2^{-/-}$ mice was shown to depend on paracrine TNFα stimulation derived from non-parenchymal cells, such as Kupffer cells (Mauad et al., 1994; Pikarsky et al., 2004). In this setting, the sustained inflammatory process observed was dependent on NF-κB activation in infiltrating immune cells. Similarly, in $Mdr2^{-/-}$ mice ablation of IL-6 in monocytes suppressed the expression of common NF-κB target genes, such as IL-6, TNFα, INF-γ and IL-1α, and thus decreased macrophage infiltration, spontaneous liver damage and HCC formation (Kong et al., 2016). Moreover, as described previously, in the DEN-induced mouse model of HCC ablation of IKKβ led to compensatory proliferation of hepatocytes, which prompted tumor initiation. In this context, the liver damage caused by DEN was shown to activate NF-κB in liver resident Kupffer cells, which in turn produced and secreted mitogenic factors and cytokines that promoted compensatory proliferation (Maeda et al., 2005). In fact, deletion of IKKβ both in hepatocytes as well as in Kupffer and B cells reduced 4-fold the HCC load, thus highlighting the role of NF-κB in lymphoid and myeloid cells to aid in HCC development. Finally, the presence of ectopic lymphoid structures (ELSs), which are leukocyte aggregates that direct B- and T-cell responses, have been shown to be an indicative of poor prognosis in HCC patients (Patman, 2015). Interestingly, NF-κB signaling has been found essential for the generation of hepatic ELSs, since enforced hepatocyte-specific IKKβ expression in a transgenic mouse model increased the presence of ELSs in the liver. This, in turn, correlated with liver damage, increased hepatocyte proliferation and HCC development (Finkin et al., 2015). These hepatocarcinogenic effects were attributed to the supportive inflammatory microniche created by ELSs for malignant hepatocytes, considering that ablation of lymphocytes resulted in a significant attenuation of HCC formation. In this scenario, LT-β, a well-known activator of the non-canonical NF-κB pathway, was identified as an important regulator of ELS assembly (Finkin et al., 2015). All in all, the

evidence highlights the crucial role of the NF-κB pathway in hepatocarcinogenesis also when activated in immune cells.

4.2 The transcription factor NF-κB

The NF-κB family of inducible transcription factors (TFs) is comprised of five members, namely NF-κB1 (p105/p50), NF-κB2 (p100/p52), RelA (p65), RelB and c-Rel. While RelA, RelB and c-Rel are produced as mature proteins and contain a transactivation domain (TAD), NF-κB1 and NF-κB2 are synthesized as inactive precursors that need to be proteolytically processed to produce mature TFs. The five members form homo- or heterodimers that bind to κB elements in promoter or enhancer regions in the DNA to induce or repress gene transcription. All NF-κB proteins contain at their N-terminal a conserved Rel-homology domain (RHD) which mediates dimerization, DNA binding, IκB interaction and nuclear localization. Whereas RelA, RelB and c-Rel all have TAD domains in their C-terminus, both p105 and p100 contain ankyrin repeats at their C-terminal region, allowing them to function in a similar fashion to inhibitor of κB (IκB) proteins (Ghosh & Hayden, 2008; Gilmore, 2006; Oeckinghaus & Ghosh, 2009; Shih et al., 2011). Once processed, p50 and p52 are capable of translocating to the nucleus and perform TF functions (Savinova et al., 2009).

Under physiological conditions, NF-κB members are commonly found sequestered in the cytoplasm through interaction with the ankyrin-rich regions of cytoplasmic IκB proteins IκBα, IκBβ and IκBε. These inhibitory proteins function by masking the nucleus localization signal (NLS) found in the RHD of the NF-κB subunits, thus remaining inactive (Ghosh & Hayden, 2008; Huxford & Ghosh, 2009). NF-κB can become activated through two different pathways: the canonical or classical pathway, and the non-canonical or alternative pathway (Hoesel & Schmid, 2013; Shih et al., 2011). Both have in common an upstream regulatory step that involves activation of the IKK complex, which consists of two catalytic subunits, IKKα and IKKβ, and a regulatory subunit, IKKγ, also known as NEMO. Activation of the classical pathway occurs upon reception of stimuli including cytokines (IL-1α, IL-1β, IL-17, etc.), TNFR ligands, pattern recognition receptor (PRR) ligands, such as lipopolysaccharide (LPS) and DNA fragments, or upon TCR and BCR stimulation. In brief, stimulation of these membrane receptors leads to activation of TGFβ-activated kinase 1 (TAK1), which forms a

complex with the regulatory subunits TAK1-binding protein (TAB)-1 and TAB2. TAB2 then facilitates recruitment of the IKK complex to TAK1 via the poly-ubiquitin chains of NEMO. Subsequently, TAK1-dependent phosphorylation activates IKKβ, which in turn phosphorylates IκBα at serines 32 and 36, thus leading to its ubiquitination and degradation in proteasome. Degradation of IκBα releases the NF-κB dimers (mainly p50/RelA and p50/c-Rel heterodimers), allowing them to translocate to the nucleus, where they initiate gene transcription (Brown et al., 2008; Hoesel & Schmid, 2013; Shih et al., 2011). Conversely, the non-canonical NF-κB pathway is only activated by a specific group of stimuli that include ligands of LTβR, BAFFR, CD40 and RANK. It is considered a supplementary signaling axis that cooperates with functions of the adaptive immune system. In this scenario, downstream signaling through NF-κB inducing kinase (NIK) activates IKKα. Together they induce p100 phosphorylation and ubiquitination for the degradation of its C-terminal domain, which contains the ankyrin repeats. Processing of p100 leads to the generation of p52, which is released in the cytoplasm and will translocate into the nucleus as p52/RelB heterodimers (Shih et al., 2011; Sun, 2017).

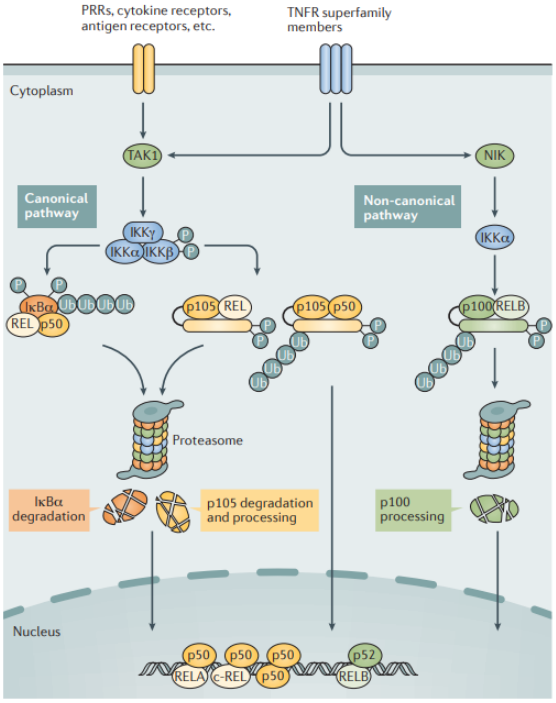

Figure 18.1. Canonical and non-canonical NF-κB pathways. The canonical NF-κB pathway responds to a variety of stimuli activating PRRs, cytokine receptors and antigen receptors. Upon receptor engagement, these activate TAK1, which ultimately leads to the phosphorylation and activation of IKKβ for the subsequent phosphorylation of IκBα. IκBα is then targeted for ubiquitin-dependent degradation in the proteasome, thus allowing for the translocation of the p50/RelA and p50/c-Rel heterodimers into the nucleus to initiate target

gene transcription. In contrast, the non-canonical NF-κB pathway is selectively activated by a subset of tumor necrosis factor receptor (TNFR) superfamily members that activate the downstream effector NIK. NIK subsequently phosphorylates and activates IKKα, which in turn phosphorylates p100 thus inducing its processing in proteasome, leading to the generation of p52. The non-canonical pathway ultimately leads to the translocation of p52/RelB heterodimers into the nucleus. Ub, ubiquitin. Obtained from (Sun, 2017).

Once in the nucleus, the NF-κB dimers bind κB elements in the DNA to initiate transcription. In some instances, target gene activation requires assistance from other TFs including activator protein 1 (AP1) members, STAT and interferon regulatory factors (IRFs) (Grivennikov & Karin, 2010; Oeckinghaus et al., 2011; Taniguchi & Karin, 2018). Common NF-κB target genes include genes encoding for pro-inflammatory cytokines (TNF, IL-1, IL-6, etc.), chemokines (IL-8, CCL2, CCL3, CCL5, CXCL1 and CXCL2) and enzymes (like cyclooxygenase 2 and inducible nitric oxide synthase), growth factors, proliferation-related genes (such as *MYC* and cyclin D1), anti-apoptotic proteins (Bcl-X_L, Bcl-2, FLIP), angiogenic factors, adhesion molecules and matrix metalloproteinases (Liu et al., 2017). Owing to this wide range of target genes, constitutive NF-κB activation has incredibly detrimental effects, and can lead to chronic inflammation and tumorigenesis. Interestingly, pathogenic NF-κB activation is rarely due to genetic alterations directly on NF-κB family members, but rather due to defects affecting upstream regulators (Taniguchi & Karin, 2018).

4.3 Atypical IκB members

While classical IκB proteins are ubiquitously expressed and exert their functions in the cytoplasm, where they bind to NF-κB dimers impeding their nuclear translocation, atypical IκB members, namely Bcl-3, IκBNS, IκBζ, IκBη and IκBL, are expressed predominantly in the nucleus in response to a broad variety of stimuli (Hinz et al., 2012). Under physiological conditions, atypical IκBs display low expression levels, except for IκBη, which is found constitutively expressed at basal levels in multiple tissues (Yamauchi et al., 2010). Upon activation of the NF-κB signaling pathway in response to a variety of inflammatory stimuli, the expression of atypical IκBs is greatly upregulated in the nucleus, where they will perform their functions (Hayden & Ghosh, 2008; Hinz et al., 2012). Atypical IκBs can function as transcriptional co-activators or co-repressors, either by stabilizing p50 homodimers on κB sites and facilitating NF-κB interaction with other factors, or by removing DNA-bound hetero- or homodimers,

respectively. Thus, their main role is to provide fine-tuning for late NF-κB-dependent gene regulation (Hinz et al., 2012; Willems et al., 2016).

4.3.1 The atypical protein IκBζ

IκBζ, which is encoded by *NFKBIZ* (also known as *MAIL*), possesses a high degree of homology with the other atypical IκB proteins Bcl3 and IκBNS (Haruta et al., 2001; Kitamura et al., 2000; Muta et al., 2003). Structurally, IκBζ is a nuclear protein that contains seven ankyrin repeats, a TAD domain in its central region that confers intrinsic transcriptional activity, and a nuclear translocation sequence (NLS) in its N-terminus (Motoyama et al., 2005; Muta et al., 2003). IκBζ exists as 3 different splice variants: IκBζ(S), IκBζ(L) and IκBζ(D). All of them share the presence of the ankyrin repeats in their C-terminal region and differ in their central or N-terminal domain. The shorter IκBζ(S) variant lacks the first 99 amino-acids from the N-terminus, while the rare IκBζ(D) isoform lacks a big segment in the central region that includes the transactivation domain, thus behaving as a dominant negative isoform (Chapman et al., 2010; Motoyama et al., 2005).

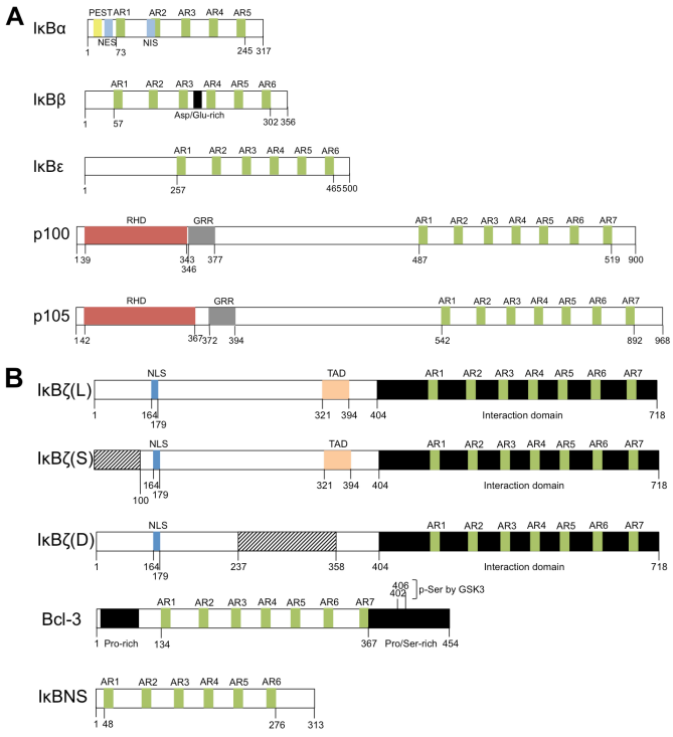

Figure 18.2. Schematic representation of the IκB family of proteins. Structural representation of the (A) cytoplasmic or typical IκB proteins and (B) nuclear or atypical IκB protein members. PEST, domain rich in proline, glutamic acid, serine and threonine; AR, ankyrin-repeat; NES, nuclear export signal; NIS, nuclear import signal; GRR, glycine-rich region. Obtained from (Willems et al., 2016).

NFKBIZ constitutes an NF-κB primary response gene that, despite being barely detectable in resting cells, is robustly induced in the nucleus upon inflammatory stimulation of IL-1R, IL-17R, BCR, TCR or TLR 2, 4, 5, 7 and 9, but not upon stimulation with TNF-α (Eto et al., 2003; Irie et al., 2000; Kitamura et al., 2000; Yamamoto et al., 2004). Engagement of IL-1R/TLR elicits the recruitment of the adaptor protein MyD88 to the Toll/interleukin-1 receptor (TIR). MyD88 subsequently recruits and activates IL-1 receptor-associated kinase (IRAK)4 and IRAK1, the latter of which then phosphorylates TRAF6. TRAF6 phosphorylation ultimately leads to TAK1-mediated IKK phosphorylation and thus, activation of the canonical NF-κB pathway, thereby inducing IκBζ expression. In fact, it has been shown that ablation of MyD88 completely abolishes IL-1 and LPS-mediated IκBζ induction (Yamamoto et al., 2004). However, NF-κB-dependent induction of IκBζ transcription is not enough to ensure IκBζ expression at protein level, since stabilization of IκBζ mRNA is a requirement for it to be fully functional (Yamazaki et al., 2005). In this regard, activation of IRAK1/4 downstream of MyD88 was proven to be essential in the post-transcriptional regulation of a 165-nucleotide cis-element found in the 3'-UTR region of IκBζ, which confers stability to its mRNA (MaruYama et al., 2016; Ohba et al., 2012). However, further studies are required to provide insights into other mechanisms regulating mRNA stability and translational activation downstream of distinct immune receptors and cell types.

MicroRNAs (miRNAs), which are non-coding RNA molecules that mediate post-transcriptional regulation of gene expression via translational inhibition or induction of mRNA cleavage, have also been shown to regulate IκBζ expression in certain cell types. For instance, a study in Hep2G cells revealed that miR-124 targets the 3'-UTR of IκBζ resulting in its translational repression, while miR-223 was shown to regulate NFKBIZ expression in glioblastoma multiforme (Huang et al., 2015; Lindenblatt et al., 2009). Moreover, a study showed that roquin-1 cooperates with the endonuclease regnase-1 in the recognition and cleavage of *NFKBIZ* mRNA, thus negatively regulating IκBζ expression. In this setting, activation of MALT1 downstream of the TCR in $CD4^+$ T cells led to the cleavage and degradation of both roquin-1 and regnase-1, thereby allowing the stabilization and expression of IκBζ, which enhances T_H17 differentiation (Garg et al., 2015; Jeltsch et al., 2014). Hence, there are several cellular mechanisms in place to regulate the expression of IκBζ, not only at a

transcriptional, but also at a post-transcriptional level. Once expressed, IκBζ mediates the removal or recruitment of NF-κB subunits and gene regulators to promoter regions to regulate the expression of a specific subset of NF-κB secondary response genes (Yamamoto et al., 2004; Yamazaki et al., 2008).

In the nucleus, IκBζ requires the interaction with NF-κB members in order to gain access to the promoter regions of its target genes and thereby regulate transcription. Therefore, NF-κB is not only required for IκBζ induction, but also contributes in the transcriptional upregulation of IκBζ genes, since silencing of the p50 or p65 subunits has been shown to downregulate or abrogate the expression of certain IκBζ target genes (Eto et al., 2003; Yamazaki et al., 2008). IκBζ preferentially forms complexes with p50/p50 homodimers (Kohda et al., 2016; Motoyama et al., 2005; Yamamoto et al., 2004). Nevertheless, it has also been shown to interact with the p52 subunit in ABC DLBCL cell lines, implying a role in the non-canonical NF-κB pathway (Nogai et al., 2013). Conversely, IκBζ binding with the p65 subunit has been reported to negatively affect its transcriptional activity in the nucleus by inhibiting the binding of p65/p50 heterodimers to the DNA (Totzke et al., 2006; Yamazaki et al., 2001). Contrary to this observation, another study reported that interaction of IκBζ with p65/p50 dimers induces IFNγ production in NK cells in response to IL-12/IL-18 stimulation (Kannan et al., 2011). Additionally, IκBζ has been shown to recruit and modulate other TFs. For instance, it was reported that IκBζ recruits the transcription factor CCAAT/enhancer binding protein beta (C/EBPβ) to the promoters of secondary response genes, thereby inducing transcriptional activation (Matsuo et al., 2007; Yamazaki et al., 2008). Such evidence highlights the dual functions of IκBζ either as an activator or repressor of transcription, which is likely dependent on the cell type, stimulus or its interaction with other cofactors. All in all, this poses an additional layer of control for the NF-κB pathway.

Studies have further provided evidence supporting a role of IκBζ mediating epigenetic changes that allow for the transcription of secondary response genes. In particular, IκBζ was shown to induce H3K4 trimethylation, which is associated with active transcription, at the promoters of secondary response genes to mediate the recruitment of the preinitiation complex comprising p65, RNA polymerase II (RNA-polII) and TATA-binding protein (TBP) (Kayama et al., 2008). Furthermore, the expression

of the secondary response genes *IL-6* and *IL-12b* in macrophages was shown to require the interaction of IκBζ with the histone-remodeling complex SWI/SNF via its members Brg1 and Akirin2 (Tartey et al., 2014). Another study highlighted the importance of post-transcriptional modifications in regulating the binding affinity of IκBζ to the histone deacetylase HDAC1. Specifically, the Ras/MAPK-mediated Thr189/193/195 phosphorylation in the N-terminal of IκBζ was shown to enhance its binding to HDAC1 in keratinocytes, thus leading to the repression of specific IκBζ target genes including *IL-6*, *CCL2*, *CXCL5* and *S100A9* (Grondona et al., 2020). Hence, the IκBζ-mediated recruitment of interaction partners involved in chromatin remodeling seems to be an important step for the regulation of a selective subset of NF-κB secondary response genes and post-translational modifications are likely important for the regulation of such interactions.

Through the modulation of NF-κB subunits and recruitment of additional cofactors, IκBζ induces a specific subset of NF-κB secondary response genes that are expressed in a delayed manner, due to the fact that they require *de novo* protein synthesis. Notable among the identified IκBζ target genes are well-characterized inflammatory and immunity players such as *IL-6*, lipocalin-2 (*Lcn2*), granulocyte-macrophage colony stimulating factor (GM-CSF or *Csf2*), granulocyte colony stimulating factor (G-CSF or *Csf3*), IL-12P40 (*IL-12b*), IL-8, IL-36 and IL-17C (Alexander et al., 2013; Annemann et al., 2016; Hildebrand et al., 2013; Hörber et al., 2016; Müller et al., 2018).

4.3.2 Role of IκBζ in cancer

As mentioned in previous sections, NF-κB activation in cancer cells and tumor microenvironment plays an essential role in the development of inflammatory processes and hepatocarcinogenesis. Owing to the role of the NF-κB primary target gene IκBζ in the induction of cytokine and chemokine production, its expression has been found to be associated with the development and progression of certain cancer types. For instance, the activated B cell-like (ABC) subtype of diffuse large B-cell lymphoma (DLBCL), characterized by its constitutive NF-κB activation, exhibits IκBζ overexpression, which has been observed to contribute to the survival of these cells via induction of growth-promoting cytokines, cell cycle-regulatory proteins and anti-apoptotic proteins (Nogai et al., 2011, 2013). IκBζ overexpression has also been observed in cases of adult T-cell leukemia (ATL), likely enhancing tumorigenesis

through the induction of GBP-1 and STAT1 expression (Kimura et al., 2013). Conversely, downregulation of *NFKBIZ* has been observed in Mycosis Fungoides (MF), the most common type of primary cutaneous T-cell lymphoma (CTCL), possibly enhancing NF-κB activity, an event which is frequently observed in this tumor type (van Kester et al., 2012). Furthermore, IL-1β induction of IκBζ in the liver cancer cell line HepG2 was linked to the downregulation of miR-124a. In this context, miR-124a was found to control IκBζ expression via translational inhibition. MiR-124a has also been shown to be silenced in glioblastoma patient specimens, thus likely contributing to the observed IκBζ upregulation in this tumor entity (Lindenblatt et al., 2009; Tivnan et al., 2014). The high levels of *NFKBIZ* identified in glioblastoma multiforme cell lines can also be attributed to the observed miR-223 silencing in this tumor type, which is also thought to target NFKBIZ mRNA (Huang et al., 2015). Nevertheless, the role of IκBζ in cancer development and progression could be complex. Some studies have found that IκBζ can inhibit the activation of STAT3 (Z. Wu et al., 2009), a well-known TF that has an essential role in inflammatory processes and is upregulated in several tumors (Huynh et al., 2019; H.-Q. Wang et al., 2022; H. Yu et al., 2014). Furthermore, IκBζ has been described as a critical regulator of SASP expression by inducing IL-6 and IL-8 (Alexander et al., 2013). However, SASP, which is associated with a release of important growth factors and cytokines, can either have an anti-tumorigenic role by eliciting an immune response to clear tumor cells, or, paradoxically, promote tumor progression depending on the tumor stage and context (C. A. Schmitt et al., 2022a). Therefore, IκBζ might have contradictory roles in cancer as observed with its inducer NF-κB.

4.4 Functions of Brd4 and its relationship with NF-κB

Bromodomain containing protein 4 (Brd4) is a member of the bromodomain and extra-terminal (BET) family of proteins that also includes Brd2, Brd3 and Brdt. BET proteins are characterized by containing two bromodomains (BD1 and BD2) which bind to acetylated lysine residues both in histone and non-histone proteins. The extra-terminal (ET) domain allows interaction of these proteins with chromatin regulators (Ali et al., 2022; Donati et al., 2018; N. Wang et al., 2021). Brd4 can also interact in a BD-independent fashion either through its phosphorylation-dependent

interaction domain (PDID) or a basic residue-rich interaction domain (BID) both located in the central region.

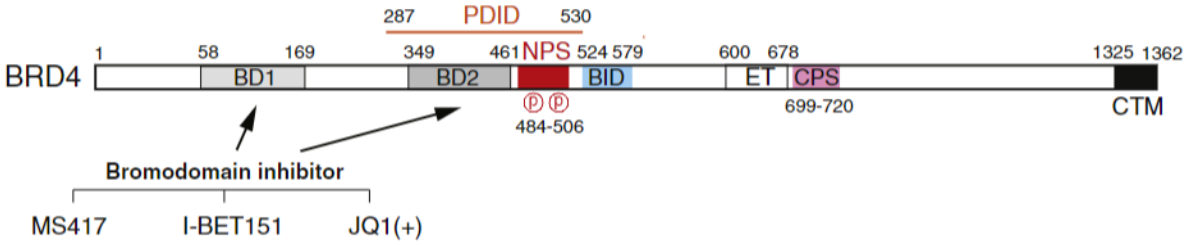

Figure 18.3. Schematic representation of Brd4. Structural representation of the BET protein member Brd4, including BD1/BD2-targeting bromodomain inhibitors. CPS, C-terminal phosphorylation sites; CTM, C-terminal motif; NPS, N-terminal cluster of CK2 phosphorylation sites. Obtained from (Chiang, 2016).

Brd4 becomes activated by phosphorylation of its N-terminal phosphorylation sites (NPS), thereby unmasking its bromodomains to allow interaction with chromatin and specific transcription factors (Chiang, 2016; S.-Y. Wu et al., 2013). Once active, Brd4 acts as an epigenetic reader, binding to acetylated histones and recruiting and regulating transcription factors or chromatin remodeling complexes to promote gene transcription (Filippakopoulos & Knapp, 2014).

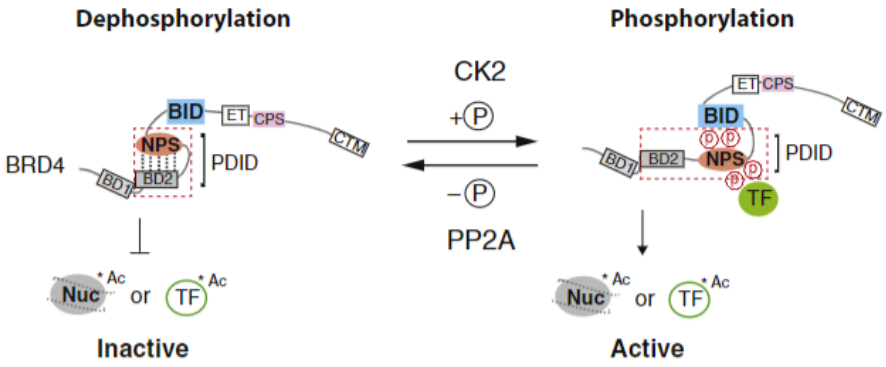

Figure 18.4. Schematic representation of Brd4's active configuration. When dephosphorylated, the NPS masks BD2, thus impairing the chromatin binding activity of BD1 and the interaction of Brd4 with acetylated transcription factors. The casein kinase 2 (CK2)-mediated phosphorylation of the NPS allows for a change in configuration, whereby NPS switches its contact to the BID, unmasking BD2. This configuration allows for the recruitment of transcription factors. Nuc, nucleosome; TF, transcription factor; Ac, acetylation; PP2A, protein phosphatase 2. Obtained from (Chiang, 2016).

One way in which Brd4 activates transcription is through recruitment of positive-transcription elongation factor b (p-TEFb), a complex comprised of cyclin T1 and cyclin-dependent kinase 9 (Cdk9), which can otherwise be found sequestered by the inhibitory ribonucleoprotein complex 7SK/HEXIM (Jang et al., 2005; Schröder et al., 2012; Z. Yang et al., 2005). Once Brd4 interacts with p-TEFb, it directs it to the transcription start sites (TSSs) in the DNA for docking, thus facilitating the Cdk9-dependent phosphorylation and release of RNA-polymerase II (RNA-pol II) into active transcription (Dey et al., 2009; Donati et al., 2018; Jonkers & Lis, 2015; Zhiyuan et al., 2008).

One proven interaction partner of Brd4 is NF-κB. A study reported that Brd4 interacts in a bromodomain-dependent manner with the NF-κB subunit RelA via its acetylated lysine-310 (Bo et al., 2009; Hajmirza et al., 2018). Interestingly, this binding was critical for the expression of typical inflammatory genes and could be attributed to the Brd4-mediated recruitment of Cdk9 to phosphorylate, and thereby activate, RNA-pol II (Bo et al., 2009). Subsequent studies have provided evidence indicative of Brd4 controlling a transcriptional module similar to that of NF-κB in oncogene-induced senescent cells (Tasdemir et al., 2016). Interestingly, the observed Brd4-regulated SASP genes are well-known NF-κB and/or IκBζ target genes. Considering this observation, the question remains whether Brd4 can directly interact with IκBζ, and whether inhibition of Brd4 could be a potential treatment strategy in cancers with a dysregulated NF-κB pathway.

4.5 Aims of the study

Hepatocellular carcinoma is the most common type of primary liver tumor. Owing to its molecular complexity and aggressiveness, the difficulty for diagnosis and the lack of effective treatment strategies for patients, HCC remains one of the deadliest cancers worldwide. HCC is a well-known inflammation-linked cancer, where the great majority of the associated risk factors pose a hepatocarcinogenic burden due to the prolonged inflammation and fibrosis they provoke. In this regard, activation of the NF-κB pathway, both in hepatocytes and immune cells infiltrating the liver parenchyma, has been shown to be important for the development and progression of HCC in the context of liver inflammation. The NF-κB primary target gene IκBζ is strongly induced in the nucleus in response to a wide variety of inflammatory stimuli, thus mediating the induction of a subset of NF-κB secondary response genes that comprise a set of cytokines, chemokines and factors that participate in inflammatory processes. Taking this into consideration, investigating the induction and functions of IκBζ in human HCC cell lines, uncovering novel target genes in the setting of liver cancer and investigating the importance of this atypical IκB protein *in vivo* is pivotal to elucidate its role in hepatocarcinogenesis.

Therefore, the aims of the study were to:

- Investigate the molecular mechanisms of IκBζ function, by identifying and validating novel interaction partners.
- Map the binding sites with its interaction partners and elucidate the functional consequences of these interactions.
- Study the functional role of IκBζ in OIS in a HCC setting.
- Identify HCC-relevant IκBζ-induced target genes and cytokines.
- Uncover effects of liver-specific IκBζ overexpression in murine models.

5 Results

5.1 Potential IκBζ interaction partners

The atypical nuclear IkB protein IκBζ lacks a typical DNA-binding domain and requires association with NF-κB subunits such as p50 homodimers to access DNA-regulatory regions (Motoyama et al., 2005; Willems et al., 2016). Owing to its transactivation domain, IκBζ can induce the transcription of NF-κB secondary response genes. To exploit this function, however, IκBζ has been proposed to bind to a series of interaction partners and epigenetic modifiers (Grondona et al., 2020; Kayama et al., 2008; Tartey et al., 2014). Our research group previously demonstrated that induction or overexpression of IκBζ is sufficient and required to drive the expression of a subset of essential NF-κB target genes. Furthermore, several plausible IκBζ interaction partners were identified in a large pull-down experiment performed on unstimulated and IL-1β-stimulated cells. Amongst the hits reported stood out the epigenetic reader Brd4 and the transcription factor STAT3. Thus, we next focused on further validating and investigating the binding of IκBζ to Brd4 and STAT3.

5.1.1 IκBζ induction

IκBζ has been shown to be induced upon stimulation with cytokines such as IL-1β and IL-17 or treatment with LPS. Hence, we were interested in examining whether IκBζ could also be induced in this manner in the context of liver cancer. For this, we treated two different HCC cell lines (SMMCs and Huh7s) with the cytokines IL-1α and IL-1β. The SMMC cell line exhibited IκBζ induction just 1 h after stimulation with recombinant human (rh) IL-1β, while in Huh7 cells IκBζ was induced after 2 h treatment (Fig. 19A). Similarly, rhIL-1α achieved IκBζ induction just after 1 h in SMMCs, while it was expressed 4 h after treatment in Huh7 cells (Fig. 19A). Moreover, we could detect IκBζ expression in primary hepatocytes after treating them for 4 h with rhIL-1β (Fig. 19B). Next, to determine the half-life of IκBζ, we treated SMMC cells for 2 h with rhIL-1β to induce IκBζ expression after which we subjected them to cycloheximide (CHX) treatment, which is a well-known protein synthesis inhibitor. Immunoblotting analyses revealed that IκBζ expression decreased just 1.5 h after induction and was undetectable after 3.5 h (Fig. 19C). Thus, IκBζ is promptly degraded and has a fast turnover in HCC cells. Interestingly, cotreatment with the Brd4 inhibitor JQ1 led to a

faster degradation of IκBζ. Altogether, our results demonstrated the efficiency of both IL-1α and IL-1β to induce IκBζ in the context of HCC and its short half-life, proving its requirement for *de novo* protein synthesis.

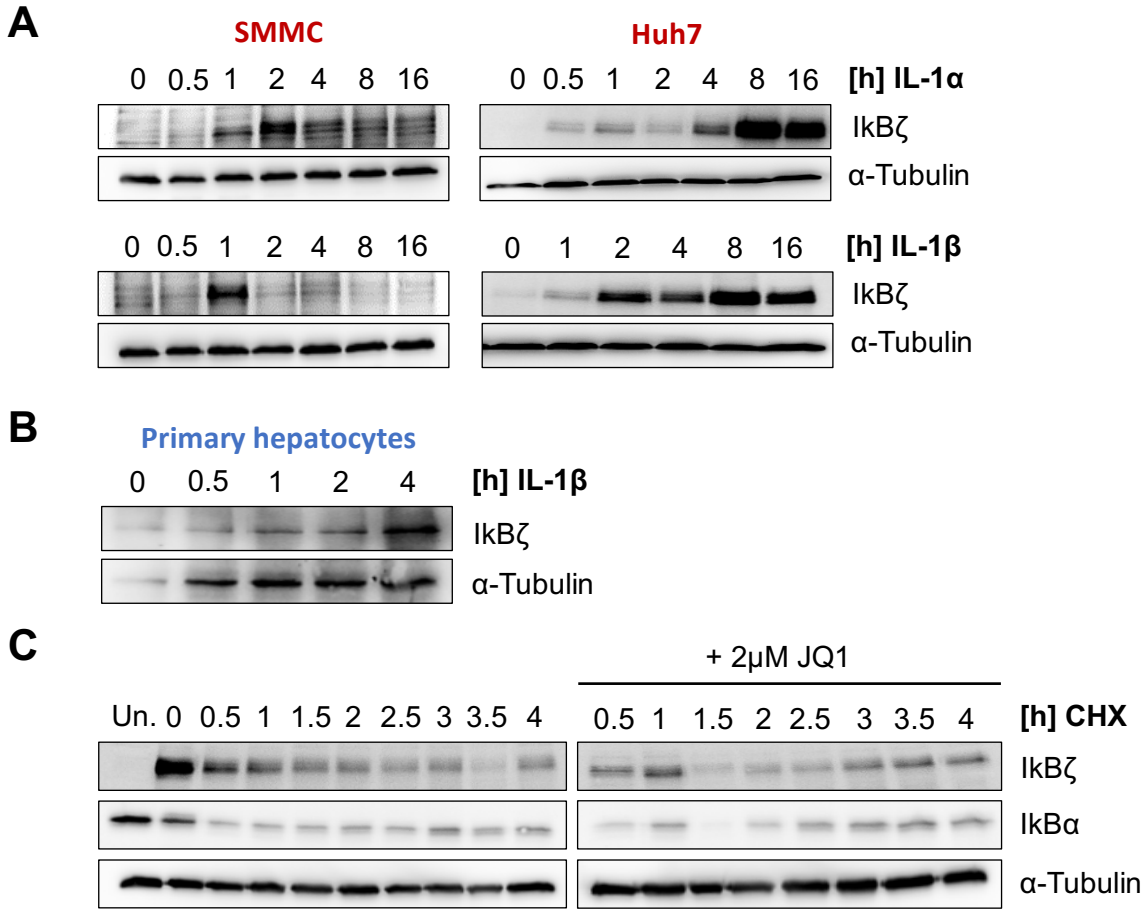

Figure 19. IL-1α and IL-1β induce IκBζ in human HCC cells. (A) SMMC and Huh7 cells were treated with 10 ng/ml rhIL-1α or 2.5 ng/ml rhIL-1β, as indicated, and IκBζ expression was assessed by immunoblot analysis. **(B)** Human primary hepatocytes were treated with 2.5 ng/ml rhIL-1β as indicated, and IκBζ expression was assessed by immunoblot analysis. **(C)** Huh7 cells were pre-treated for 2 h with 2.5 ng/ml rhIL-1β and then treated every 30 min with 10 ng/ml CHX. IκBζ and IκBα expression was then assessed by immunoblotting. **(A-C)** Tubulin served as loading control.

5.1.2 IκBζ interaction partners

5.1.2.1 Brd4 binding to IκBζ

Previous research performed by our working group revealed that IκBζ requires the presence of Brd4 in order to effectively induce the expression of a group of IκBζ target genes (data not published). To investigate whether IκBζ and Brd4 physically interact in the nucleus for the regulation of IκBζ-related genes, we performed a FLAG pull-down assay in HEK293T cells expressing FLAG-tagged Brd4 in combination with

Strep-tagged p50 and Strep-tagged IκBζ. By immunoblotting, we could detect both p50 and IκBζ interaction with Brd4 (Fig. 20A). Interestingly, the presence of p50 seemed to reinforce the binding of Brd4 with IκBζ. Moreover, treatment with the bromodomain inhibitors JQ1 or iBET-762 did not impair the interaction between Brd4 and IκBζ (Fig. 20B-D). Altogether, these results suggest that the interaction between Brd4, IκBζ and p50 is bromodomain independent.

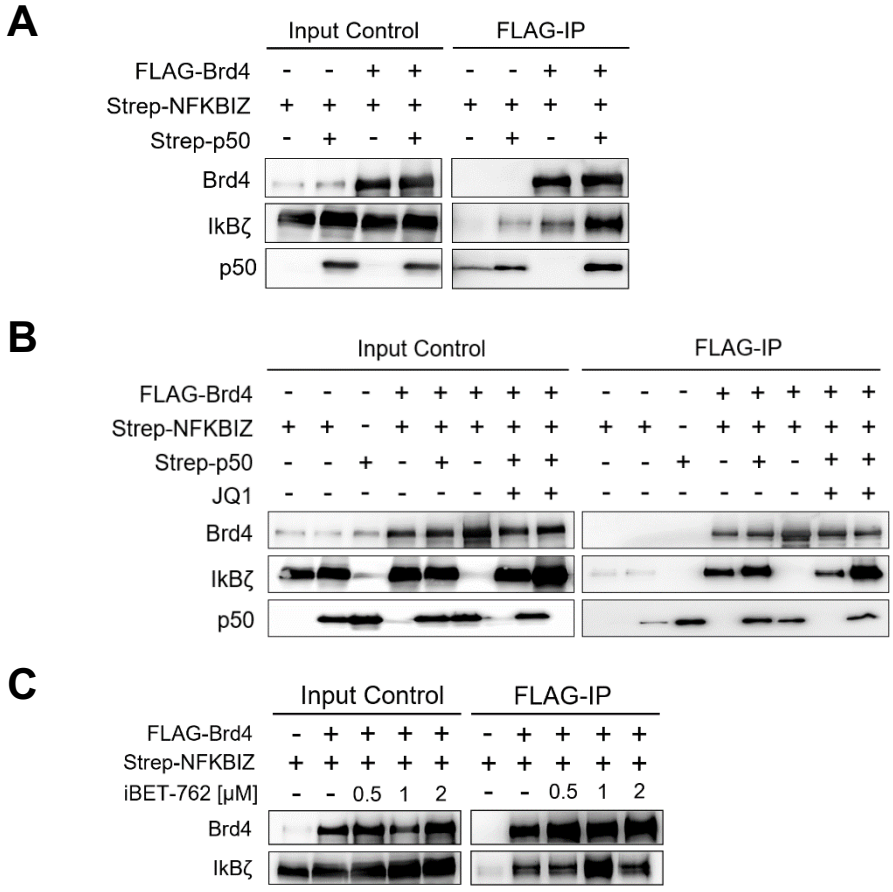

Figure 20. IκBζ interacts with Brd4 in a bromodomain-independent manner. HEK2932T cells were transiently transfected with **(A-D)** FLAG-tagged Brd4 and Strep-tagged IκBζ alone or in combination with **(A-B)** Strep-tagged p50. **(B-D)** HEK293T cells were treated with **(B)** 2 μM JQ1, or **(C)** 0.5, 1 or 2 μM iBET-762 for 24 h. **(A-C)** Expression of IκBζ, Brd4 and p50 was assessed by immunoblot analysis.

5.1.2.2 Cdk9 binding to IκBζ

Because Brd4 is essential for the activation of the p-TEFb complex, which allows the release of RNA-polymerase II into active transcription (Z. Yang et al., 2005), we next studied the interaction between IκBζ, Brd4 and the p-TEFb complex member Cdk9. To assess interaction, a FLAG pull-down assay was performed in HEK293T cells expressing FLAG-IκBζ, Strep-Brd4 and HA-Cdk9, and revealed that Cdk9 precipitates with IκBζ even in the absence of Brd4 (Fig. 21A). Furthermore, treatment with JQ1 did not interfere with the interaction between IκBζ and Cdk9 (Fig. 21A). Thus, the interaction between the two is neither Brd4 nor bromodomain-dependent; proving that Cdk9 can directly bind to IκBζ.

In order to corroborate these interactions, IκBζ overexpression was induced in Huh7/Tet-ON-IκBζ cells via 48 h doxycycline treatment followed by immunoprecipitation for endogenous Brd4. Strikingly, Brd4 co-precipitated with IκBζ and Cdk9, proving interaction between the three (Fig. 21B). Cotreatment with JQ1 failed to impair the binding of Brd4 with IκBζ and Cdk9, further indicating that this interaction is bromodomain-independent.

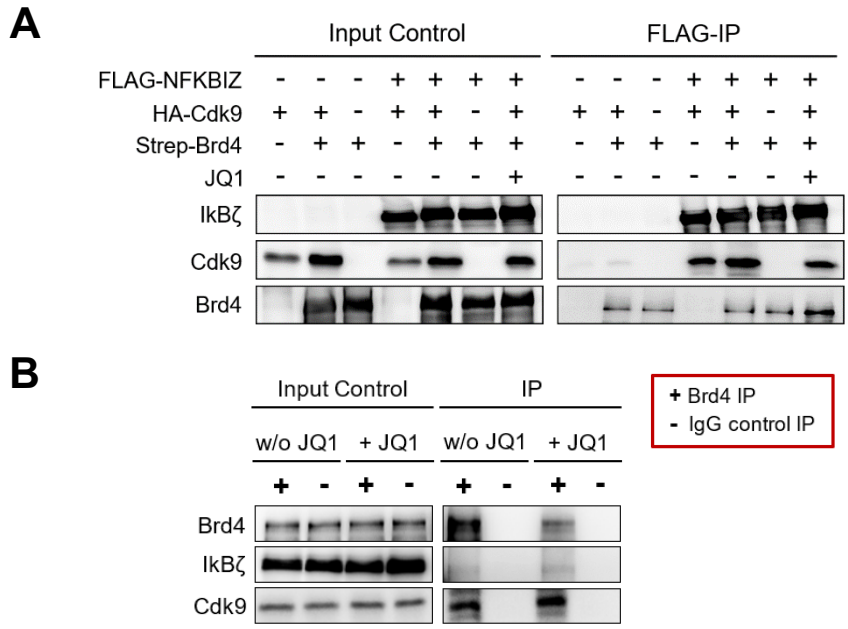

Figure 21. IκBζ and Brd4 interact with Cdk9 in a bromodomain-independent manner. (A) HEK2932T cells were transiently transfected with FLAG-tagged IκBζ, HA-tagged Cdk9 and Strep-tagged Brd4, and treated with 2 μM JQ1 for 48 h. Expression of IκBζ, Brd4 and Cdk9 was assessed by immunoblot analysis. **(B)** Huh7/Tet-ON-IκBζ cells were initially treated for 24 h with 1 μg/ml doxycycline (dox) alone or in combination with 2 μM JQ1. After 24 h, cells were treated for 2 h with 2.5 ng/ml rhIL-1β. Brd4 antibody was used for immunoprecipitation (IP) of endogenous Brd4. IgG antibody was used as negative IP control.

5.1.2.3 STAT3 binding to IκBζ

Considering that STAT3 was identified as a potential IκBζ interaction partner in the large pull-down assay performed by our research group, we hypothesized that STAT3 requires binding with IκBζ in order to transactivate the expression of a subset of its target genes. To prove interaction between the two, we co-transfected HEK293T cells with FLAG-Brd4, Strep-IκBζ and Strep-STAT3 expression plasmids and performed a FLAG pull-down. Interestingly, not only did STAT3 interact with IκBζ, but it was also able to bind Brd4 even in the absence of IκBζ (Fig. 22A). In fact, presence of IκBζ seemed to weaken the interaction between STAT3 and Brd4, especially after treatment with JQ1 (Fig. 22A). However, increasing the amount of Strep-Brd4 transfected did not alter the binding to STAT3 or IκBζ (Fig. 22B), indicating that Brd4 does not bind to either of the two in a competitive manner.

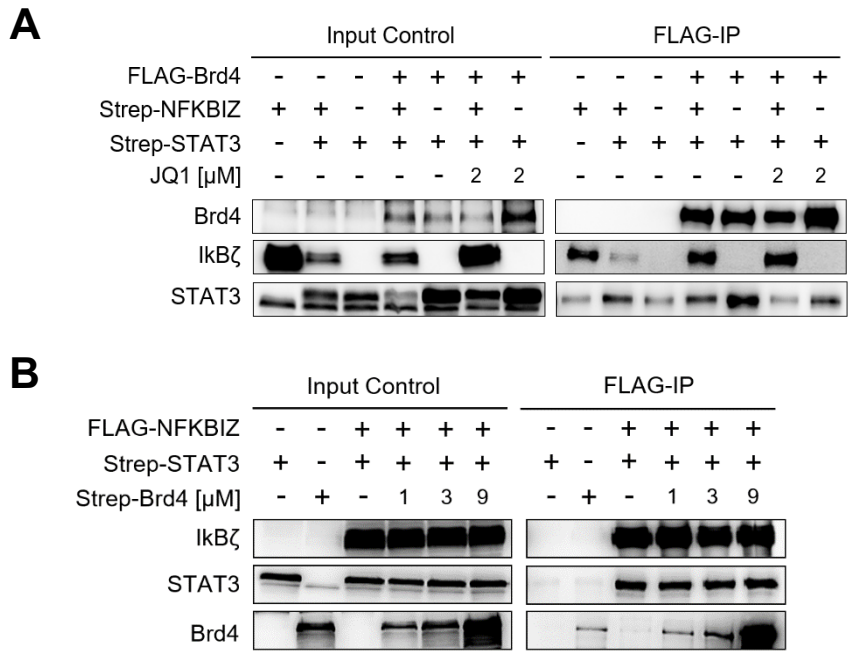

Figure 22. IκBζ and Brd4 interact with STAT3 in a bromodomain-independent manner. HEK2932T cells were transiently transfected with **(A)** FLAG-tagged Brd4, Strep-tagged IκBζ and Strep-tagged STAT3 or **(B)** FLAG-tagged IκBζ, Strep-tagged STAT3 and 1, 3 or 9 μg of Strep-tagged Brd4. HEK293T cells were then treated with **(A)** 2 μM JQ1 for 24 h. **(A-B)** FLAG-IP was performed to pull down **(A)** Brd4, or **(B)** IκBζ and expression of IκBζ, Brd4 and STAT3 was subsequently assessed by immunoblot analysis.

5.1.3 Mapping of IκBζ and Brd4 interaction

Next, we tried to elucidate the binding site responsible for the interaction between Brd4 and IκBζ. For this, we co-transfected HEK293T cells with Strep-Brd4 and truncated FLAG-IκBζ expression vectors and then performed a streptavidin pull-down. As expected, only the expression vector encoding for the N-terminal region of IκBζ (NFKBIZ AA 1-442) precipitated with Strep-Brd4 (Fig. 23A-B).

We then assessed whether Brd4 phosphorylation affects IκBζ binding. For this, we repeated the streptavidin pull down assay after co-transfection of HEK2932T cells with FLAG-tagged Brd4 mutants that either cannot be phosphorylated by CK2 (7A mutant) or that mimic constitutive phosphorylation (7D mutant). Furthermore, to examine the role that the bromodomain plays in the interaction, we expressed an exogenous bromodomain-inactivated mutant (BD mutant). We found that the 7A mutant displays weaker IκBζ binding when compared to full-length Brd4 and 7D-mutant (Fig. 23C), likely indicating the importance of Brd4 phosphorylation for its interaction with IκBζ. Surprisingly, the BD mutant seemed to have higher affinity for IκBζ than the full-length Brd4 (Fig. 23C), further reinforcing the observation that the bromodomain is dispensable for Brd4 and IκBζ interaction.

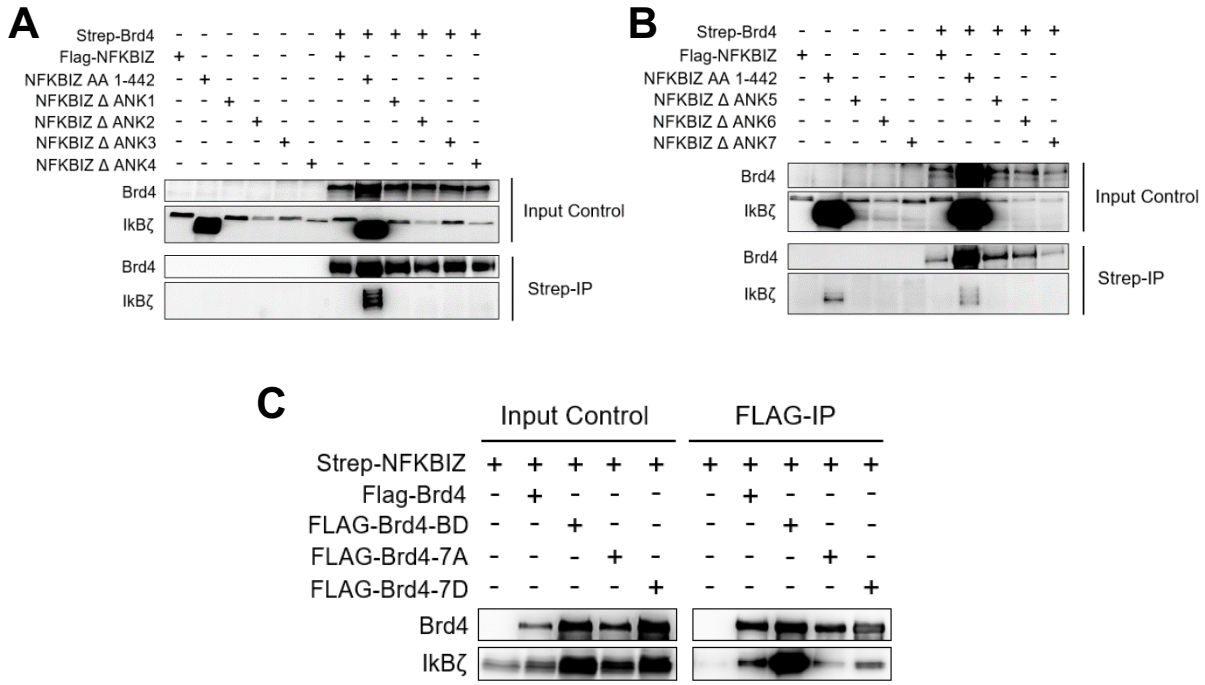

Figure 23. Brd4 interact with the C-terminal of IκBζ. (A-B) HEK2932T cells were transiently transfected with Strep-tagged Brd4, FLAG-tagged IκBζ^{WT} and FLAG-tagged truncated versions of IκBζ lacking the indicated ankyrin repeats. **(A, B)** Expression of IκBζ and Brd4 was assessed by immunoblot analysis after streptavidin-IP to pull down IκBζ. **(C)** HEK2932T cells were transiently transfected with Strep-tagged IκBζ, FLAG-tagged Brd4^{WT} and the truncated FLAG-tagged Brd4 mutants Brd4-BD, Brd4-7A and Brd4-7D. Streptavidin-IP was performed to pull down IκBζ and expression of IκBζ and Brd4 was subsequently assessed by immunoblot analysis.

5.1.4 Oncogenic Ras induction of IκBζ and its role in senescence

Oncogenic Ras expression has been associated with the induction of senescence (Dimauro & David, 2010), while Brd4 has been shown to be required for the expression of genes characteristic of the senescence associated secretory phenotype (Tasdemir et al., 2016). Moreover, a study revealed that IκBζ regulates the induction of common SASP factors in DNA-damage and oncogene-induced senescent cells (Alexander et al., 2013). Knowing that both Brd4 and IκBζ are required for the induction of the SASP, we wondered whether interaction between the two is crucial for oncogene-induced senescence and expression of SASP-related genes. First, we explored whether oncogenic Ras expression could lead to the induction of senescence in SMMC cells. For this, we generated SMMC/*RAS*^{G12V} cells (Ras-SMMC) that expressed the oncogenic Ras^{G12V} protein under the control of the Tet-ON system. Doxycycline treatment of these cells resulted in a robust induction of Ras (Fig. 24B). Doxycycline treatment of Ras-SMMC cells for 3 consecutive days followed by 4 days without

treatment effectively induced senescence, as determined by SA-β-gal staining and morphology (Fig. 24A). When examining the effects of *RAS*^{G12V} expression in SMMC cells, we found that not only was senescence induced, but also IκBζ expression at protein level (Fig. 24B). Furthermore, induction of *RAS*^{G12V} expression in Ras-SMMC cells via doxycycline treatment led to a marked increase in characteristic senescence-associated and IκBζ target genes, such as *IL-1A*, *IL-1B*, *IL-6*, *IL-8*, *CXCL1*, *CXCL10* and *p21,* when compared to the empty vector SMMC control cells (Φ-SMMC) (Fig. 24C).

We next examined the effects of exposing SMMC cells to the cytokine and chemokine-rich SASP supernatant (SN) obtained from *RAS*^{G12V}-expressing SMMC cells and observed that 1 h exposure led to a marked upregulation of STAT3 phosphorylation when compared exposure to the SNs obtained from the control counterparts (Fig. 24D). This phospho-STAT3 upregulation was maintained up to 48 h after exposure (data not shown). Next, we knocked out IκBζ (via CRISPR/Cas9) or silenced STAT3 (via shRNA) in Ras-SMMC cells and harvested their supernatant 48 h after to examine its effects. As expected, exposure of SMMC cells to these supernatants failed to induce STAT3 phosphorylation (Fig. 24D). Interestingly, SN from JQ1 or PFI-1-treated Ras-SMMC cells also failed to induce phospho-STAT3 in a paracrine manner (Fig. 24F). Similarly, treatment with the Cdk9 inhibitor THAL-SNS-032 also negatively affected the induction of STAT3 phosphorylation (Fig. 24E). These results indicate that IκBζ is indispensable for the induction of SASP-related genes. Moreover, the transcription of these genes seems to require the interaction between IκBζ, STAT3, Brd4 and Cdk9, since inhibition or silencing of any of these proteins led to the inability of IκBζ to fully induce the expression of its target genes.

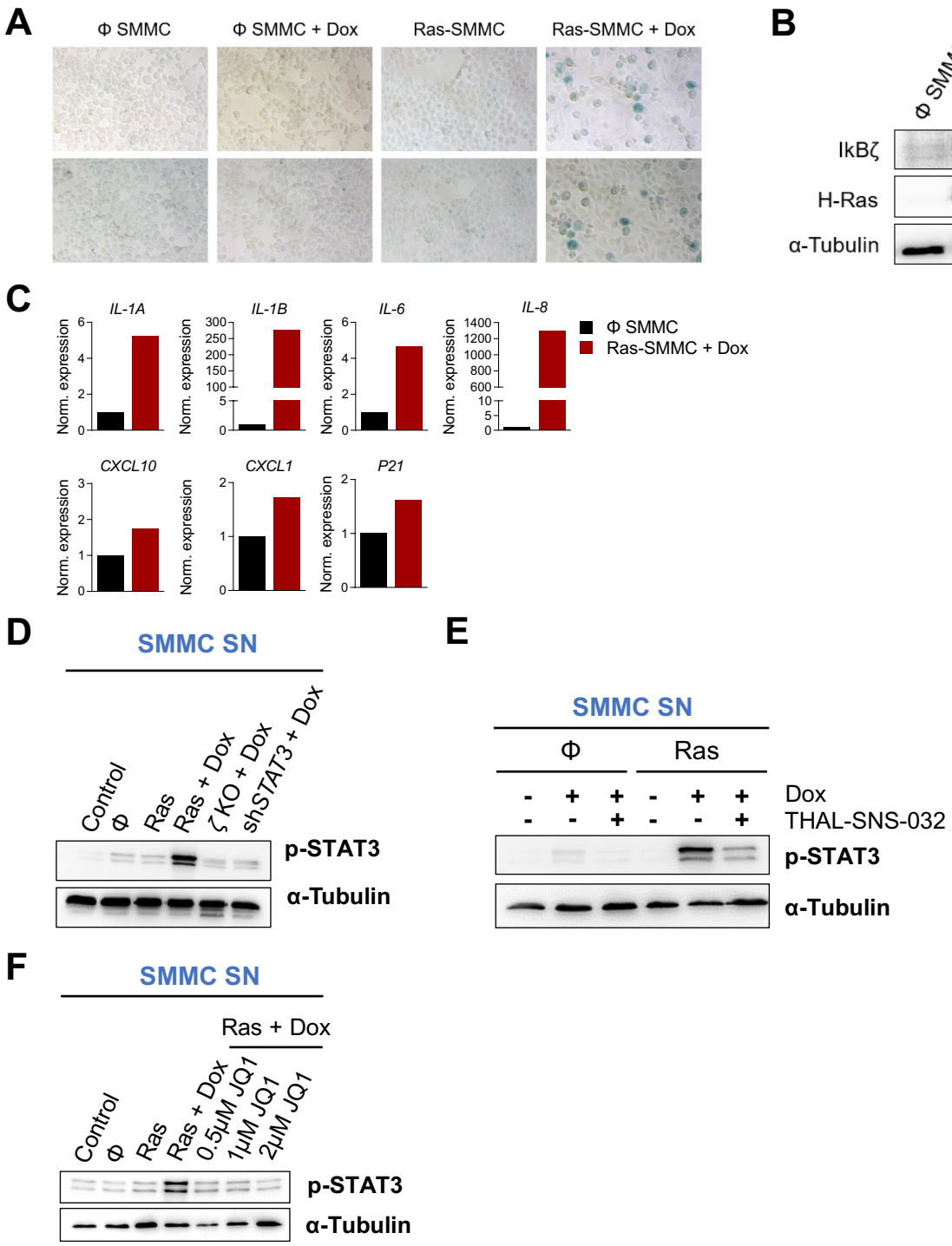

Figure 24. Oncogenic Ras induces senescence and IκBζ target gene expression. **(A)** SMMC cells expressing a control or *RAS*^{G12V} vector were either left untreated or were treated with 1 μg/ml doxycycline for 3 days. Senescence induction was then assessed by SA-β-gal staining. **(B)** The efficacy of lentiviral transduction of *RAS*^{G12V} in SMMC cells, as well as IκBζ expression, were controlled by immunoblotting after 48 h treatment with 1 μg/ml doxycycline. **(C)** Expression of typical IκBζ target genes was evaluated by RT-qPCR in control and *RAS*^{G12V}-expressing SMMC cells. Biological triplicates were measured. *RPL37A* was used as the housekeeping gene. **(D-F)** SMMC cells were exposed for 1 h to the supernatants (SN) of SMMC cells that had been pre-treated as indicated in the depicted figures. Phosphorylation of STAT3 was then assessed by immunoblot analysis. Tubulin served as loading control.

5.2 Identification of novel IκBζ target genes

When activated, IκBζ strongly induces the expression of a subset of well-known NF-κB secondary response genes (Alexander et al., 2013; Hildebrand et al., 2013; Kayama et al., 2008). However, we wondered what other genes never identified before are also induced by IκBζ in the context of liver cancer and whether they could play a role in inflammatory responses.

5.2.1 Novel IκBζ-dependent target genes

In order to characterize novel IκBζ target genes, we focused on validating the expression of a subset of genes that had been previously identified through RNA-sequencing (RNA-seq) analysis by our research group. This gene subset appeared to be upregulated exclusively in rhIL-1β-treated Huh7 cells when compared to the unstimulated Huh7 counterparts, thus potentially indicating their dependence on IκBζ activity. Interestingly, many of these genes, such as *SLC2A1* and *SLC2A3* (encoding for glucose transporters GLUT1 and GLUT3 respectively), *IGFBP6*, *HAS2* and *HILPDA,* are related with metabolic functions; whereas *BCL6*, *BATF3*, *PI3*, *CXCL6*, *CD44* and *PTX3,* which were also upregulated in rhIL-1β-stimulated Huh7, are related with immune functions. In order to evaluate their potential as IκBζ-target genes, we next assessed the expression of this gene subset in IκBζ-overexpressing Huh7/Tet-ON-IκBζ cells. Using RT-qPCR analysis, we observed that rhIL-1β treatment of Huh7 cells led to the upregulation of many of the aforementioned genes when compared to the untreated counterparts (Fig. 25A). As expected, doxycycline-induced IκBζ overexpression in Huh7/Tet-ON-IκBζ cells further increased the expression of this gene subset (Fig. 25A). In contrast RT-qPCR analysis performed on rhIL-1β-treated IκBζ-knockout Huh7 cells (Huh7/CRISPR/Cas9-IκBζ-KO) revealed a stark downregulation of these genes when compared to the rhIL-1β-treated Huh7 control cells (Fig. 25B), thus characterizing them as IκBζ target genes.

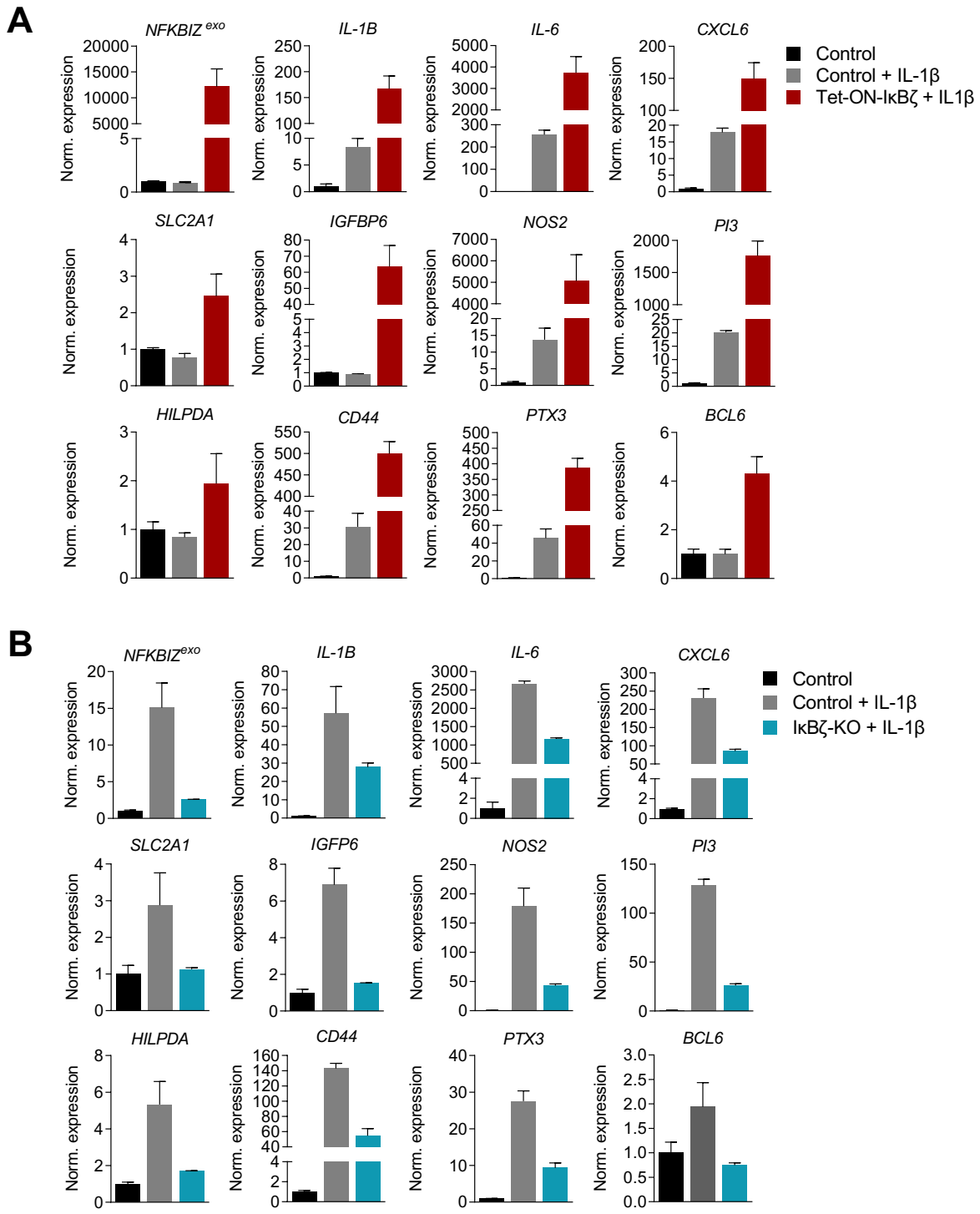

Figure 25. Validation of novel IκBζ target genes. (A) Tet-ON Huh7 cells were initially treated for 48 h with 1 µg/ml doxycycline to induce IκBζ overexpression (OE). Subsequently, control and IκBζ-overexpressing Huh7 cells were left untreated or were stimulated for 2 h with 2.5 ng/ml with rhIL-1β. Expression of novel IκBζ target genes was evaluated by RT-qPCR. **(B)** Control and IκBζ-knockout Huh7 cells were left untreated or were stimulated for 2 h with 2.5 ng/ml with rhIL-1β. Expression of novel IκBζ target genes was evaluated by RT-qPCR. **(A-B)** Biological triplicates were measured. *RPL37A* was used as the housekeeping gene. Error bars correspond to the mean ± SD.

5.3 Liver-specific *NFKBIZ* overexpression in mice

To study the effects of liver-specific *NFKBIZ* overexpression *in vivo*, we crossed Rosa26 transgenic mice containing a Cre/loxP conditional FLAG-*NFKBIZ* expression vector under the control of a reverse tetracycline transactivator (rtTA), with Albumin-Cre transgenic mice to generate F1-offspring that would allow spatiotemporal control of IκBζ expression (as explained in section 7.1.15). In this setting, doxycycline was required for the induction of our chosen transgene (FLAG-*NFKBIZ*). We referred to these mice as AlbCre-Flagζ. In subsequent experiments, we used the parental line Rosa26 tm(rtTA*FLAG-*NFKBIZ*) as the control group and referred to them as rtTA-Flagζ mice.

5.3.1 *NFKBIZ* overexpression *in vivo* has detrimental effects on mouse livers

An initial pilot experiment was performed in 8-week-old AlbCre-Flagζ mice, which were either left untreated or were exposed to doxycycline for 2 weeks to induce IκBζ overexpression. After the 2-week treatment, livers were excised for initial macroscopical examination, which revealed evident alterations in the liver surface, including the presence of multiple nodules characteristic by their white color, as well as enlarged vessels and translucent droplets that had the consistency of lipid droplets (Fig. 26A). Furthermore, via RT-qPCR analysis, we could determine that several IκBζ target genes were markedly upregulated, thus proving efficient IκBζ overexpression in AlbCre-Flagζ mice after exposure to doxycycline (Fig. 26B). When evaluating the expression of common lymphoid and myeloid markers, we noted an upregulation of the typical neutrophil marker myeloperoxidase (*MPO*), as well as an increase in *CD4* and *CD19* expression (Fig. 26B). Surprisingly, we also observed an upregulation of *LIPIN* in the context of liver-specific IκBζ overexpression (Fig. 26B). All in all, this initial experiment suggested that IκBζ overexpression in the liver has a pro-inflammatory effect.

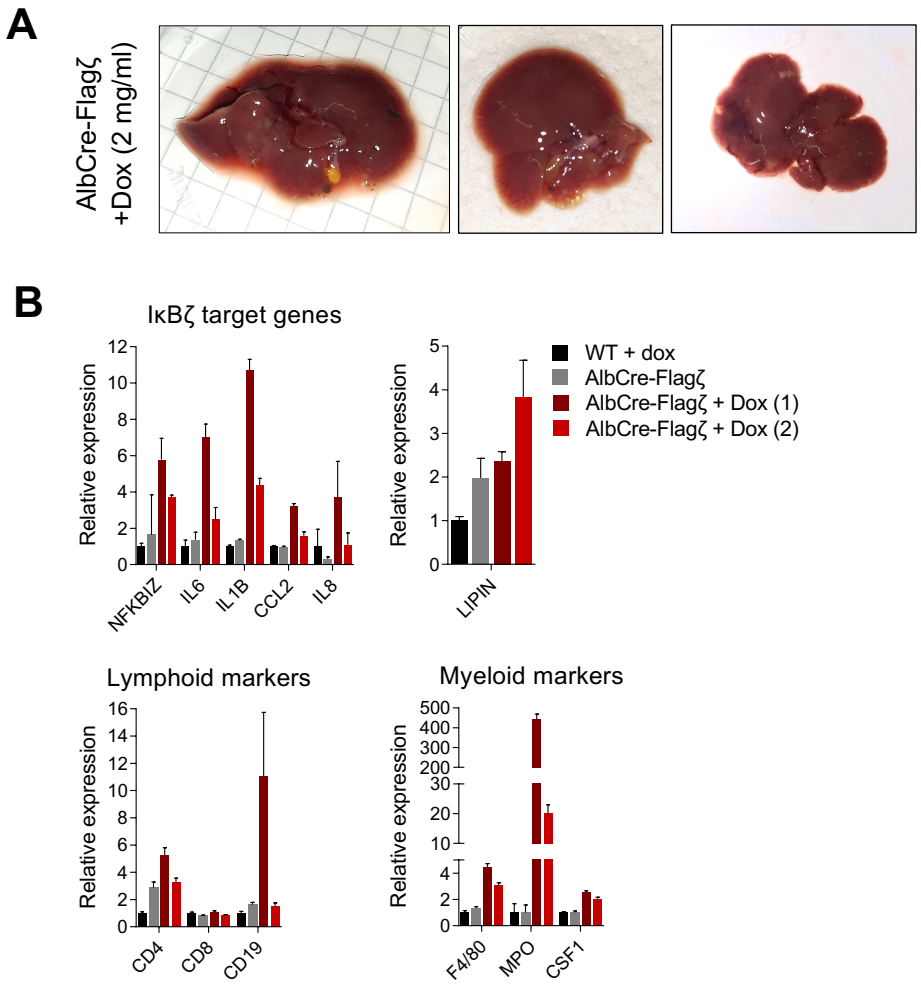

Figure 26. Livers from IκBζ-overexpressing mice exhibit phenotypic alterations that correlate with upregulation of IκBζ target genes. (A) Representative photographs of livers excised from untreated or dox-treated (2 mg/ml for 2 weeks) AlbCre-Flagζ mice. **(B)** Livers from WT, untreated or dox-treated (2 mg/ml for 2 weeks) AlbCre-Flagζ mice were harvested and processed for RNA isolation. Expression of common IκBζ-target genes, myeloid and lymphoid markers was assessed via RT-qPCR. Biological triplicates were measured. *RPL37A* was used as the housekeeping gene. Error bars correspond to the mean ± SD.

Liver harvest of rtTA-Flagζ and AlbCre-Flagζ mice at week 7 after birth that had been exposed to doxycycline for the last 2 weeks confirmed the macroscopical presence of wide-spread white nodules, lipid droplet-like structures and blood clotting after *NFKBIZ* overexpression. Interestingly, the appearance of this phenotype was exclusive to those mice harboring marked IκBζ upregulation, as determined by RT-qPCR and immunoblot analyses (Fig. 27A-B). Livers excised from AlbCre-Flagζ mice in which *NFKBIZ* expression had remained low, with expression levels comparable to those observed in rtTA-Flagζ mice, did not show any of the previously mentioned characteristics. Additionally, expression of typical IκBζ target genes, such as *IL-6*, *IL-1B*, *CCL2* and *IL-8*, as well as common immune markers including *CD4*, *CSF1*, *Ly6G* and *MPO* were

starkly upregulated in those AlbCre-Flagζ mice with *NFKBIZ* overexpression (Fig. 27B). Cytokine arrays further validated the secretion of well-known inflammatory factors. Livers excised from AlbCre-Flagζ mice harboring elevated *NFKBIZ* expression exhibited an upregulation in the secretion of IL-1β, IL-1ra, IL-16, IL-23, CXCL10, CXCL1, CCL2, CXCL9, CCL, CXCL12, TIMP1 and TREM1 (Fig. 27D), some of which are known IκBζ target genes.

AlbCre-Flagζ mice as young as 4 weeks old already showed IκBζ expression at protein level after a 2-week exposure to doxycycline, which correlated with an upregulation in *NFKBIZ*, *IL-1B* and *MPO* expression at mRNA level as determined by RT-qPCR (data not shown). Furthermore, macroscopical examination of the livers of two doxycycline-treated AlbCre-Flagζ mice found dead in cage at just 3 weeks after birth revealed massive alterations of the liver anatomy. Approximately 20-30% of the liver surface exhibited inflammation and/or fibrosis and presented an accumulation of the previously described nodules and lipid droplet-like structures, having lost their normal appearance (Fig. 27C). Altogether, these results indicate that liver-specific IκBζ overexpression is extremely detrimental especially in developing livers. However, the exact mechanisms of action remain to be elucidated.

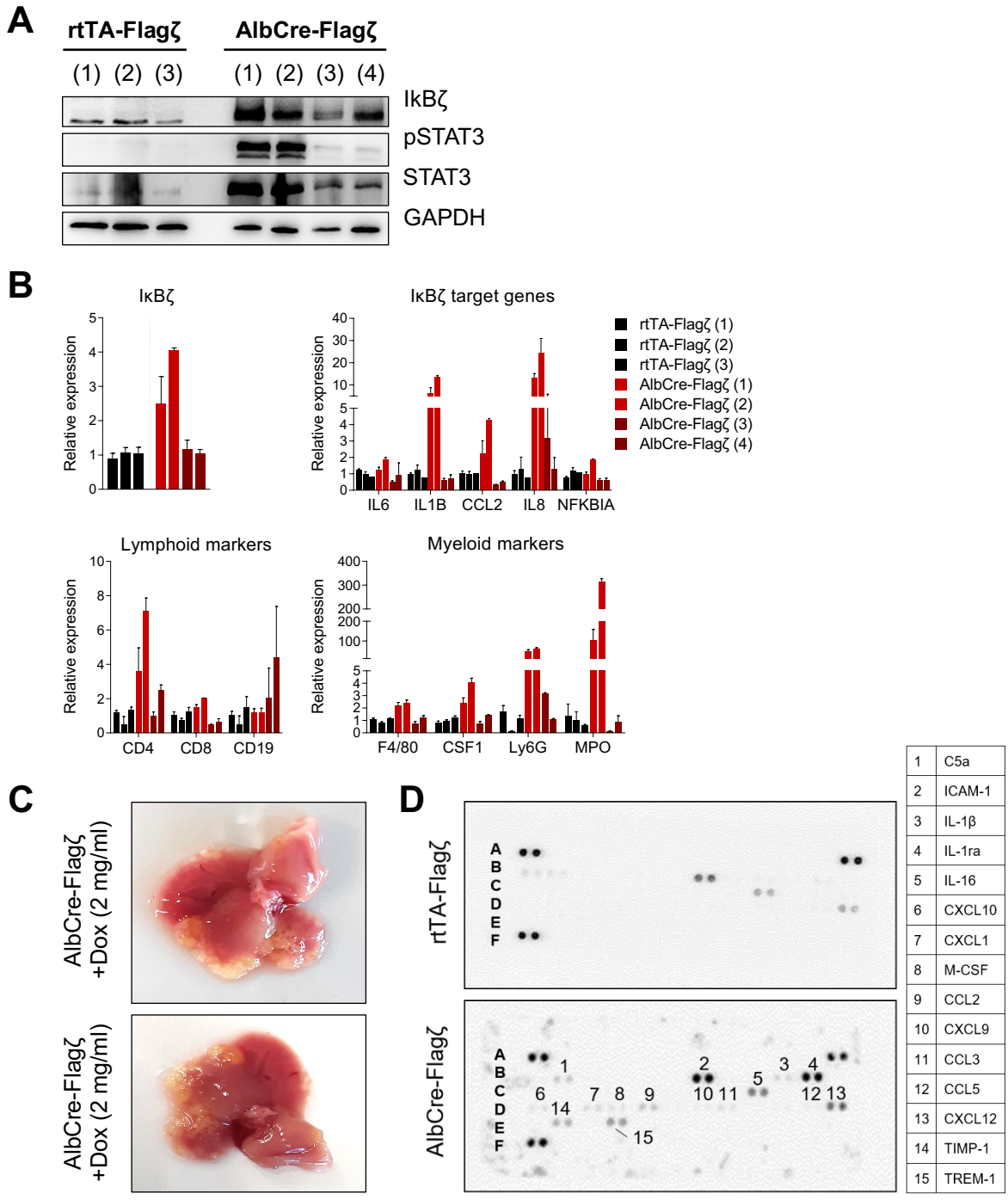

Figure 27. IκBζ overexpression provokes liver inflammation. (A-B) Livers from rtTA-Flagζ (n=3) and AlbCre-Flagζ (n=4) mice that were exposed for 2 weeks to doxycycline (2 mg/ml) were harvested at week 7 after birth and processed for protein and RNA isolation. IκBζ expression was then assessed via **(A)** immunoblot analysis and **(B)** RT-qPCR**. (B)** Common IκBζ-target genes, myeloid and lymphoid markers were also assessed via RT-qPCR. Biological triplicates were measured. *RPL37A* was used as the housekeeping gene. **(C)** Representative photographs from livers of doxycycline-treated (2 mg/ml) 3-week-old AlbCre-Flagζ mice exhibiting phenotypic and macroscopic alterations. **(D)** Livers from rtTA-Flagζ (n=1) and AlbCre-Flagζ (n=1) mice that were exposed for 2 weeks to doxycycline (2 mg/ml) were excised at week 7 after birth, lysed and run on the Mouse Cytokine Array Panel A for detection of common mouse cytokines and chemokines. The table on the right indicates the specific

cytokine/chemokine corresponding to each depicted number. Error bars correspond to the mean ± SD.

5.3.2 Characterization of the IκBζ-induced phenotypic alterations

Having identified a clear phenotype in the livers of IκBζ overexpressing mice, we sought to characterize and determine the origin of the lesions and nodules found in these livers. Previous studies identified the presence of complex lymphoid aggregates that resemble secondary lymphoid organs in aggressive hepatocellular carcinomas both in humans and in mice (Finkin et al., 2015; Patman, 2015). These aggregates are known as ectopic lymphoid-like structures (ELS) and are visible in the surface of affected livers as white-colored nodules. To assess whether the resembling nodules displayed in AlbCre-Flagζ livers could potentially be characterized as ELSs, we analyzed the expression of the genes comprised in the ELS gene signature. Strikingly, we found that 8 out of the 12 genes comprising the ELS gene signature were strongly upregulated in AlbCre-Flagζ mice (Fig. 28A). This upregulation was unique to the AlbCre-Flagζ mice exhibiting *NFKBIZ* overexpression. As a result, these findings suggest a direct correlation between IκBζ expression and the appearance of ELS in the liver.

Next, we attempted at characterizing the lesions observed in the liver of young AlbCre-Flagζ mice. Knowing that IκBζ regulates the expression of typical inflammatory genes, and that liver inflammation strongly correlates with fibrosis, we questioned whether the structural alterations observed after IκBζ overexpression indicated a fibrotic event. For this, we examined the expression of well-known fibrosis-related genes and observed that AlbCre-Flagζ mice exhibiting a strong IκBζ expression markedly upregulated fibrosis-related genes, such as *TGFβ*, *TNFα*, *SCF*, *TIMP1*, *ACTA2*, *PDGFB* and *Col1A1* (Fig. 29B). Furthermore, genes known to modify the tumor microenvironment such as *MMP2*, *MMP9*, *S100A8* and *S100A9*, were also upregulated (Fig. 28B). Altogether, these results indicate that IκBζ overexpression in the liver context can lead to inflammatory events that trigger fibrosis as well as immune cell infiltration.

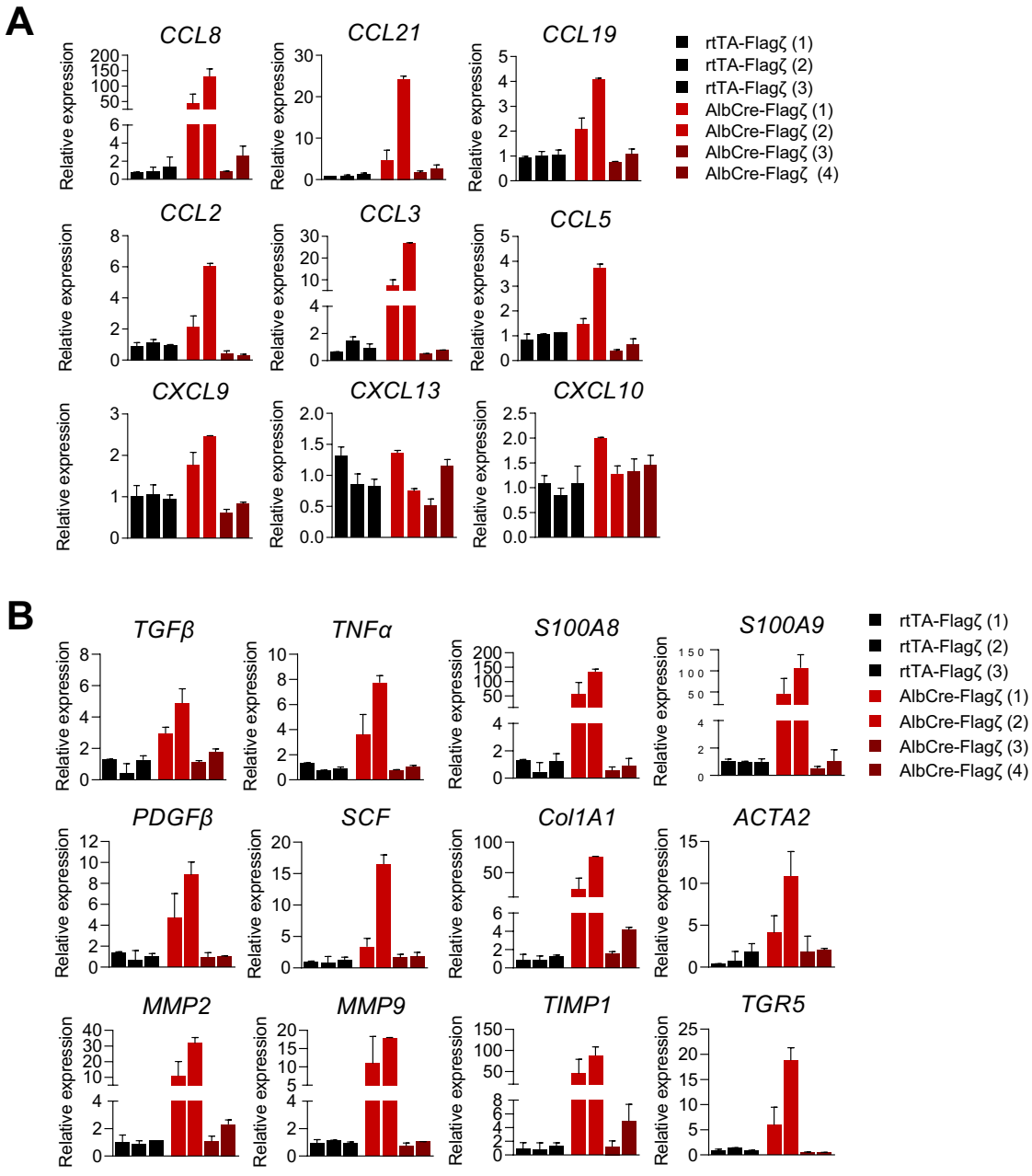

Figure 28. Livers from IκBζ-overexpressing mice express common ELS and fibrosis markers. (A-B) Livers from doxycycline-treated (2 mg/ml) rtTA-Flagζ (n=3) and AlbCre-Flagζ (n=4) mice were harvested at week 7 after birth and processed for RNA isolation. Expression of **(A)** ELS-signature genes and **(B)** typical fibrosis markers was subsequently assessed via RT-qPCR**.** Biological triplicates were measured. *RPL37A* was used as the housekeeping gene. Error bars correspond to the mean ± SD.

5.4 *NFKBIZ* expression in liver disease patients

5.4.1 *NFKBIZ* expression is elevated in human liver disease

To study whether IκBζ plays a role in liver disease development and progression in humans, we examined *NFKBIZ* expression via RNAscope, a technique that allows for RNA analysis via *in situ* hybridization (ISH) of formalin-fixed, paraffin-embedded tissue specimens, in two distinct tissue microarrays (TMAs). One of the TMAs was specific for hepatocellular carcinoma patients, while the other TMA contained sections of a wide array of liver diseases, including chronic hepatitis, non-alcoholic fatty liver disease (NAFLD), cirrhosis and HCC together with unaffected liver tissue. Strikingly, RNA ISH revealed that *NFKBIZ* expression tends to be higher in early stages of liver inflammation and disease, with approximately 46% of chronic hepatitis specimens showing *NFKBIZ* positivity. The percentage of *NFKBIZ*-positive sections went down to 39% in cirrhosis patients and it was the lowest in HCC cases, with only 21% of the sections exhibiting *NFKBIZ* expression (Fig. 29A, D). Interestingly, more than 80% of the hepatitis specimens described as NAFLD/NASH that exhibited *NFKBIZ* positivity, were also positive for HBV (Fig. 29C), thus suggesting a plausible relationship between HBV infection, IκBζ induction and increased fatty acid accumulation and fatty degeneration in the liver.

Regarding the pattern of IκBζ mRNA expression, we observed that it was dispersed within the tissue rather than focalized to specific areas and did not correlate with the presence of particular cell types. Interestingly, *NFKBIZ* expression positively correlated with an increase in immune cell infiltration with 71% of IκBζ+ specimens exhibiting immune cells in the liver parenchyma (Fig. 29B). However, it remains to be determined what type of immune cells preferentially co-localize with IκBζ+ hepatocytes and the role they play in disease progression.

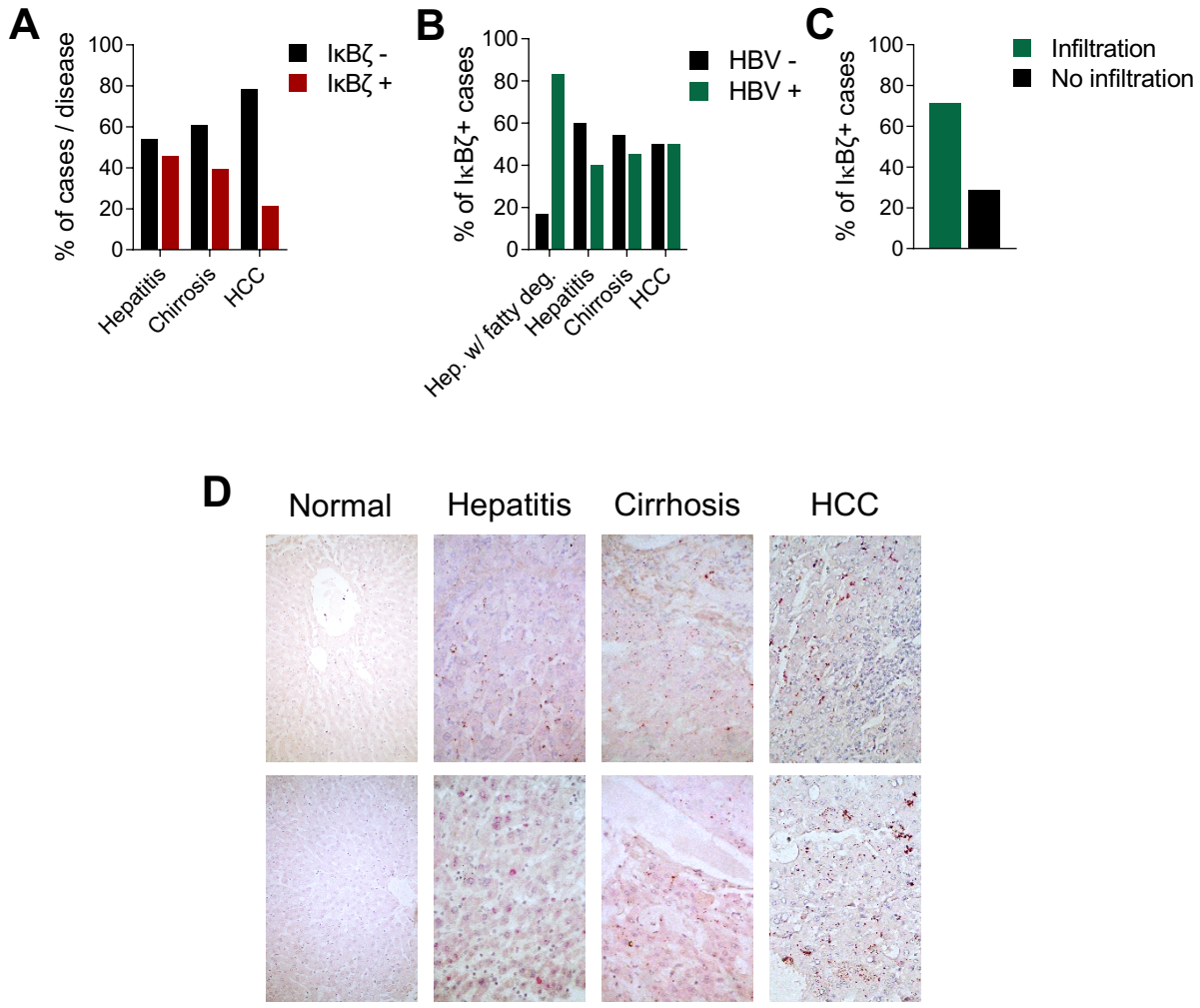

Figure 29. IκBζ is predominantly expressed at early stages of liver disease. (A-B) Tissue microarrays of human liver disease progression were stained using the RNAscope technique to detect *NFKBIZ* mRNA expression via microscopy. Quantification of IκBζ positivity for each liver disease specimen was individually determined as indicated by the manufacturer. **(B)** Immune cell infiltration in each liver disease specimen was determined by cell morphology. **(C)** Information about HBV positivity was obtained from the liver disease progression TMA data sheet. **(D)** Representative photographs of IκBζ RNAscope staining of normal and diseased liver specimens from a human liver disease progression TMA.

6 Discussion

Hepatocellular carcinoma is the most common and severe type of primary liver tumor and accounts for approximately 90% of all newly diagnosed liver cancer cases (Llovet, Kelley, et al., 2021; Sung et al., 2021). It is a well-characterized inflammation-linked cancer that frequently develops from a pre-existing liver disease with a continuous cycle of damage-inflammation-regeneration (J. D. Yang et al., 2019; YM. Yang et al., 2019). The etiology of the underlying liver disease varies widely and is associated with specific geographical regions. For instance, in developed countries, nonalcoholic fatty liver disease and non-alcoholic steatohepatitis have become one of the major risk factors for HCC development together with hepatitis C viral infection (Welzel et al., 2013; YM. Yang et al., 2019; Younossi et al., 2015). On the other hand, in countries with scarce medical resources infection by hepatitis B virus tends to be the leading etiology, whereas exposure to aflatoxin B from contaminated food, also common in these regions, strongly interacts with HBV thereby enhancing liver cancer risk (Levrero & Zucman-Rossi, 2016; Llovet, Kelley, et al., 2021; Turner et al., 2002). Moreover, these distinct etiologies give rise to different mechanisms of hepatocarcinogenesis that contribute to the molecular diversity of hepatocellular carcinoma. HCC patients tend to be diagnosed at late stages of the disease, which combined with the high heterogeneity and complexity of genetic lesions present in this tumor type, hinders the treatment options (Llovet, De Baere, et al., 2021; Llovet et al., 2008; Llovet, Kelley, et al., 2021; Villanueva, 2019). Hence, the prognosis for these patients remains poor and HCC remains one of the deadliest cancer types worldwide (J.-W. Park et al., 2015; Sung et al., 2021; J. D. Yang & Roberts, 2010).

6.1 IκBζ induction and regulation in human HCC cell lines

The NF-κB pathway is frequently dysregulated in several tumor types including HCC. NF-κB is considered a master regulator of inflammation and immune responses (Luedde & Schwabe, 2011; Refolo et al., 2020; YM. Yang et al., 2019). Hence, given the pivotal role of inflammation in the development of HCC, the activation of this pathway has been linked to liver tumorigenesis. However, as described previously, the role of NF-κB in hepatocarcinogenesis remains controversial, mainly owing to the wide

array of target genes and stimulatory signals, as well as the context and cell type in which this transcription factor becomes activated. In physiological conditions, NF-κB is tightly regulated by several control layers that also regulate the selective expression of specific target genes depending on the setting. Generally, NF-κB family members form homo- and heterodimers that will translocate to the nucleus once the pathway becomes activated to induce the expression of specific target genes (Hayden & Ghosh, 2008a; Huxford & Ghosh, 2009; Oeckinghaus & Ghosh, 2009; Shih et al., 2011b). Commonly, p50 and p52 homodimers are associated with transcriptional repression. However, the atypical IκB member IκBζ, which lacks a typical DNA-binding domain, binds to these subunits that provide it with access to DNA-regulatory regions (Kohda et al., 2016; Motoyama et al., 2005; Yamamoto et al., 2004). Once bound to the DNA, it can initiate transcription of a subset of NF-κB secondary response genes thanks to its transactivation domain (Alexander et al., 2013; Annemann et al., 2016; Hildebrand et al., 2013; Müller et al., 2018). Previous studies by our research group identified novel IκBζ target genes that are strongly related with immunosuppressive functions, such as *CCL2*, *CXCL5*, *LIF*, *ARG1* and *CCL7* amongst others. Other well-characterized IκBζ target genes include a set of cytokines, chemokines and factors that participate in inflammatory processes, such as *IL-6*, *CCL8*, *CSF2*, *CSF3* and *IL-1B* (Alexander et al., 2013; Kitamura et al., 2000; Yamazaki et al., 2008). Interestingly, the expression of many of these IκBζ-regulated genes is enhanced in HCC, and IL-6 in particular has been observed to play a key role together with STAT3 in the promotion of hepatocarcinogenesis (Bergmann et al., 2017; Grohmann et al., 2018; G. He et al., 2013; E. J. Park et al., 2010). All in all, based on these insights regarding the important role of IκBζ in the regulation of a crucial subset of NF-κB response genes, we hypothesized that IκBζ is likely induced in the context of liver disease and inflammation, thereby promoting liver carcinogenesis through different mechanisms.

In order to evaluate this hypothesis, we first focused on exploring the stimuli that trigger IκBζ induction in hepatocytes and in the setting of human HCC. Previous studies have shown that cytokines such as IL-1β and IL-17 or treatment with LPS and double-stranded RNA can elicit strong IκBζ induction upon stimulation of the TLR/IL-1 receptor pathway (Grondona et al., 2020; Yamamoto et al., 2004). In this regard, we observed that both IL-1α and IL-1β successfully induced IκBζ expression at protein

level in two different human HCC cell lines, as well as in primary hepatocytes (Fig. 19A-B).

There are multiple layers of control regulating IκBζ expression. Studies have provided evidence indicating that stabilization of *NFKBIZ* mRNA is essential for efficient protein expression (Yamazaki et al., 2005). In fact, IκBζ mRNA is regulated at a post-transcriptional level through the action of miRNAs and ribonucleases, that will determine its protein translation (Garg et al., 2015; Huang et al., 2015; Jeltsch et al., 2014; Lindenblatt et al., 2009). Moreover, it is well known that classical IκB proteins are intrinsically unstable and are rapidly degraded in proteasome (O'Dea & Hoffmann, 2010). Similarly, IκBζ expression has also been shown to be transient in keratinocytes upon zymosan A treatment (Grondona et al., 2020). In this context, post-trantranslational modifications or interaction with other proteins could potentially confer protein stability to IκBζ. Indeed, when performing a cycloheximide (CHX) chase assay in IL-1β-treated SMMC, we observed a rapid degradation of the IκBζ protein, the expression of which was undetectable by immunoblotting analysis just after 3.5 h of CHX treatment (Fig. 19C). Surprisingly, cotreatment with the Brd4 inhibitor JQ1 accelerated the degradation process (Fig. 19C). Based on the latter results, we speculated that the epigenetic reader Brd4 likely interacts with IκBζ, granting it stability and enhancing its half-life. All in all, these results demonstrate the efficient induction of the nuclear protein IκBζ after IL-1 receptor stimulation and its short half-life in HCC cells. Interestingly, IL-1β signaling has been identified as a key player in chronic liver inflammation and has been shown to be implicated in the development of HCC (Litmanovich et al., 2018; Szabo & Csak, 2012). High IL-1β levels have been observed in hepatitis, liver fibrosis, cirrhosis and HCC cases, meaning it is present from the very initial steps of liver inflammation and disease all the way through to HCC formation (Litmanovich et al., 2018; Su et al., 2015; Szabo & Csak, 2012). In fact, the number and sizes of liver tumors developed in IL-1β-deficient obese mice were strikingly reduced as compared with wild-type mice. In this same obesity-induced HCC mouse model, IL-1β was described as an upstream inducer of IL-6 expression, which would be in accordance with our observed results (Yoshimoto et al., 2013). These findings support our notion that an inflammatory liver microenvironment rich in IL-1β can activate the NF-κB pathway, and thus, IκBζ for the induction of further inflammatory cytokines and chemokines which contribute to hepatocarcinogenesis.

We next wanted to analyze the molecular mechanisms of IκBζ function and its manner of regulation, since it has not yet been fully elucidated. As mentioned previously, albeit IκBζ contains a transactivation domain, it is unable to induce target gene expression by itself. First of all, IκBζ requires binding to p50/p50, p52/p52 and, to a lesser extent, p50/p65 dimers in order to gain access to the DNA and initiate transcription (Eto et al., 2003; Kannan et al., 2011; Kohda et al., 2016; Nogai et al., 2013; Yamazaki et al., 2008). Furthermore, previous analyses revealed that IκBζ is required to recruit NF-κB dimers onto the target promoter in a gene-specific manner, thereby regulating the expression of particular NF-κB target genes (Kohda et al., 2016). Also, studies suggest that IκBζ associates with key transcription regulators and specific target promoters in order to induce selective gene expression. Thus, our research group performed a large pull-down assay in order to identify plausible IκBζ interaction partners. This assay revealed that IκBζ likely associates with Brd4 and/or STAT3 upon IL-1β stimulation, meaning when IκBζ is transcriptionally active. To validate these interactions, we performed pull-down assays on HEK293T cells transfected with Strep- or FLAG-tagged Brd4, p50, STAT3 and IκBζ expression vectors. As expected, FLAG-Brd4 co-immunoprecipitated with IκBζ independently of the presence of p50 (Fig. 20A). However, presence of p50 seemed to enhance the interaction between IκBζ and Brd4, which suggests that binding of IκBζ to p50 could potentially stabilize the association with Brd4 (Fig. 20A-B). As explained in the introduction, Brd4 has two bromodomains that bind to acetylated lysine residues thereby allowing its interaction with other proteins and transcription regulators (Donati et al., 2018). Hence, at first, we hypothesized that interaction between IκBζ and Brd4 might occur through binding of its bromodomains to acetylated residues in IκBζ. Therefore, we next assessed the interaction of both proteins after treatment with JQ1. JQ1 is a BET bromodomain inhibitor; hence, if the interaction were to be BD-dependent, IκBζ would no longer co-immunoprecipitate with Brd4 in the presence of JQ1. Still, IκBζ was effectively pulled down with Flag-Brd4, with p50 enhancing the strength of this interaction independent of JQ1 treatment (Fig. 20B). We further evaluated the strength of the interactions after treatment with another BET inhibitors, namely iBET-762, and could demonstrate that the interaction between IκBζ and Brd4 continued to occur despite inhibition of the bromodomains (Fig. 20C).

To structurally determine the binding site responsible for the interaction between Brd4 and IκBζ, we initially examined the association of Brd4 with constructs encoding exclusively for either the N-terminal domain (*NFKBIZ* AA 1-442) (NTD) or C-terminal domain (NFKBIZ 436-718) (CTD) of the IκBζ protein and observed that Brd4 specifically binds to the NTD of IκBζ (Fig. 23A-B). To further verify these observations, we assessed by co-immunoprecipitation the binding of Brd4 to distinct IκBζ mutants encoding for C-terminal regions lacking each specific ankyrin repeat. Our results proved that Brd4 exclusively binds to the NTD of IκBζ (Fig. 23A-B). However, further studies should be performed in order to determine the exact binding region and whether post-translational modifications of IκBζ contribute to the interaction.

Next, we attempted at identifying the site responsible for IκBζ's binding to Brd4. Interactions with Brd4 have been reported to occur through the bromodomains or through alternative binding sites such as the phosphorylation-dependent interaction domain (PDID), the basic residue-enriched interaction domain (BID), the N-terminal cluster of CK2 phosphorylation sites (NPS) and the extraterminal domain (ET), all of which are not affected by BET inhibitors (Chiang, 2016; S.-Y. Wu et al., 2013). Since BET inhibitors did not affect binding of IκBζ to Brd4, we sought to explore other binding sites by performing co-immunoprecipitation assays using truncated Brd4 constructs encoding for specific fragments spanning the entire length of the protein. IκBζ was efficiently pulled-down by the truncated Brd4 expression vectors encoding for sections of its N-terminal domain (data not shown). To explore in more detail other possible interaction sites, we made use of exogenous FLAG-tagged Brd4 constructs encoding mutants that either cannot be phosphorylated by CK2 (Brd4-7A), that mimic constitutive phosphorylation (Brd4-7D), or a bromodomain-inactivated mutant (Brd4-BD). We then assessed the interaction of IκBζ to the Brd4 truncated mutants by co-immunoprecipitation and observed that Brd4-7A barely co-precipitated with IκBζ (Fig. 23C), suggesting that phosphorylation by CK2 may be crucial for their interaction. Taking these results into account, it would be of interest to study the interaction between IκBζ and Brd4 in the presence of DC-1 and DC-2 peptides, which are able to block phospho-NPS interaction with transcription factors, since the PDID seems to be of importance for the interaction between the two.

Brd4 is known to aid in the initiation of transcription by releasing and thus recruiting to the DNA the p-TEFb complex (Z. Yang et al., 2005). This complex comprises the kinase Cdk9 and cyclin T1. Cdk9 plays a critical role in RNA polymerase II transcription initiation, elongation, and termination by phosphorylating its C-terminal domain (CTD) at serine 2 (Dey et al., 2009; Jang et al., 2005; Pang et al., 2022; Zhiyuan et al., 2008). Therefore, we next examined whether IκBζ can directly interact with Cdk9. Our findings revealed that, even in the absence of Brd4, IκBζ was able to interact with Cdk9 (Fig. 21A). Moreover, to further validate these results, we performed a co-immunoprecipitation assay targeting endogenous Brd4 in doxycycline-induced Huh/Tet-ON-IκBζ cells. As expected, both IκBζ and Cdk9 precipitated together with Brd4 even after treatment with JQ1 inhibitor (Fig. 21B). Collectively, we speculate that IκBζ likely regulates the transcription of a select set of target genes through its interaction with Brd4 and Cdk9. Hypothetically, Brd4 would recruit IκBζ-p50/p50 complexes to specific target gene promoter or enhancer regions for binding, while subsequent Cdk9 association would allow for transcription initiation.

Another plausible interaction partner identified by our research group in the ChIP-sequencing analysis was STAT3. Previous studies have shown that binding of IκBζ to the coiled coil domain of STAT3 inhibits its SRC stimulated transcriptional activity (Z. Wu et al., 2009). However, in discrepancy with these results, analyses performed by our research group identified that IκBζ increases STAT3 DNA-binding and its transactivation activity. We initially proposed that IκBζ forms a complex comprised of a p50 homodimer, that would give it the required access to the DNA, Brd4 and Cdk9, to direct IκBζ to specific target sites and induce transcription initiation, respectively, and finally STAT3 would potentially enhance the transcription of specific target genes. However, co-immunoprecipitation analyses showed that in absence of IκBζ, STAT3 effectively co-precipitated with Brd4, but this interaction was impaired in the presence of IκBζ (Fig. 22B). Nevertheless, further studies are required to fully characterize the role, mechanism and function of the interaction between IκBζ, Brd4 and STAT3 as a complex, since it is of interest regarding HCC development and progression.

6.2 Oncogenic Ras-mediated IκBζ induction and its role in senescence

Ras is one of the most frequently mutated oncogenes in human cancers, with mutations in approximately 30% of all tumors (Uprety & Adjei, 2020). Sequencing analyses have revealed that approximately 20% of HCC cases present mutations in the *KRAS* gene, which, when compared to other tumor types, accounts for a relatively low mutation rate (Turhal et al., 2015). However, Ras tends to be hyperactivated during hepatocarcinogenesis independently of any mutations in the Ras oncogene itself (Q. Wang et al., 2001). In fact, nowadays several mouse models of hepatocellular carcinoma have been developed via hydrodynamic delivery of transposons expressing activated Ras combined with either *TP53* downregulation, β-catenin activation or c-Myc overexpression (Ju et al., 2016). In this context, previous studies have demonstrated that oncogenic Ras is required for the activation of NF-κB in cancer cells via mediation of phosphorylation of p65 at Ser-536, which allows for nuclear translocation and transcriptional activation (Tago et al., 2019). Another study provided evidence indicating that oncogenic Ras indirectly leads to the activation of NF-κB and cytokine production (Catanzaro et al., 2014). Interestingly, oncogenic Ras signaling led to specific upregulation of *IL-6*, *IL-8*, *CXCL1*, *G-CSF* and *GM-CSF*, all of which are well known IκBζ target genes. Based on these findings, we speculated that hyperactivation of Ras could lead to the activation of NF-κB, which subsequently would induce IκBζ expression and thus, cytokine and chemokine production and release. In order to prove this hypothesis, we first established a doxycycline-inducible RAS^{G12V} expression system in SMMC cells. Interestingly, expression of RAS^{G12V} oncogene led to IκBζ expression at protein level (Fig 24B). This was corresponded with an upregulation of common IκBζ target genes, such as *IL-1A*, *IL-1B*, *IL-6*, *IL-8* and *CXCL1* (Fig. 24C). Owing to these results, we could determine that oncogenic Ras leads to cytokine production through the induction of IκBζ.

Oncogenic Ras has been shown to provoke a premature cell cycle arrest in association with p53 and p16 induction in response to the abnormal mitogenic signaling (Serrano et al., 1997). This permanent growth arrest is widely known as oncogene-induced senescence (OIS) and is associated with phenotypic changes, with the most common features being a flat and enlarged morphology, β-galactosidase activity in acidic

conditions, formation of heterochromatic foci and secretion of a series of factors and proteins known as the senescence-associated secretory phenotype (SASP) (Braig & Schmitt, 2006; Dimauro & David, 2010; Mooi & Peeper, 2006). The factors released through the SASP reinforce the senescent arrest, alter the microenvironment and trigger immune surveillance of the senescent cells (Chien et al., 2011). Interestingly, NF-κB has been shown to act as a master regulator of the SASP (Rovillain et al., 2011; Salminen et al., 2012), while a more recent study showed that Brd4 is required for the SASP and paracrine signaling via cooperation with transcription factors for the regulation of target genes (Tasdemir et al., 2016b). Furthermore, atypical IκBζ was proved to be an essential mediator for the induction of conserved SASP cytokines in senescent cells (Alexander et al., 2013). These results led us to believe that the interaction between Brd4 and IκBζ is essential for the induction of the SASP and the secretion of these inflammation-related factors. We proceeded to study this by first validating the induction of senescence upon oncogenic Ras with the inducible *RAS*^{G12V} SMMC (Ras-SMMC) cell system. As expected, SMMC cells became senescent after *RAS*^{G12V} expression for 3 consecutive days followed by a 4-day resting period, as we could observe via SA-β-gal staining (Fig. 24A). We then harvested the supernatant from the cultured senescent cells and exposed SMMC cells to it for up to 48 h. Interestingly, upon exposure to senescent supernatant, SMMC cells exhibited STAT3 phosphorylation, which was not the case in SMMC cells exposed to supernatants from Ras-SMMC cells that had been knocked out for IκBζ, knocked down for STAT3 or where Brd4 or Cdk9 had been inhibited via a BET or Cdk9 inhibitors, respectively (Fig. 24D-F). One of the main factors secreted in the SASP is IL-6. Janus kinases are known to elicit signals from the IL-6 receptor family to activate STAT3. Thus, the observation that STAT3 phosphorylation was abrogated after exposure to supernatants from Ras-SMMC cells that had undergone IκBζ knockout or STAT3 knockdown, or Brd4 and Cdk9 inhibition, indicates an impairment in SASP induction in these cells. Altogether, these results suggest that the interaction between IκBζ, Brd4 and/or STAT3 is crucial for the induction of SASP-specific factors, among which is IL-6.

The senescence-associated secretory phenotype has been shown to be important for immunosurveillance of pre-malignant cells and mediation of tumor cell clearance (Xue et al., 2007). However, the cytokines and chemokines secreted in the SASP also have detrimental effects depending on the context. For instance, some chemokines robustly

expressed by senescent cells attract suppressive innate immune cells, which tend to favor tumor progression by creating an immunosuppressive microenvironment. In this regard, the SASP-derived IκBζ target gene IL-6 was reported to promote a suppressive environment by increasing the presence of granulocytic myeloid derived suppressor cells that limit cytotoxic T-lymphocyte function (Ruhland et al., 2016). On the other hand, certain cytokines released in the SASP contribute in creating a pro-inflammatory microenvironment that promotes tumor cell survival, proliferation, invasion and angiogenesis (C. A. Schmitt et al., 2022; L. Wang et al., 2022). Conclusively, the role of IκBζ together with Brd4 and STAT3 in the induction of senescence, and therefore their impact in the development and progression of HCC, should be studied in more detail.

6.3 Novel IκBζ target genes

IκBζ is required for the induction of a subset of NF-κB secondary response genes (Eto et al., 2003; Kitamura et al., 2000; Motoyama et al., 2005; Yamamoto et al., 2004), the expression of which is delayed since they require *de novo* protein synthesis. Several of these target genes have already been identified by our research group and others in different cell types and in response to different stimuli. In this regard, we sought out novel putative IκBζ-dependent target genes in the context of hepatocellular carcinoma. For this, we initially analyzed the results obtained from an RNA-seq performed previously by our working group in Huh7 cells treated with IL-1β, to select a subset of genes upregulated after IκBζ induction when compared to the unstimulated control. Subsequently, to confirm that IκBζ was indeed responsible for the induction of these genes, we generated Huh7 cells with doxycycline-inducible expression of *NFKBIZ* (Huh7/Tet-ON-IκBζ) or Huh7 cells knocked-out for *NFKBIZ* via a CRISPR/Cas9 system (IκBζ-KO Huh7). Interestingly, Tet-ON-IκBζ cells exhibited a stark upregulation of the subset of genes identified in the RNA-seq when compared to the unstimulated controls. This gene subset included *CXCL6*, *GLUT1*, *GLUT3*, *IGFBP6*, *NOS2*, *PI3*, *HILPDA*, *CD44*, *PTX3* and *BCL6* (Fig. 25A). All these genes were conversely downregulated in IκBζ-KO Huh7 cells despite IL-1β stimulation (Fig. 25B), thus further validating their status as IκBζ target genes. Among the genes examined, the identification of *CD44* as an IκBζ target gene was of special interest, considering that several studies have

highlighted its role in HCC initiation and progression (Asai et al., 2019; Dhar et al., 2018; Zhang et al., 2021). Interestingly, one of these studies reported that CD44 expression is rapidly induced in carcinogen-exposed hepatocytes in a STAT3-dependent manner, the activation of which is preceded by IL-6 induction (Dhar et al., 2018). This finding suggests that IκBζ could initially trigger the induction of IL-6 in the setting of carcinogenic exposure, which would subsequently activate STAT3 for the upregulation of CD44. Considering the crucial role of CD44 for hepatocarcinogenesis, the question that remains to be answered is whether IκBζ could potentially trigger HCC formation through CD44 upregulation.

Another interesting IκBζ target gene identified by RNA-seq was hypoxia inducible lipid droplet associated (*HILPDA*). *HILPDA* promotes lipid storage in hepatocytes in the form of lipid droplets (LPs), which are specialized organelles that store esterified triglycerides. Certain liver diseases such as alcoholic and non-alcoholic steatohepatitis are characterized by expansion and accumulation of LDs (de la Rosa Rodriguez & Kersten, 2020; Gluchowski et al., 2017; Mashek et al., 2015). However, when investigating lipid droplet formation after exposure of Huh7 cells to the mono-unsaturated fatty acid (MUFA) oleic acid, we observed that IκBζ-KO Huh7 cells showed no impairment in the formation of LDs (data not shown). Contrarily, exposure to oleic acid did provoke a slight upregulation of *NFKBIZ*, IκBζ target genes, *STAT3* and *NFKBIA* expression (data not shown). This implies that an increase in fatty acid accumulation in hepatocytes might lead to a direct activation of inflammation-related pathways, such as IκBζ, NF-κB and STAT3. Indeed, these pathways have been observed to be activated in cases of NAFLD and NASH (Grivennikov & Karin, 2010; Grohmann et al., 2018; G. He & Karin, 2011; Lee & Cheung, 2019).

CXCL6, a pro-angiogenic chemokine that has been associated with HCC progression, invasion and metastasis, and that is correlated with a poor outcome (Tian et al., 2014) was also identified as a novel IκBζ target gene and was increased in Huh7 upon IκBζ overexpression. Furthermore, pentraxin 3 (PTX3), a member of the pentraxin superfamily that is produced and released in response to inflammatory signals such as TLR ligands, TNFα and IL1-β and connects innate immunity, inflammation, tissue repair and cancer (Deng et al., 2020; Garlanda et al., 2004; Wirestam et al., 2017), was also upregulated specifically after IκBζ overexpression. PTX3 has also been

identified as a biomarker of HCC in chronic HBV infection, and its levels seem to increase with liver disease severity (Deng et al., 2020; Han et al., 2021). Finally, elafin, also known as peptidase inhibitor 3 (PI3), is a serine protease inhibitor crucial for host defense that has been found in several inflammatory skin diseases such as psoriasis. Interestingly, elafin has been reported to be increased in HCC tissues, to correlate with aggressive phenotypes and poor prognosis and to drive metastasis and therapy resistance (C. Wang et al., 2021). In our analyses, PI3 was also identified as a novel IκBζ target gene and IκBζ knock-out dramatically decreased its levels in Huh7 cells. In summary, IκBζ induction during liver disease progression could potentially be a contributing factor to the observed increase in CXCL6, PI3 and PTX3 expression observed in HCC, thus participating in the progression of liver inflammation and disease to drive hepatocarcinogenesis. Hence, further studies performed in *in vivo* murine models of liver cancer would be of interest to elucidate the correlation between IκBζ expression and the subsequent induction of these novel target genes in hepatocarcinogenesis.

Taken together, these results imply that IκBζ regulates the expression of an extensive array of genes, many of which are implicated in the mounting of inflammatory responses and the regulation of innate and adaptive immune cells. Furthermore, our insights provide evidence for a role of IκBζ in cellular metabolism, considering that some of the novel target genes identified regulate glucose and fatty acid uptake and accumulation, respectively. Considering that many of these genes identified have been reported to play a role in the initiation, progression and invasion of HCC, we speculate that IκBζ plays an important role in liver disease and hepatocarcinogenesis. However, the stage at which IκBζ might participate remains to be determined.

6.4 Effects of liver-specific IκBζ overexpression *in vivo*

Murine models have demonstrated contradictory roles of NF-κB in the development and progression of hepatocellular carcinoma. Studies have provided insight that indicate that, in the presence of an inflammatory environment, NF-κB can promote hepatocarcinogenesis through the induction of pro-inflammatory cytokines, as well as by triggering the expression of chemokines and growth factors that not only modulate the immune cell repertoire infiltrating the tumor, but also stimulate the growth and

survival of malignant cancer cells (Haybaeck et al., 2009; Mauad et al., 1994; Pikarsky et al., 2004b). Moreover, the activation of the NF-κB pathway in infiltrating immune cells, such as Kupfer cells, monocytes and lymphocytes, has been shown to further promote carcinogenesis in the liver (Finkin et al., 2015; Haybaeck et al., 2009; Kong et al., 2016).

In our study, we found that IκBζ overexpression in HCC cell lines leads to the induction of several novel target genes that have been previously demonstrated to play a role in liver disease progression, as well as HCC initiation, progression, angiogenesis and metastasis (Fig. 25A-B). Moreover, the induction of OIS in the HCC cell line SMMC led to an IκBζ/Brd4/Cdk9-dependent senescence-associated secretory phenotype (Fig. 24A-F), which has been shown to be a double-edged sword when it comes to carcinogenesis. In fact, a study performed in a murine model of HCC triggered by obesity and DEN exposure provided evidence pointing towards the crucial role of the hepatic stellate cell (HSC)-derived SASP in the development of HCC (Yoshimoto et al., 2013). Taking this into account, we sought to investigate the effects of liver-specific IκBζ overexpression *in vivo*. Strikingly, hepatocyte-specific IκBζ overexpression had severely detrimental effects on the livers of AlbCre-Flagζ mice that had been treated with doxycycline for 2 weeks, especially at young ages. We could observe a clear phenotype in the livers of *NFKBIZ*-overexpressing mice, which presented with white nodules, lipid droplet-like structures, blood clots and fibrotic structures that could be observed at a macromolecular level (Fig. 26A). Interestingly, the appearance of phenotypical defects on AlbCre-Flagζ mice correlated with an upregulation of typical IκBζ target genes, as well as common myeloid markers, such as *Ly6G* and *MPO* (Fig. 26B, Fig. 27B), possibly indicating neutrophil and monocytic infiltrates. Furthermore, they exhibited a stark increase in the expression of liver damage, inflammation and fibrosis markers, including *Col1A1*, *S100A8*, *S100A9*, *MMP2*, *MMP9*, *PDGFβ*, *ACTA2*, *TIMP1* and *TNFα* (Fig. 28B). Importantly, all the genes whose expression appeared to be increased were exclusively upregulated in mice exhibiting a clear IκBζ overexpression, both at mRNA and protein level. Furthermore, we also reported that IκBζ overexpressing mice exhibited STAT3 phosphorylation (Fig. 27A), possibly indicating the presence of an IκBζ-IL-6-STAT3 axis. We speculate that this signaling loop likely participates in the inflammation-derived injury observed in the livers of doxycycline-treated AlbCre-Flagζ mice.

Another very prominently expressed gene in the livers of AlbCre-Flagζ mice was *TGR5* (Fig. 28B), which in physiological conditions participates in bile acid production and homeostasis (Pols et al., 2011). TGR5 is a G protein-coupled receptor which is expressed in cholangiocytes and plays a role in bile composition. Interestingly, studies have shown that TGR5 can also modulate the immune response by inhibiting the production of proinflammatory cytokines such as TNFα, IL-1α, IL-1β, IL-6 and IL-8 (Kawamata et al., 2003; Pols et al., 2011). Interestingly, most of the cytokines downregulated by *TGR5* expression are IκBζ target genes. These observations indicate that IκBζ-induced inflammatory cytokine release may trigger a counteracting mechanism in which *TGR5* is upregulated in order to diminish the excessive inflammatory stimuli to avoid subsequent liver injury. However, whether *TGR5* expression is under the regulation of IκBζ, or whether TGR5 negatively impacts IκBζ activation to impede transactivation of its target genes has yet to be determined. Furthermore, it would be of interest to investigate the role of *TGR5* and its expression during liver disease, HCC initiation and progression.

Insights provided by this research further suggest that IκBζ may be a key player in the formation of the so-called ectopic lymphoid structures, which are structures that have an organization similar to secondary lymphoid organs but are formed in non-lymphoid tissues (Marinkovic & Marinkovic, 2021). ELSs have been shown to play a pathological role in liver cancer and to be associated with a poor prognosis (Finkin et al., 2015; Patman, 2015). A study reported that ELSs form microniches where malignant hepatocytes thrive in a cytokine-rich milieu to develop into full blown HCC (Finkin et al., 2015). In this context, multiple ELSs developed at 7 months in mice constitutively expressing IKKβ in hepatocytes, whereas mice harboring a single allele of IKKβ exhibited a decrease in the number and size of ELSs at 14 months, thereby highlighting the association between NF-κB activation and ELS formation. Owing to these observations, we speculated that the white nodules present in the surface of livers excised from AlbCre-Flagζ mice could be characterized as ELSs. Moreover, the immune markers shown to be upregulated in IκBζ overexpressing AlbCre-Flagζ mice (namely *Ly6G*, *MPO* and *CD4*) (Fig. 26B, Fig. 27B) paralleled the ones observed in the previously mentioned study, with T lymphocytes, macrophages and neutrophils being the most prominent immune infiltrates. To further validate the identity of these nodules as ELSs, we harvested them from affected livers and quantified by RT-qPCR

the expression of the 12 genes that comprise the ELS gene signature. Interestingly, 8 out of the 12 ELS signature genes were upregulated when compared to unaffected livers, likely indicating their status as ELSs (Fig. 28A).

Collectively, these observations suggest a crucial role for IκBζ expression in the initiation of liver injury, fibrosis and inflammation characterized by immune cell infiltration. Knowing that previous studies have underlined an essential role of NF-κB-driven inflammation and fibrosis during the development of severe liver disease that progress into HCC, our data imply that IκBζ expression could play a pivotal role throughout this process, enhancing the severity of liver fibrosis, lipid accumulation in hepatocytes and immune cell infiltration, and thus contributing to hepatocarcinogenesis.

6.5 IκBζ expression in human liver disease

The NF-κB pathway has been repeatedly shown to be dysregulated in multiple tumor types, and its activation plays a crucial role in the development and progression of liver diseases of multiple etiologies. IκBζ, an NF-κB primary response gene that is rapidly induced upon inflammatory stimuli, is involved in various inflammation-mediated diseases such as psoriasis, owing to its role as a coactivator of cytokine and chemokine expression (Gautam et al., 2022). In this context, chronic inflammation in the liver has also been shown to have detrimental effects, leading to continuous cycles of tissue damage and repair that are attributed to oxidative stress, endoplasmic reticulum stress, autophagy and constant exposure to intestine-derived toxins. This tissue destruction and repair is associated with the appearance of cirrhosis, which can eventually drive HCC development (YM. Yang et al., 2019). NF-κB being a master regulator of inflammation can participate in the initiation and progression of HCC depending on the microenvironmental context. Thus, we initially hypothesized that IκBζ expression may lead to hepatocarcinogenesis through the induction of pro-inflammatory cytokines. Interestingly, RNA in situ hybridization analyses that we performed in human progressive liver disease and HCC tissue microarrays (TMAs) to investigate *NFKBIZ* expression, revealed that *NFKBIZ* is starkly induced in *earlier* stages of liver disease, such as cases of chronic hepatitis and NASH, while its expression is progressively lost as the disease progresses into HCC (Fig. 29A, D).

These results seemingly indicate the participation or induction of IκBζ in the initial stages of liver disease, during the cycle of tissue destruction and repair associated with proinflammatory signals that precede cirrhosis. Regarding this data, IκBζ would be primordially required for disease progression and malignant transformation of hepatocytes but may become dispensable once the tumor is fully developed.

On a different note, NF-κB activation has been previously associated not only with the development of NASH, but also upon hepatitis B virus infection. Accordingly, our data indicated a possible correlation between HBV infection, IκBζ induction and NAFLD development, considering that among the IκBζ+ hepatitis cases with fatty degeneration, more than 80% were HBV positive. This data leads us to speculate that HBV infection might derive in NF-κB-induced IκBζ expression, which would predispose hepatocytes to fatty acid and triglyceride accumulation (Fig. 29C). However, in contradiction to our results, a recent study reported a protective role of IκBζ in the development of NAFLD after L-amino acid-defined high-fat diet (CDAHFD) treatment (Ishikawa et al., 2022). The preventive effect by IκBζ was associated with changes in the expression of factors related with triglyceride biosynthesis and lipoprotein uptake. However, this study failed to demonstrate a downregulation of well-known, immune response-related IκBζ target genes in a liver-specific *NFKBIZ* knockout mouse model. Furthermore, they failed to observe a change in the expression of fibrosis-related genes, even after CHAHFD treatment, which is in conflict with our observed results in IκBζ overexpressing mice. However, these contradictory results likely underscore the dual role of IκBζ as an inducer or attenuator of the immune response and inflammation, which could be modulated by the cellular and microenvironmental context.

Activation of the NF-κB pathway leads to the induction of chemokines such as CCL2, CCL5, CXCL13, CCL19 and CCL21, that are essential for the recruitment of immune cells which further contribute and enhance the inflammatory response (Carragher et al., 2004). In agreement with these observations, we found that approximately 70% of IκBζ+ samples exhibited immune cell infiltration as determined by microscopy (Fig. 29B), compared to 46% of the IκBζ- counterparts. Thus, we hypothesize that the IκBζ-induced production and release of cytokines and chemokines from parenchymal liver cells likely prompts the recruitment of immune cells to the site of injury. These newly recruited immune cells could either further enhance inflammation via the release

of pro-inflammatory cytokines or, on the contrary, could induce an immunosuppressive microenvironment as a counteractive mechanism.

However, further studies in our murine model of liver-specific *NFKBIZ* overexpression are required in order to determine which type of immune cell is recruited to the site of inflammation and fibrosis, to analyze in more detail the phenotypic characteristics and polarization status of these cells, and whether their presence can enhance or accelerate liver disease progression and HCC initiation. Nevertheless, it is important to remark that the RNAscope data presented in this research is based on a small subset of liver disease and HCC patient specimens, and thus, cannot be extrapolated to what occurs in the general population. Furthermore, the majority of HCC specimens displayed in the TMA were of grade 1-2, meaning that the results might not be representative of what occurs at later stages in HCC. Therefore, further studies in different liver disease and HCC murine models are required, where IκBζ expression is investigated in more detail to uncover its functions and determine its importance as a tumor-promoter.

All in all, IκBζ is a pleiotropic member of the atypical IκB family of proteins, the expression of which is tightly regulated through multiple layers of control, including post-transcriptional modifications, and the function of which varies depending on the stimulus eliciting its induction and the context in which it is activated, as well as on its binding to different transcription regulators and epigenetic modifiers. However, the data we obtained from both *in vitro* and *in vivo* experiments performed in the setting of HCC suggest that IκBζ acts in collaboration with Brd4, Cdk9 and/or STAT3 in order to induce the expression of pro-inflammatory cytokines and chemokines, thereby promoting the cycle of inflammation-injury-regeneration characteristic of liver disease.

7 Materials and Methods

7.1 Materials

7.1.1 Cell culture consumables

Product	Provider	Catalog No.
384-Multiwell plates LightCycler® 480, white	Roche	04729749001
96-well F-bottom with lid	Faust	TPP92096
96-well U-bottom with lid	Faust	TPP92697
96-well F-bottom, white, lumitrac	Greiner bio-one	655075
96-well F-bottom, black, fluotrac	Greiner bio-one	GB655076
24-well F-bottom with lid	Faust	TPP92024
12-well F-bottom with lid	Faust	TPP92012
10 cm tissue culture dish	TPP	93040
15 ml conical tubes	Greiner bio-one	188271
50 ml conical tubes	Greiner bio-one	227270
5 ml round-bottom polystyrene test tubes	Corning	352052
Cell culture flasks: T25 and T75	Greiner bio-one	690175-TRI, 658175-TRI
Cell freezing container	VWR	432138
Combitips advanced: 0.5, 1, 2.5, 5 and 10 ml	Eppendorf	0030089421, 0030089430, 0030089650, 0030089456, 0030089677
Eppendorf Safe-Lock tubes: 1.5 and 2 ml	Eppendorf	0030120086, 0030120094
Filtration unit Stericup®, 0.22 µM	Carl Roth	X340.1
MACS Columns 25LS	Miltenyi Biotec	130-042-401
NC-Chamber Slide A8™	Chemometec	942-0003
Nunc Cryotube Vials	ThermoFisher Scientific	375418PK
PCR tubes, 0.2 mL	BioRad	TBC0802
Pipette tips: 10, 200, 1000 µl	Nerbe plus	07-372-2015, 07-375-2015, 07-379-2015
Serological pipettes: 5, 10, 25 and 50 ml	Corning	357543, 356551, 356535, 356550

7.1.2 Cell culture media, supplements and antibiotics

Name	Provider	Composition
DMEM	Sigma-Aldrich	D5030
IMDM	Sigma-Aldrich	I6529-500ML
RPMI 1640	Sigma-Aldrich	R8758-500ML
RPMI 1640, no glutamine	Gibco	21870076
PB-MAX™ Karyotyping Medium	Thermo Fisher	12557013
X-VIVO™ 15	Lonza	BE02-053Q
HEPES Buffer (1M)	Sigma-Aldrich	H0887
DPBS (1x)	Sigma-Aldrich	D8537-500ML
HBSS	Sigma-Aldrich	H8264-500ML
Fetal Calf Serum	Sigma-Aldrich	F7524
Human Serum	Sigma-Aldrich	H3667
Penicillin/Streptomycin	Sigma-Aldrich	P11-010
Plasmocin™ prophylactic	Invivogen	Ant-mpp
Doxycycline	AppliChem	A2951,0025
Puromycin	Invivogen	Ant-pr-1

7.1.3 Chemicals and reagents

Name	Provider	Catalog No.
2-Propanol	Carl Roth	T403.1
7-AAD	BD	51-68981E
2% Bis-acrylamide	Serva	29195.02
40% Acrylamide	AppliChem	A3658
α-Tocopherol	Sigma-Aldrich	258024
β-mercaptoethanol	Sigma-Aldrich	M3148
AO-DAPI staining reagent	Chemometec	910-3018
Adenine	Sigma-Aldrich	A2786
Agarose Standard	Carl Roth	3810.3
Albumin Fraction V	Carl Roth	8076.4
Ammonium hydroxide, 28-30%	Sigma-Aldrich	320145
Ammonium persulfate	Sigma-Aldrich	A3678-25G
Ascorbic acid	Selleckchem	S3114
BODIPY™ 581/591 C11	Themo Fisher	D3861
Bromophenol blue	Sigma-Aldrich	B0126
CellROX™ green reagent	Thermo Fisher	C10444
DBE-4 dibasic ester	Sigma-Aldrich	112755
Dimethyl 2-ketoglutarate (DM-KG)	Sigma-Aldrich	349631
Dimethyl fumarate (DMF)	Sigma-Aldrich	242926

Dimethyl (*S*)-(−)-Malate	Sigma-Aldrich	374318
Dimethyl sulfoxide (DMSO)	Sigma-Aldrich	D2650-100ML
EcoMount	Biocare	EM897L
Ethylenediamine (EDTA)	Carl Roth	CN06.3
Ethanol 96% pure	AppliChem	A1615,2500PE
FLAG M2 agarose beads	Sigma-Aldrich	A2220
Glycerol anhydrous	AppliChem	A1123,1000
Glycine	Carl Roth	3908.3
H2DCFDA	ThermoFisher	D399
Hydrogen peroxide solution (30%)	Sigma-Aldrich	H1009-100ML
MitoTEMPO	MedChemExpress	HY-112879
MitoSOX™	ThermoFisher	M36008
NADP	Sigma-Aldrich	10128031001
β-NADPH sodium salt	Sigma-Aldrich	N8035-15VL
N-Acetylcysteine	Sigma-Aldrich	A7250
Non-fat milk	AppliChem	A0830,1000
Oxaloacetic acid	Sigma-Aldrich	O7753
PageRuler™ prestained protein ladder	ThermoFisher Scientific	26617
Propidium Iodide/ RNase staining solution	Cell Signaling Technology	4087S
Protease inhibitor cocktail	Roche	04-693-132-001
Protein A agarose beads	Thermo Fisher	20333
Protein assay dye reagent concentrate	Bio-Rad	5000006
QIAzol lysis reagent	Qiagen	79306
Sepharose 6B beads	Sigma-Aldrich	6B100
SDS pellets	Carl Roth	CN30.3
Sodium azide	Sigma-Aldrich	71290
Sodium chloride	Carl Roth	0601.2
Sodium orthovanadate	Sigma-Aldrich	S6508
Strep-tactin®	IBA	2-5030-002
Sulfuric acid	Sigma-Aldrich	339741
SYTOX™ blue dead cell stain	Thermo Fisher	S34857
TEMED	Carl Roth	2367.1
Tetramethylrhodamin, Ethylester (TMRE)	Thermo Fisher	T669
Tetra-natriumdiphosphate decahydrate	Carl Roth	T883.3
Tris-HCl	Carl Roth	9090.1
TritonX100	Sigma-Aldrich	X100-5ML
Trizma® base	Sigma-Aldrich	T1503-500G
Tween-20	Sigma-Aldrich	P1379
Xylene	Sigma-Aldrich	108633

7.1.4 Immortalized human cell lines

Name	Description	Media (% FCS)
HEK293T	Human embryonic kidney 293 cells	DMEM (10%)
BJAB	GCB DLBCL	RPMI 1640 (10%)
DOHH2	GCB DLBCL	RPMI 1640 (10%)
HBL-1	ABC DLBCL	RPMI 1640 (20%)
HT	GCB DLBCL	RPMI 1640 (10%)
Huh-7	HCC	DMEM (10%)
Karpas-422	GCB DLBCL	RPMI 1640 (10%)
OCI-Ly3	ABC DLBCL	RPMI 1640 (20%)
OCI-Ly10	ABC DLBCL	IMDM + (20% human serum)
OCI-Ly19	GCB DLBCL	IMDM (10%)
Pfeiffer	GCB DLBCL	RPMI 1640 (10%)
RIVA	ABC DLBCL	RPMI 1640 (20%)
SMMC-7721	HCC	DMEM (10%)
SU-DHL-2	ABC DLBCL	RPMI 1640 (20%)
SU-DHL-4	GCB DLBCL	RPMI 1640 (10%)
SU-DHL-6	GCB DLBCL	RPMI 1640 (10%)
SU-DHL-8	GCB DLBCL	RPMI 1640 (20%)
Toledo	GCB DLBCL	RPMI 1640 (10%)
U2932	ABC DLBCL	RPMI 1640 (20%)
WSU-DLCL2	GCB DLBCL	RPMI 1640 (10%)

7.1.5 Formulations

Name	Composition
10x Migration buffer	60.6 g Tris base 288 g Glycine 20 g SDS 2 L H_2O
10x Blotting buffer	50 g Tris base 238 g Glycine 2 L H_2O
AnnexinV binding buffer	10 mM HEPES 150 mM NaCl 2.5 mM $CaCl_2$ in 1x PBS

Acrylamide 10%	125 ml 40% Acrylamide 49 ml 2% Bis-acrylamide 125 ml 1.5 M tris-HCl, pH 8.8 up to 500 ml with H_2O
Acrylamide 25%	312 ml 40% Acrylamide 17 ml 2% Bis-acrylamide 125 ml 1,5 M Tris-HCl, pH 8.8 up to 500 ml with H_2O
FACS buffer	2% FCS 2 mM EDTA in 1x DPBS
Freezing buffer	10% (v/v) DMSO in FCS
MACS buffer	1% FCS 0.5 mM EDTA in 1x DPBS
PBS-T (1x)	1 L 10x PBS 50 ml Tween-20 9 L H_2O
Primary B cell culture media	10% FCS 25 mM HEPES in RPMI 1640
Resuspension buffer	0.1% BSA 0.01 M HEPES 0.1% Saponin in 1x PBS
Sample buffer for SDS-PAGE	7.5 ml 1 M Tris-HCl, pH 7.4 2.4 g SDS 12 mg Bromophenol blue 30% Glycerol 4 ml 14.3 M β-mercaptoethanol up to 100 ml with H_2O adjust to pH 6.8
Stacking gel	31.25 ml 40% Acrylamide 16.25 ml 2% Bis-acrylamide 31.25 ml 1 M Tris-HCl, pH 6.8 add 250 ml H_2O
Supplemented cell lysis buffer	150 mM NaCl 50 mM tris-HCl, pH 7.4 1% triton X-100 50 mM NaF 10 mM Na4P2O7 10 mM Na3VO4 Protease inhibitor 1x (Complete, Roche)
Wash buffer	0.05% Tween in 1x DPBS

7.1.6 Kits and systems

Name	Provider	Catalog No.
B cell isolation kit II, human	Miltenyi Biotec	130-091-151
CellTiter-Glo® 2.0 Cell viability assay	Promega	G9241
CellTiter 96® AQueous one solution cell proliferation assay (MTS)	Promega	G3580
CellTiter-Fluor™ Cell viability assay	Promega	G6081
ECL Western blotting substrate	Promega	W1001
GSH/GSSG-Glo™ assay	Promega	V6611
Human IL-6 Uncoated ELISA Kit	Invitrogen	88-7066-88
Human IL-6 High sensitivity ELISA	Invitrogen	BMS213HS
Human IL-10 Uncoated ELISA Kit	Invitrogen	88-7106-88
NADP/NADPH-Glo™ assay	Promega	G9081
RNAscope™ 2.5 HD Detection Reagents-RED	ACD	322360
RNAscope™ 2.5 HD Reagent Kit-RED	ACD	322350
RNAscope™ 2.5 VS Probe-Hs-NFKBIZ	ACD	497859
Senescence β-Galactosidase staining kit	Cell Signaling	9860
WesternBright Sirius detection kit	Advansta	K-12043-D10

7.1.7 Materials for qPCR

Name	Provider	Catalog No.
Biozym cDNA synthesis kit	Biozym	331470
Green mastermix (2x), No ROX for qPCR	Genaxxon Bioscience	M3023.0500
Proteome profiler mouse cytokine array kit, panel A	R&D	ARY006
Qiashredder	QIAGEN	79656
RNeasy mini kit	QIAGEN	74106
Wizard® Genomic DNA purification kit	Promega	A1120

7.1.8 Oligonucleotides

Name	Forward (5'-3')	Reverse (3'-5')
hBCL6	GGAGTCGAGACATCTTGACTGA	ATGAGGACCGTTTTATGGGCT
hCCL2	CAGCCAGATGCAATCAATGCC	TGGAATCCTGAACCCACTTCT

hCD44	CTGCCGCTTTGCAGGTGTA	CATTGTGGGCAAGGTGCTATT
hCSF2	TCCTGAACCTGAGTAGAGACAC	TGCTGCTTGTAGTGGCTGG
hCXCL6	AGAGCTGCGTTGCACTTGTT	GCAGTTTACCAATCGTTTTGGGG
hCXCL8	TTTTGCCAAGGAGTGCTAAAGA	AACCCTCTGCACCCAGTTTTC
hCXCL10	GTGGCATTCAAGGAGTACCTC	TGATGGCCTTCGATTCTGGATT
hGLUT1	GGCCAAGAGTGTGCTAAAGAA	ACAGCGTTGATGCCAGACAG
hGLUT3	GCTGGGCATCGTTGTTGGA	GCACTTTGTAGGATAGCAGGAAG
hHILPDA	AAGCATGTGTTGAACCTCTACC	TGTGTTGGCTAGTTGGCTTCT
hIGFBP6	AGGAGTGCGGGGTCTACAC	CTCTGCGGTTCACATCCTGT
hIL1A	TGGTAGTAGCAACCAACGGGA	ACTTTGATTGAGGGCGTCATTC
hIL1B	ATGATGGCTTATTACAGTGGCAA	GTCGGAGATTCGTAGCTGGA
hIL6	ACTCACCTCTTCAGAACGAATTG	CCATCTTTGGAAGGTTCAGGTTG
hLCN2	CCACCTCAGACCTGATCCCA	CCCCTGGAATTGGTTGTCCTG
hNFKBIA	CTCCGAGACTTTCGAGGAAATAC	GCCATTGTAGTTGGTAGCCTTCA
hNFKBIZ (exo)	AAGTGCCAGCCCTTTCAAGT	GTCGAACAGGTTAGGCTCGT
hNOS2	TTCAGTATCACAACCTCAGCAAG	TGGACCTGCAAGTTAAAATCCC
hPI3	CACGGGAGTTCCTGTTAAAGG	TCTTTCAAGCAGCGGTTAGGG
hPTX3	CATCTCCTTGCGATTCTGTTTTG	CCATTCCGAGTGCTCCTGA
msACTA2	CCCAGACATCAGGGAGTAATGG	TCTATCGGATACTTCAGCGTCA
msCCL2	TAAAAACCTGGATCGGAACCAAA	GCATTAGCTTCAGATTTACGGGT
msCCL3	TGTACCATGACACTCTGCAAC	CAACGATGAATTGGCGTGGAA
msCCL5	TTTGCCTACCTCTCCCTCG	CGACTGCAAGATTGGAGCACT
msCCL8	TCTACGCAGTGCTTCTTTGCC	AAGGGGGATCTTCAGCTTTAGTA
msCCL19	CCTGGGAACATCGTGAAAGC	TAGTGTGGTGAACACAACAGC
msCCL21	GTGATGGAGGGGGTCAGGA	GGGATGGGACAGCCTAAACT
msCD4	CTAGCTGTCACTCAAGGGAAGA	CGAAGGCGAACCTCCTCTAA
msCD8	CCGTTGACCCGCTTTCTGT	TTCGGCGTCCATTTTCTTTGG
msCD19	CTTGGTATCGAGGTAACCAGTCA	ACAATCACTAGCAAGATGCCC
msCOL1A1	GCTCCTCTTAGGGGCCACT	ATTGGGGACCCTTAGGCCAT
msCSF1	GTGTCAGAACACTGTAGCCAC	TCAAAGGCAATCTGGCATGAAG
msCXCL9	GGAGTTCGAGGAACCCTAGTG	GGGATTTGTAGTGGATCGTGC
msCXCL10	CCAAGTGCTGCCGTCATTTTC	GGCTCGCAGGGATGATTTCAA
msCXCL13	GGCCACGGTATTCTGGAAGC	ACCGACAACAGTTGAAATCACTC
msF4/80	CTGCACCTGTAAACGAGGCTT	GCAGACTGAGTTAGGACCACAA
msIL1A	TCTATGATGCAAGCTATGGCTCA	CGGCTCTCCTTGAAGGTGA
msIL1B	GAAATGCCACCTTTTGACAGTG	TGGATGCTCTCATCAGGACAG
msIL6	CTGCAAGAGACTTCCATCCAG	AGTGGTATAGACAGGTCTGTTGG
msIL8	TCGAGACCATTTACTGCAACAG	CATTGCCGGTGGAAATTCCTT
msIL36G	CAGGTGTGGATCTTTCGTAATCA	CATGGGAGGATAGTCACGCTG
msLy6G	GACTTCCTGCAACACAACTACC	ACAGCATTACCAGTGATCTCAGT
msMMP2	ACCTGAACACTTTCTATGGCTG	CTTCCGCATGGTCTCGATG
msMMP9	GCAGAGGCATACTTGTACCG	TGATGTTATGATGGTCCCACTTG

msMPO	AGGGCCGCTGATTATCTACAT	CTCACGTCCTGATAGGCACA
msNFKBIZ (endo)	TGCTACACATCCGAAGCAACA	CACTGCACTCTTCAGGTCTGT
msNFKBIA	TGAAGGACGAGGAGTACGAGC	TGCAGGAACGAGTCTCCGT
msPDGFB	CATCCGCTCCTTTGATGATCTT	GTGCTCGGGTCATGTTCAAGT
msS100A8	AAATCACCATGCCCTCTACAAG	CCCACTTTTATCACCATCGCAA
msS100A9	GCACAGTTGGCAACCTTTATG	TGATTGTCCTGGTTTGTGTCC
msSCF	GAATCTCCGAAGAGGCCAGAA	GCTGCAACAGGGGGTAACAT
msTGFB	CCACCTGCAAGACCATCGAC	CTGGCGAGCCTTAGTTTGGAC
msTGR5	TGCTTCTTCCTAAGCCTACTACT	CTGATGGTTCCGGCTCCATAG
msTIMP1	CGAGACCACCTTATACCAGCG	ATGACTGGGGTGTAGGCGTA
msTNFA	CAGGCGGTGCCTATGTCTC	CGATCACCCCGAAGTTCAGTAG

7.1.9 Materials for protein expression systems

7.1.9.1 Transient expression

Name	Backbone	Source
FLAG-BRD4	pcDNA5	addgene
FLAG-IκBζ	pCR3	previously generated
FLAG-BRD4-BD	pcDNA5 frt/to	addgene
FLAG-BRD4-7A	pcDNA5 frt/to	addgene
FLAG-BRD4-7D	pcDNA5 frt/to	addgene
Strep-BRD4	pEXPR-IBA103	previously generated
Strep-IκBζ	pCR3	previously generated
Strep-p50	pCR3	previously generated
Strep-STAT3	pCR3	previously generated
HA-Cdk9	pcDNA6/3HA	addgene
Xpress-BRD4 (1-470)	pcDNA4	addgene
Xpress-BRD4 (1-594)	pcDNA4	addgene
Xpress-BRD4 (471-730)	pcDNA4	addgene
Xpress-BRD4 (595-1362)	pcDNA4	addgene
Xpress-BRD4 (1047-1362)	pcDNA4	addgene
NFKBIZ AA 1-442	pCR3	previously generated
NFKBIZ AA 436-718	pCR3	previously generated
NFKBIZ Δ ANK1	pCR3	previously generated
NFKBIZ Δ ANK2	pCR3	previously generated
NFKBIZ Δ ANK3	pCR3	previously generated

NFKBIZ Δ ANK4	pCR3	previously generated
NFKBIZ Δ ANK5	pCR3	previously generated
NFKBIZ Δ ANK6	pCR3	previously generated
NFKBIZ Δ ANK7	pCR3	previously generated

7.1.9.2 Lentiviral expression

Name	Backbone	Source
Empty CRIPSR	Lenti-CRISPRv2	addgene
IκBζ CRISPR/Cas9	Lenti-CRISPRv2	previously generated
Empty Tet-ON	pInducer 20	addgene
FLAG-NFKBIZ WT Tet-ON	pInducer 20	previously generated
Ras (G12V) Tet-ON	pInducer 20	previously generated
Ras (G12V) Tet-ON	pInducer 20	previously generated
Lentiviral empty vector	pLKO.1	Open Biosystems
shRNA-STAT3	pTRIPZ	Dharmacon
shRNA-GLS1	pLKO.1	Sigma Aldrich

Unless otherwise specified, all plasmids are from human origin. *Cloning was performed by Dr. Anja Schmitt, Caroline Schönfeld, Melanie Grimm, Dr. Paula Grondona, in collaboration with the students Tobias Kaster, Barbara Streibl, Jens Bauer, Lisa Schmid or Marie Elen Tuchel.

7.1.10 Antibodies

Name	Provider	Catalog No.
AKT	Cell Signaling	#4691
p-AKT (Ser473)	Cell Signaling	#9271T
AnnexinV-PE/Cy7	BioLegend	640949
Anti-mouse IgG	Jackson Immuno Research	115-005-003
Anti-rabbit IgG	Jackson Immuno Research	111-035-003
c-Jun	Cell Signaling	#9165
c-Myc	Cell Signaling	#9402
Erk1/2	Santa Cruz	514302
p-Erk1/2 (Thr202/Tyr204)	Cell Signaling	#4370T
IkBα	Cell Signaling	#9242
p-IkBα (Ser32/36)	Cell Signaling	#9246
IkBζ	Cell Signaling	#9244

JNK1/2	Cell Signaling	#9258
p-JNK1/2 (Thr183/Tyr185)	Cell Signaling	#4668
Flag	Cell Signaling	#14793S
GAPDH	Cell Signaling	2118S
GLS1 (E4T9Q)	Cell Signaling	#49363
GLS2	Thermo Fisher	PA5-78475
H3K9-me3	Cell Signaling	#13969
H3K27-me3	Cell Signaling	#9733S
STAT3	Cell Signaling	#9139
p-STAT3 (Thy705)	Cell Signaling	#9145
p-4E-BP1 (Thr37/46)	Cell Signaling	#2855
p-elF-4E (Ser209)	Cell Signaling	#9741
p-elF2α (Ser51)	Cell Signaling	#9721
p-S6 (235/236)	Cell Signaling	#81736
Tubulin alpha (DM1A)	Sigma-Aldrich	T9026

All antibodies were dissolved in 1x PBST with 5% (w/v) non-fat dried milk powder or with 5% (w/v) BSA according to the manufacturer's specifications. In addition, NaN3 was added to prevent contamination. Prepared diluted antibodies were used up to 10 times and stored at -20ºC.

7.1.11 Pharmacological inhibitors

Name	Provider	Catalog No.
ABT-199 (Venetoclax)	Selleckchem	S8048
Antimycin A	Sigma Aldrich	66-81-9
BPTES	Selleckchem	S7753
CB-839	Cayman	Cay22038-10
Cycloheximide (CHX)	Sigma Aldrich	S7243
Ferrostatin-1	Selleckchem	S7243
iBET-762 (Molibresib)	Selleckchem	S7189
JQ1	Selleckchem	S7110
MG-132	Selleckchem	S2619
PFI-1	Selleckchem	S1216
Rapamycin	Selleckchem	S1039
Rotenone	Sigma-Aldrich	R8875
THAL-SNS-032	Selleckchem	S8979

7.1.12 Biological reagents and agents used for stimulation

Name	Provider	Catalog No.
Collagenase type IV	Sigma-Aldrich	C4-BIOC
Collagen coating solution	Sigma-Aldrich	125-50
PMA/Ionomycin (P/I)	Sigma-Aldrich	P1585, 56092-81-0
Recombinant human IL-1α	Immunotools	11349012
Recombinant human IL-1β	Immunotools	11340012
Recombinant human IL-4	Immunotools	11340043
Recombinant human IL-6	Immunotools	11340064
Recombinant human IL-10	Immunotools	11340103
Recombinant human sCD40 ligand	Immunotools	11343343
Liver disease spectrum TMA	Tissue Array	LV20812b
Liver cancer survey TMA	Tissue Array	LV2084

7.1.13 Devices

Device	Provider
Axio Vert.A microscope	Zeiss
DMI6000 Microscope	Leica
Fusion FX Vilber Lourmat	Peqlab
Genesys 10S UV-Vis spectrophotometer	Thermo Scientific
HybEZ™ II Hybridization System	ACD
Infinite M200 Reader	Tecan
Lightcycler® 480 II	Roche
LSRII Flow cytometer	BD
NanoDrop 1000 photometer	Peqlab
NuceloCounter® NC-250™	Chemometec
Power supply	BioRad
Thermoshaker	Cell Media
Ultra-Turrax T25 basic	IKA
Vapo.protect Mastercycler® Pro	Eppendorf

7.1.14 Software for data analysis

Product	Provider
CompuSyn	ComboSyn, Inc., Paramus, USA
Combenefit	Cambridge Institute, Cambridge, UK
Flow Jo (Version 10)	Tree Star, Inc., Ashland, USA
GraphPad PRISM (Version 9)	GaphPad Software, Inc., San Diego, USA

7.1.15 Mouse strains

Albumin-Cre (B6.Cg-*Speer6-ps1Tg(Alb-cre)21Mgn*/J)

Albumin-Cre mice, which is a transgenic mouse line expressing Cre recombinase under the control of the mouse albumin enhancer/promoter, were purchased directly from The Jackson Laboratory. Mice were kept under pathogen-free conditions in the animal facility of the Core Facility Transgene Tiere (Tübingen, Germany).

Rosa26-tm(rtTA*Flag-NFKBIZ)J

A transgenic mouse model (C57BL/6 background) with inducible expression of Flag-*NFKBIZ* (controlled by TetO (TRE3G) operator) was designed by Dr. Stephan Hailfinger (UK Münster, Münster, Germany) and Dr. Daniela Krammer (Mainz University, Mainz, Germany) and generated by Ingenious targeting laboratory. These mice utilize the Rosa-Express™ system (Ingenious targeting laboratory) which allows for inducible and tissue specific control of the transgene of interest from the Rosa26 locus. Specifically, the Rosa26 locus incorporated a floxed Neomycin-Stop cassette inserted downstream of a CAG promoter, followed by a reverse tetracycline transactivator component, a TRE3G (tetO) promoter and the Flag-*NFKBIZ* transgene. These mice constituted our parental line and were used as controls. Mice were kept under pathogen-free conditions in the animal facility of the Core Facility Transgene Tiere (Tübingen, Germany). Experiments were performed in accordance with government and institutional guidelines and regulations.

Rosa26-tm(Alb-rtTA*Flag-NFKBIZ)J

Rosa26-tm(rtTA*Flag-*NFKBIZ*)J mice were mated with albumin-cre mice, in order to generate Rosa26-tm(Alb-rtTA*Flag-*NFKBIZ*)J mice. Mating with the tissue-specific

albumin-cre recombinase mouse line allows for removal of the floxed Stop cassette, permitting the expression of the rtTA specifically in hepatocytes. These mice overexpress Flag-*NFKBIZ* specifically in the liver and only after administration of 2 mg/ml doxycycline in the drinking water, which should allow the rtTA to bind to the TRE3G promoter to activate transgene expression. Mice were kept under pathogen-free conditions in the animal facility of the Core Facility Transgene Tiere (Tübingen, Germany). Experiments were performed in accordance with government and institutional guidelines and regulations.

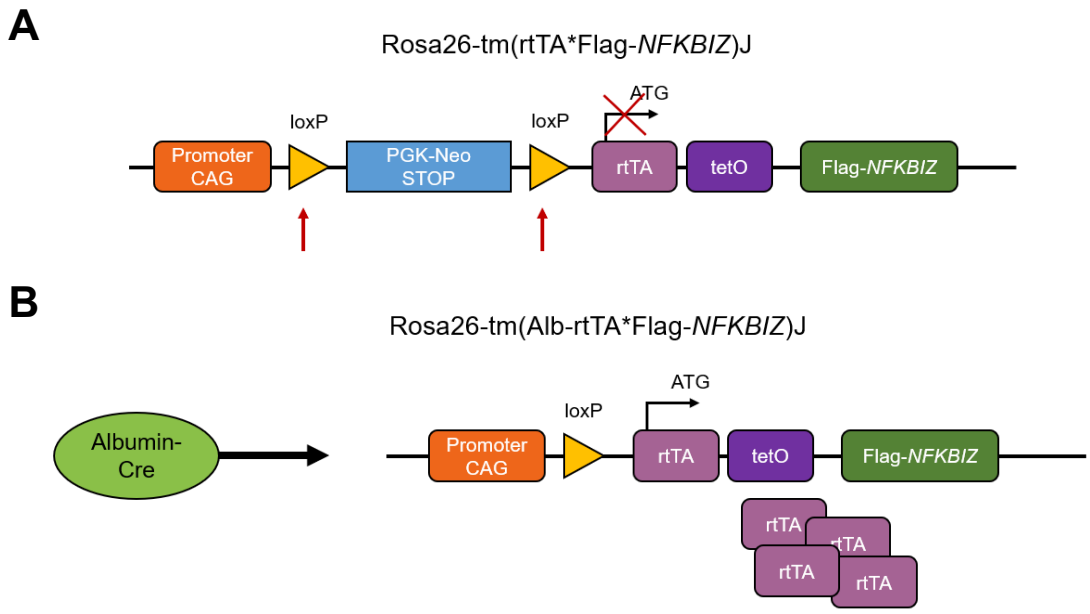

Figure 30. Strategy to generate Rosa26-tm(Alb-rtTA*Flag-*NFKBIZ*)J. (A) Schematic representation of the Rosa26-tm(rtTA*Flag-*NFKBIZ*)J mice provided by Ingenious targeting laboratory. The PGK-Neo STOP cassette prevents rtTA, and Flag-*NFKBIZ* expression. The red arrows indicate the excision sites for the removal of the floxed PGK-Neo STOP cassette. **(B)** Schematic representation of the generation of F1 Rosa26-tm(Alb-rtTA*Flag-*NFKBIZ*)J mice. Mating of the mouse line described in Fig30A with albumin-cre recombinase mice allows for removal of the floxed PGK-Neo STOP cassette, for expression of rtTA from the CAG promoter. Doxycycline introduction allows binding of the rtTA to the TRE3G promoter to activate expression of Flag-*NFKBIZ*. PGK-Neo STOP, PGK-Nemomycin STOP cassette; rtTA, reverse tetracyclin transactivator; tetO, tet operon.

7.2 Methods and protocols

7.2.1 Cell culture methods

7.2.1.1 Culture of immortalized cell lines

All cell lines were kept at 37°C, 5% CO2 in their corresponding media (Table 7.1.2). Immortalized DLBCL cell lines (Table 7.1.4) were cultured in 25 or 75 cm^2 flasks and split every 2 days by 1:4-1:10 in order to keep a density of less than $0.5x10^6$ cells/ml. The HEK293T cell line was cultured in 10 mm plates and split every 2-3 days at a ratio of 1:10.

7.2.1.2 Isolation and culture of human primary B cells

Untouched B cells were isolated from human peripheral blood mononuclear cells (PBMCs) using the B cell isolation kit II, human (Table 7.1.6) according to the manufacturer's instructions and plated at a concentration of $5x10^5$ cells/ml. For their maintenance, four different culture mediums were tested to find the most optimal culture conditions: PB-Max™ Karyotyping medium, X-VIVO™ 15 hematopoietic cell medium, RPMI supplemented with 10% FCS, 100 ng/ml rhsCD40 Ligand and 10 ng/ml rhIL-4 and RPMI supplemented with 10% FCS and 25 mM Hepes.

7.2.1.3 Freezing and thawing of cells

Approximately $4\text{-}5x10^6$ cells were harvested by centrifugation, resuspended in 1-1.5 ml freezing media (Table 7.1.5) and transferred to cryopreservation vials. Then the cryovials were kept for two days in freezing containers at -80°C and subsequently stored in a liquid nitrogen tank for long-term. For thawing of cells, cryovials were partially immersed in a 37°C water bath and transferred to 15 ml centrifuge tubes containing culture media. Cells were centrifuged, resuspended in 10 ml of the respective culture media and transferred to the corresponding cell culture container.

7.2.1.4 Determination of cell number, proliferation and viability

Cell counting

Cell number was assessed using an automated cell counter (Table 7.1.13). In brief, 19 µl of cell suspension were mixed with 1 µl of AO•DAPI (Table 7.1.3). The mixture

was transferred to an A8 Chemometec glass slide (Table 7.1.1) and cell number was quantified automatically using the NucleoCounter® NC-250 device.

Cell viability assays

For long-term survival and cell viability assays, cells were seeded at a density of $2x10^5$ cells/ml either in 96-well plates, 12-well plates or in 25 cm^2 flasks and exposed to the inhibitors or chemical reagents of interest for 2 to 7 consecutive days – depending on the assay. Cells were then counted daily using the cell analyzer (Table) and retreated daily with the respective inhibitor, chemical reagent or solvent control. Every second day the cells were split, seeded in fresh media and treated again. To determine potential synergism between two inhibitors, cells were seeded at a concentration of $2x10^5$ cells/ml in 96-well plates, treated daily for 2 consecutive days and quantified using the MTS assay or the Cell-Titer Fluor™ assay (Table 7.1.6) according to the manufacturer's specifications. After 30 min - 4 h, depending on the assay, absorbance (490 nm) or fluorescence (380–400nm_{Ex}/505nm_{Em}) was measured in a Tecan M200 reader. The value of 490 nm absorbance or 505nm_{Em} fluorescence is directly proportional to the number of living cells in culture. The combination index (CI) was then calculated with the Combenefit software (Di Veroli et al., 2016).

7.2.2 Transient and stable expression systems

7.2.2.1 Calcium phosphate transfection

For transient expression, HEK293T cells were transfected using calcium phosphate. In brief, $1x10^6$ HEK293T cells were seeded in 10 cm^2 plates 24 hours before transfection in supplemented DMEM media. The day after, 50 µl 2.5 M $CaCl_2$ were mixed with 450 µl nuclease-free water in a 1.5 ml reaction tube (one tube was prepared per plate) and 5-10 µg of expressing plasmid were added per tube. Next, while vortexing each reaction tube, 500 µl of 2xHeBs buffer (280 mM NaCl, 1.5 mM Na_2HPO_4, 10 mM Hepes, pH 7.05) were added drop by drop. After a 10 min incubation at RT, the prepared mixtures were added to the corresponding HEK293T culture dish making sure to distribute it equally throughout the plate. Experiments were performed 24-48 h after transfection.

7.2.2.2 Lentiviral transduction

Stable expression of constructs containing lentiCRISPRv2, pInducer or shRNA constructs in adherent (Huh7) or suspension cells (DLBCL cell lines) was achieved by lentiviral transduction using a second-generation packaging system. First, viral particles were produced. In brief, initially HEK2932T cells were transfected as described in section 3.2.2.1 using the lentiviral expressing constructs of interest together with the plasmids coding for the packaging elements, namely pCMV-VSV-G (3 µl per reaction tube) and psPAX2 (6.5 µl per reaction tube). The day after transfection, the medium was exchanged for 6 ml of fresh medium. After 48 h, the lentiviral suspension was filtered with a syringe (0.45 µM) and added to the cells of interest, which had been pre-seeded at a concentration of 0.2-0.3x10^6 cells/ml. Two days after infection, cells were washed twice with pre-warmed medium and seeded in medium containing the corresponding antibiotic for selection (puromycin for shRNA and CRISPRv2, and G418 for pInducer plasmids). For the Tet-ON system, doxycycline was added to the cells in order to achieve protein expression. Puromycin and G418 concentrations were adjusted depending on the cell line. Cells were kept in selection medium for up to 7 days prior to experiments. For experiments involving sh*GLS,* experiments were started just 2 days after selection due to the high cytotoxicity of glutaminase inhibition.

7.2.3 RNA methods

7.2.3.1 RNA isolation and cDNA generation

At least 2x10^6 cells per condition were harvested and subjected to RNA isolation using either the QIAzol method (primary hepatocytes) or the Qiagen RNA kit (liver samples and HCC cell lines) according to manufacturer's instructions. Importantly, for liver samples, 30-60 µg of tissue were transferred into a 2 ml reaction tube and immediately mixed with 300-600 ml of buffer RLT and 1% β-mercaptoethanol. Then liver tissue was lysed with the use of a rotor-stator homogenizer before proceeding with the rest of the protocol. After isolation, RNA concentrations and purity were determined with the use of Nanodrop spectrophotometer and stored at -80ºC until use.

Reverse transcription of total RNA into complementary single-stranded DNA (cDNA) was done using the cDNA Synthesis Kit (Table 7.1.6) and hexamer primers following manufacturer's protocol. Resulting cDNA was diluted 1:5 prior to RT-qPCR analysis.

7.2.3.2 Real time-quantitative PCR

For the measurement of cDNA expression levels, the Green MasterMix (Table 7.1.6) was used. Following user guidelines, an initial reaction mix was prepared with the following components:

Nuclease-free H_2O	3.25 µL
10 µM forward primer	0.25 µL
10 µM reverse primer	0.25 µL
Diluted cDNA	2 µL
Green MasterMix	6.25 µL

The reaction mix was then carefully resuspended and pipetted in triplicates in a 384-well plate. The plate was then shortly centrifuged for 1 min at 1500 x g and then the PCR was performed with the following conditions: 1 cycle at 95ºC for 15 min for denaturation, followed by 40 cycles at 95ºC for 15 sec and 60ºC for 4 sec. Real-time PCR data was analyzed using Microsoft Excel 2010. Relative quantification of cDNA expression was calculated using the $2^{-\Delta\Delta CT}$ method (Livak & Schmittgen, 2001). ΔΔCt values of each mRNA were divided by the ΔΔCt value of the housekeeping gene (RPL37A or GAPDH) and normalized to the corresponding value of internal reference (untreated/control sample).

7.2.3.3 RNAscope®

The RNAscope® assy uses a method of *in situ* hybridization (ISH) to visualize single RNA molecules in samples mounted on slides. We used this method in order to quantify IkBζ mRNA in TMAs of human progressive liver disease and HCC. Following manufacturer's instructions, we complied with the following workflow (provided by Advanced Cell Diagnostics) with the reagents included in the RNAscope® assay kit:

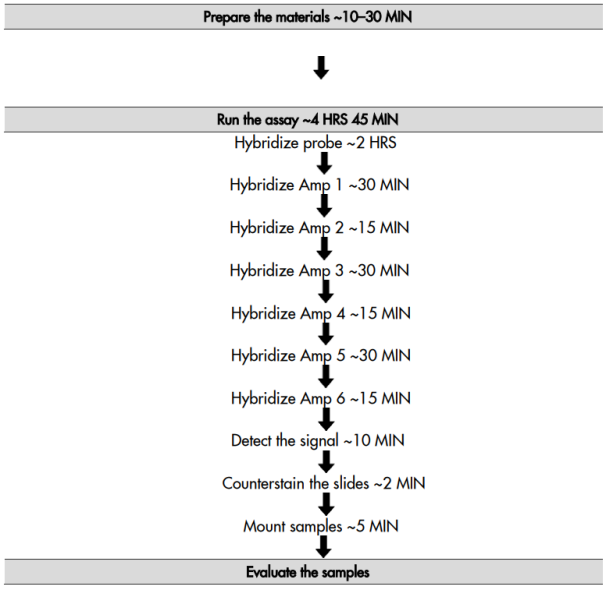

In our case, the samples were hybridized with the RNAscope™ 2.5 VS Probe-Hs-NFKBIZ to detect IkBζ mRNA. For each hybridization step, 4 drops of each specified probe were added per sample and incubated for the indicated amounts of time in the provided oven at 40ºC (Amp 1 - Amp 4) or at RT (Amp 5 - Amp 6). Between each of these initial steps, samples were washed 3 times with Wash Buffer at RT. For the detection step, Fast RED-B was mixed with Fast RED-A at a 1:60 ratio to prepare a total of 120 µl of RED solution per sample. After incubation for 10 min at RT, samples were submerged in distilled water, and then rinsed in fresh tap water. Finally, tissues were counterstained with 50% Hematoxylin for 2 min at RT and washed 3-5 times in tap water until slides were clear. To finish, samples were dried at 60ºC in a dry oven for at least 15 min, dipped in fresh pure xylene and mounted with 1-2 drops of EcoMount and a coverslip.

7.2.4 Protein methods

Cell harvesting and lysate preparation

DLBCL suspension cells were seeded and treated as mentioned in 7.2.1.1. After treatment, all cells were transferred to a 15 ml centrifuge tube. Then, cells were centrifuged at 1800 rpm for 3 minutes and twice washed in 1x PBS. After washing, cells were transferred to 1.5 ml reaction tubes and resuspended in at least 2x the pelleted volume with lysis buffer supplemented with protease and phosphatase inhibitors (Table 7.1.3). Cells were then incubated on ice for 10 minutes with intermittent vortexing followed by sonication for 5 min. Next, cells were centrifuged at

14.000 g for 10 min at 4ºC and the resulting supernatant, corresponding to the whole cell extract, was harvested and transferred to a new 1.5 ml reaction tube.

Determination of whole protein concentration

Protein concentrations of each sample were measured in duplicates using the Bio-Rad Protein Assay Dye Reagent Concentrate. To measure the protein concentration, the protein assay dye concentrate was initially diluted in a 1:5 ratio with ddH_2O to generate the working reagent (WR). Next, 0.5 µl of each lysate was mixed with 1 ml of WR in a 1.5 ml reaction tube and thoroughly vortexed. The absorbance of the samples was then measured at λ = 562 nm using the Genesys 10S UV-Vis spectrophotometer (Table 7.1.13). Protein concentrations were calculated with an according calibration curve.

Protein sample preparation

Cell lysates were diluted accordingly in 3x sample buffer to obtain a total of 30-120µg of protein per sample and were heated up for 5 min at 95ºC to induce protein denaturation. For long-term storage lysates were kept at -20°C.

Immunoprecipitation

To assess possible IκBζ interaction partners, wild-type Brd4, STAT3, p50 and IκBζ or truncated Brd4 and IκBζ mutants were ectopically expressed in HEK293T cells and assessed via steptavidin or FLAG pull-down assays. In brief, after cell lysis and subsequent protein concentration determination, which was performed as described in section 3.2, 30 µl of the resulting protein fraction were transferred to a 1.5 ml reaction tube and stored at -20ºC to serve as input-control. The remaining lysate was then precleared with pre-washed sepharose 6B beads for 30 min at 4ºC in a rotating wheel. After preclearing, samples were centrifuged for 1 min at 3000 rpm to collect the resulting supernatant, which constitutes the precleared lysate. This precleared lysate was then incubated with pre-washed anti-FLAG M2 agarose beads or streptavidin affinity beads (Table 7.1.2) for 1 h at 4ºC in a rotating wheel. After incubation, the resulting samples were centrifuged for 1 min at 3000 rpm and washed 3 times with 1 ml lysis buffer. Finally, the resulting pellet was resuspended in 80 µl of 3x sample buffer and boiled at 95ºC for 5 min. Immunoprecipitated complexes were resolved with SDS-PAGE by loading 10 µl of input control and 20-30 µl of immunoprecipitated samples.

Interaction partners of endogenous IκBζ were evaluated in the NFKBIZ-OE Huh7 cell line after induction of IκBζ expression with doxycycline treatment for 48 h via protein A pull-down assays. All steps followed were identical to the ones explained above with the following differences:

I. Preclearing was performed using protein A agarose beads.
II. Pre-cleared lysates were incubated with an anti-Brd4 or an IgG isotype control antibody (diluted 1:50) overnight at 4ºC in a rotating wheel.

After incubation, steps proceeded as explained previously and immunoprecipitated complexes were resolved with SDS-PAGE by loading 10 µl of input control and 20-30 µl of immunoprecipitated samples.

SDS-PAGE and immunoblotting

Detection of protein expression in whole cell extracts was assessed by Western Blot. First, lysates were loaded into a 10-15% SDS-PAGE (consisting of an upper collection gel and a lower separating gel) according to the components in Table 7.1.2 and 7.1.5 using the Peqlab PerfectBlue gel system Twin ExW S. To be able to determine the proteins' molecular weight, one or more protein ladders were loaded into each gel. Initially, the gels were run at 80 V for 10-30 min, which was then increased to 120 V and run for 2-3 hours in 1x migration buffer. After protein separation with gel electrophoresis, the proteins were transferred from the gel to a nitrocellulose membrane by electroblotting with the BioRad Trans-Blot® Cell in 1x blotting buffer (Table 7.1.5). The transfer conditions were 100 V for 90-120 minutes, after which the membranes were stained briefly with 5 ml of Ponceau reagent for 5 min at RT to evaluate the efficiency of the transfer. After washing out the Ponceau staining, the membranes were incubated for 30-60 min in 5% nonfat dry milk in TBS-T to block nonspecific binding sites. Then, membranes were incubated overnight with the corresponding primary antibody diluted in 5% milk or BSA depending on the specifications (Table 7.1.10) at 4°C on a shaker. The next day, membranes were washed three times for 5 min in PBS-T to remove excess or unspecific binding of primary antibody, and incubated with mouse or rabbit secondary antibodies (Table 7.1.10) for 3-4 hours at RT. After incubation, membranes were washed 3 more times with PBS-T and developed using ECL substrate at room temperature in dark

conditions. The chemiluminescence signals were detected with the Fusion SL detection system.

7.2.5 Enzyme-linked immunosorbent assay (ELISA)

Detection of secreted IL-6 or IL-10 from DLBCL cell lines (Fig. 5.3) was assessed by ELISA with the kits listed in table 7.1.6. In brief, cells were seeded at a concentration of $3x10^5$ cells/ml in 25 cm^2 flasks in triplicates and treated for 24 or 48 h with the corresponding inhibitors or their solvent control. After treatment, the cell suspensions were transferred to 15 ml centrifugation tubes and centrifuged at 1800 rpm for 3 min. After centrifugation, supernatants were transferred to new 15 ml tubes. Samples were diluted in cell medium at a ratio of 1:10 before proceeding with the IL-10 ELISA kit, while samples assayed via the IL-6 ELISA kit were left undiluted. Subsequently, the ELISAs were performed according to the manufacturer's instructions. For long-term storage the supernatants were kept at -20°C degrees.

7.2.6 Senescence assays

7.2.6.1 Senescence induction

To induce senescence in the human HCC cell line SMMC, we initially generated an SMMC/Tet-ON-Ras^{G12V} cell line (Ras-SMMC cells) (as described in section 3.2.2.2) that could express oncogenic Ras (Ras^{G12V}) in an inducible manner via doxycycline treatment. Once generated, $5x10^5$ Ras-SMMC cells were first plated in 6-well plates and treated with 1 µg/ml doxycycline for 3 consecutive days, after which the medium was exchanged for fresh medium, and cells were left untreated for 4 consecutive days. After this 7-day period, Ras-SMMC cells started exhibiting a clear senescent morphology (Fig.24A).

7.2.6.2 β-Galactosidase Staining (SA-β-gal)

Senescent cells express β-galactosidase at pH6 and can easily be detected via SA-β-gal staining. To monitor the induction of oncogene-induced senescence in Ras-SMMC cells, we performed SA-β-gal staining according to manufacturer's protocol (Table 7.1.6). In brief, after senescence induction as indicated in section 3.2.6.1, Ras-SMMC cells washed with 2 ml 1x PBS and then fixed for 10 min with 1 ml of 1x Fixative Solution. After fixation, cells were washed twice with 1x PBS and 1 ml of

β-Galactosidase Staining Solution was added to each well. The plate was then sealed with parafilm and incubated at 37ºC overnight in a dry incubator. For microscopic visualization, the β-Galactosidase Staining Solution was removed, and cells were overlaid with 70% glycerol. For long term storage, plates were kept at 4ºC.

7.2.7 Fluorescence activated cell sorting (FACS)

To examine the effects of glutaminase inhibition on cell cycle, apoptosis, lipid peroxidation, accumulation of reactive oxygen species and mitochondrial membrane potential, flow cytometry analyses were performed. For all assays, $5x10^5$ - $1x10^6$ cells were initially transferred to a test tube for staining and measurement.

7.2.7.1 Surface staining

Analysis of lipid peroxidation

To monitor ferroptosis induction, cells were stained with the lipid peroxidation sensor BODIPY 581/591 undecanoic acid (BODIPY C11; Thermo Fisher Scientific). In brief, cells were stained with 2 mM of BODIPY C11 in Hanks' balanced salt solution (HBSS) for 15 min at 37ºC. Cells were then centrifuged at 1800 rpm for 3 min and washed twice in 1 ml HBSS. After washing, dead cells were stained using SYTOX Blue dead cell stain (Table 7.1.2). The percentage of oxidized BODIPY C11 cells and mean fluorescence intensity of oxidized BODIPY C11 were quantified by flow cytometry (BD LSRII) normalized to the mean fluorescence intensity of the reduced probe. FlowJo (V10) software was used for histograms.

Analysis of lipid peroxidation

To monitor ferroptosis induction, cells were stained with the lipid peroxidation sensor BODIPY 581/591 undecanoic acid (BODIPY C11; Thermo Fisher Scientific). In brief, cells were stained with 2 mM of BODIPY C11 in Hanks' balanced salt solution (HBSS) for 15 min at 37ºC. Cells were then centrifuged at 1800 rpm for 3 min and washed twice in 1 ml HBSS. After washing, dead cells were stained using SYTOX Blue dead cell stain (Table 7.1.2). The percentage of oxidized BODIPY C11 cells and mean fluorescence intensity of oxidized BODIPY C11 were quantified by flow cytometry (BD LSRII) normalized to the mean fluorescence intensity of the reduced probe. FlowJo (V10) software was used for histograms.

Analysis of mitochondrial and intracellular ROS

To monitor accumulation of mitochondrial ROS, cells were stained with the mitochondrial-specific superoxide sensor MitoSOX (Table 7.1.2). In brief, cells were washed once in 1 ml HBSS and then stained with 1 µM of MitoSOX in HBSS for 10 min at 37ºC. After washing a second time, dead cells were stained using SYTOX Blue dead cell stain (Table 7.1.2). The percentage of MitoSOX-positive cells and mean fluorescence intensity of MitoSOX were quantified by flow cytometry (BD LSRII) and normalized to the mean fluorescence intensity of the untreated probe. FlowJo (V10) software was used for histograms. To assay the accumulation of intracellular ROS, the same procedure as described above was followed, with two main differences:

I. Cells were stained with 5 µM of the live cell-specific ROS sensor CellROX (Table 7.1.2).
II. Incubation was performed for 30 min at 37ºC.

Analysis of cytosolic ROS

Shortly before treatment, cells were resuspended in pre-warmed HBSS containing 1 µM of H_2DCFDA and incubated at 37ºC for 45 min. After dye loading, cells were centrifuged, resuspended in pre-warmed media and $5x10^5$ cells were seeded per well in a 12-well plate in triplicates. Cells were then treated as indicated in Fig.12C for the specified amount of time. After treatment, $5x10^5$ cells were transferred to test tubes, washed twice in 1 ml HBSS, after which fluorescence was quantified by flow cytometry (BD LSRII) and normalized to the intensity of the untreated or solvent control probe. FlowJo (V10) software was used for histograms.

Analysis of mitochondrial membrane potential (MMP) and activity

To monitor mitochondrial activity and alterations in the MMP, cells were stained with the cell permeable, positively charged tetramethylrhodamine, ethyl ester (TMRE) (Table 7.1.2). In brief, cells were washed once in 1 ml 1x PBS and then stained with 50 nM of TMRE in PBS for 30 min at 37ºC. After washing two more times, dead cells were stained using SYTOX Blue dead cell stain (Table 7.1.2). The percentage of TMRE-positive cells and mean fluorescence intensity of TMRE were quantified by flow cytometry (BD LSRII) and normalized to the mean fluorescence intensity of the untreated probe. FlowJo (V10) software was used for histograms.

7.2.7.2 Intracellular staining

Propidium Iodide (PI)/RNase staining

To analyze cell cycle alterations after glutaminase inhibition, cells were stained with the DNA and RNA intercalating agent PI. PI/RNase is used to specifically determine DNA content, since it contains a ribonuclease that removes RNA from the samples. Previous to the staining, cells were washed once with 1 ml of pre-warmed 1x PBS and resuspended in 500 µl resuspension buffer (Table 7.1.5) in order to permeabilize the cells. Then 500 µl of PI/RNase solution were added per sample and these were incubated for 1 h in the dark at RT. Samples were then centrifuged at 2000 rpm for 3 min and washed once with 1 ml 1x PBS. For measurement, pellets were resuspended in 250 µl 1x PBS and fluorescence was quantified by flow cytometry (BD LSRII). FlowJo (V10) software was used for histograms.

7-AAD/AnnexinV staining

In order to assess apoptosis after glutaminase inhibition, we stained the cells with 7-AAD and AnnexinV-PE/Cy7. 7-AAD will intercalate with double-stranded DNA only in dead cells with compromised cellular membranes. AnnexinV, on the other hand, binds to phosphatidylserine, which translocates to the outer plasma membrane during early apoptosis. Hence, staining with AnnexinV and 7-AAD allows for discrimination between live, early apoptotic and late apoptotic cells.

In brief, cells were first washed twice in FACS buffer and resuspended in 100 µl of AnnexinV binding buffer. Next, 5 µl of AnnexinV-PE/Cy7 and 5 µl of 7-AAD were added to the cell suspension, gently vortexed and incubated for 15 min at RT in the dark. For measurement, pellets were resuspended in 400 µl AnnexinV buffer and fluorescence was quantified by flow cytometry (BD LSRII). FlowJo (V10) software was used for histograms.

7.2.8 Luminescence and fluorescence assays

7.2.8.1 Quantification of cellular GSH levels

Levels of reduced (GSH) and oxidized (GSSG) glutathione in cellular lysates were quantified using the GSH/GSSG-Glo Assay (Table 7.1.6) according to the manufacturer's protocol. For this assay, $5x10^5$ of pretreated cells were initially resuspended in 250 µl 1x PBS. In brief, each sample was divided into two different wells (in triplicates): one of the wells was treated with 25 µl of Total Glutathione Lysis Reagent, which converts all glutathione (both oxidized and reduced) into the reduced form of GSH, while the other well was treated with 25 µl of Oxidized Glutathione Lysis Reagent, which contains N-Ethylmaleimide (NEM), which reacts with GSH so that only oxidized GSH is reduced to GSH. Next, 50 µl of Luciferin Generation Reagent were added per well. This reagent generates luciferin from the GSH present in the sample through the action of GST. Hence, the amount of luciferin generated depends on the moles of reduced GSH present in the sample. Finally, 100 µl of Luciferin Detection Reagent were added to each well to initiate luminescence signal via the action of luciferase. The amount of luminescence detected is directly proportional to the amount of GSH derived from total glutathione or oxidized glutathione alone. The ratio of oxidized to reduced glutathione present in each sample were then calculated following manufacturer's instructions.

7.2.8.2 Quantification of cellular NADPH levels

Levels of reduced (NADPH) and oxidized nicotinamide adenine dinucleotide phosphate (NADP) in cellular lysates were quantified using the NADP+/NADPH-Glo Assay (Table 7.1.6) according to the manufacturer's protocol. For this assay, $1,25x10^6$ of pretreated cells were initially resuspended in 250 µl 1x PBS. Similar to the GSH quantification assay, 50 µl of each sample were pipetted into two different wells (in triplicates) and received a different treatment in order to quantify $NADP^+$ and NADPH separately. Initially, all cells were lysed with 50 µl of base solution with 1% DTAB. For the measurement of NADP+, 25 µl of 0.4 M HCl to one of the wells. Next, plates were incubated for 15 min at 60ºC and equilibrated for 10 min at RT. 25 µl of 0.5 M Trizma® base were added to the acid-treated samples, while the other samples received 50 µl of HCl/Trizma®. Finally, 100 µl of NADP/NADPH-Glo™ Detection Reagent were added

to each well, which allows for the emission of luminescent signal proportional to the original amount of $NADP^+$ or NADPH present in the samples.

7.2.8.3 Quantification of cellular ATP levels

This assay is utilized to determine the number of viable cells in culture by quantifying the amount of ATP present. The assay is designed so that luciferin is catalyzed by luciferase only in the presence of Mg^{2+} and ATP. Hence, only viable cells will emit luminescence. First, cells were plated as indicated in section 3.2.1.4 and treated with the inhibitor of interest or its solvent control. 48 h after treatment start, the plate was first equilibrated to RT for 30 min and then 150 µl of CellTiter-Glo® 2.0 Reagent (Table 7.1.6) were added per well and plate was shaken briefly. After a 10 min incubation period at RT, luminescence was recorded using the Tecan M200 plate reader.

7.2.8.4 CellTiter-Fluor™ cell viability assay

The CellTiter-Fluor™ viability assay is a non-lytic fluorescence assay that measures the activity of a conserved protease that is constitutively active in live cells, and therefore serves as a marker of cell viability. In brief, cells were initially plated as determined in section 3.2.1.4 (Cell viability assays) and treated as indicated for 48 h. After treatment, cells were resuspended and 50 µl of each sample (in triplicates) were transferred to a new 96-well plate. Finally, 50 µl of CellTiter-Fluor™ Reagent (Table 7.1.6) were added to all wells, mixed briefly and incubated for 30 min at 37ºC. After incubation, fluorescence was measured using the Tecan M200 reader (Table 7.1.13) every 30 min up to a total time of 3 h.

7.2.9 Microscopy

Imaging and detection of IkBζ mRNA expressed in human tissue microarrays of liver disease and HCC was performed after staining with the RNAscope® *in situ* hybridization method. After mounting of samples, images were acquired with the confocal microscope Zeiss 710 (Table 7.1.13) using immersion oil when required.

8 Acknowledgements

First of all, I would like to thank my primary supervisor Prof. Dr. Stephan Hailfinger for for his excellent guidance, support and advice throughout my doctoral thesis. Thank you for your positivity and encouragement when times got hard, for creating such an enjoyable working atmosphere in the lab, for all the interesting discussions at lunch time and for always being present and willing to help, even in the distance. You have been missed in Tübingen. Thank you for giving me the opportunity to work on these exciting projects. I would also like to express my gratitude to Professor Dr. Klaus Schulze-Osthoff for the opportunity to work in this lab and for the very useful insights into this project.

I would like to thank all the people that have contributed in one way or another to this project. Caro and Meli, thank you so much for everything that you taught me in the lab and for your continuous technical support and good working atmosphere. I would also like to thank all the new KSO lab members, but especially Aylin and Vanessa, for always helping in whatever they could (lab or otherwise), for all the support handling the two projects when it was getting hard and, of course, for the all the laughs during lunch time. The lab is definitely in good hands with both of you in it. I would like to give a special thanks to my colleagues Anja and Philip. Anja, many thanks for all the useful comments and corrections, for your scientific advice and for your mentoring in the lab. Philip, you make the lab such a fun place to work at. Thank you for your kindness, for always being so positive, and for the countless times you helped me out, even when I was going through difficult personal times.

Por supuesto, no me olvido de mi familia y amigos, a los que he echado mucho de menos durante este tiempo. Quiero agradecer a mis personas “vitamina”, Elena, Mireia, María M, Marieta, María L., Raquel, Patricia y Cristina, que se han mantenido a mi lado a pesar de la distancia y a pesar del tiempo. Las pocas veces que os he podido ver durante los últimos años, me habéis dado la energía para poder continuar y sé que siempre puedo contar con vosotras. Un agradecimiento especial va para Neus y Jordi. No sé qué habría hecho sin vosotros. Habéis sido mis pilares de apoyo, me habéis levantado cuando me he caído y habéis aguantado mis incesantes quejas.

Gracias a vosotros nunca me he sentido sola y he podido seguir adelante a pesar de todo.

Finalmente, me gustaría agraceder a mi familia por todas sus palabras de aliento. Gracias a mis padres, por haberme llevado hasta donde estoy ahora. Gracias por confiar en mi, por impulsarme en el camino y por vuestro apoyo. Papá, gracias por siempre ser capaz de relativizar los problemas, por tus consejos y por siempre estar ahí cuando lo he necesitado. Mamá, todos mis logros son tuyos. Tu fuerza, valentía y saber estar han sido un ejemplo. Gracias a mi hermano Álvaro, por todo el cariño que siempre das y que tan necesario es. Gracias por siempre poner una sonrisa en mi cara. Abuela, gracias por creer en mí y por recordarme siempre que lo más importante es ser feliz.

Toby, I can't imagine having made it this far without you. A big thank you for always being willing to bring me to the lab at ridiculous hours during weekends and never complaining about it. Thank you for your constant words of encouragement, for making me feel that I can accomplish anything I set my mind to, and especially for the many beautiful moments and experiences you have given me during this time, which have allowed me to enjoy every step of this difficult journey.

9 References

Abla, H., Sollazzo, M., Gasparre, G., Iommarini, L., & Porcelli, A. M. (2020). The multifaceted contribution of α-ketoglutarate to tumor progression: An opportunity to exploit? *Seminars in Cell & Developmental Biology*, *98*, 26–33.

Abubaker, J., Bavi, P. P., Al-Harbi, S., Siraj, A. K., Al-Dayel, F., Uddin, S., & Al-Kuraya, K. (2007). PIK3CA mutations are mutually exclusive with PTEN loss in diffuse large B-cell lymphoma. *Leukemia*, *21*(11), 2368–2370.

Advani, R. H., Buggy, J. J., Sharman, J. P., Smith, S. M., Boyd, T. E., Grant, B., Kolibaba, K. S., Furman, R. R., Rodriguez, S., Chang, B. Y., Sukbuntherng, J., Izumi, R., Hamdy, A., Hedrick, E., & Fowler, N. H. (2012). Bruton Tyrosine Kinase Inhibitor Ibrutinib (PCI-32765) Has Significant Activity in Patients With Relapsed/Refractory B-Cell Malignancies. *Journal of Clinical Oncology*, *31*(1), 88–94.

Aleksandrova, K., Boeing, H., Nöthlings, U., Jenab, M., Fedirko, V., Kaaks, R., Lukanova, A., Trichopoulou, A., Trichopoulos, D., Boffetta, P., Trepo, E., Westhpal, S., Duarte-Salles, T., Stepien, M., Overvad, K., Tjønneland, A., Halkjær, J., Boutron-Ruault, M.-C., Dossus, L., … Pischon, T. (2014). Inflammatory and metabolic biomarkers and risk of liver and biliary tract cancer. *Hepatology*, *60*(3), 858–871.

Alexander, E., Hildebrand, D. G., Kriebs, A., Obermayer, K., Manz, M., Rothfuss, O., Schulze-Osthoff, K., & Essmann, F. (2013). IκBζ is a regulator of the senescence-associated secretory phenotype in DNA damage- and oncogene-induced senescence. *Journal of Cell Science*, *126*(16), 3738–3745.

Ali, H. A., Li, Y., Bilal, A. H. M., Qin, T., Yuan, Z., & Zhao, W. (2022). A Comprehensive Review of BET Protein Biochemistry, Physiology, and Pathological Roles. *Frontiers in Pharmacology*, *13*.

Alizadeh, A. A., Eisen, M. B., Davis, R. E., Ma, C., Lossos, I. S., Rosenwald, A., Boldrick, J. C., Sabet, H., Tran, T., Yu, X., Powell, J. I., Yang, L., Marti, G. E., Moore, T., Hudson, J., Lu, L., Lewis, D. B., Tibshirani, R., Sherlock, G., … Staudt, L. M. (2000). Distinct types of diffuse large B-cell lymphoma identified by gene expression profiling. *Nature*, *403*(6769), 503–511.

Altman, B. J., Stine, Z. E., & Dang, C. v. (2016). From Krebs to clinic: glutamine metabolism to cancer therapy. *Nature Reviews Cancer*, *16*(10), 619–634.

Amandine David, Nicolas Arnaud, Magali Fradet, Hélène Lascaux, Catherine Ouk-Martin, Nathalie Gachard, Ursula Zimber-Strobl, Jean Feuillard, & Nathalie Faumont. (2017). c-Myc dysregulation is a co-transforming event for nuclear factor-κB activated B cells. *Haematologica*, *102*(5), 883–894.

Annemann, M., Plaza-Sirvent, C., Schuster, M., Katsoulis-Dimitriou, K., Kliche, S., Schraven, B., & Schmitz, I. (2016). Atypical IκB proteins in immune cell differentiation and function. *Immunology Letters*, *171*, 26–35.

Ardlie, K. G., Deluca, D. S., Segrè, A. v, Sullivan, T. J., Young, T. R., Gelfand, E. T., Trowbridge, C. A., Maller, J. B., Tukiainen, T., Lek, M., Ward, L. D., Kheradpour, P., Iriarte, B., Meng, Y., Palmer, C. D., Esko, T., Winckler, W., Hirschhorn, J. N., … Dermitzakis, E. T. (2015). The Genotype-Tissue Expression (GTEx) pilot analysis: Multitissue gene regulation in humans. *Science*, *348*(6235), 648–660.

Armitage, J. O., Gascoyne, R. D., Lunning, M. A., & Cavalli, F. (2017). Non-Hodgkin lymphoma. *The Lancet*, *390*(10091), 298–310.

Asai, R., Tsuchiya, H., Amisaki, M., Makimoto, K., Takenaga, A., Sakabe, T., Hoi, S., Koyama, S., & Shiota, G. (2019). CD44 standard isoform is involved in maintenance of cancer stem cells of a hepatocellular carcinoma cell line. *Cancer Medicine*, *8*(2), 773–782.

Bergmann, J., Müller, M., Baumann, N., Reichert, M., Heneweer, C., Bolik, J., Lücke, K., Gruber, S., Carambia, A., Boretius, S., Leuschner, I., Becker, T., Rabe, B., Herkel, J., Wunderlich, F. T., Mittrücker, H.-W., Rose-John, S., & Schmidt-Arras, D. (2017). IL-6 trans-signaling is essential for the development of hepatocellular carcinoma in mice. *Hepatology*, *65*(1), 89–103.

Bo, H., Xiao-Dong, Y., Ming-Ming, Z., Keiko, O., & Lin-Feng, C. (2009). Brd4 Coactivates Transcriptional Activation of NF-κB via Specific Binding to Acetylated RelA. *Molecular and Cellular Biology*, *29*(5), 1375–1387.

Botman, D., Tigchelaar, W., & Van Noorden, C. J. F. (2014). Determination of Glutamate Dehydrogenase Activity and Its Kinetics in Mouse Tissues using Metabolic Mapping (Quantitative Enzyme Histochemistry). *Journal of Histochemistry & Cytochemistry*, *62*(11), 802–812.

Bowzyk Al-Naeeb, A., Ajithkumar, T., Behan, S., & Hodson, D. J. (2018). Non-Hodgkin lymphoma. *BMJ*, *362*, k3204.

Bradshaw, P. C. (2021). Acetyl-CoA Metabolism and Histone Acetylation in the Regulation of Aging and Lifespan. *Antioxidants*, *10*(4).

Braig, M., & Schmitt, C. A. (2006). Oncogene-Induced Senescence: Putting the Brakes on Tumor Development. *Cancer Research*, *66*(6), 2881–2884.

Brown, K. D., Claudio, E., & Siebenlist, U. (2008). The roles of the classical and alternative nuclear factor-kappaB pathways: potential implications for autoimmunity and rheumatoid arthritis. *Arthritis Research & Therapy*, *10*(4), 212.

Cacace, A., Sboarina, M., Vazeille, T., & Sonveaux, P. (2017). Glutamine activates STAT3 to control cancer cell proliferation independently of glutamine metabolism. *Oncogene*, *36*(15), 2074–2084.

Camicia, R., Winkler, H. C., & Hassa, P. O. (2015). Novel drug targets for personalized precision medicine in relapsed/refractory diffuse large B-cell lymphoma: a comprehensive review. *Molecular Cancer*, *14*(1), 207.

Caro, P., Kishan, A. U., Norberg, E., Stanley, I. A., Chapuy, B., Ficarro, S. B., Polak, K., Tondera, D., Gounarides, J., Yin, H., Zhou, F., Green, M. R., Chen, L., Monti, S., Marto, J. A., Shipp, M. A., & Danial, N. N. (2012). Metabolic Signatures Uncover Distinct Targets in Molecular Subsets of Diffuse Large B Cell Lymphoma. *Cancer Cell*, *22*(4), 547–560.

Carragher, D., Johal, R., Button, A., White, A., Eliopoulos, A., Jenkinson, E., Anderson, G., & Caamaño, J. (2004). A Stroma-Derived Defect in NF-κB2−/− Mice Causes Impaired Lymph Node Development and Lymphocyte Recruitment1. *The Journal of Immunology*, *173*(4), 2271–2279.

Catanzaro, J. M., Sheshadri, N., Pan, J.-A., Sun, Y., Shi, C., Li, J., Powers, R. S., Crawford, H. C., & Zong, W.-X. (2014). Oncogenic Ras induces inflammatory cytokine production

by upregulating the squamous cell carcinoma antigens SerpinB3/B4. *Nature Communications*, *5*(1), 3729.

Chapman, S. J., Khor, C. C., Vannberg, F. O., Rautanen, A., Segal, S., Moore, C. E., Davies, R. J. O., Day, N. P., Peshu, N., Crook, D. W., Berkley, J. A., Williams, T. N., Scott, J. A., & Hill, A. V. S. (2010). NFKBIZ polymorphisms and susceptibility to pneumococcal disease in European and African populations. *Genes & Immunity*, *11*(4), 319–325.

Chapuy, B., Stewart, C., Dunford, A. J., Kim, J., Kamburov, A., Redd, R. A., Lawrence, M. S., Roemer, M. G. M., Li, A. J., Ziepert, M., Staiger, A. M., Wala, J. A., Ducar, M. D., Leshchiner, I., Rheinbay, E., Taylor-Weiner, A., Coughlin, C. A., Hess, J. M., Pedamallu, C. S., … Shipp, M. A. (2018). Molecular subtypes of diffuse large B cell lymphoma are associated with distinct pathogenic mechanisms and outcomes. *Nature Medicine*, *24*(5), 679–690.

Cheng, A.-L., Qin, S., Ikeda, M., Galle, P. R., Ducreux, M., Kim, T.-Y., Lim, H. Y., Kudo, M., Breder, V., Merle, P., Kaseb, A. O., Li, D., Verret, W., Ma, N., Nicholas, A., Wang, Y., Li, L., Zhu, A. X., & Finn, R. S. (2022). Updated efficacy and safety data from IMbrave150: Atezolizumab plus bevacizumab vs sorafenib for unresectable hepatocellular carcinoma. *Journal of Hepatology*, *76*(4), 862–873.

Cheson, B. D., Nowakowski, G., & Salles, G. (2021). Diffuse large B-cell lymphoma: new targets and novel therapies. In *Blood Cancer Journal* (Vol. 11, Issue 4). Springer Nature.

Chiang, C.-M. (2016). Phospho-BRD4: transcription plasticity and drug targeting. *Drug Discovery Today: Technologies*, *19*, 17–22.

Chien, Y., Scuoppo, C., Wang, X., Fang, X., Balgley, B., Bolden, J. E., Premsrirut, P., Luo, W., Chicas, A., Lee, C. S., Kogan, S. C., & Lowe, S. W. (2011). Control of the senescence-associated secretory phenotype by NF-κB promotes senescence and enhances chemosensitivity. *Genes & Development*, *25*(20), 2125–2136.

Coiffier, B., Thieblemont, C., van den Neste, E., Lepeu, G., Plantier, I., Castaigne, S., Lefort, S., Marit, G., Macro, M., Sebban, C., Belhadj, K., Bordessoule, D., Fermé, C., & Tilly, H. (2010). Long-term outcome of patients in the LNH-98.5 trial, the first randomized study comparing rituximab-CHOP to standard CHOP chemotherapy in DLBCL patients: a study by the Groupe d'Etudes des Lymphomes de l'Adulte. *Blood*, *116*(12), 2040–2045.

Compagno, M., Lim, W. K., Grunn, A., Nandula, S. v, Brahmachary, M., Shen, Q., Bertoni, F., Ponzoni, M., Scandurra, M., Califano, A., Bhagat, G., Chadburn, A., Dalla-Favera, R., & Pasqualucci, L. (2009). Mutations of multiple genes cause deregulation of NF-κB in diffuse large B-cell lymphoma. *Nature*, *459*(7247), 717–721.

Correia, C., Lee, S.-H., Meng, X. W., Vincelette, N. D., Knorr, K. L. B., Ding, H., Nowakowski, G. S., Dai, H., & Kaufmann, S. H. (2015). Emerging understanding of Bcl-2 biology: Implications for neoplastic progression and treatment. *Biochimica et Biophysica Acta (BBA) - Molecular Cell Research*, *1853*(7), 1658–1671.

Cory, J. G., & Cory, A. N. N. H. (2006). Critical Roles of Glutamine as Nitrogen Donors in Purine and Pyrimidine Nucleotide Synthesis: Asparaginase Treatment in Childhood Acute Lymphoblastic Leukemia. *In Vivo*, *20*(5), 587.

Curi R., Newsholme P., Procopio J., Lagranha C., Gorjão R., & Pithon-Curi TC. Glutamine, gene expression, and cell function. F. Biosci. 2007 J. 1;12:344-57. doi: 10. 2741/2068. P.

17127303. (2007). Glutamine, gene expression, and cell function. *Font Biosci.*, *12*, 344–357.

Czabotar, P. E., Lessene, G., Strasser, A., & Adams, J. M. (2014). Control of apoptosis by the BCL-2 protein family: implications for physiology and therapy. *Nature Reviews Molecular Cell Biology*, *15*(1), 49–63.

Davids, M. S., Seymour, J. F., Gerecitano, J. F., Kahl, B. S., Pagel, J. M., Wierda, W. G., Anderson, M. A., Rudersdorf, N., Gressick, L. A., Montalvo, N. P., Yang, J., Zhu, M., Dunbar, M., Cerri, E., Enschede, S. H., Humerickhouse, R., & Roberts, A. W. (2014). Phase I study of ABT-199 (GDC-0199) in patients with relapsed/refractory (R/R) non-Hodgkin lymphoma (NHL): Responses observed in diffuse large B-cell (DLBCL) and follicular lymphoma (FL) at higher cohort doses. *Journal of Clinical Oncology*, *32*(15_suppl), 8522.

Davis, R. E., Brown, K. D., Siebenlist, U., & Staudt, L. M. (2001). Constitutive Nuclear Factor κB Activity Is Required for Survival of Activated B Cell–like Diffuse Large B Cell Lymphoma Cells. *Journal of Experimental Medicine*, *194*(12), 1861–1874.

Davis, R. E., Ngo, V. N., Lenz, G., Tolar, P., Young, R. M., Romesser, P. B., Kohlhammer, H., Lamy, L., Zhao, H., Yang, Y., Xu, W., Shaffer, A. L., Wright, G., Xiao, W., Powell, J., Jiang, J., Thomas, C. J., Rosenwald, A., Ott, G., … Staudt, L. M. (2010). Chronic active B-cell-receptor signalling in diffuse large B-cell lymphoma. *Nature*, *463*(7277), 88–92.

DeBerardinis, R. J., Mancuso, A., Daikhin, E., Nissim, I., Yudkoff, M., Wehrli, S., & Thompson, C. B. (2007). Beyond aerobic glycolysis: Transformed cells can engage in glutamine metabolism that exceeds the requirement for protein and nucleotide synthesis. *Proceedings of the National Academy of Sciences*, *104*(49), 19345–19350.

Dejure, F. R., Royla, N., Herold, S., Kalb, J., Walz, S., Ade, C. P., Mastrobuoni, G., Vanselow, J. T., Schlosser, A., Wolf, E., Kempa, S., & Eilers, M. (2017). The MYC mRNA 3′-UTR couples RNA polymerase II function to glutamine and ribonucleotide levels. *The EMBO Journal*, *36*(13), 1854–1868.

de la Rosa Rodriguez, M. A., & Kersten, S. (2020). Regulation of lipid droplet homeostasis by hypoxia inducible lipid droplet associated HILPDA. *Biochimica et Biophysica Acta (BBA) - Molecular and Cell Biology of Lipids*, *1865*(9), 158738.

Delbridge, A. R. D., Grabow, S., Strasser, A., & Vaux, D. L. (2016). Thirty years of BCL-2: translating cell death discoveries into novel cancer therapies. *Nature Reviews Cancer*, *16*(2), 99–109.

Deng, H., Fan, X., Wang, X., Zeng, L., Zhang, K., Zhang, X., Li, N., Han, Q., Lv, Y., & Liu, Z. (2020). Serum pentraxin 3 as a biomarker of hepatocellular carcinoma in chronic hepatitis B virus infection. *Scientific Reports*, *10*(1), 20276.

Dey, A., Nishiyama, A., Karpova, T., McNally, J., & Ozato, K. (2009). Brd4 Marks Select Genes on Mitotic Chromatin and Directs Postmitotic Transcription. *Molecular Biology of the Cell*, *20*(23), 4899–4909.

Dhar, D., Antonucci, L., Nakagawa, H., Kim, J. Y., Glitzner, E., Caruso, S., Shalapour, S., Yang, L., Valasek, M. A., Lee, S., Minnich, K., Seki, E., Tuckermann, J., Sibilia, M., Zucman-Rossi, J., & Karin, M. (2018). Liver Cancer Initiation Requires p53 Inhibition by CD44-Enhanced Growth Factor Signaling. *Cancer Cell*, *33*(6), 1061-1077.e6.

Dimauro, T., & David, G. (2010). Ras-induced senescence and its physiological relevance in cancer. *Cancer Drug Targets*, *10(8)*, 869–876.

Ding, B. B., Yu, J. J., Yu, R. Y.-L., Mendez, L. M., Shaknovich, R., Zhang, Y., Cattoretti, G., & Ye, B. H. (2008). Constitutively activated STAT3 promotes cell proliferation and survival in the activated B-cell subtype of diffuse large B-cell lymphomas. *Blood*, *111*(3), 1515–1523.

Donati, B., Lorenzini, E., & Ciarrocchi, A. (2018). BRD4 and Cancer: going beyond transcriptional regulation. *Molecular Cancer*, *17*(1), 164.

Donato, F., Tagger, A., Gelatti, U., Parrinello, G., Boffetta, P., Albertini, A., Decarli, A., Trevisi, P., Ribero, M. L., Martelli, C., Porru, S., & Nardi, G. (2002). Alcohol and Hepatocellular Carcinoma: The Effect of Lifetime Intake and Hepatitis Virus Infections in Men and Women. *American Journal of Epidemiology*, *155*(4), 323–331.

Dunleavy, K. (2014). Double-hit lymphomas: current paradigms and novel treatment approaches. *Hematology*, *2014*(1), 107–112.

Dunleavy, K., Pittaluga, S., Czuczman, M. S., Dave, S. S., Wright, G., Grant, N., Shovlin, M., Jaffe, E. S., Janik, J. E., Staudt, L. M., & Wilson, W. H. (2009). Differential efficacy of bortezomib plus chemotherapy within molecular subtypes of diffuse large B-cell lymphoma. *Blood*, *113*(24), 6069–6076.

Dunleavy, K., & Wilson, W. H. (2011). Differential Role of BCL2 in Molecular Subtypes of Diffuse Large B-cell Lymphoma. *Clinical Cancer Research*, *17*(24), 7505–7507.

Effenberger, M., Bommert, K. S., Kunz, V., Kruk, J., Leich, E., Rudelius, M., Bargou, R., & Bommert, K. (2017). Glutaminase inhibition in multiple myeloma induces apoptosis via MYC degradation. *Oncotarget*, *8*, 85858–85867.

El-Serag, H. B., & Mason, A. C. (2000). Risk Factors for the Rising Rates of Primary Liver Cancer in the United States. *Archives of Internal Medicine*, *160*(21), 3227–3230.

Eto, A., Muta, T., Yamazaki, S., & Takeshige, K. (2003). Essential roles for NF-κB and a Toll/IL-1 receptor domain-specific signal(s) in the induction of IκB-ζ. *Biochemical and Biophysical Research Communications*, *301*(2), 495–501.

Filippakopoulos, P., & Knapp, S. (2014). Targeting bromodomains: epigenetic readers of lysine acetylation. *Nature Reviews Drug Discovery*, *13*(5), 337–356.

Finkin, S., Yuan, D., Stein, I., Taniguchi, K., Weber, A., Unger, K., Browning, J. L., Goossens, N., Nakagawa, S., Gunasekaran, G., Schwartz, M. E., Kobayashi, M., Kumada, H., Berger, M., Pappo, O., Rajewsky, K., Hoshida, Y., Karin, M., Heikenwalder, M., … Pikarsky, E. (2015). Ectopic lymphoid structures function as microniches for tumor progenitor cells in hepatocellular carcinoma. *Nature Immunology*, *16*(12), 1235–1244.

Finn, R. S., Qin, S., Ikeda, M., Galle, P. R., Ducreux, M., Kim, T.-Y., Kudo, M., Breder, V., Merle, P., Kaseb, A. O., Li, D., Verret, W., Xu, D.-Z., Hernandez, S., Liu, J., Huang, C., Mulla, S., Wang, Y., Lim, H. Y., … Cheng, A.-L. (2020). Atezolizumab plus Bevacizumab in Unresectable Hepatocellular Carcinoma. *New England Journal of Medicine*, *382*(20), 1894–1905.

Fontán, L., & Melnick, A. (2013). Molecular Pathways: Targeting MALT1 Paracaspase Activity in Lymphoma. *Clinical Cancer Research*, *19*(24), 6662–6668.

Fontan, L., Yang, C., Kabaleeswaran, V., Volpon, L., Osborne, M. J., Beltran, E., Garcia, M., Cerchietti, L., Shaknovich, R., Yang, S. N., Fang, F., Gascoyne, R. D., Martinez-Climent, J. A., Glickman, J. F., Borden, K., Wu, H., & Melnick, A. (2012). MALT1 Small Molecule Inhibitors Specifically Suppress ABC-DLBCL In Vitro and In Vivo. *Cancer Cell*, *22*(6), 812–824.

Fontes-Cal, T. C. M., Mattos, R. T., Medeiros, N. I., Pinto, B. F., Belchior-Bezerra, M., Roque-Souza, B., Dutra, W. O., Ferrari, T. C. A., Vidigal, P. V. T., Faria, L. C., Couto, C. A., & Gomes, J. A. S. (2021). Crosstalk Between Plasma Cytokines, Inflammation, and Liver Damage as a New Strategy to Monitoring NAFLD Progression. *Frontiers in Immunology*, *12*.

Forner, A., Reig, M., & Bruix, J. (2018). Hepatocellular carcinoma. *The Lancet*, *391*(10127), 1301–1314.

Franchina, D. G., Grusdat, M., & Brenner, D. (2018). B-Cell Metabolic Remodeling and Cancer. In *Trends in Cancer* (Vol. 4, Issue 2, pp. 138–150). Cell Press.

Franco, R., & Cidlowski, J. A. (2009). Apoptosis and glutathione: beyond an antioxidant. *Cell Death & Differentiation*, *16*(10), 1303–1314.

Fu, K., Weisenburger, D. D., Choi, W. W. L., Perry, K. D., Smith, L. M., Shi, X., Hans, C. P., Greiner, T. C., Bierman, P. J., Bociek, R. G., Armitage, J. O., Chan, W. C., & Vose, J. M. (2008). Addition of Rituximab to Standard Chemotherapy Improves the Survival of Both the Germinal Center B-Cell–Like and Non–Germinal Center B-Cell–Like Subtypes of Diffuse Large B-Cell Lymphoma. *Journal of Clinical Oncology*, *26*(28), 4587–4594.

Ganne-Carrié, N., & Nahon, P. (2019). Hepatocellular carcinoma in the setting of alcohol-related liver disease. *Journal of Hepatology*, *70*(2), 284–293.

Gao, P., Tchernyshyov, I., Chang, T.-C., Lee, Y.-S., Kita, K., Ochi, T., Zeller, K. I., de Marzo, A. M., van Eyk, J. E., Mendell, J. T., & Dang, C. v. (2009). c-Myc suppression of miR-23a/b enhances mitochondrial glutaminase expression and glutamine metabolism. *Nature*, *458*(7239), 762–765.

Garg, A. V., Amatya, N., Chen, K., Cruz, J. A., Grover, P., Whibley, N., Conti, H. R., Hernandez Mir, G., Sirakova, T., Childs, E. C., Smithgall, T. E., Biswas, P. S., Kolls, J. K., McGeachy, M. J., Kolattukudy, P. E., & Gaffen, S. L. (2015). MCPIP1 Endoribonuclease Activity Negatively Regulates Interleukin-17-Mediated Signaling and Inflammation. *Immunity*, *43*(3), 475–487.

Garlanda, C., Bottazzi, B., Bastone, A., & Mantovani, A. (2004). Pentraxins at the crossroads between innate immunity, inflammation, matrix deposition, and female fertility. *Annual Review of Immunology*, *23*(1), 337–366.

Gautam, P., Maenner, S., Cailotto, F., Reboul, P., Labialle, S., Jouzeau, J.-Y., Bourgaud, F., & Moulin, D. (2022). Emerging role of IκBζ in inflammation: Emphasis on psoriasis. *Clinical and Translational Medicine*, *12*(10).

Ghosh, S., & Hayden, M. S. (2008). New regulators of NF-κB in inflammation. *Nature Reviews Immunology*, *8*(11), 837–848.

Gilmore, T. D. (2006). Introduction to NF-κB: players, pathways, perspectives. *Oncogene*, *25*(51), 6680–6684.

Global Burden of Disease Liver Cancer Collaboration, Akinyemiju, T., & Abera, S. (2017). The Burden of Primary Liver Cancer and Underlying Etiologies From 1990 to 2015 at the Global, Regional, and National Level: Results From the Global Burden of Disease Study 2015. *JAMA Oncology*, *3*(12), 1683–1691.

Gluchowski, N. L., Becuwe, M., Walther, T. C., & Farese, R. V. (2017). Lipid droplets and liver disease: from basic biology to clinical implications. *Nature Reviews Gastroenterology & Hepatology*, *14*(6), 343–355.

Godwin, A. K., Meister, A., O'Dwyer, P. J., Huang, C. S., Hamilton, T. C., & Anderson, M. E. (1992). High resistance to cisplatin in human ovarian cancer cell lines is associated with marked increase of glutathione synthesis. *Proceedings of the National Academy of Sciences*, *89*(7), 3070–3074.

Gong, T., Zheng, C., Ou, X., Zheng, J., Yu, J., Chen, S., Duan, Y., & Liu, W. (2022). Glutamine metabolism in cancers: Targeting the oxidative homeostasis. *Frontiers in Oncology*, *12*.

Gouas, D., Shi, H., & Hainaut, P. (2009). The aflatoxin-induced TP53 mutation at codon 249 (R249S): Biomarker of exposure, early detection and target for therapy. *Cancer Letters*, *286*(1), 29–37.

Gregory, M. A., Nemkov, T., Park, H. J., Zaberezhnyy, V., Gehrke, S., Adane, B., Jordan, C. T., Hansen, K. C., D'Alessandro, A., & DeGregori, J. (2019). Targeting Glutamine Metabolism and Redox State for Leukemia Therapy. *Clinical Cancer Research*, *25*(13), 4079–4090.

Grivennikov, S. I., & Karin, M. (2010). Dangerous liaisons: STAT3 and NF-κB collaboration and crosstalk in cancer. *Cytokine & Growth Factor Reviews*, *21*(1), 11–19.

Grohmann, M., Wiede, F., Dodd, G. T., Gurzov, E. N., Ooi, G. J., Butt, T., Rasmiena, A. A., Kaur, S., Gulati, T., Goh, P. K., Treloar, A. E., Archer, S., Brown, W. A., Muller, M., Watt, M. J., Ohara, O., McLean, C. A., & Tiganis, T. (2018). Obesity Drives STAT-1-Dependent NASH and STAT-3-Dependent HCC. *Cell*, *175*(5), 1289-1306.e20.

Grondona, P., Bucher, P., Schmitt, A., Schönfeld, C., Streibl, B., Müller, A., Essmann, F., Liberatori, S., Mohammed, S., Hennig, A., Kramer, D., Schulze-Osthoff, K., & Hailfinger, S. (2020). Threonine Phosphorylation of IκBζ Mediates Inhibition of Selective Proinflammatory Target Genes. *Journal of Investigative Dermatology*, *140*(9), 1805-1814.

Grondona, P., Bucher, P., Schulze-Osthoff, K., Hailfinger, S., & Schmitt, A. (2018). NF-κB Activation in Lymphoid Malignancies: Genetics, Signaling, and Targeted Therapy. *Biomedicines*, *6*(2).

Gross, M. I., Demo, S. D., Dennison, J. B., Chen, L., Chernov-Rogan, T., Goyal, B., Janes, J. R., Laidig, G. J., Lewis, E. R., Li, J., MacKinnon, A. L., Parlati, F., Rodriguez, M. L. M., Shwonek, P. J., Sjogren, E. B., Stanton, T. F., Wang, T., Yang, J., Zhao, F., & Bennett, M. K. (2014). Antitumor activity of the glutaminase inhibitor CB-839 in triple-negative breast cancer. *Molecular Cancer Therapeutics*, *13*(4), 890–901.

Gupta, M., Han, J. J., Stenson, M., Maurer, M., Wellik, L., Hu, G., Ziesmer, S., Dogan, A., & Witzig, T. E. (2012). Elevated serum IL-10 levels in diffuse large B-cell lymphoma: a mechanism of aberrant JAK2 activation. *Blood*, *119*(12), 2844–2853.

Hailfinger, S., Lenz, G., Ngo, V., Posvitz-Fejfar, A., Rebeaud, F., Guzzardi, M., Penas, E.-M. M., Dierlamm, J., Chan, W. C., Staudt, L. M., & Thome, M. (2009). Essential role of MALT1

protease activity in activated B cell-like diffuse large B-cell lymphoma. *Proceedings of the National Academy of Sciences*, *106*(47), 19946–19951.

Hailfinger, S., Nogai, H., Pelzer, C., Jaworski, M., Cabalzar, K., Charton, J.-E., Guzzardi, M., Décaillet, C., Grau, M., Dörken, B., Lenz, P., Lenz, G., & Thome, M. (2011). Malt1-dependent RelB cleavage promotes canonical NF-κB activation in lymphocytes and lymphoma cell lines. *Proceedings of the National Academy of Sciences*, *108*(35), 14596–14601.

Hainsworth, J. D., Arrowsmith, E. R., McCleod, M., Hsi, E. D., Hamid, O., Shi, P., Lin, B. K., & Fayad, L. E. (2016). A randomized, phase 2 study of R-CHOP plus enzastaurin vs R-CHOP in patients with intermediate- or high-risk diffuse large B-cell lymphoma. *Leukemia & Lymphoma*, *57*(1), 216–218.

Hajmirza, A., Emadali, A., Gauthier, A., Casasnovas, O., Gressin, R., & Callanan, M. B. (2018). BET Family Protein BRD4: An Emerging Actor in NFκB Signaling in Inflammation and Cancer. *Biomedicines*, *6*(1).

Han, Q., Deng, H., Fan, X., Wang, X., Zhang, X., Zhang, K., Li, N., Lv, Y., & Liu, Z. (2021). Increased Serum Pentraxin 3 Levels are Associated with Poor Prognosis of Hepatitis B Virus-Related Hepatocellular Carcinoma. *Journal of Hepatocellular Carcinoma*, *8*, 1367–1373.

Haruta, H., Kato, A., & Todokoro, K. (2001). Isolation of a Novel Interleukin-1-inducible Nuclear Protein Bearing Ankyrin-repeat Motifs*. *Journal of Biological Chemistry*, *276*(16), 12485–12488.

Hashwah, H., Bertram, K., Stirm, K., Stelling, A., Wu, C.-T., Kasser, S., Manz, M. G., Theocharides, A. P., Tzankov, A., & Müller, A. (2019). The IL-6 signaling complex is a critical driver, negative prognostic factor, and therapeutic target in diffuse large B-cell lymphoma. *EMBO Molecular Medicine*, *11*(10).

Hassan, M. M., Hwang, L.-Y., Hatten, C. J., Swaim, M., Li, D., Abbruzzese, J. L., Beasley, P., & Patt, Y. Z. (2002). Risk factors for hepatocellular carcinoma: Synergism of alcohol with viral hepatitis and diabetes mellitus. *Hepatology*, *36*(5), 1206–1213.

Haybaeck, J., Zeller, N., Wolf, M. J., Weber, A., Wagner, U., Kurrer, M. O., Bremer, J., Iezzi, G., Graf, R., Clavien, P.-A., Thimme, R., Blum, H., Nedospasov, S. A., Zatloukal, K., Ramzan, M., Ciesek, S., Pietschmann, T., Marche, P. N., Karin, M., … Heikenwalder, M. (2009). A Lymphotoxin-Driven Pathway to Hepatocellular Carcinoma. *Cancer Cell*, *16*(4), 295–308.

Hayden, M. S., & Ghosh, S. (2008). Shared Principles in NF-kappaB Signaling. *Cell*, *132*(3), 344–362.

Hayes, J. D., Dinkova-Kostova, A. T., & Tew, K. D. (2020). Oxidative Stress in Cancer. *Cancer Cell*, *38*(2), 167–197.

He, G., Dhar, D., Nakagawa, H., Font-Burgada, J., Ogata, H., Jiang, Y., Shalapour, S., Seki, E., Yost, S. E., Jepsen, K., Frazer, K. A., Harismendy, O., Hatziapostolou, M., Iliopoulos, D., Suetsugu, A., Hoffman, R. M., Tateishi, R., Koike, K., & Karin, M. (2013). Identification of Liver Cancer Progenitors Whose Malignant Progression Depends on Autocrine IL-6 Signaling. *Cell*, *155*(2), 384–396.

He, G., & Karin, M. (2011). NF-κB and STAT3 – key players in liver inflammation and cancer. *Cell Research*, *21*(1), 159–168.

He, L., Wu, J., Tang, W., Zhou, X., Lin, Q., Luo, F., Yin, Y., & Li, T. (2018). Prevention of Oxidative Stress by α-Ketoglutarate via Activation of CAR Signaling and Modulation of the Expression of Key Antioxidant-Associated Targets in Vivo and in Vitro. *Journal of Agricultural and Food Chemistry*, *66*(43), 11273–11283.

He, M. Y., & Kridel, R. (2021). Treatment resistance in diffuse large B-cell lymphoma. In *Leukemia* (Vol. 35, Issue 8, pp. 2151–2165). Springer Nature.

Hermine, O., Haioun, C., Lepage, E., d'Agay, M.-F., Briere, J., Lavignac, C., Fillet, G., Salles, G., Marolleau, J.-P., Diebold, J., Reyes, F., & (GELA) for the Groupe d'Etude des Lymphomes de l'Adulte, P. G. (1996). Prognostic Significance of bcl-2 Protein Expression in Aggressive Non-Hodgkin's Lymphoma. *Blood*, *87*(1), 265–272.

Hildebrand, D. G., Alexander, E., Hörber, S., Lehle, S., Obermayer, K., Münck, N.-A., Rothfuss, O., Frick, J.-S., Morimatsu, M., Schmitz, I., Roth, J., Ehrchen, J. M., Essmann, F., & Schulze-Osthoff, K. (2013). IκBζ Is a Transcriptional Key Regulator of CCL2/MCP-1. *The Journal of Immunology*, *190*(9), 4812–4820.

Hinz, M., Arslan, SÇ., & Scheidereit, C. (2012). It takes two to tango: IκBs, the multifunctional partners of NF-κB. *Immunological Reviews*, *246(1)*, 59–76.

Hoesel, B., & Schmid, J. A. (2013). The complexity of NF-κB signaling in inflammation and cancer. *Molecular Cancer*, *12*(1), 86.

Hörber, S., Hildebrand, D. G., Lieb, W. S., Lorscheid, S., Hailfinger, S., Schulze-Osthoff, K., & Essmann, F. (2016). kappaB, IkappaB-zeta Controls Macrophage Interleukin-10 Expression. *Journal of Biological Chemistry*, *291*(24), 12851–12861.

Hosios, A. M., Hecht, V. C., Danai, L. V., Johnson, M. O., Rathmell, J. C., Steinhauser, M. L., Manalis, S. R., & Vander Heiden, M. G. (2016). Amino Acids Rather than Glucose Account for the Majority of Cell Mass in Proliferating Mammalian Cells. *Developmental Cell*, *36*(5), 540–549.

Huang, Y.-T., Hsu, T., Kelsey, K. T., & Lin, C.-L. (2015). Integrative Analysis of Micro-RNA, Gene Expression, and Survival of Glioblastoma Multiforme. *Genetic Epidemiology*, *39*(2), 134–143.

Hu, Q., Zhang, Y., Lou, H., Ou, Z., Liu, J., Duan, W., Wang, H., Ge, Y., Min, J., Wang, F., & Ju, Z. (2021). GPX4 and vitamin E cooperatively protect hematopoietic stem and progenitor cells from lipid peroxidation and ferroptosis. *Cell Death & Disease*, *12*(7), 706.

Hu, W., Zhang, C., Wu, R., Sun, Y., Levine, A., & Feng, Z. (2010). Glutaminase 2, a novel p53 target gene regulating energy metabolism and antioxidant function. *Proceedings of the National Academy of Sciences*, *107*(16), 7455–7460.

Huxford, T., & Ghosh, G. (2009). A Structural Guide to Proteins of the NF-κB Signaling Module. *Cold Spring Harbor Perspectives in Biology*, *1*(3).

Huynh, J., Chand, A., Gough, D., & Ernst, M. (2019). Therapeutically exploiting STAT3 activity in cancer — using tissue repair as a road map. *Nature Reviews Cancer*, *19*(2), 82–96.

Indo, H. P., Davidson, M., Yen, H.-C., Suenaga, S., Tomita, K., Nishii, T., Higuchi, M., Koga, Y., Ozawa, T., & Majima, H. J. (2007). Evidence of ROS generation by mitochondria in

cells with impaired electron transport chain and mitochondrial DNA damage. *Mitochondrion*, *7*(1), 106–118.

Iqbal, J., Greiner, T. C., Patel, K., Dave, B. J., Smith, L., Ji, J., Wright, G., Sanger, W. G., Pickering, D. L., Jain, S., Horsman, D. E., Shen, Y., Fu, K., Weisenburger, D. D., Hans, C. P., Campo, E., Gascoyne, R. D., Rosenwald, A., Jaffe, E. S., … (LLMPP), for the L. M. P. P. (2007). Distinctive patterns of BCL6 molecular alterations and their functional consequences in different subgroups of diffuse large B-cell lymphoma. *Leukemia*, *21*(11), 2332–2343.

Irie, T., Muta, T., & Takeshige, K. (2000). TAK1 mediates an activation signal from toll-like receptor(s) to nuclear factor-κB in lipopolysaccharide-stimulated macrophages. *FEBS Letters*, *467*(2–3), 160–164.

Ishikawa, H., Hayakawa, M., Baatartsogt, N., Kakizawa, N., Ohto-Ozaki, H., Maruyama, T., Miura, K., Suzuki, K., Rikiyama, T., & Ohmori, T. (2022). IκBζ regulates the development of nonalcoholic fatty liver disease through the attenuation of hepatic steatosis in mice. *Scientific Reports*, *12*(1), 11634.

Jang, M. K., Mochizuki, K., Zhou, M., Jeong, H.-S., Brady, J. N., & Ozato, K. (2005). The Bromodomain Protein Brd4 Is a Positive Regulatory Component of P-TEFb and Stimulates RNA Polymerase II-Dependent Transcription. *Molecular Cell*, *19*(4), 523–534.

Jeltsch, K. M., Hu, D., Brenner, S., Zöller, J., Heinz, G. A., Nagel, D., Vogel, K. U., Rehage, N., Warth, S. C., Edelmann, S. L., Gloury, R., Martin, N., Lohs, C., Lech, M., Stehklein, J. E., Geerlof, A., Kremmer, E., Weber, A., Anders, H.-J., … Heissmeyer, V. (2014). Cleavage of roquin and regnase-1 by the paracaspase MALT1 releases their cooperatively repressed targets to promote TH17 differentiation. *Nature Immunology*, *15*(11), 1079–1089.

Jiang, X., Stockwell, B. R., & Conrad, M. (2021). Ferroptosis: mechanisms, biology and role in disease. *Nature Reviews Molecular Cell Biology*, *22*(4), 266–282.

Johnson, N. A., Slack, G. W., Savage, K. J., Connors, J. M., Ben-Neriah, S., Rogic, S., Scott, D. W., Tan, K. L., Steidl, C., Sehn, L. H., Chan, W. C., Iqbal, J., Meyer, P. N., Lenz, G., Wright, G., Rimsza, L. M., Valentino, C., Brunhoeber, P., Grogan, T. M., … Gascoyne, R. D. (2012). Concurrent Expression of MYC and BCL2 in Diffuse Large B-Cell Lymphoma Treated With Rituximab Plus Cyclophosphamide, Doxorubicin, Vincristine, and Prednisone. *Journal of Clinical Oncology*, *30*(28), 3452–3459.

Ju, H.-L., Han, K.-H., Lee, J. D., & Ro, S. W. (2016). Transgenic mouse models generated by hydrodynamic transfection for genetic studies of liver cancer and preclinical testing of anti-cancer therapy. *International Journal of Cancer*, *138*(7), 1601–1608.

Kannan, Y., Yu, J., Raices, R. M., Seshadri, S., Wei, M., Caligiuri, M. A., & Wewers, M. D. (2011). IκBζ augments IL-12– and IL-18–mediated IFN-γ production in human NK cells. *Blood*, *117*(10), 2855–2863.

Katt, W. P., Lukey, M. J., & Cerione, R. A. (2017). A tale of two glutaminases: homologous enzymes with distinct roles in tumorigenesis. *Future Medicinal Chemistry*, *9*(2), 223–243.

Kawamata, Y., Fujii, R., Hosoya, M., Harada, M., Yoshida, H., Miwa, M., Fukusumi, S., Habata, Y., Itoh, T., Shintani, Y., Hinuma, S., Fujisawa, Y., & Fujino, M. (2003). A G Protein-coupled Receptor Responsive to Bile Acids. *Journal of Biological Chemistry*, *278*(11), 9435–9440.

Kayama, H., Ramirez-Carrozzi, V. R., Yamamoto, M., Mizutani, T., Kuwata, H., Iba, H., Matsumoto, M., Honda, K., Smale, S. T., & Takeda, K. (2008). Class-specific Regulation of Pro-inflammatory Genes by MyD88 Pathways and IκBζ. *Journal of Biological Chemistry*, *283*(18), 12468–12477.

Khatun, M., Ray, R., & Ray, R. B. (2021). Chapter Three - Hepatitis C virus associated hepatocellular carcinoma. In D. Sarkar & P. B. Fisher (Eds.), *Advances in Cancer Research* (Vol. 149, pp. 103–142). Academic Press.

Kimura, R., Senba, M., Cutler, S. J., Ralph, S. J., Xiao, G., & Mori, N. (2013). Human T Cell Leukemia Virus Type I Tax-Induced IκB-ζ Modulates Tax-Dependent and Tax-Independent Gene Expression in T Cells. *Neoplasia*, *15*(9), 1110–1124.

Kitamura, H., Kanehira, K., Okita, K., Morimatsu, M., & Saito, M. (2000). MAIL, a novel nuclear IκB protein that potentiates LPS-induced IL-6 production. *FEBS Letters*, *485*(1), 53–56.

Klein, U., Casola, S., Cattoretti, G., Shen, Q., Lia, M., Mo, T., Ludwig, T., Rajewsky, K., & Dalla-Favera, R. (2006). Transcription factor IRF4 controls plasma cell differentiation and class-switch recombination. *Nature Immunology*, *7*(7), 773–782.

Knittel, G., Liedgens, P., Korovkina, D., Pallasch, C. P., & Reinhardt, H. C. (2016). Rewired NFκB signaling as a potentially actionable feature of activated B-cell-like diffuse large B-cell lymphoma. *European Journal of Haematology*, *97*(6), 499–510.

Kohda, A., Yamazaki, S., & Sumimoto, H. (2016). The Nuclear Protein IkappaB-zeta; Forms a Transcriptionally Active Complex with Nuclear Factor-kappaB p50 and the Lcn2 Promoter via the N- and C-terminal Ankyrin Repeat Motifs. *Journal of Biological Chemistry*, *291*(39), 20739–20752.

Kong, L., Zhou, Y., Bu, H., Lv, T., Shi, Y., & Yang, J. (2016). Deletion of interleukin-6 in monocytes/macrophages suppresses the initiation of hepatocellular carcinoma in mice. *Journal of Experimental & Clinical Cancer Research*, *35*(1), 131.

Kuo, H.-P., Ezell, S. A., Schweighofer, K. J., Cheung, L. W. K., Hsieh, S., Apatira, M., Sirisawad, M., Eckert, K., Hsu, S. J., Chen, C.-T., Beaupre, D. M., Versele, M., & Chang, B. Y. (2017). Combination of Ibrutinib and ABT-199 in Diffuse Large B-Cell Lymphoma and Follicular Lymphoma. *Molecular Cancer Therapeutics*, *16*(7), 1246–1256.

Küppers, R. (2005). Mechanisms of B-cell lymphoma pathogenesis. In *Nature Reviews Cancer* (Vol. 5, Issue 4, pp. 251–262).

Lacey, J. M., & Wilmore, D. W. (1990). Is Glutamine a Conditionally Essential Amino Acid? *Nutrition Reviews*, *48*(8), 297–309.

Ladanyi, M., Offit, K., Jhanwar, S. C., Filippa, D. A., & Chaganti, R. S. K. (1991). MYC Rearrangement and Translocations Involving Band 8q24 in Diffuse Large Cell Lymphomas. *Blood*, *77*(5), 1057–1063.

Lam, L. T., Davis, R. E., Pierce, J., Hepperle, M., Xu, Y., Hottelet, M., Nong, Y., Wen, D., Adams, J., Dang, L., & Staudt, L. M. (2005). Small Molecule Inhibitors of IκB Kinase Are Selectively Toxic for Subgroups of Diffuse Large B-Cell Lymphoma Defined by Gene Expression Profiling. *Clinical Cancer Research*, *11*(1), 28–40.

Lam, L. T., Wright, G., Davis, R. E., Lenz, G., Farinha, P., Dang, L., Chan, J. W., Rosenwald, A., Gascoyne, R. D., & Staudt, L. M. (2008). Cooperative signaling through the signal

transducer and activator of transcription 3 and nuclear factor-κB pathways in subtypes of diffuse large B-cell lymphoma. *Blood*, *111*(7), 3701–3713.

Lee, C., & Cheung, S. T. (2019). STAT3: An Emerging Therapeutic Target for Hepatocellular Carcinoma. *Cancers*, *11*(11).

Lencioni, R., de Baere, T., Soulen, M. C., Rilling, W. S., & Geschwind, J. H. (2016). Lipiodol transarterial chemoembolization for hepatocellular carcinoma: A systematic review of efficacy and safety data. *Hepatology*, *64*(1).

Lenz, G., Davis, R. E., Ngo, V. N., Lam, L., George, T. C., Wright, G. W., Dave, S. S., Zhao, H., Xu, W., Rosenwald, A., Ott, G., Muller-Hermelink, H. K., Gascoyne, R. D., Connors, J. M., Rimsza, L. M., Campo, E., Jaffe, E. S., Delabie, J., Smeland, E. B., … Staudt, L. M. (2008). Oncogenic CARD11 Mutations in Human Diffuse Large B Cell Lymphoma. *Science*, *319*(5870), 1676–1679.

Lenz, G., Nagel, I., Siebert, R., Roschke, A. v, Sanger, W., Wright, G. W., Dave, S. S., Tan, B., Zhao, H., Rosenwald, A., Muller-Hermelink, H. K., Gascoyne, R. D., Campo, E., Jaffe, E. S., Smeland, E. B., Fisher, R. I., Kuehl, W. M., Chan, W. C., & Staudt, L. M. (2007). Aberrant immunoglobulin class switch recombination and switch translocations in activated B cell–like diffuse large B cell lymphoma. *Journal of Experimental Medicine*, *204*(3), 633–643.

Lenz, G., & Staudt, L. M. (2010). Aggressive Lymphomas. *New England Journal of Medicine*, *362*(15), 1417–1429.

Lenz, G., Wright, G., Dave, S. S., Xiao, W., Powell, J., Zhao, H., Xu, W., Tan, B., Goldschmidt, N., Iqbal, J., Vose, J., Bast, M., Fu, K., Weisenburger, D. D., Greiner, T. C., Armitage, J. O., Kyle, A., May, L., Gascoyne, R. D., … Staudt, L. M. (2008). Stromal Gene Signatures in Large-B-Cell Lymphomas. *New England Journal of Medicine*, *359*(22), 2313–2323.

Lenz, G., Wright, G. W., Emre, N. C. T., Kohlhammer, H., Dave, S. S., Davis, R. E., Carty, S., Lam, L. T., Shaffer, A. L., Xiao, W., Powell, J., Rosenwald, A., Ott, G., Muller-Hermelink, H. K., Gascoyne, R. D., Connors, J. M., Campo, E., Jaffe, E. S., Delabie, J., … Staudt, L. M. (2008). Molecular subtypes of diffuse large B-cell lymphoma arise by distinct genetic pathways. *Proceedings of the National Academy of Sciences*, *105*(36), 13520–13525.

Levrero, M., & Zucman-Rossi, J. (2016). Mechanisms of HBV-induced hepatocellular carcinoma. *Journal of Hepatology*, *64*(1), S84–S101.

Lewerenz, J., Hewett, S. J., Huang, Y., Lambros, M., Gout, P. W., Kalivas, P. W., Massie, A., Smolders, I., Methner, A., Pergande, M., Smith, S. B., Ganapathy, V., & Maher, P. (2012). The Cystine/Glutamate Antiporter System xc− in Health and Disease: From Molecular Mechanisms to Novel Therapeutic Opportunities. *Antioxidants & Redox Signaling*, *18*(5), 522–555.

Li, B., Cao, Y., Meng, G., Qian, L., Xu, T., Yan, C., Luo, O., Wang, S., Wei, J., Ding, Y., & Yu, D. (2019). Targeting glutaminase 1 attenuates stemness properties in hepatocellular carcinoma by increasing reactive oxygen species and suppressing Wnt/beta-catenin pathway. *EBioMedicine*, *39*, 239–254.

Liberti, M. v, & Locasale, J. W. (2016). The Warburg Effect: How Does it Benefit Cancer Cells? *Trends in Biochemical Sciences*, *41*(3), 211–218.

Lindenblatt, C., Schulze-Osthoff, K., & Totzke, G. (2009). IκBζ expression is regulated by miR-124a. *Cell Cycle*, *8*(13), 2019–2023.

Li, N., Ragheb, K., Lawler, G., Sturgis, J., Rajwa, B., Melendez, J. A., & Robinson, J. P. (2003). Mitochondrial Complex I Inhibitor Rotenone Induces Apoptosis through Enhancing Mitochondrial Reactive Oxygen Species Production *. *Journal of Biological Chemistry*, *278*(10), 8516–8525.

Litmanovich, A., Khazim, K., & Cohen, I. (2018). The Role of Interleukin-1 in the Pathogenesis of Cancer and its Potential as a Therapeutic Target in Clinical Practice. *Oncology and Therapy*, *6*(2), 109–127.

Liu, T., Zhang, L., Joo, D., & Sun, S.-C. (2017). NF-κB signaling in inflammation. *Signal Transduction and Targeted Therapy*, *2*(1), 17023.

Llovet, J. M., De Baere, T., Kulik, L., Haber, P. K., Greten, T. F., Meyer, T., & Lencioni, R. (2021). Locoregional therapies in the era of molecular and immune treatments for hepatocellular carcinoma. *Nature Reviews Gastroenterology & Hepatology*, *18*(5), 293–313.

Llovet, J. M., Kelley, R. K., Villanueva, A., Singal, A. G., Pikarsky, E., Roayaie, S., Lencioni, R., Koike, K., Zucman-Rossi, J., & Finn, R. S. (2021). Hepatocellular carcinoma. *Nature Reviews Disease Primers*, *7*(1), 6.

Llovet, J. M., Real, M. I., Montaña, X., Planas, R., Coll, S., Aponte, J., Ayuso, C., Sala, M., Muchart, J., Solà, R., Rodés, J., & Bruix, J. (2002). Arterial embolisation or chemoembolisation versus symptomatic treatment in patients with unresectable hepatocellular carcinoma: a randomised controlled trial. *The Lancet*, *359*(9319), 1734–1739.

Llovet, J. M., Ricci, S., Mazzaferro, V., Hilgard, P., Gane, E., Blanc, J.-F., de Oliveira, A. C., Santoro, A., Raoul, J.-L., Forner, A., Schwartz, M., Porta, C., Zeuzem, S., Bolondi, L., Greten, T. F., Galle, P. R., Seitz, J.-F., Borbath, I., Häussinger, D., … Bruix, J. (2008). Sorafenib in Advanced Hepatocellular Carcinoma. *New England Journal of Medicine*, *359*(4), 378–390.

Luedde, T., Beraza, N., Kotsikoris, V., van Loo, G., Nenci, A., de Vos, R., Roskams, T., Trautwein, C., & Pasparakis, M. (2007). Deletion of NEMO/IKKγ in Liver Parenchymal Cells Causes Steatohepatitis and Hepatocellular Carcinoma. *Cancer Cell*, *11*(2), 119–132.

Luedde, T., & Schwabe, R. F. (2011). NF-κB in the liver—linking injury, fibrosis and hepatocellular carcinoma. *Nature Reviews Gastroenterology & Hepatology*, *8*(2), 108–118.

Lukey, M. J., Cluntun, A. A., Katt, W. P., Lin, M. J., Druso, J. E., Ramachandran, S., Erickson, J. W., Le, H. H., Wang, Z.-E., Blank, B., Greene, K. S., & Cerione, R. A. (2019). Liver-Type Glutaminase GLS2 Is a Druggable Metabolic Node in Luminal-Subtype Breast Cancer. *Cell Reports*, *29*(1), 76-88.

Lukey, M. J., Greene, K. S., Erickson, J. W., Wilson, K. F., & Cerione, R. A. (2016). The oncogenic transcription factor c-Jun regulates glutaminase expression and sensitizes cells to glutaminase-targeted therapy. *Nature Communications*, *7*(1), 11321.

Lukey, M. J., Wilson, K. F., & Cerione, R. A. (2013). Therapeutic strategies impacting cancer cell glutamine metabolism. *Future Medicinal Chemistry*, *5*(14), 1685–1700.

Maeda, S., Kamata, H., Luo, J.-L., Leffert, H., & Karin, M. (2005). IKKβ Couples Hepatocyte Death to Cytokine-Driven Compensatory Proliferation that Promotes Chemical Hepatocarcinogenesis. *Cell*, *121*(7), 977–990.

Mandelbaum, J., Bhagat, G., Tang, H., Mo, T., Brahmachary, M., Shen, Q., Chadburn, A., Rajewsky, K., Tarakhovsky, A., Pasqualucci, L., & Dalla-Favera, R. (2010). BLIMP1 Is a Tumor Suppressor Gene Frequently Disrupted in Activated B Cell-like Diffuse Large B Cell Lymphoma. *Cancer Cell*, *18*(6), 568–579.

Marinkovic, T., & Marinkovic, D. (2021). Biological mechanisms of ectopic lymphoid structure formation and their pathophysiological significance. *International Reviews of Immunology*, *40*(4), 255–267.

Marquez, J., Mate, J. M., Alonso, F. J., Martin-Rufian, M., Lobo, C., & Campos-Sandoval, J. A. (2015). Canceromics Studies Unravel Tumor's Glutamine Addiction After Metabolic Reprogramming. *Mazurek S, Shoshan M, Editors. Tumor Cell Metabolism* .

Márquez, J., Matés, J. M., & Campos-Sandoval, J. A. (2016). Glutaminases. *Advances in Neurobiology*, *13*, 133–171.

Martelli, M., Ferreri, A. J. M., Agostinelli, C., di Rocco, A., Pfreundschuh, M., & Pileri, S. A. (2013). Diffuse large B-cell lymphoma. *Critical Reviews in Oncology/Hematology*, *87*(2), 146–171.

MaruYama, T., Sayama, A., Ishii, K. J., & Muta, T. (2016). Screening of posttranscriptional regulatory molecules of IκB-*ζ*. *Biochemical and Biophysical Research Communications*, *469*(3), 711–715.

Masamha, CP., & LaFontaine, P. (2018). Molecular targeting of glutaminase sensitizes ovarian cancer cells to chemotherapy. *Journal of Cellular Biochemistry*, *119(7)*, 6136–6145.

Mashek, D. G., Khan, S. A., Sathyanarayan, A., Ploeger, J. M., & Franklin, M. P. (2015). Hepatic lipid droplet biology: Getting to the root of fatty liver. *Hepatology*, *62*(3), 964–967.

Masisi, B. K., el Ansari, R., Alfarsi, L., Rakha, E. A., Green, A. R., & Craze, M. L. (2020). The role of glutaminase in cancer. *Histopathology*, *76*(4), 498–508.

Matés, J. M., Campos-Sandoval, J. A., & Márquez, J. (2018). Glutaminase isoenzymes in the metabolic therapy of cancer. *Biochimica et Biophysica Acta (BBA) - Reviews on Cancer*, *1870*(2), 158–164.

Matsuo, S., Yamazaki, S., Takeshige, K., & Muta, T. (2007). Crucial roles of binding sites for NF-κB and C/EBPs in IκB-ζ-mediated transcriptional activation. *Biochemical Journal*, *405*(3), 605–615.

Mauad, T. H., van Nieuwkerk, C. M., Dingemans, K. P., Smit, J. J., Schinkel, A. H., Notenboom, R. G., van den Bergh Weerman, M. A., Verkruisen, R. P., Groen, A. K., & Oude Elferink, R. P. (1994). Mice with homozygous disruption of the mdr2 P-glycoprotein gene. A novel animal model for studies of nonsuppurative inflammatory cholangitis and hepatocarcinogenesis. *The American Journal of Pathology*, *145(5)*, 1237–1245.

Meng, D., Yang, Q., Wang, H., Melick, C. H., Navlani, R., Frank, A. R., & Jewell, J. L. (2020). Glutamine and asparagine activate mTORC1 independently of Rag GTPases. *Journal of Biological Chemistry*, *295*(10), 2890–2899.

Metallo, C. M., Gameiro, P. A., Bell, E. L., Mattaini, K. R., Yang, J., Hiller, K., Jewell, C. M., Johnson, Z. R., Irvine, D. J., Guarente, L., Kelleher, J. K., vander Heiden, M. G., Iliopoulos, O., & Stephanopoulos, G. (2012). Reductive glutamine metabolism by IDH1 mediates lipogenesis under hypoxia. *Nature*, *481*(7381), 380–384.

Meyer, N., & Penn, L. Z. (2008). Reflecting on 25 years with MYC. *Nature Reviews Cancer*, *8*(12), 976–990.

Monti, S., Savage, K. J., Kutok, J. L., Feuerhake, F., Kurtin, P., Mihm, M., Wu, B., Pasqualucci, L., Neuberg, D., Aguiar, R. C. T., Cin, P. D., Ladd, C., Pinkus, G. S., Salles, G., Harris, N. L., Dalla-Favera, R., Habermann, T. M., Aster, J. C., Golub, T. R., & Shipp, M. A. (2005). Molecular profiling of diffuse large B-cell lymphoma identifies robust subtypes including one characterized by host inflammatory response. *Blood*, *105*(5), 1851–1861.

Mooi, W. J., & Peeper, D. S. (2006). Oncogene-Induced Cell Senescence — Halting on the Road to Cancer. *New England Journal of Medicine*, *355*(10), 1037–1046.

Motoyama, M., Yamazaki, S., Eto-Kimura, A., Takeshige, K., & Muta, T. (2005). Positive and Negative Regulation of Nuclear Factor-κB-mediated Transcription by IκB-ζ an Inducible Nuclear Protein. *Journal of Biological Chemistry*, *280*(9), 7444–7451.

Müller, A., Hennig, A., Lorscheid, S., Grondona, P., Schulze-Osthoff, K., Hailfinger, S., & Kramer, D. (2018). IκBζ is a key transcriptional regulator of IL-36–driven psoriasis-related gene expression in keratinocytes. *Proceedings of the National Academy of Sciences*, *115*(40), 10088–10093.

Muta, T., Yamazaki, S., Eto, A., Motoyama, M., & Takeshige, K. (2003). IkappaB-zeta, a new anti-inflammatory nuclear protein induced by lipopolysaccharide, is a negative regulator for nuclear factor-kappaB. *Journal of Endotoxin Research*, *9 3*, 187–191.

Nakagawa, H., Maeda, S., Yoshida, H., Tateishi, R., Masuzaki, R., Ohki, T., Hayakawa, Y., Kinoshita, H., Yamakado, M., Kato, N., Shiina, S., & Omata, M. (2009). Serum IL-6 levels and the risk for hepatocarcinogenesis in chronic hepatitis C patients: An analysis based on gender differences. *International Journal of Cancer*, *125*(10), 2264–2269.

Nakamura, H., & Takada, K. (2021). Reactive oxygen species in cancer: Current findings and future directions. *Cancer Science*, *112*(10), 3945–3952.

Naugler, W. E., Sakurai, T., Kim, S., Maeda, S., Kim, K., Elsharkawy, A. M., & Karin, M. (2007). Gender Disparity in Liver Cancer Due to Sex Differences in MyD88-Dependent IL-6 Production. *Science*, *317*(5834), 121–124.

Ngo, V. N., Young, R. M., Schmitz, R., Jhavar, S., Xiao, W., Lim, K.-H., Kohlhammer, H., Xu, W., Yang, Y., Zhao, H., Shaffer, A. L., Romesser, P., Wright, G., Powell, J., Rosenwald, A., Muller-Hermelink, H. K., Ott, G., Gascoyne, R. D., Connors, J. M., … Staudt, L. M. (2011). Oncogenically active MYD88 mutations in human lymphoma. *Nature*, *470*(7332), 115–119.

Nguyen, L., Papenhausen, P., & Shao, H. (2017). The Role of c-MYC in B-Cell Lymphomas: Diagnostic and Molecular Aspects. *Genes*, *8*(4).

Nguyen, T., & Durán, R. (2018). Glutamine metabolism in cancer therapy. *Cancer Drug Resist*, *1*, 126–138.

Nicklin, P., Bergman, P., Zhang, B., Triantafellow, E., Wang, H., Nyfeler, B., Yang, H., Hild, M., Kung, C., Wilson, C., Myer, V. E., MacKeigan, J. P., Porter, J. A., Wang, Y. K., Cantley, L. C., Finan, P. M., & Murphy, L. O. (2009). Bidirectional Transport of Amino Acids Regulates mTOR and Autophagy. *Cell*, *136*(3), 521–534.

Nogai, H., Dörken, B., & Lenz, G. (2011). Pathogenesis of Non-Hodgkin's Lymphoma. *Journal of Clinical Oncology*, *29*(14), 1803–1811.

Nogai, H., Wenzel, S.-S., Hailfinger, S., Grau, M., Kaergel, E., Seitz, V., Wollert-Wulf, B., Pfeifer, M., Wolf, A., Frick, M., Dietze, K., Madle, H., Tzankov, A., Hummel, M., Dörken, B., Scheidereit, C., Janz, M., Lenz, P., Thome, M., & Lenz, G. (2013). IκB-ζ controls the constitutive NF-κB target gene network and survival of ABC DLBCL. *Blood*, *122*(13), 2242–2250.

Nowakowski, G. S., & Czuczman, M. S. (2015). ABC, GCB, and Double-Hit Diffuse Large B-Cell Lymphoma: Does Subtype Make a Difference in Therapy Selection? *American Society of Clinical Oncology Educational Book*, *35*, e449–e457.

Oeckinghaus, A., & Ghosh, S. (2009). The NF-κB Family of Transcription Factors and Its Regulation. *Cold Spring Harbor Perspectives in Biology*, *1*(4).

Oeckinghaus, A., Hayden, M. S., & Ghosh, S. (2011). Crosstalk in NF-κB signaling pathways. *Nature Immunology*, *12*(8), 695–708.

Ohba, T., Ariga, Y., Maruyama, T., Truong, N. K., Inoue, J., & Muta, T. (2012). Identification of interleukin-1 receptor-associated kinase 1 as a critical component that induces post-transcriptional activation of IκB-ζ. *The FEBS Journal*, *279*(2), 211–222.

Olive, V., Bennett, M. J., Walker, J. C., Ma, C., Jiang, I., Cordon-Cardo, C., Li, Q.-J., Lowe, S. W., Hannon, G. J., & He, L. (2009). miR-19 is a key oncogenic component of mir-17-92. *Genes & Development*, *23*(24), 2839–2849.

Otto, C., Schmidt, S., Kastner, C., Denk, S., Kettler, J., Müller, N., Germer, C. T., Wolf, E., Gallant, P., & Wiegering, A. (2019). Targeting bromodomain-containing protein 4 (BRD4) inhibits MYC expression in colorectal cancer cells. *Neoplasia*, *21*(11), 1110–1120.

Pang, Y., Bai, G., Zhao, J., Wei, X., Li, R., Li, J., Hu, S., Peng, L., Liu, P., & Mao, H. (2022). The BRD4 inhibitor JQ1 suppresses tumor growth by reducing c-Myc expression in endometrial cancer. *Journal of Translational Medicine*, *20*(1), 336.

Panieri, E., & Santoro, M. M. (2016). ROS homeostasis and metabolism: a dangerous liason in cancer cells. *Cell Death & Disease*, *7*(6), e2253–e2253.

Pan, R., Hogdal, L. J., Benito, J. M., Bucci, D., Han, L., Borthakur, G., Cortes, J., DeAngelo, D. J., Debose, L., Mu, H., Döhner, H., Gaidzik, V. I., Galinsky, I., Golfman, L. S., Haferlach, T., Harutyunyan, K. G., Hu, J., Leverson, J. D., Marcucci, G., … Letai, A. G. (2014). Selective BCL-2 Inhibition by ABT-199 Causes On-Target Cell Death in Acute Myeloid Leukemia. *Cancer Discovery*, *4*(3), 362–375.

Park, E. J., Lee, J. H., Yu, G.-Y., He, G., Ali, S. R., Holzer, R. G., Österreicher, C. H., Takahashi, H., & Karin, M. (2010). Dietary and Genetic Obesity Promote Liver Inflammation and Tumorigenesis by Enhancing IL-6 and TNF Expression. *Cell*, *140*(2), 197–208.

Park, J.-W., Chen, M., Colombo, M., Roberts, L. R., Schwartz, M., Chen, P.-J., Kudo, M., Johnson, P., Wagner, S., Orsini, L. S., & Sherman, M. (2015). Global patterns of hepatocellular carcinoma management from diagnosis to death: the BRIDGE Study. *Liver International*, *35*(9), 2155–2166.

Park, W. H., Han, Y. W., Kim, S. H., & Kim, S. Z. (2007). An ROS generator, antimycin A, inhibits the growth of HeLa cells via apoptosis. *Journal of Cellular Biochemistry*, *102(1)*, 98–109.

Pasqualucci, L., Compagno, M., Houldsworth, J., Monti, S., Grunn, A., Nandula, S. v, Aster, J. C., Murty, V. v, Shipp, M. A., & Dalla-Favera, R. (2006). Inactivation of the PRDM1/BLIMP1 gene in diffuse large B cell lymphoma. *The Journal of Experimental Medicine*, *203*, 311–317.

Pasqualucci, L., Dominguez-Sola, D., Chiarenza, A., Fabbri, G., Grunn, A., Trifonov, V., Kasper, L. H., Lerach, S., Tang, H., Ma, J., Rossi, D., Chadburn, A., Murty, V. v, Mullighan, C. G., Gaidano, G., Rabadan, R., Brindle, P. K., & Dalla-Favera, R. (2011). Inactivating mutations of acetyltransferase genes in B-cell lymphoma. *Nature*, *471*(7337), 189–195.

Patman, G. (2015). Ectopic lymphoid structures promote carcinogenesis in the liver. *Nature Reviews Gastroenterology & Hepatology*, *12*(12), 671.

Peirs, S., Matthijssens, F., Goossens, S., van de Walle, I., Ruggero, K., de Bock, C. E., Degryse, S., Canté-Barrett, K., Briot, D., Clappier, E., Lammens, T., de Moerloose, B., Benoit, Y., Poppe, B., Meijerink, J. P., Cools, J., Soulier, J., Rabbitts, T. H., Taghon, T., … van Vlierberghe, P. (2014). ABT-199 mediated inhibition of BCL-2 as a novel therapeutic strategy in T-cell acute lymphoblastic leukemia. *Blood*, *124*(25), 3738–3747.

Pfreundschuh, M., Kuhnt, E., Trümper, L., Österborg, A., Trneny, M., Shepherd, L., Gill, D. S., Walewski, J., Pettengell, R., Jaeger, U., Zinzani, P.-L., Shpilberg, O., Kvaloy, S., de Nully Brown, P., Stahel, R., Milpied, N., López-Guillermo, A., Poeschel, V., Grass, S., … Murawski, N. (2011). CHOP-like chemotherapy with or without rituximab in young patients with good-prognosis diffuse large-B-cell lymphoma: 6-year results of an open-label randomised study of the MabThera International Trial (MInT) Group. *The Lancet Oncology*, *12*(11), 1013–1022.

Pikarsky, E., Porat, R. M., Stein, I., Abramovitch, R., Amit, S., Kasem, S., Gutkovich-Pyest, E., Urieli-Shoval, S., Galun, E., & Ben-Neriah, Y. (2004a). NF-kB functions as a tumour promoter in inflammation-associated cancer. *Nature Reviews Cancer*, *4*(10), 753.

Pikarsky, E., Porat, R. M., Stein, I., Abramovitch, R., Amit, S., Kasem, S., Gutkovich-Pyest, E., Urieli-Shoval, S., Galun, E., & Ben-Neriah, Y. (2004b). NF-κB functions as a tumour promoter in inflammation-associated cancer. *Nature*, *431*(7007), 461–466.

Pols, T. W. H., Noriega, L. G., Nomura, M., Auwerx, J., & Schoonjans, K. (2011). The Bile Acid Membrane Receptor TGR5: A Valuable Metabolic Target. *Digestive Diseases*, *29*(1), 37–44.

Quek, L.-E., van Geldermalsen, M., Guan, Y. F., Wahi, K., Mayoh, C., Balaban, S., Pang, A., Wang, Q., Cowley, M. J., Brown, K. K., Turner, N., Hoy, A. J., & Holst, J. (2022). Glutamine addiction promotes glucose oxidation in triple-negative breast cancer. *Oncogene*, *41*(34), 4066–4078.

Raimondi, V., Ciccarese, F., & Ciminale, V. (2020). Oncogenic pathways and the electron transport chain: a dangeROS liaison. *British Journal of Cancer*, *122*(2), 168–181.

Rathore, M. G., Saumet, A., Rossi, J.-F., de Bettignies, C., Tempé, D., Lecellier, C.-H., & Villalba, M. (2012). The NF-κB member p65 controls glutamine metabolism through miR-23a. *The International Journal of Biochemistry & Cell Biology*, *44*(9), 1448–1456.

Récher, C., Coiffier, B., Haioun, C., Molina, T. J., Fermé, C., Casasnovas, O., Thiéblemont, C., Bosly, A., Laurent, G., Morschhauser, F., Ghesquières, H., Jardin, F., Bologna, S., Fruchart, C., Corront, B., Gabarre, J., Bonnet, C., Janvier, M., Canioni, D., … Tilly, H. (2011). Intensified chemotherapy with ACVBP plus rituximab versus standard CHOP plus rituximab for the treatment of diffuse large B-cell lymphoma (LNH03-2B): an open-label randomised phase 3 trial. *The Lancet*, *378*(9806), 1858–1867.

Reddy, A., Zhang, J., Davis, N. S., Moffitt, A. B., Love, C. L., Waldrop, A., Leppa, S., Pasanen, A., Meriranta, L., Karjalainen-Lindsberg, M.-L., Nørgaard, P., Pedersen, M., Gang, A. O., Høgdall, E., Heavican, T. B., Lone, W., Iqbal, J., Qin, Q., Li, G., … Dave, S. S. (2017). Genetic and Functional Drivers of Diffuse Large B-Cell Lymphoma. *Cell*, *171*(2), 481-494.

Refolo, M. G., Messa, C., Guerra, V., Carr, B. I., & D'Alessandro, R. (2020). Inflammatory Mechanisms of HCC Development. *Cancers*, *12*(3).

Riihijärvi, S., Koivula, S., Nyman, H., Rydström, K., Jerkeman, M., & Leppä, S. (2010). Prognostic impact of protein kinase C β II expression in R-CHOP-treated diffuse large B-cell lymphoma patients. *Modern Pathology*, *23*(5), 686–693.

Roberts, A. W., Davids, M. S., Pagel, J. M., Kahl, B. S., Puvvada, S. D., Gerecitano, J. F., Kipps, T. J., Anderson, M. A., Brown, J. R., Gressick, L., Wong, S., Dunbar, M., Zhu, M., Desai, M. B., Cerri, E., Heitner Enschede, S., Humerickhouse, R. A., Wierda, W. G., & Seymour, J. F. (2015). Targeting BCL2 with Venetoclax in Relapsed Chronic Lymphocytic Leukemia. *New England Journal of Medicine*, *374*(4), 311–322.

Robertson, M. J., Kahl, B. S., Vose, J. M., de Vos, S., Laughlin, M., Flynn, P. J., Rowland, K., Cruz, J. C., Goldberg, S. L., Musib, L., Darstein, C., Enas, N., Kutok, J. L., Aster, J. C., Neuberg, D., Savage, K. J., LaCasce, A., Thornton, D., Slapak, C. A., & Shipp, M. A. (2007). Phase II Study of Enzastaurin, a Protein Kinase C Beta Inhibitor, in Patients With Relapsed or Refractory Diffuse Large B-Cell Lymphoma. *Journal of Clinical Oncology*, *25*(13), 1741–1746.

Roschewski, M., Staudt, L. M., & Wilson, W. H. (2014). Diffuse large B-cell lymphoma—treatment approaches in the molecular era. *Nature Reviews Clinical Oncology*, *11*(1), 12–23.

Rosenwald, A., Wright, G., Chan, W. C., Connors, J. M., Campo, E., Fisher, R. I., Gascoyne, R. D., Muller-Hermelink, H. K., Smeland, E. B., Giltnane, J. M., Hurt, E. M., Zhao, H., Averett, L., Yang, L., Wilson, W. H., Jaffe, E. S., Simon, R., Klausner, R. D., Powell, J., … Staudt, L. M. (2002). The Use of Molecular Profiling to Predict Survival after Chemotherapy for Diffuse Large-B-Cell Lymphoma. *New England Journal of Medicine*, *346*(25), 1937–1947.

Roth, E., Oehler, R., Manhart, N., Exner, R., Wessner, B., Strasser, E., & Spittler, A. (2002). Regulative potential of glutamine—relation to glutathione metabolism. *Nutrition*, *18*(3), 217–221.

Rovillain, E., Mansfield, L., Caetano, C., Alvarez-Fernandez, M., Caballero, O. L., Medema, R. H., Hummerich, H., & Jat, P. S. (2011). Activation of nuclear factor-kappa B signalling promotes cellular senescence. *Oncogene*, *30*(20), 2356–2366.

Ruan, J., Martin, P., Furman, R. R., Lee, S. M., Cheung, K., Vose, J. M., LaCasce, A., Morrison, J., Elstrom, R., Ely, S., Chadburn, A., Cesarman, E., Coleman, M., & Leonard, J. P. (2010). Bortezomib Plus CHOP-Rituximab for Previously Untreated Diffuse Large B-Cell Lymphoma and Mantle Cell Lymphoma. *Journal of Clinical Oncology*, *29*(6), 690–697.

Ruhland, M. K., Loza, A. J., Capietto, A.-H., Luo, X., Knolhoff, B. L., Flanagan, K. C., Belt, B. A., Alspach, E., Leahy, K., Luo, J., Schaffer, A., Edwards, J. R., Longmore, G., Faccio, R., DeNardo, D. G., & Stewart, S. A. (2016). Stromal senescence establishes an immunosuppressive microenvironment that drives tumorigenesis. *Nature Communications*, *7*(1), 11762.

Ruiz-Rodado, V., Lita, A., Dowdy, T., Celiku, O., Saldana, A. C., Wang, H., Yang, C. Z., Chari, R., Li, A., Zhang, W., Song, H., Zhang, M., Ahn, S., Davis, D., Chen, X., Zhuang, Z., Herold-Mende, C., Walters, K. J., Gilbert, M. R., & Larion, M. (2020). Metabolic plasticity of IDH1-mutant glioma cell lines is responsible for low sensitivity to glutaminase inhibition. *Cancer & Metabolism*, *8*(1), 23.

Ruminy, P., Etancelin, P., Couronné, L., Parmentier, F., Rainville, V., Mareschal, S., Bohers, E., Burgot, C., Cornic, M., Bertrand, P., Lenormand, B., Picquenot, J.-M., Jardin, F., Tilly, H., & Bastard, C. (2011). The isotype of the BCR as a surrogate for the GCB and ABC molecular subtypes in diffuse large B-cell lymphoma. *Leukemia*, *25*(4), 681–688.

Saha, S. K., Islam, S. M. R., Abdullah-AL-Wadud, M., Islam, S., Ali, F., & Park, K. S. (2019). Multiomics Analysis Reveals that GLS and GLS2 Differentially Modulate the Clinical Outcomes of Cancer. *Journal of Clinical Medicine*, *8*(3).

Salminen, A., Kauppinen, A., & Kaarniranta, K. (2012). Emerging role of NF-κB signaling in the induction of senescence-associated secretory phenotype (SASP). *Cellular Signalling*, *24*(4), 835–845.

Savinova, O. v, Hoffmann, A., & Ghosh, G. (2009). The Nfkb1 and Nfkb2 Proteins p105 and p100 Function as the Core of High-Molecular-Weight Heterogeneous Complexes. *Molecular Cell*, *34*(5), 591–602.

Schaub, F. X., Dhankani, V., Berger, A. C., Trivedi, M., Richardson, A. B., Shaw, R., Zhao, W., Zhang, X., Ventura, A., Liu, Y., Ayer, D. E., Hurlin, P. J., Cherniack, A. D., Eisenman, R. N., Bernard, B., Grandori, C., & Network, C. G. A. (2018). Pan-cancer Alterations of the MYC Oncogene and Its Proximal Network across the Cancer Genome Atlas. *Cell Systems*, *6(3)*, 282–300.

Schmitt, A., Xu, W., Bucher, P., Grimm, M., Konantz, M., Horn, H., Zapukhlyak, M., Berning, P., Brändle, M., Jarboui, M.-A., Schönfeld, C., Boldt, K., Rosenwald, A., Ott, G., Grau, M., Klener, P., Vockova, P., Lengerke, C., Lenz, G., … Hailfinger, S. (2021). Dimethyl fumarate induces ferroptosis and impairs NF-κB/STAT3 signaling in DLBCL. *Blood*, *138*(10), 871–884.

Schmitt, C. A., Wang, B., & Demaria, M. (2022a). Senescence and cancer — role and therapeutic opportunities. *Nature Reviews Clinical Oncology*, *19*(10), 619–636.

Schmitz, R., Wright, G. W., Huang, D. W., Johnson, C. A., Phelan, J. D., Wang, J. Q., Roulland, S., Kasbekar, M., Young, R. M., Shaffer, A. L., Hodson, D. J., Xiao, W., Yu, X., Yang, Y., Zhao, H., Xu, W., Liu, X., Zhou, B., Du, W., … Staudt, L. M. (2018). Genetics and Pathogenesis of Diffuse Large B-Cell Lymphoma. *New England Journal of Medicine*, *378*(15), 1396–1407.

Schneider, C., Pasqualucci, L., & Dalla-Favera, R. (2011). Molecular pathogenesis of diffuse large B-cell lymphoma. *Seminars in Diagnostic Pathology*, *28*(2), 167–177.

Schröder, S., Cho, S., Zeng, L., Zhang, Q., Kaehlcke, K., Mak, L., Lau, J., Bisgrove, D., Schnölzer, M., Verdin, E., Zhou, M.-M., & Ott, M. (2012). Two-pronged Binding with Bromodomain-containing Protein 4 Liberates Positive Transcription Elongation Factor b from Inactive Ribonucleoprotein Complexes. *Journal of Biological Chemistry*, *287*(2), 1090–1099.

Sener, Z., Cederkvist, F. H., Volchenkov, R., Holen, H. L., & Skålhegg, B. S. (2016). T Helper Cell Activation and Expansion Is Sensitive to Glutaminase Inhibition under Both Hypoxic and Normoxic Conditions. *PLOS ONE*, *11*(7), e0160291-.

Serrano, M., Lin, A. W., McCurrach, M. E., Beach, D., & Lowe, S. W. (1997). Oncogenic ras Provokes Premature Cell Senescence Associated with Accumulation of p53 and p16/INK4a. *Cell*, *88*(5), 593–602.

Shaffer, A. L., Young, R. M., & Staudt, L. M. (2012). Pathogenesis of Human B Cell Lymphomas. *Annual Review of Immunology*, *30*(1), 565–610.

Shaffer, A. L., Yu, X., He, Y., Boldrick, J., Chan, E. P., & Staudt, L. M. (2000). BCL-6 Represses Genes that Function in Lymphocyte Differentiation, Inflammation, and Cell Cycle Control. *Immunity*, *13*(2), 199–212.

Shakiba, E., Ramezani, M., & Sadeghi, M. (2018). Evaluation of serum interleukin-6 levels in hepatocellular carcinoma patients: a systematic review and meta-analysis. *Clinical and Experimental Hepatology*, *4*(3), 182–190.

Shamas-Din, A., Kale, J., Leber, B., & Andrews, D. W. (2013). Mechanisms of Action of Bcl-2 Family Proteins. *Cold Spring Harbor Perspectives in Biology*, *5*(4).

Shankland, K. R., Armitage, J. O., & Hancock, B. W. (2012). Non-Hodgkin lymphoma. *The Lancet*, *380*(9844), 848–857.

Shen, Y.-A., Hong, J., Asaka, R., Asaka, S., Hsu, F.-C., Suryo Rahmanto, Y., Jung, J.-G., Chen, Y.-W., Yen, T.-T., Tomaszewski, A., Zhang, C., Attarwala, N., DeMarzo, A. M., Davidson, B., Chuang, C.-M., Chen, X., Gaillard, S., Le, A., Shih, I.-M., & Wang, T.-L. (2020). Inhibition of the MYC-Regulated Glutaminase Metabolic Axis Is an Effective Synthetic Lethal Approach for Treating Chemoresistant Ovarian Cancers. *Cancer Research*, *80*(20), 4514–4526.

Sheron, N., Bird, G., Goka, J., Alexander, G., & Williams, R. (1991). Elevated plasma interleukin-6 and increased severity and mortality in alcoholic hepatitis. *Clinical and Experimental Immunology*, *84(3)*, 449–453.

Shih, V. F.-S., Tsui, R., Caldwell, A., & Hoffmann, A. (2011). A single NFκB system for both canonical and non-canonical signaling. *Cell Research*, *21*(1), 86–102.

Shiina, S., Sato, K., Tateishi, R., Shimizu, M., Ohama, H., Hatanaka, T., Takawa, M., Nagamatsu, H., & Imai, Y. (2018). Percutaneous Ablation for Hepatocellular Carcinoma: Comparison of Various Ablation Techniques and Surgery. *Canadian Journal of Gastroenterology and Hepatology*, *2018*, 4756147. https://doi.org/10.1155/2018/4756147

Singh, R., Shaik, S., Negi, B. S., Rajguru, J. P., Patil, P. B., Parihar, A. S., & Sharma, U. (2020). Non-Hodgkin's lymphoma: A review. *Journal of Family Medicine and Primary Care*, *9*(4).

Smith, S. M., van Besien, K., Karrison, T., Dancey, J., McLaughlin, P., Younes, A., Smith, S., Stiff, P., Lester, E., Modi, S., Doyle, L. A., Vokes, E. E., & Pro, B. (2010). Temsirolimus Has Activity in Non–Mantle Cell Non-Hodgkin's Lymphoma Subtypes: The University of Chicago Phase II Consortium. *Journal of Clinical Oncology*, *28*(31), 4740–4746.

Son, J., Lyssiotis, C. A., Ying, H., Wang, X., Hua, S., Ligorio, M., Perera, R. M., Ferrone, C. R., Mullarky, E., Shyh-Chang, N., Kang, Y., Fleming, J. B., Bardeesy, N., Asara, J. M., Haigis, M. C., DePinho, R. A., Cantley, L. C., & Kimmelman, A. C. (2013). Glutamine supports pancreatic cancer growth through a KRAS-regulated metabolic pathway. *Nature*, *496*(7443), 101–105.

Souers, A. J., Leverson, J. D., Boghaert, E. R., Ackler, S. L., Catron, N. D., Chen, J., Dayton, B. D., Ding, H., Enschede, S. H., Fairbrother, W. J., Huang, D. C. S., Hymowitz, S. G., Jin, S., Khaw, S. L., Kovar, P. J., Lam, L. T., Lee, J., Maecker, H. L., Marsh, K. C., … Elmore, S. W. (2013). ABT-199, a potent and selective BCL-2 inhibitor, achieves antitumor activity while sparing platelets. *Nature Medicine*, *19*(2), 202–208.

Staudt, L. M., & Dave, S. (2005). The Biology of Human Lymphoid Malignancies Revealed by Gene Expression Profiling. In *Advances in Immunology* (Vol. 87, pp. 163–208). Academic Press.

Staudt, L. M., & Wilson, W. H. (2002). Focus on lymphomas. *Cancer Cell*, *2*(5), 363–366.

Su, B., Luo, T., Zhu, J., Fu, J., Zhao, X., Chen, L., Zhang, H., Ren, Y., Yu, L., Yang, X., Wu, M., Feng, G., Li, S., Chen, Y., & Wang, H. (2015). Interleukin-1β/Iinterleukin-1 receptor-associated kinase 1 inflammatory signaling contributes to persistent Gankyrin activation during hepatocarcinogenesis. *Hepatology*, *61*(2), 585–597.

Sung, H., Ferlay, J., Siegel, R. L., Laversanne, M., Soerjomataram, I., Jemal, A., & Bray, F. (2021). Global Cancer Statistics 2020: GLOBOCAN Estimates of Incidence and Mortality Worldwide for 36 Cancers in 185 Countries. *CA: A Cancer Journal for Clinicians*, *71*(3), 209–249.

Sun, R. C., & Denko, N. C. (2014). Hypoxic Regulation of Glutamine Metabolism through HIF1 and SIAH2 Supports Lipid Synthesis that Is Necessary for Tumor Growth. *Cell Metabolism*, *19*(2), 285–292.

Sun, S.-C. (2017). The non-canonical NF-κB pathway in immunity and inflammation. *Nature Reviews Immunology*, *17*(9), 545–558.

Suzuki, S., Tanaka, T., Poyurovsky, M. v, Nagano, H., Mayama, T., Ohkubo, S., Lokshin, M., Hosokawa, H., Nakayama, T., Suzuki, Y., Sugano, S., Sato, E., Nagao, T., Yokote, K., Tatsuno, I., & Prives, C. (2010). Phosphate-activated glutaminase (GLS2), a p53-inducible regulator of glutamine metabolism and reactive oxygen species. *Proceedings of the National Academy of Sciences*, *107*(16), 7461–7466.

Suzuki, S., Venkatesh, D., Kanda, H., Nakayama, A., Hosokawa, H., Lee, E., Miki, T., Stockwell, B. R., Yokote, K., Tanaka, T., & Prives, C. (2022). GLS2 Is a Tumor Suppressor and a Regulator of Ferroptosis in Hepatocellular Carcinoma. *Cancer Research*, *82*(18), 3209–3222.

Svinka, J., Mikulits, W., & Eferl, R. (2013). STAT3 in hepatocellular carcinoma: new perspectives. *Hepatic Oncology*, *1*(1), 107–120.

Szabo, G., & Csak, T. (2012). Inflammasomes in liver diseases. *Journal of Hepatology*, *57*(3), 642–654.

Szeliga M., Obara-Michlewska M., & Matyja E. (2009). Transfection with liver-type glutaminase cDNA alters gene expression and reduces survival, migration and proliferation of T98G glioma cells. *Glia*, *57(9)*, 1014-1023.

Tago, K., Funakoshi-Tago, M., Ohta, S., Kawata, H., Saitoh, H., Horie, H., Aoki-Ohmura, C., Yamauchi, J., Tanaka, A., Matsugi, J., & Yanagisawa, K. (2019). Oncogenic Ras mutant causes the hyperactivation of NF-κB via acceleration of its transcriptional activation. *Molecular Oncology*, *13*(11), 2493–2510.

Taniguchi, K., & Karin, M. (2018). NF-κB, inflammation, immunity and cancer: coming of age. *Nature Reviews Immunology*, *18*(5), 309–324.

Tartey, S., Matsushita, K., Vandenbon, A., Ori, D., Imamura, T., Mino, T., Standley, D. M., Hoffmann, J. A., Reichhart, J.-M., Akira, S., & Takeuchi, O. (2014). Akirin2 is critical for inducing inflammatory genes by bridging IκB-ζ and the SWI/SNF complex. *The EMBO Journal*, *33*(20), 2332–2348.

Tasdemir, N., Banito, A., Roe, J.-S., Alonso-Curbelo, D., Camiolo, M., Tschaharganeh, D. F., Huang, C.-H., Aksoy, O., Bolden, J. E., Chen, C.-C., Fennell, M., Thapar, V., Chicas, A., Vakoc, C. R., & Lowe, S. W. (2016). BRD4 Connects Enhancer Remodeling to Senescence Immune Surveillance. *Cancer Discovery*, *6*(6), 612–629.

Teperino, R., Schoonjans, K., & Auwerx, J. (2010). Histone Methyl Transferases and Demethylases; Can They Link Metabolism and Transcription? *Cell Metabolism*, *12*(4), 321–327. https://doi.org/10.1016/j.cmet.2010.09.004

Thandra, K. C., Barsouk, A., Saginala, K., Padala, S. A., Barsouk, A., & Rawla, P. (2021). Epidemiology of Non-Hodgkin's Lymphoma. *Medical Sciences*, *9*(1).

Thangadurai, S., Bajgiran, M., Manickam, S., Mohana-Kumaran, N., & Azzam, G. (2022). CTP synthase: the hissing of the cellular serpent. *Histochemistry and Cell Biology*, *158*(6), 517–534.

Tian, H., Huang, P., Zhao, Z., Tang, W., & Xia, J. (2014). HIF-1α Plays a Role in the Chemotactic Migration of Hepatocarcinoma Cells Through the Modulation of CXCL6 Expression. *Cellular Physiology and Biochemistry*, *34*(5), 1536–1546.

Tivnan, A., Zhao, J., Johns, T. G., Day, B. W., Stringer, B. W., Boyd, A. W., Tiwari, S., Giles, K. M., Teo, C., & McDonald, K. L. (2014). The tumor suppressor microRNA, miR-124a, is regulated by epigenetic silencing and by the transcriptional factor, REST in glioblastoma. *Tumor Biology*, *35*(2), 1459–1465.

Totzke, G., Essmann, F., Pohlmann, S., Lindenblatt, C., Jänicke, R. U., & Schulze-Osthoff, K. (2006). A Novel Member of the IkappaB Family, Human IkappaB-zeta, Inhibits Transactivation of p65 and Its DNA Binding. *Journal of Biological Chemistry*, *281*(18), 12645–12654.

Trépo, C., Chan, H. L. Y., & Lok, A. (2014). Hepatitis B virus infection. *The Lancet*, *384*(9959), 2053–2063.

Tsukada, Y., Fang, J., Erdjument-Bromage, H., Warren, M. E., Borchers, C. H., Tempst, P., & Zhang, Y. (2006). Histone demethylation by a family of JmjC domain-containing proteins. *Nature*, *439*(7078), 811–816.

Turhal, N. S., Savaş, B., Çoşkun, Ö., Baş, E., Karabulut, B., Nart, D., Korkmaz, T., Yavuzer, D., Demir, G., Doğusoy, G., & Artaç, M. (2015). Prevalence of K-Ras mutations in hepatocellular carcinoma: A Turkish Oncology Group pilot study. *Molecular and Clinical Oncology*, *3*(6), 1275—1279.

Turner, P. C., Sylla, A., Diallo, M. S., Castegnaro, J.-J., Hall, A. J., & Wild, C. P. (2002). The role of aflatoxins and hepatitis viruses in the etiopathogenesis of hepatocellular carcinoma: A basis for primary prevention in Guinea–Conakry, West Africa. *Journal of Gastroenterology and Hepatology*, *17*(s4), S441–S448.

Uprety, D., & Adjei, A. A. (2020). KRAS: From undruggable to a druggable Cancer Target. *Cancer Treatment Reviews*, *89*.

US National Library of Medicine. (2012). ClinicalTrials.Gov [Online].

US National Library of Medicine. (2019). *ClinicalTrials.Gov*.

Van der Heiden, M. G., Cantley, L. C., & Thompson, C. B. (2009). Understanding the Warburg Effect: The Metabolic Requirements of Cell Proliferation. *Science*, *324*(5930), 1029–1033.

Van de Voorde, J., Ackermann, T., Pfetzer, N., Sumpton, D., Mackay, G., Kalna, G., Nixon, C., Blyth, K., Gottlieb, E., & Tardito, S. (2023). Improving the metabolic fidelity of cancer models with a physiological cell culture medium. *Science Advances*, *5*(1), eaau7314.

Van Kester, M. S., Borg, M. K., Zoutman, W. H., Out-Luiting, J. J., Jansen, P. M., Dreef, E. J., Vermeer, M. H., van Doorn, R., Willemze, R., & Tensen, C. P. (2012). A meta-analysis of gene expression data identifies a molecular signature characteristic for tumor-stage mycosis fungoides. *The Journal of Investigative Dermatology*, *132*(8), 2050–2059.

Villanueva, A. (2019). Hepatocellular Carcinoma. *New England Journal of Medicine*, *380*(15), 1450–1462.

Wang, C., Liao, Y., He, W., Zhang, H., Zuo, D., Liu, W., Yang, Z., Qiu, J., Yuan, Y., Li, K., Zhang, Y., Wang, Y., Shi, Y., Qiu, Y., Gao, S., Yuan, Y., & Li, B. (2021). Elafin promotes tumour metastasis and attenuates the anti-metastatic effects of erlotinib via binding to EGFR in hepatocellular carcinoma. *Journal of Experimental & Clinical Cancer Research*, *40*(1), 113.

Wang, H.-Q., Man, Q.-W., Huo, F.-Y., Gao, X., Lin, H., Li, S.-R., Wang, J., Su, F.-C., Cai Lulu, Shi, Y., Liu Bing, & Bu, L.-L. (2022). STAT3 pathway in cancers: Past, present, and future. *MedComm*, *3*(2), e124.

Wang, L., Lankhorst, L., & Bernards, R. (2022). Exploiting senescence for the treatment of cancer. *Nature Reviews Cancer*, *22*(6), 340–355.

Wang, N., Wu, R., Tang, D., & Kang, R. (2021). The BET family in immunity and disease. *Signal Transduction and Targeted Therapy*, *6*(1), 23.

Wang, Q., Lin, ZY., & Feng, XL. (2001). Alterations in metastatic properties of hepatocellular carcinoma cell following H-ras oncogene transfection. *World Journal of Gastroenterology*, *7(3)*, 335–339.

Wang, Y., Liu, J., Burrows, P. D., & Wang, J.-Y. (2020). B Cell Development and Maturation. In J.-Y. Wang (Ed.), *B Cells in Immunity and Tolerance* (pp. 1–22). Springer Singapore.

Wang, Z., Liu, F., Fan, N., Zhou, C., Li, D., Macvicar, T., Dong, Q., Bruns, C. J., & Zhao, Y. (2020). Targeting Glutaminolysis: New Perspectives to Understand Cancer Development and Novel Strategies for Potential Target Therapies. *Frontiers in Oncology*, *10*.

Welzel, T. M., Graubard, B. I., Quraishi, S., Zeuzem, S., Davila, J. A., El-Serag, H. B., & McGlynn, K. A. (2013). Population-Attributable Fractions of Risk Factors for Hepatocellular Carcinoma in the United States. *Official Journal of the American College of Gastroenterology | ACG*, *108*(8).

Willems, M., Dubois, N., Musumeci, L., Bours, V., & Robe, P. A. (2016). IκBζ: an emerging player in cancer. *Oncotarget*, *7*, 66310–66322.

Wilson, W. H., Gerecitano, J. F., Goy, A., de Vos, S., Kenkre, V. P., Barr, P. M., Blum, K. A., Shustov, A. R., Advani, R. H., Lih, J., Williams, M., Schmitz, R., Yang, Y., Pittaluga, S., Wright, G., Kunkel, L. A., McGreivy, J., Balasubramanian, S., Cheng, M., … Staudt, L. M. (2012). The Bruton's Tyrosine Kinase (BTK) Inhibitor, Ibrutinib (PCI-32765), Has Preferential Activity in the ABC Subtype of Relapsed/Refractory De Novo Diffuse Large B-Cell Lymphoma (DLBCL): Interim Results of a Multicenter, Open-Label, Phase 2 Study. *Blood*, *120*(21), 686.

Wilson, W. H., Wright, G. W., Huang, D. W., Hodkinson, B., Balasubramanian, S., Fan, Y., Vermeulen, J., Shreeve, M., & Staudt, L. M. (2021). Effect of ibrutinib with R-CHOP chemotherapy in genetic subtypes of DLBCL. *Cancer Cell*, *39*(12), 1643-1653.e3.

Wirestam, L., Enocsson, H., Skogh, T., Eloranta, M. L., Rönnblom, L., Sjöwall, C., & Wetterö, J. (2017). Interferon-α coincides with suppressed levels of pentraxin-3 (PTX3) in systemic lupus erythematosus and regulates leucocyte PTX3 in vitro. *Clinical and Experimental Immunology*, *189*(1), 83–91.

Wise, D. R., DeBerardinis, R. J., Mancuso, A., Sayed, N., Zhang, X.-Y., Pfeiffer, H. K., Nissim, I., Daikhin, E., Yudkoff, M., McMahon, S. B., & Thompson, C. B. (2008). Myc regulates a transcriptional program that stimulates mitochondrial glutaminolysis and leads to glutamine addiction. *Proceedings of the National Academy of Sciences*, *105*(48), 18782–18787.

Wise, D. R., & Thompson, C. B. (2010). Glutamine addiction: a new therapeutic target in cancer. In *Trends in Biochemical Sciences* (Vol. 35, Issue 8, pp. 427–433).

Witzig, T. E., Reeder, C. B., LaPlant, B. R., Gupta, M., Johnston, P. B., Micallef, I. N., Porrata, L. F., Ansell, S. M., Colgan, J. P., Jacobsen, E. D., Ghobrial, I. M., & Habermann, T. M. (2011). A phase II trial of the oral mTOR inhibitor everolimus in relapsed aggressive lymphoma. *Leukemia*, *25*(2), 341–347.

Wong, V. W.-S., Yu, J., Cheng, A. S.-L., Wong, G. L.-H., Chan, H.-Y., Chu, E. S.-H., Ng, E. K.-O., Chan, F. K.-L., Sung, J. J.-Y., & Chan, H. L.-Y. (2009). High serum interleukin-6 level predicts future hepatocellular carcinoma development in patients with chronic hepatitis B. *International Journal of Cancer*, *124*(12), 2766–2770.

Wright, G., Tan, B., Rosenwald, A., Hurt, E. H., Wiestner, A., & Staudt, L. M. (2003). A gene expression-based method to diagnose clinically distinct subgroups of diffuse large B cell lymphoma. *Proceedings of the National Academy of Sciences*, *100*(17), 9991–9996.

Wright, G. W., Huang, D. W., Phelan, J. D., Coulibaly, Z. A., Roulland, S., Young, R. M., Wang, J. Q., Schmitz, R., Morin, R. D., Tang, J., Jiang, A., Bagaev, A., Plotnikova, O., Kotlov, N., Johnson, C. A., Wilson, W. H., Scott, D. W., & Staudt, L. M. (2020). A Probabilistic

Classification Tool for Genetic Subtypes of Diffuse Large B Cell Lymphoma with Therapeutic Implications. *Cancer Cell*, *37*(4), 551-568.e14.

Wu, S.-Y., Lee, A.-Y., Lai, H.-T., Zhang, H., & Chiang, C.-M. (2013). Phospho Switch Triggers Brd4 Chromatin Binding and Activator Recruitment for Gene-Specific Targeting. *Molecular Cell*, *49*(5), 843–857. ht

Wu, Z., Zhang, X., Yang, J., Wu, G., Zhang, Y., Yuan, Y., Jin, C., Chang, Z., Wang, J., Yang, X., & He, F. (2009). Nuclear protein IκB-ζ inhibits the activity of STAT3. *Biochemical and Biophysical Research Communications*, *387*(2), 348–352.

Wyndham H. Wilson, Sin-Ho Jung, Pierluigi Porcu, David Hurd, Jeffrey Johnson, S. Eric Martin, Myron Czuczman, Raymond Lai, Jonathan Said, Amy Chadburn, Dan Jones, Kieron Dunleavy, George Canellos, Andrew D. Zelenetz, Bruce D. Cheson, & Eric D. Hsi. (2012). A Cancer and Leukemia Group B multi-center study of DA-EPOCH-rituximab in untreated diffuse large B-cell lymphoma with analysis of outcome by molecular subtype. *Haematologica*, *97*(5), 758–765.

Xiang, Y., Stine, Z. E., Xia, J., Lu, Y., O'Connor, R. S., Altman, B. J., Hsieh, A. L., Gouw, A. M., Thomas, A. G., Gao, P., Sun, L., Song, L., Yan, B., Slusher, B. S., Zhuo, J., Ooi, L. L., Lee, C. G. L., Mancuso, A., McCallion, A. S., … Dang, C. v. (2015). Targeted inhibition of tumor-specific glutaminase diminishes cell-autonomous tumorigenesis. *The Journal of Clinical Investigation*, *125*(6), 2293–2306.

Xia, X., Zhou, W., Guo, C., Fu, Z., Zhu, L., Li, P., Xu, Y., Zheng, L., Zhang, H., Shan, C., & Gao, Y. (2018). Glutaminolysis Mediated by MALT1 Protease Activity Facilitates PD-L1 Expression on ABC-DLBCL Cells and Contributes to Their Immune Evasion. *Frontiers in Oncology*, *8*.

Xia, Y., & Zhang, X. (2020). The Spectrum of MYC Alterations in Diffuse Large B-Cell Lymphoma. *Acta Haematologica*, *143*(6), 520–528.

Xue, W., Zender, L., Miething, C., Dickins, R. A., Hernando, E., Krizhanovsky, V., Cordon-Cardo, C., & Lowe, S. W. (2007). Senescence and tumour clearance is triggered by p53 restoration in murine liver carcinomas. *Nature*, *445*(7128), 656–660.

Xu, L., Zhou, D., Li, F., & Ji, L. (2020). Glutaminase 2 functions as a tumor suppressor gene in gastric cancer. *Transl Cancer Res.*, *9(8)*, 4906–4913.

Xu, X., Meng, Y., Li, L., Xu, P., Wang, J., Li, Z., & Bian, J. (2019). Overview of the Development of Glutaminase Inhibitors: Achievements and Future Directions. *Journal of Medicinal Chemistry*, *62*(3), 1096–1115.

Yamamoto, M., Yamazaki, S., Uematsu, S., Sato, S., Hemmi, H., Hoshino, K., Kaisho, T., Kuwata, H., Takeuchi, O., Takeshige, K., Saitoh, T., Yamaoka, S., Yamamoto, N., Yamamoto, S., Muta, T., Takeda, K., & Akira, S. (2004). Regulation of Toll/IL-1-receptor-mediated gene expression by the inducible nuclear protein IkappaBzeta. *Nature*, *430(6996)*, 218–222.

Yamauchi, S., Ito, H., & Miyajima, A. (2010). IκBη, a nuclear IκB protein, positively regulates the NF-κB–mediated expression of proinflammatory cytokines. *Proceedings of the National Academy of Sciences*, *107*(26), 11924–11929.

Yamazaki, S., Matsuo, S., Muta, T., Yamamoto, M., Akira, S., & Takeshige, K. (2008). Gene-specific Requirement of a Nuclear Protein, IkappaB-zeta, for Promoter Association of

Inflammatory Transcription Regulators. *Journal of Biological Chemistry*, *283*(47), 32404–32411.

Yamazaki, S., Muta, T., Matsuo, S., & Takeshige, K. (2005). Stimulus-specific Induction of a Novel Nuclear Factor-kappaB Regulator, IkappaB-zeta, via Toll/Interleukin-1 Receptor Is Mediated by mRNA Stabilization. *Journal of Biological Chemistry*, *280*(2), 1678–1687.

Yamazaki, S., Muta, T., & Takeshige, K. (2001). A Novel IκB Protein, IκB-ζ, Induced by Proinflammatory Stimuli, Negatively Regulates Nuclear Factor-κB in the Nuclei*. *Journal of Biological Chemistry*, *276*(29), 27657–27662.

Yang, C., Ko, B., Hensley, C. T., Jiang, L., Wasti, A. T., Kim, J., Sudderth, J., Calvaruso, M. A., Lumata, L., Mitsche, M., Rutter, J., Merritt, M. E., & DeBerardinis, R. J. (2014). Glutamine Oxidation Maintains the TCA Cycle and Cell Survival during Impaired Mitochondrial Pyruvate Transport. *Molecular Cell*, *56*(3), 414–424.

Yang, J. D., Hainaut, P., Gores, G. J., Amadou, A., Plymoth, A., & Roberts, L. R. (2019). A global view of hepatocellular carcinoma: trends, risk, prevention and management. *Nature Reviews Gastroenterology & Hepatology*, *16*(10), 589–604.

Yang, J. D., Larson, J. J., Watt, K. D., Allen, A. M., Wiesner, R. H., Gores, G. J., Roberts, L. R., Heimbach, J. A., & Leise, M. D. (2017). Hepatocellular Carcinoma Is the Most Common Indication for Liver Transplantation and Placement on the Waitlist in the United States. *Clinical Gastroenterology and Hepatology*, *15*(5), 767-775.e3.

Yang, J. D., & Roberts, L. R. (2010). Hepatocellular carcinoma: a global view. *Nature Reviews Gastroenterology & Hepatology*, *7*(8), 448–458.

Yang, J., Liao, X., Agarwal, M. K., Barnes, L., Auron, P. E., & Stark, G. R. (2007). Unphosphorylated STAT3 accumulates in response to IL-6 and activates transcription by binding to NFκB. *Genes & Development*, *21*(11), 1396–1408.

Yang, L., Venneti, S., & Nagrath, D. (2017). Glutaminolysis: A Hallmark of Cancer Metabolism. *Annual Review of Biomedical Engineering*, *19*(1), 163–194.

Yang, W.-H., Qiu, Y., Stamatatos, O., Janowitz, T., & Lukey, M. J. (2021). Enhancing the Efficacy of Glutamine Metabolism Inhibitors in Cancer Therapy. *Trends in Cancer*, *7*(8), 790–804.

Yang, YM., Kim, SY., & Seki, E. (2019). Inflammation and Liver Cancer: Molecular Mechanisms and Therapeutic Targets. *Seminars in Liver Disease*, *39*(01), 26–42.

Yang, Z., Yik, J. H. N., Chen, R., He, N., Jang, M. K., Ozato, K., & Zhou, Q. (2005). Recruitment of P-TEFb for Stimulation of Transcriptional Elongation by the Bromodomain Protein Brd4. *Molecular Cell*, *19*(4), 535–545.

Ying, M., You, D., Zhu, X., Cai, L., Zeng, S., & Hu, X. (2021). Lactate and glutamine support NADPH generation in cancer cells under glucose deprived conditions. *Redox Biology*, *46*, 102065.

Yin, L., Li, H., Li, A.-J., Lau, W. Y., Pan, Z., Lai, E. C. H., Wu, M., & Zhou, W.-P. (2014). Partial hepatectomy vs transcatheter arterial chemoembolization for resectable multiple hepatocellular carcinoma beyond Milan criteria: A RCT. *Journal of Hepatology*, *61*(1), 82–88.

Yoo, H. C., Yu, Y. C., Sung, Y., & Han, J. M. (2020). Glutamine reliance in cell metabolism. *Experimental & Molecular Medicine*, *52*(9), 1496–1516.

Yoshimoto, S., Loo, T. M., Atarashi, K., Kanda, H., Sato, S., Oyadomari, S., Iwakura, Y., Oshima, K., Morita, H., Hattori, M., Honda, K., Ishikawa, Y., Hara, E., & Ohtani, N. (2013). Obesity-induced gut microbial metabolite promotes liver cancer through senescence secretome. *Nature*, *499*(7456), 97–101.

Younes, A., Flinn, I., Berdeja, J. G., Friedberg, J. W., Alberti, S., Thieblemont, C., Morschhauser, F., Hellemans, P., Hall, B., Smit, J., Skee, D., de Vries, R., Todorovic, M., Khan, I., Fourneau, N., & Oki, Y. (2013). Phase Ib study combining ibrutinib with rituximab, cyclophosphamide, doxorubicin, vincristine, and prednisone (R-CHOP) in patients with CD20-positive B-cell non-Hodgkin lymphoma (NHL). *Journal of Clinical Oncology*, *31*(15_suppl), 8502.

Younes, A., Thieblemont, C., Morschhauser, F., Flinn, I., Friedberg, J. W., Amorim, S., Hivert, B., Westin, J., Vermeulen, J., Bandyopadhyay, N., de Vries, R., Balasubramanian, S., Hellemans, P., Smit, J. W., Fourneau, N., & Oki, Y. (2014). Combination of ibrutinib with rituximab, cyclophosphamide, doxorubicin, vincristine, and prednisone (R-CHOP) for treatment-naive patients with CD20-positive B-cell non-Hodgkin lymphoma: a non-randomised, phase 1b study. *The Lancet Oncology*, *15*(9), 1019–1026.

Younossi, ZM., Otgonsuren, M., & Henrym, L. (2015). Association of nonalcoholic fatty liver disease (NAFLD) with hepatocellular carcinoma (HCC) in the United States from 2004 to 2009. *Hepatology*, *62(6)*, 1723–1730.

Yuen, M.-F., Chen, D.-S., Dusheiko, G. M., Janssen, H. L. A., Lau, D. T. Y., Locarnini, S. A., Peters, M. G., & Lai, C.-L. (2018). Hepatitis B virus infection. *Nature Reviews Disease Primers*, *4*(1), 18035.

Yu, H., Lee, H., Herrmann, A., Buettner, R., & Jove, R. (2014). Revisiting STAT3 signalling in cancer: new and unexpected biological functions. *Nature Reviews Cancer*, *14*(11), 736–746.

Yu, J., Yu, X., Han, Z., Cheng, Z., Liu, F., Zhai, H., Mu, M., Liu, Y., & Liang, P. (2017). Percutaneous cooled-probe microwave versus radiofrequency ablation in early-stage hepatocellular carcinoma: a phase III randomised controlled trial. *Gut*, *66*(6), 1172.

Zeppa, P., & Cozzolino, I. (2017). Non-Hodgkin Lymphoma. In *Monographs in Clinical Cytology* (Vol. 23, pp. 34–51).

Zhang, J., He, X., Wan, Y., Zhang, H., Tang, T., Zhang, M., Yu, S., Zhao, W., & Chen, L. (2021). CD44 promotes hepatocellular carcinoma progression via upregulation of YAP. *Experimental Hematology & Oncology*, *10*(1), 54.

Zhang, J., Mao, S., Guo, Y., Wu, Y., Yao, X., & Huang, Y. (2019). Inhibition of GLS suppresses proliferation and promotes apoptosis in prostate cancer. *Bioscience Reports*, *39*(6), BSR20181826.

Zhang, J., Pavlova, N. N., & Thompson, C. B. (2017). Cancer cell metabolism: the essential role of the nonessential amino acid, glutamine. *The EMBO Journal*, *36*(10), 1302–1315.

Zhao, X., Petrashen, A. P., Sanders, J. A., Peterson, A. L., & Sedivy, J. M. (2019). SLC1A5 glutamine transporter is a target of MYC and mediates reduced mTORC1 signaling and

increased fatty acid oxidation in long-lived Myc hypomorphic mice. *Aging Cell*, *18*(3), e12947.

Zhiyuan, Y., Nanhai, H., & Qiang, Z. (2008). Brd4 Recruits P-TEFb to Chromosomes at Late Mitosis To Promote G1 Gene Expression and Cell Cycle Progression. *Molecular and Cellular Biology*, *28*(3), 967–976.

Zhu, L., Tang, F., Lei, Z., Guo, C., Song, Y., Huang, J., & Xia, X. (2019). Antiapoptotic properties of MALT1 protease are associated with redox homeostasis in ABC-DLBCL cells. *Molecular Carcinogenesis*, *58*(12), 2340–2352.

Zuber, J., Shi, J., Wang, E., Rappaport, A. R., Herrmann, H., Sison, E. A., Magoon, D., Qi, J., Blatt, K., Wunderlich, M., Taylor, M. J., Johns, C., Chicas, A., Mulloy, J. C., Kogan, S. C., Brown, P., Valent, P., Bradner, J. E., Lowe, S. W., & Vakoc, C. R. (2011). RNAi screen identifies Brd4 as a therapeutic target in acute myeloid leukaemia. *Nature*, *478*(7370), 524–528.